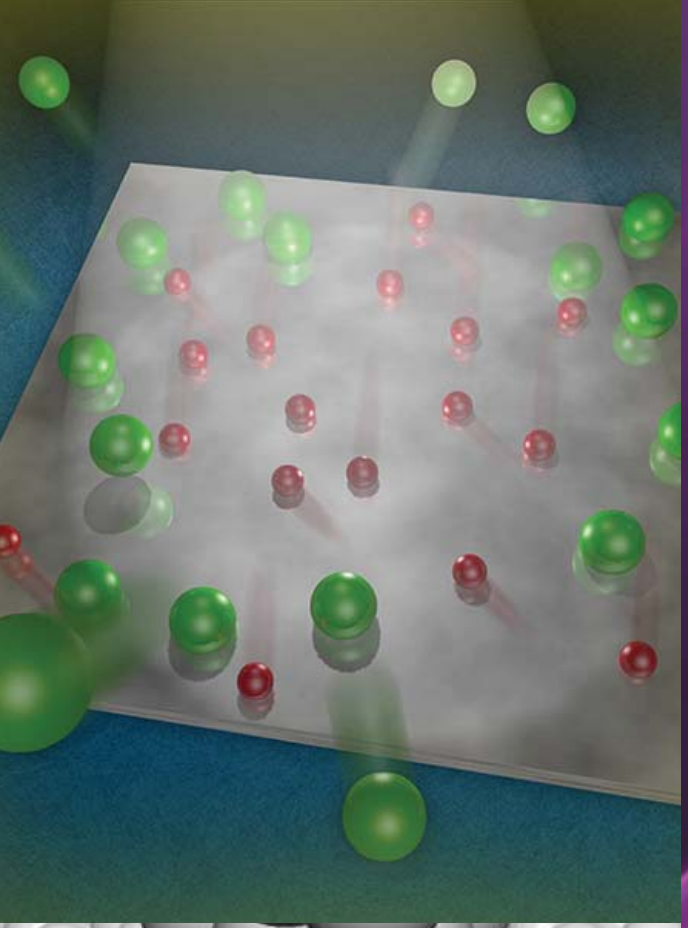

CPIMS 10

Tenth Condensed Phase and Interfacial Molecular Science (CPIMS) Research Meeting

Bolger Conference Center
Potomac, MD
October 19 - 22, 2014

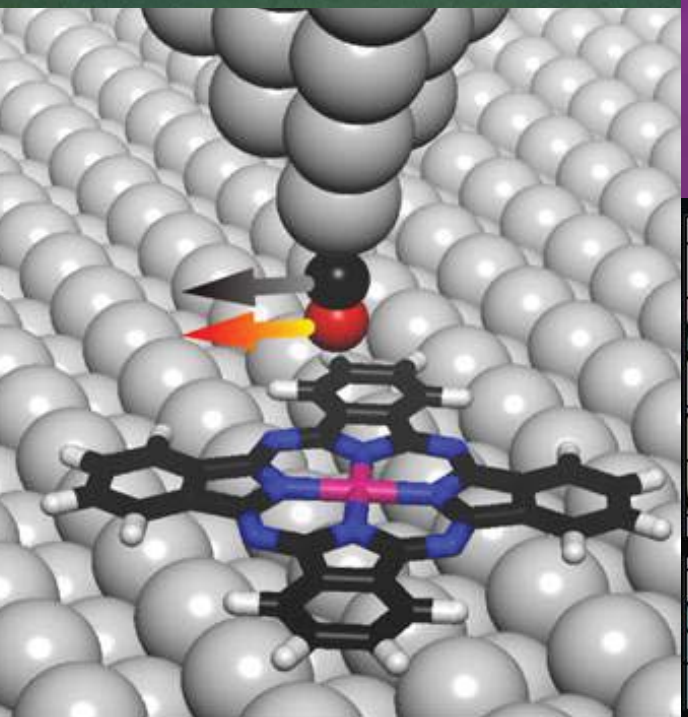

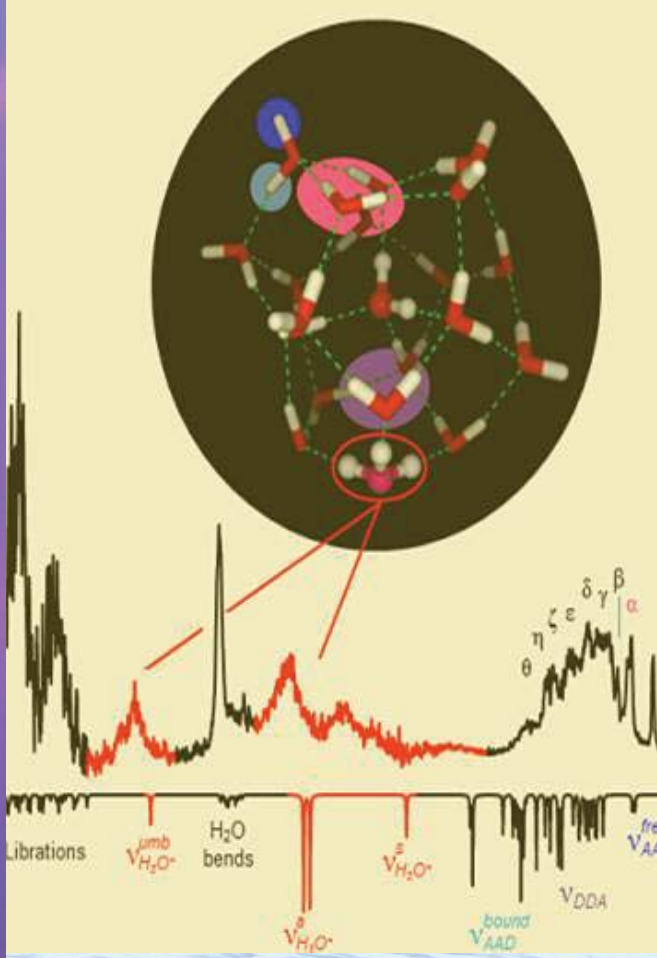

U.S. DEPARTMENT OF ENERGY | Office of Science
Office of Basic Energy Sciences
Chemical Sciences, Geosciences & Biosciences Division

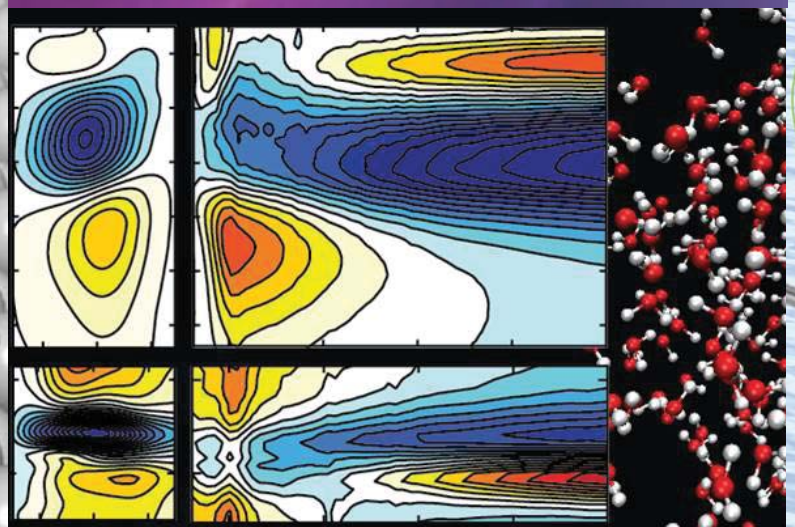

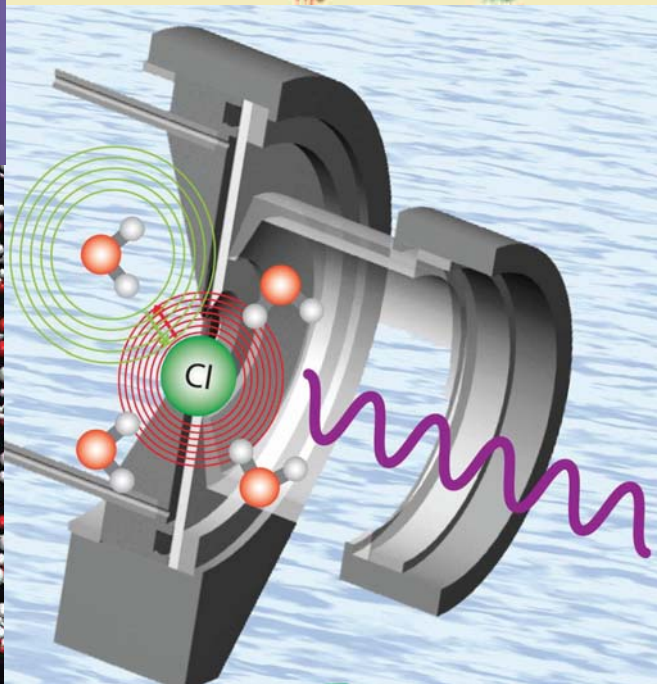

CPIMS 10

About the Cover Graphics

Weakly-bound species, such as Kr, CO_2, and N_2, were used to probe the photochemistry of chemisorbed oxygen on TiO_2(110). Ultraviolet irradiation of oxygen co-adsorbed with the probe species led to photon-stimulated desorption (PSD) of the most weakly-bound species, such as Kr. Without chemisorbed oxygen, the PSD yields of all the probes were very low. Surprisingly, photo-excitation of O_2 and oxygen adatoms resulted in desorption of the probe species due to collisions with neighboring co-adsorbates. To our knowledge, this is the first evidence for photo-activity of oxygen adatoms on TiO_2(110). The observations also provide a new tool for studying photochemical processes on surfaces.

N. G. Petrik and G. A. Kimmel, *Phys. Chem. Chem. Phys.* 2014, **DOI:**10.1039/c3cp54195a

Submitted by Greg A. Kimmel (Pacific Northwest National Laboratory)

A new and generally applicable technique based on the scanning tunneling microscope (STM) provides real space images of molecular structures. A tip terminated with a single carbon monoxide (CO) molecule was scanned over a single cobalt-phthalocyanine (CoPc) molecule adsorbed on Ag(110) surface at 600 mK while monitoring the hindered translational vibration of the CO. The variation in the vibrational intensity in the scan provides the contrast in the CoPc skeletal structure due to the CO molecule sensing the electrostatic potential inside the CoPc. Such images provide an understanding into the relation of structure and function of molecules.

C. Chiang, C. Xu, Z. Han and W. Ho, *Science* 2014, **DOI:**10.1126/science.1253405

Submitted by Wilson Ho (University of California, Irvine)

Using a new sub-70-femtosecond, broadband mid-infrared source, we performed two-dimensional infrared, transient absorption and polarization anisotropy spectroscopy of liquid water by exciting the OH stretching transition and characterizing the response from 1,350 cm^{-1} to 4,000 cm^{-1}. The two-dimensional infrared spectrum (left) and transient absorption spectrum (right) provide insight into the ultrafast dynamics. We find that the O–H stretching mode is delocalized over many water molecules and is mixed with low-frequency intermolecular modes. Such results change the way that molecular vibrations in water are perceived, which significantly impacts future discussion of aqueous chemical reactions.

K. Ramasesha, L. De Marco, A. Mandal, and A. Tokmakoff, *Nature Chemistry* 2013, **DOI:**10.1038/nchem.1757

Submitted by Andrei Tokmakoff (University of Chicago)

Cryogenic ion vibrational predissociation (CIVP) spectroscopy has been used to solve a long-standing puzzle regarding the vibrational signature of the proton defect in the "magic number" $H^+(H_2O)_{21}$ cluster ion. The new information was obtained by first slowly cooling the parent ion in a 10K RF ion trap, where weakly bound D_2 molecules were attached prior to vibrational excitation in a photofragmentation mass spectrometer. By combining the photon energy range accessible with table top and free electron lasers (Fritz Haber Institute, Asmis group), spectra were obtained from 200 to 4,000 cm^{-1}, thus providing an unprecedented spectroscopic view of an archetypal, three dimensional H-bonded water network.

J. A. Fournier, C. J. Johnson, C. T. Wolke, G. H. Weddle, A. B. Wolk, and M. A. Johnson, *Science* 2014, **DOI:**10.1126/science.1253788

Submitted by Mark Johnson (Yale University)

The existence of chloride-hydronium contact ion pairs even in moderate concentration hydrochloric acid (2.5 m) demonstrates that the counterions do not behave merely as spectators. Through comparison of recent extended X-ray absorption fine structure (EXAFS) measurements to state-of-the-art density functional theory (DFT) simulations, we are able to obtain a unique view into the molecular structure of medium-to-high concentrated electrolytes.

M.D. Baer, J.L. Fulton, M. Balasubramanian, G.K. Schenter, and C.J. Mundy, *Journal of Physical Chemistry B* 2014, **DOI:**10.1021/jp501091h

Submitted by Christopher Mundy, John Fulton, and Gregory Schenter (Pacific Northwest National Laboratory)

Program and Abstracts for

CPIMS 10

Tenth Research Meeting of the Condensed Phase and Interfacial Molecular Science (CPIMS) Program

Bolger Conference Center
Potomac, MD
October 19-22, 2014

U.S. DEPARTMENT OF ENERGY | Office of Science

Office of Basic Energy Sciences
Chemical Sciences, Geosciences & Biosciences Division

The research grants and contracts described in this document are supported by the U.S. DOE Office of Science, Office of Basic Energy Sciences, Chemical Sciences, Geosciences and Biosciences Division.

FOREWORD

This volume summarizes the scientific content of the Tenth Research Meeting on Condensed Phase and Interfacial Molecular Science (CPIMS) sponsored by the U. S. Department of Energy (DOE), Office of Basic Energy Sciences (BES). The research meeting is held for the DOE laboratory and university principal investigators within the BES CPIMS Program to facilitate scientific interchange among the PIs and to promote a sense of program awareness and identity.

This year's speakers are gratefully acknowledged for their investment of time and for their willingness to share their ideas with the meeting participants. The agenda for CPIMS 10 is nearly identical to that for CPIMS 9, which was cancelled because of the lapse in appropriations that took place in October of 2013. We acknowledge the extra effort of those speakers who agreed to create presentations for both CPIMS 10 and CPIMS 9. We also delight in the knowledge that a similar lapse in appropriations is unlikely to interrupt the CPIMS 10 meeting.

The abstracts in this book represent progress reports for each of the projects that receive support from the CPIMS program. Therefore, the book represents a snapshot in time of the scope of CPIMS-supported research. We thank Dawn Adin for her creative efforts in assembling this volume. A recent tradition is the use of the cover of this book to display research highlights from CPIMS investigators. This year, we have included five research highlights on the cover. These images were selected from highlights submitted by CPIMS investigators during the past two years. We thank the investigators for allowing us to place their images on the cover of this book, and we thank all CPIMS investigators who submitted research highlights. CPIMS Investigators are encouraged to submit highlight of their results; we will continue to receive these stories of success with great pride.

We are deeply indebted to the members of the scientific community who have contributed valuable time toward the review of proposals and programs. These thorough and thoughtful reviews are central to the continued vitality of the CPIMS Program. We appreciate the privilege of serving in the management of this research program. In carrying out these tasks, we learn from the achievements and share the excitement of the research of the many sponsored scientists and students whose work is summarized in the abstracts published on the following pages.

Special thanks are reserved for the staff of the Oak Ridge Institute for Science and Education, in particular, Connie Lansdon and Tim Ledford. We also thank Diane Marceau, Robin Felder, and Michaelene Kyler-Leon in the Chemical Sciences, Biosciences, and Geosciences Division for their indispensable behind-the-scenes efforts in support of the CPIMS program.

Gregory J. Fiechtner, Mark R. Pederson, and Jeffrey L. Krause
Chemical Sciences, Geosciences and Biosciences Division
Office of Basic Energy Sciences

Agenda

CPIMS 10

U.S. DEPARTMENT OF ENERGY | Office of Science

Office of Basic Energy Sciences
Chemical Sciences, Geosciences & Biosciences Division

Tenth Condensed Phase and Interfacial Molecular Science (CPIMS) Research Meeting

Sunday, October 19

3:00-6:00 pm	**** Registration ****
6:00 pm	**** Reception (No host, Pony Express Bar & Grill) ****
7:00 pm	**** Dinner (Osgood's Restaurant) ****

Monday, October 20

7:30 am **** Breakfast (Osgood's Restaurant) ****

All Presentations Held in Stained Glass Hall

8:30 am *Introductory Remarks*
Gregory J. Fiechtner, DOE Basic Energy Sciences

Session I Chair: **Cynthia J. Jenks**, Ames Laboratory

9:00 am *A New Approach for Studying Cobalt's Surface Chemistry with Cobalt Nanoparticles*
E. Charles H. Sykes, Tufts University

9:30 am *Complexity in Mechanisms for Zr Catalyzed Hydroamination Reactions*
Theresa L. Windus, Ames Laboratory

10:00 am *The Dissociative Chemisorption of Methane on Metal Surfaces: Mode-Selective Chemistry and the Effects of Lattice Motion*
Bret Jackson, University of Massachusetts, Amherst

10:30 am **** Break ****

Session II Chair: **William A. Tisdale**, Massachusetts Institute of Technology

11:00 am *The Role of Fast Charge Dynamics in Heterogeneous Catalysis*
Tanja Cuk, Lawrence Berkeley National Laboratory

11:30 am *Single-Molecule Interfacial Electron Transfer Dynamics*
H. Peter Lu, Bowling Green State University

12:00 noon *Dynamics of Electrons at Interfaces on Ultrafast Timescales as Applied to Electronic Materials*
Benjamin Caplins, Lawrence Berkeley National Laboratory

12:30 pm **** Lunch (Osgood's Restaurant) ****

1:30 pm–4:30 pm Free/Discussion Time

Session III Chair: **Wayne Hess**, Pacific Northwest National Laboratory

4:30 pm *Photo-Induced Electron Transfer in Nanometer-Sized Junctions*
Eric Potma, University of California, Irvine

5:00 pm *Recent Advances in Methods and Substrates for Molecular Scale Chemical Imaging*
Mark C. Hersam, Northwestern University

5:30 pm *Imaging Chemical Bond and Molecular Structure*
Wilson Ho, University of California, Irvine

6:00 pm **** Reception (no host, Pony Express Bar & Grill) ****

7:00 pm **** Dinner (Osgood's Restaurant) ****

Tuesday, October 21

7:30 am **** Breakfast (Osgood's Restaurant) ****

Session IV Chair: **Etienne Garand**, University of Wisconsin - Madison

8:30 am *Heterogeneous Free Radical Reactions on Droplets and Nanoparticles*
Kevin R. Wilson, Lawrence Berkeley National Laboratory

9:00 am *Structural Motifs in Ionic Liquids and the Hydrated Proton with Cryogenic Ion Vibrational Spectroscopy*
Mark Johnson, Yale University

9:30 am *Computational Studies of the Structure and Vibrational Spectra of $H^+(H_2O)_n^+$ Clusters and of the Dynamics of Proton-coupled Electron Transfer in Pyridine-Water Complexes*
Kenneth D. Jordan, University of Pittsburgh

10:00 am *Photodissociation Spectroscopy and Dynamics of Metal-Molecular Complexes*
Michael A. Duncan, University of Georgia

10:30 am **** Break ****

11:00 am *Special Session: Strategic Planning for the CPIMS Program*

11:30 am **** Lunch (Osgood's Restaurant) ****

12:30 pm–4:30 pm Free/Discussion Time

Session V Chair: **Andrei Tokmakoff**, University of Chicago

4:30 pm *New Forms of Potential Energy Functions Describing Intermolecular Interactions: From the Very Weak to the Very Strong*
Sotiris S. Xantheas, Pacific Northwest National Laboratory

5:00 pm *Dynamics Inside Nanoconfined Systems*
Michael D. Fayer, Stanford University

5:30 pm *X-Ray Spectroscopy of Aqueous Carbonic Acid*
Rich Saykally, Lawrence Berkeley National Laboratory

6:00 pm **** Reception (No Host, Pony Express Bar & Grill) ****

7:00 pm **** Dinner (Osgood's Restaurant) ****

Wednesday, October 22

7:30 am **** Breakfast (Osgood's Restaurant) ****

Session VI Chair: **Mark Spitler**, DOE Basic Energy Sciences

8:30 am *Combinations of Aromatic and Aliphatic Radiolysis*
Jay A. LaVerne, Notre Dame Radiation Laboratory

9:00 am *Geminate Recombination in Tetrahydrofuran*
John R. Miller, Brookhaven National Laboratory

9:30 am *Interfacial Chemistry between Gas-Phase Molecules and GaAs Surfaces Probed by Near-Ambient Pressure X-ray Photoelectron Spectroscopy*
Sylwia Ptasinska, Radiation Laboratory and Department of Physics, University of Notre Dame

10:00 am **** Break ****

10:30 am *Energetics of Nitric Oxide Reduction and Reactivity of the Nitroxyl Products*
Sergei Lymar, Brookhaven National Laboratory

11:00 am *Chemistry of Anion and Radical Species — From Clusters to Bulk Solution*
Marat Valiev, Pacific Northwest National Laboratory

11:30 am *Closing Remarks*
Gregory J. Fiechtner, DOE Basic Energy Sciences

12:00 noon **** Meeting Adjourns ****

Table of Contents

TABLE OF CONTENTS

Abstracts

Synchrotron, Laser & Mass Spectrometry based approaches to probe Surfaces, Interfaces and Clusters.

Musahid Ahmed
MS 6R-2100, 1 Cyclotron road, Chemical Sciences Division
Lawrence Berkeley National Laboratory, Berkeley, CA 94720
mahmed@lbl.gov

Program scope - Mass spectrometry coupled with synchrotron radiation, lasers and ambient ionization methods are applied to probe chemistry on surfaces, interfaces and clusters. The systems being investigated range from fundamental studies of proton and charge transfer in model systems which are theoretically tractable to complex chemical phenomenon in biological systems. Novel cluster studies with molecular beams provides insight to the chemical physics of nucleation. Ambient ionization methods (NanoDESI) are implemented to study molecules ranging from small organic compounds to complex bio-molecules from surfaces while lasers allow visualization of the self-assembly of nanoparticles at interfaces.

Recent progress –

Synchrotron Laser Desorption Post Ionization mass spectrometry allows characterization of the molecular properties of organic compounds such as melanin, lignin and soil organic matter. The understanding of the chemical composition of melanin remains limited, due to a paucity of direct measurements. Avian feathers have an unparalleled diversity of melanin-based color mirroring their complex chemistry. Synchrotron-based photoionization mass spectrometry in conjunction with statistical analysis is used to determine the chemical composition of melanin from samples of black, brown, grey and iridescent feathers. Our analyses suggest that black color in avian melanin originates from eumelanin (clusters of oxidized forms of DHI and DHICA). Brown color is composed mostly of pheomelanin (composed of oxidized versions of benzothiazine, benzothiazole, and isoquinolines) with also various contributions from eumelanin. Finally grey color is derived mostly from pheomelanic building blocks with minimal contributions from eumelanin, and isoquinoline derivatives. (*Liu et al. RSC Advances*)

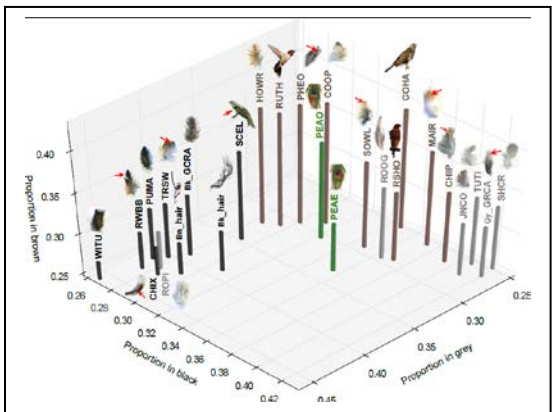

Figure 1: Peak probability contrasts (PPC) analysis projected onto three dimensions for black, brown, grey, and Peacock (green) feathers.

Differentiation of microbial species and strains in co-culture biofilms was obtained by multivariate analysis of laser desorption post-ionization mass spectra. (*Bharadwaj et al. Analyst*) Secondary Ion Mass Spectrometry (SIMS) in combination with FTIR spectroscopy was employed to study the gas plasma flux on endotoxin lipid A film and the deactivation behavior under relatively high O-radical flux exposure (10^{16} cm^{-2} s^{-1}) in an inductively coupled plasma (ICP) is compared with a much lower radical flux (10^{13} cm^{-2} s^{-1}) exposure in a vacuum beam system. This study shows that lipid A film deactivation is sensitive to the magnitude of reactive species flux. The extent of surface modification appears to be significantly different under low and high flux conditions and a chemical model was proposed to explain this effect. (*Chang et al. J. Phys. D*)

Nucleation is a phenomenon which is central to many interdisciplinary research areas such as aerosol physics, atmospheric chemistry, and material science. We have developed an experimental strategy for understanding the role of small ions or neutrals as a "seed" for nucleation phenomenon using in source ionization of molecular beams with tunable VUV synchrotron radiation. Methanol was chosen as a model system and by varying the distance between ionization and source, a new method of studying ion induced nucleation was enabled. The dominant distribution are protonated methanol clusters $(CH_3OH)_nH^+$),

followed by protonated methanol ($((CH_3OH)_n)(H_2O)H^+$) and protonated dimethyl ether ($((CH_3)_2O(CH_3OH)_nH^+$) clusters. Figure 2 shows the intensity distributions of these clusters at various distances (x = 15, 25, 35, 45 mm). The intensity distributions show signatures for both ion induced and neutral nucleation, e.g., a rapid drop followed by a plateau and can be qualitatively modelled by Thomson's liquid drop model. Furthermore a kinetic model was also employed to explain the ion distributions. A judicious combination of modelling and novel experimental design (a new quadruple ion guide and selector is being incorporated into the apparatus) should allow for a systematic study of nucleation and solvation in a variety of systems which will be theoretically tractable.

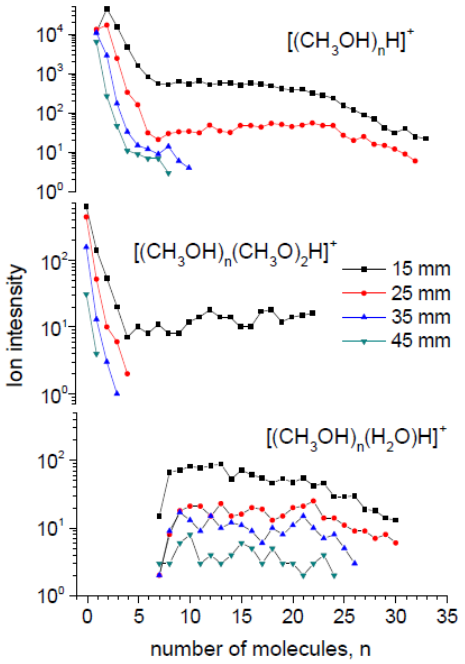

Figure 2: Ion Intensity distributions for various nozzle to ionization distances.

At present all the work described above is done in the static regime and the dynamics are mostly ascertained by theory. In an attempt to directly probe excited state dynamics of molecules and clusters using ultrafast lasers and synchrotron, we have recently measured the core level excitation (N- and O- edges) of 2-Nitrophenol in a velocity map imaging (VELMI) machine. This work is ongoing and a tunable OPA pumped by a 4 KHz femtosecond laser synchronized to X-rays will enable gas phase laser-synchrotron pump-probe experiments in the near future.

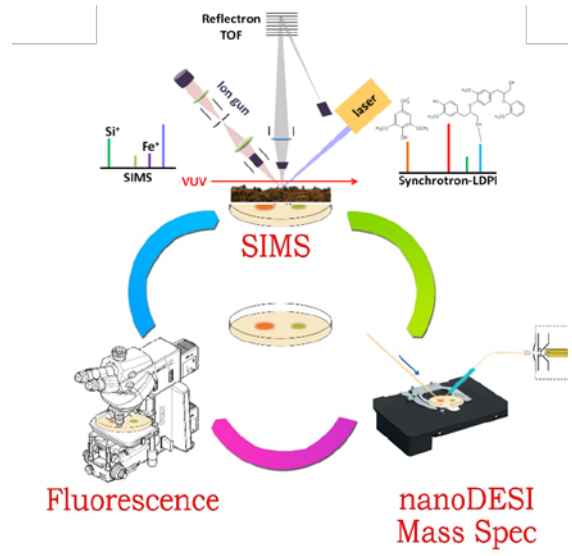

Figure 3: Correlated optical, fluorescence & mass spectrometry approaches to chemically image surfaces.

Future plans-

An experimental platform, Nanospray Desorption Electrospray Ionization (nanoDESI) is being developed to interrogate chemical transformations on surfaces. Derived from its predecessors Electrospray Ionization (ESI) and Desorption-ESI (DESI), nanoDESI is capable of performing 2D mass spectrometry imaging under ambient conditions, adding an additional dimension to ESI and providing better spatial resolution and collection efficiency compared to DESI. This approach facilitates work with nanogram-sized samples, enabling direct analysis of small molecules as well as large molecules off surfaces, without any sample preparation. This technique will be applied to probe reactive surfaces and interfaces. In addition, nanoDESI-MS is being combined with fluorescence microscopy to acquire multi-dimensional data, to provide insights into sample components, distribution and reaction mechanisms under ambient and aqueous conditions. High resolution ion beam based secondary ion mass spectrometry imaging is also part of the experimental suite and a LabVIEW based interface is being implemented to provide a seamless integration of scales for various modes of chemical imaging. (Figure 3) Initial experiments will focus on probing interfacial chemical transformations of hydrocarbons on catalytic surfaces.

Plasmon-induced hot electron generation at the metal-semiconductor interface of nanostructured materials is a path for solar energy conversion in photovoltaic and photocatalytic devices. Silver or gold

nanoparticles (NP) dispersed in TiO_2 are particularly efficient for such applications. Recently it has been demonstrated the self-organized growth of silver nanoparticles in TiO_2 films occurs upon visible laser exposure. This self-arrangement of metallic nanoparticles within TiO_2 layers allows the films to act as light concentrators by diffraction-induced excitation of guided modes within TiO_2. This effect maximizes light interaction with silver NPs and could improve the enhancement of optical, physical or chemical effects due to plasmon resonances. Our work aims both at better characterizing the mechanisms leading to the self-arrangement of metallic NPs under laser exposure within the TiO_2 films using diffraction and time resolved Raman spectroscopy methods.

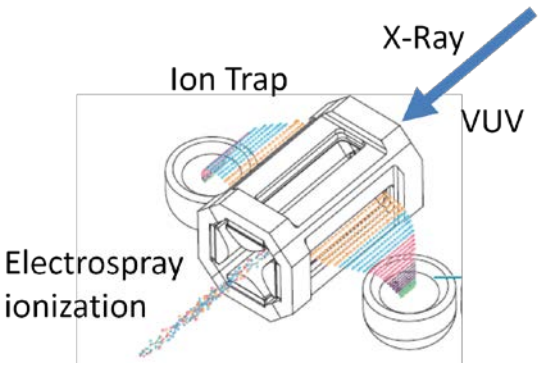

Figure 4: Ion trap to be implemented at a synchrotron for X-ray absorption and VUV photofragmentation action spectroscopy

A crucial aspect of solution chemistry is the interaction of metal ions in their various charge states and coordination environment surrounded by solvents. Motivated to attain a comprehensive grasp about the structure-property relationships, several spectroscopic techniques using synchrotron radiation have been employed to study size-selected metal-ligand complexes in the gas phase. However, soft X-ray Absorption Spectroscopy (XAS) on these systems remains largely unexplored because of low ion-densities. The advantage of XAS over other techniques is that it probes local electronic structure of a metal or a particular atom in the ligand, which in turn reveals precise effects of microsolvation. On the other hand, VUV photoionization has opened up an unprecedented method of tandem mass spectroscopy via clean ionization/fragmentation of the precursor ions providing important information about the solvent structures and coordination environment around a metal center. We propose to substantially advance the molecular level understanding of ion solvation by both XAS and VUV studies. A commercial mass spectrometer suitable for ion trapping and ESI experiments at the ALS will be acquired in the very near future to perform these experiments. (Figure 4)

Two classes of molecules will be explored to study intermolecular and intramolecular interactions and upon microsolvation will lead to solution chemistry. Metal ions can bind in different ligand sites in flavin molecule – on reactive C=O sites, nitrogen lone pairs, or can form π-complexes with aromatic rings. Since near edge (C, N, or O) XAS is a powerful technique to probe local electronic structures and bonding, XAS would show a shift in absorption spectra as a result of complexation. Spectroscopic studies of $(ML_n)^{x+}$ complexes will also allow one to generate a seamless continuum from gas phase to solution via increasing cluster size.

A second focus is to use mass spectrometry with synchrotron radiation to develop technologies and smart nano-structured catalysts to achieve hydrocarbon transformations. We propose a multi-component detection of homogeneous and heterogeneous catalytic hydrocarbon transformations in micro-droplet reactors using synchrotron X-rays and mass spectrometry. Using microfluidic and droplet delivery methods, reactants in solution phase will be delivered through a silica capillary tube to a detection zone where a liquid droplet of 20-150 μm diameters (i.e. micro-droplet) will form and will act as a reactor where reactions will take place. The micro droplet will be continuously illuminated with X-ray beams and the chemical transients will be monitored via X-ray fluorescence, and absorption while simultaneously monitoring the mass spectra. XANES spectra of catalyst compounds can be monitored at relevant timescales (seconds to minutes) to obtain oxidation state of organometallic compounds while mass spectrometry will follow chemical change. The successful demonstration of studying *operando* structural (i.e. mass spectral analysis) and chemical (i.e. XANES) evaluation of liquid catalytic reactions in a novel micro-droplet reactor has enormous implications for studies of well-defined and carefully tuned catalyst materials (e.g. single-site organometallic compounds, clusters and nanoparticles)

Papers citing CPIMS-DOE support. (2013 to present)

S. Y. Liu, M. D. Shawkey, D. Parkinson, T. P. Troy & M. Ahmed, *"Elucidation of the chemical composition of avian melanin"* RSC Advances (In press)

H-W. Chang, C-C. Hsu, M. Ahmed, S.Y. Liu, Y. Fang, J. Soeg, G. Oehrlein, D. Graves, *"Plasma Flux Dependent Lipid A Deactivation"*, J. Phys. D: Appl. Phys., (2014) **47** 224015

M. Perera, K. M. Roenitz, R. B. Metz, O. Kostko, and M. Ahmed, *"VUV photoionization measurements and electronic structure calculations of the ionization energies of gas-phase tantalum oxides TaOx (x=3-6)."* J. Spectroscopy and Dynamics. (2014), **4**, 1

C. Bhardwaj, Y. Cui, T. Hofstetter, S. Y. Liu, H. C. Bernstein, R. Carlson, M. Ahmed, and L. Hanley. *"Differentiation of Microbial Species and Strains in Coculture Biofilms by Multivariate Analysis of Laser Desorption Postionization Mass Spectra*." Analyst (2013), **138**, 6844

F. Bell, Q.N. Ruan, A. Golan, P. R. Horn, M. Ahmed, S. R. Leone, and M. Head-Gordon. *"Dissociative Photoionization of Glycerol and its Dimer Occurs predominantly via a ternary hydrogen bonded ion-molecule complex,"* J. Am. Chem. Soc. **135**, 14229 (2013)

K. Khistyaev, A. Golan, K.B. Bravaya, N. Orms, A. I. Krylov, and M. Ahmed. *"Proton Transfer in Nucleobases is Mediated by Water"*, J. Phys. Chem. A 117, 6789 (2013)

S-Y. Liu, M. Kleber, L. K. Takahashi, P. Nico, M. Keiluweit, and M. Ahmed. *"Synchrotron based mass spectrometry to investigate the molecular properties of mineral-organic associations,"* Anal. Chem. **85**, 6100 (2013)

M. Perera, R. B. Metz, O. Kostko, and M. Ahmed, *"Vacuum Ultraviolet Photoionization Studies of $PtCH_2$ and H-Pt-CH_3: A Potential Energy Surface for the Pt + CH_4 reaction.*" Angew. Chem. Int. Ed. **125**, 922 (2013)

Model Catalysis by Size-Selected Cluster Deposition

PI: Scott L. Anderson
Chemistry Department, University of Utah
315 S. 1400 E. Rm 2020
Salt Lake City, UT 84112
anderson@chem.utah.edu

Program Scope

The goal of our research is to explore correlations between supported cluster size, electronic and morphological structure, the distributions of reactant binding sites, and catalytic activity, for model catalysts prepared using size-selected metal cluster deposition. The work to date has focused on catalysts with catalytically active metal clusters deposited on metal oxide supports, and on aqueous electrocatalysis by metal clusters on glassy carbon and indium tin oxide electrodes.

The experimental setup is quite flexible. The instrument has a mass-selecting ion deposition beamline fed by a laser vaporization source that produces high fluxes at low deposition energies (~10^9 Pd_{10}/sec in a 2 mm diameter spot at 1 eV/atom, for example). Typical samples with 0.1 ML-equivalent of metal, deposited in the form of M_n^+ can be prepared in 2 to 5 minutes, and our analysis methods are also quite fast. Speed is important, because even in UHV these samples are highly efficient at collecting adventitious contaminants, due to substrate-mediated adsorption. Sample morphology is probed by low energy He^+ ion scattering (ISS), electronic structure is probed by x-ray and UV photoelectron spectroscopy and ion neutralization spectroscopy (XPS, UPS, INS), and reactivity is studied using a differentially pumped mass spectrometer surrounded by a cluster of pulsed and cw gas inlets that can be used to dose the sample while various temperature programs are executed.

The main UHV analysis chamber has a port in the bottom, equipped with a gate valve and a triple differential seal. One of several interchangeable antechambers with their own pumping systems can be connected here, and when the sample is positioned in the antechamber is it isolated from the main UHV system. This antechamber is used for high pressure procedures such as alumina film growth or *in situ* electrochemical studies, and also as a load-lock.

Recent Progress

Electronic Structure - Activity Correlations under UHV conditions

Following on our earlier demonstration(*1*) of a one-to-one anti-correlation between the binding energy of metal core orbitals, and the activity for CO oxidation of $Pd_n/TiO_2(110)$, we examined similar behavior for Pd_n/alumina/Ta(110)(*2*) and Pd_n/alumina/Re(0001).(*3*) Activity was measured as a function of alumina thickness in the 1 to 10 nm range, with the result that activity became thickness-independent at about 4 nm. The Pd_n on alumina/Ta(110) were found to highly efficient CO oxidation catalysts under the conditions studied (10 times more efficient than Pd_n/TiO_2), and as a result, the activity was not found to be strongly dependent on Pd_n size. Nonetheless, the 25% size-dependent variation in activity was quite nicely anticorrelated with the Pd 3d binding energy. These studies also examined Pd_n morphology and how it changed after reaction, and used UPS to look at correlations between the core level binding energies and the energy of the top of the metal valence band. Because these have appeared in print, the balance of the abstract will focus on newer work.

Electrochemistry studies: Several years ago we did the first *in situ* electrochemistry study over size-selected clusters, without air exposure. The focus was on oxygen reduction in acidic electrolyte over Pt_n deposited on glassy carbon.(*4*) Air exposure was found to passivate the samples, and for such small clusters, it was not possible to remove adventitious adsorbates by electrochemical cleaning, as is typically done in electrochemistry work. The conditions studied were 0.1 M $HClO_4$, either O_2-saturated or O_2-free, with the goal of studying the oxygen reduction reaction (ORR). It was found that some clusters (7, 10, 11 atoms) showed normal looking ORR activity, but most of the small clusters showed, instead, very high activity for carbon oxidation by water. This reaction is a well known problem for carbon-supported electrocatalysts, but normally carbon oxidation is negligible except at high potentials (E > ~1.2 V vs. NHE). For the very small clusters, however, carbon oxidation was found to have almost no overpotential,

generating 100s of mA/cm^2 even at potentials as low as 0.3 V, and burning visible holes into the electrode. As shown in Figure 1, one of the really interesting aspects of this chemistry was that the efficiency of the Pt_n as carbon oxidation catalysts is anti-correlated with the Pt 4f binding energy, measured by XPS after cluster deposition.

Several changes were made in the past year to enable more detailed electrochemical work. A new, three compartment electrochemical cell was developed, along with a new antechamber to house it. The other change was to switch to a non-oxidizable electrode substrate (indium tin oxide EOR activity is found to vary strongly (factor of ten) and non-monotonically with Pt_n cluster size. The EOR reaction has complex cyclic voltammograms (CVs), determined by potential-dependent competition between various ethanol reaction pathways and poisoning of the surface by species such as oxide, CO, and acetate. There are three peaks associated with EOR under the conditions studied (0.1 M $HClO_4$ with 1 vol.% ethanol), and the samples also catalyze HER at ~0.0 V, and the oxygen evolution reaction (OER) at potentials over ~1.5 V. The ITO substrates are inert in the potential range of interest for EOR.

Fig. 2 shows CVs for select Pt_n/ITO under EOR conditions. It is obvious that the EOR peak intensities are strongly dependent on deposited Pt_n size, with maximum activity for Pt_4 and Pt_{10}, and minimum activity for Pt_1 and Pt_7-Pt_8. For the most reactive sizes, the activity per gram Pt is roughtly an order of magnitude higher than that for a conventional electrode with ~5 – 10 nm Pt particles. Interestingly, even though the peak currents vary with size by a factor of 5 to 10, there is little variation in the potential dependence of the EOR activity. It turns out that the Pt 4d BEs are also strong size-dependent, and the variations in activity are one-to-one anti-correlated with the 4d BE.

This anticorrelation, and those mentioned earlier, suggest that clusters that are in electron-rich environments are highly active oxidation catalysts, while electron-poor clusters have low activity. It may seem counterintuitive that being electron rich should enhance activity for oxidation catalysis, which

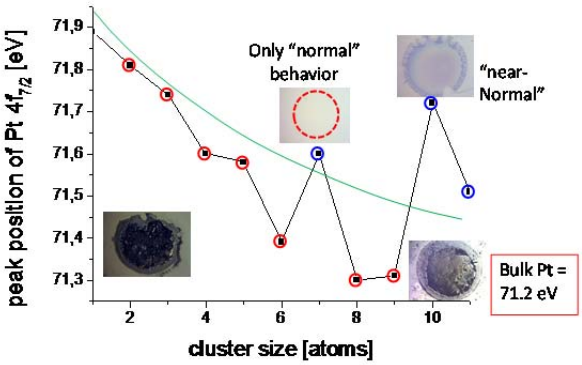

Fig. 1. Pt $4f_{7/2}$ BEs for Pt_n/glassy carbon. Those with high BEs (blue) do not catalyze carbon oxidation. Those with low BEs do.

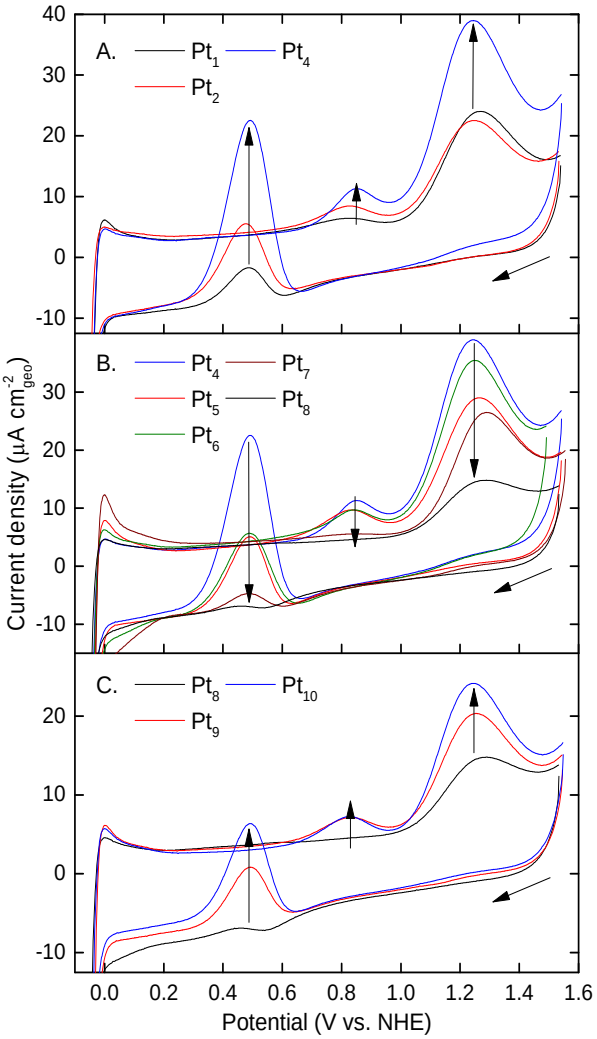

Fig. 2. CVs for Pt_n/ITO (n = 1, 2, 4-10)

involves transfer of electrons to the Pt_n electrodes. These reactions all involve various CH, OH, and OO bond activation processes, however, thus the electron-rich clusters may have high activity because they are able to transfer electrons to antibonding orbitals, weakening the bonds.

Future plans

The focus of proposed future work will be on relatively simple electrochemical systems such as EOR, ORR, CO_2 reduction, and water splitting. We are interested in looking at other metals, possibly including small alloy clusters, and also at supports such as HOPG. The work will combine *in situ* electrochemistry studies with complementary UHV surface science studies relating to the electrochemical systems. For example, in reactions like EOR or ORR, it would be very useful to understand how the binding to the clusters and substrate, of various reactant, intermediate, and product molecules, varies with cluster size. The work will use the existing cluster deposition instrument, and the electrochemical antechamber, however, we have learned a few tricks that should improve the precision and repeatability of the experiment significantly, and will construct an improved electrochemical cell and mounting system to implement them.

References Cited

1. W. E. Kaden, T. Wu, W. A. Kunkel, S. L. Anderson, Electronic Structure Controls Reactivity of Size-Selected Pd Clusters Adsorbed on TiO2 Surfaces. *Science* **326**, 826-829 (2009)10.1126/science.1180297).
2. M. D. Kane, F. S. Roberts, S. L. Anderson, Alumina support and Pdn cluster size effects on activity of Pdn for catalytic oxidation of CO. *Faraday Disc.* **162**, 323 - 340 (2013).
3. M. D. Kane, F. S. Roberts, S. L. Anderson, Mass-selected supported cluster catalysts: Size effects on CO oxidation activity, electronic structure, and thermal stability of Pd_n/alumina ($n \leq 30$) model catalysts. *International Journal of Mass Spectrometry* **370**, 1-15 (2014)10.1016/j.ijms.2014.06.018 and see also 10.1016/j.ijms.2014.07.044).
4. S. Proch, M. Wirth, H. S. White, S. L. Anderson, Strong Effects of Cluster Size and Air Exposure on Oxygen Reduction and Carbon Oxidation Electrocatalysis by Size-Selected Pt_n ($n \leq 11$) on Glassy Carbon Electrodes. *J. Am. Chem. Soc.* **135**, 3073−3086 (2013)10.1021/ja309868z).

Recent Publications acknowledging DOE support

"Size-dependent oxidation of Pd_n ($n \leq 13$) on alumina/NiAl(110): Correlation with Pd core level binding energies." Tianpin Wu, William E. Kaden, William A. Kunkel, and Scott L. Anderson, Surf. Sci. 603 (2009) 2764-77.

"Electronic Structure Controls Reactivity of Size-Selected Pd Clusters Adsorbed on TiO_2 Surfaces", William E. Kaden, Tianpin Wu, William A. Kunkel, Scott L. Anderson, Science. 326 (2009) 826 - 9.

"CO Adsorption and Desorption on Size-Selected Pd_n/TiO_2 Model Catalysts: Size Dependence of Binding Sites and Energies, and Support-Mediated Adsorption" William E. Kaden, William A. Kunkel, F. Sloan Roberts, Matthew Kane and Scott L. Anderson, J. Chem. Phys. 136 (2012) 204705 12 pages, doi: 10.1063/1.4721625

"Strong effects of cluster size and air exposure on oxygen reduction and carbon oxidation electrocatalysis by size-selected Pt_n ($n \leq 11$) on glassy carbon electrodes", Sebastian Proch, Mark Wirth, Henry S. White, and Scott L. Anderson, J. Am. Chem. Soc. 135 (2013) 3073−3086, DOI: 10.1021/ja309868z

"Alumina support and Pd_n cluster size effects on activity of Pd_n for catalytic oxidation of CO", Matthew D. Kane, R. Sloan Roberts, and Scott L. Anderson, Faraday Disc., 162 (2013) 323 - 340, DOI: 10.1039/c3fd20151a

"Mass-selected supported cluster catalysts: Size effects on CO oxidation activity, electronic structure, and thermal stability of Pd_n/alumina ($n \leq 30$) model catalysts." Matthew D. Kane, R. Sloan Roberts, and Scott L. Anderson International Journal of Mass Spectrometry 370 (2014) 1-15, DOI: 10.1016/j.ijms.2014.06.018 and see also 10.1016/j.ijms.2014.07.044).

FUNDAMENTAL ADVANCES IN RADIATION CHEMISTRY

Principal Investigators:

DM Bartels (bartels.5@nd.edu), I Carmichael, DM Chipman, I Janik, JA LaVerne, S Ptasińska
Notre Dame Radiation Laboratory, University of Notre Dame, Notre Dame, IN 46556

SCOPE

Research in fundamental advances in radiation chemistry is organized around two themes. First, energy deposition and transport seeks to describe how energetic charged particles and photons interact with matter to produce tracks of highly reactive transients, whose recombination and escape ultimately determine the chemical effect of the impinging radiation. The work described in this part is focused on fundamental problems specific to the action of ionizing radiation. Particular projects include measurement of radiolytic product yields in low temperature aqueous ices, experimental study and theoretical treatment of the VUV spectrum of water up to supercritical conditions, investigation of spur and track recombination and radiolytic yields in aromatic hydrocarbon liquids and the determination of recombination and yields in various supercritical fluids. The second thrust deals with structure, properties and reactions of radicals in condensed phases. Challenges being addressed include the experimental and theoretical investigation of solvated electron reaction rates, measurement of radical reaction rates as a function of density in supercritical fluids, theoretical characterization of free radical structure and solvation, and time-resolved resonance Raman investigation of free radical transients.

PROGRESS AND PLANS

Quantum diffusion of hydrogen isotopes was investigated in water using a pulse radiolysis/time-resolved pulsed EPR technique. Free induction decays of the hydrogen atom and of the deuterium atom were measured in the presence of paramagnetic (triplet) Ni^{2+} ions. Encounters of the atomic species with Ni^{2+} causes spin relaxation by the spin exchange mechanism. This process is expected to be purely "diffusion-limited", and so the rate constant and activation energy of spin relaxation are expected to reflect the diffusion of the atomic species in water. The same information can be obtained for the light muonium isotope (formed from a positive muon and electron) in a muon spin resonance experiment. Collaboration with workers at Paul Scherrer Institute in Switzerland produced data for diffusion of Mu, H, and D atoms all in 90% D_2O. The muonium was found to diffuse 40% faster than H even though its mass is only 0.11amu. H diffusion was found to be 10% faster than D atom. Obviously the diffusion is limited by the water fluid and does not scale by square root of the mass as it would in the gas phase. Recent ring polymer molecular dynamics (RPMD) calculations of Manolopoulos and coworkers on quantum diffusion predict that muonium should actually diffuse slower than H due to its larger De Broglie wavelength. (Their calculation of the isotope effect for H and D atoms is exactly correct.) RPMD calculations are currently being carried out in our laboratory to investigate whether quantized water librational motions are responsible for counteracting the larger effective "size" of the muonium.

The solvation structure of the hydrated electron has been the subject of debate since its discovery. For many years a "cavity model" produced by a one-electron pseudopotential in SPC water MD simulations has been broadly accepted as a correct structure. Several years ago Larson, Glover and Schwartz produced an improved pseudopotential and much to their surprise obtained a very different solvation structure. Rather than producing a cavity, the water became more dense in the region of the electron. This LGS model produced much controversy, but

Schwartz and coworkers have shown that their model is in substantial agreement with experiments (Raman, optical absorption vs. temperature, optical hole burning) where the traditional cavity model calculation fails. Detractors of the LGS model note that it must predict a zero or negative partial molar volume, whereas a laser photoacoustic experiment has produced a positive (27 cc/mole) number for this quantity. The partial molar volume is most reliably measured by the pressure effect on an equilibrium constant. Consequently we have used pulse radiolysis and optical absorption to investigate the equilibrium $(e^-)_{aq} + NH_4^+ \Leftrightarrow H + NH_3$. At Notre Dame we have checked the pressure effect on the equilibrium level of $(e^-)_{aq}$ up to 400 bar. There was no measurable change. With the S/N level available we could certainly have seen a 50% change in the equilibrium constant. Using the known partial molar volumes of the other species (assuming H and H_2 are virtually identical), this allows us to conclude that the electron partial molar volume is greater than zero, but less than 60 cc/mole. Presently collaborators in Paris are using a higher pressure cell to measure the equilibrium up to 4000 bar, but we have no reason to doubt the accuracy of the existing laser photoacoustic measurement. Consequently we reject BOTH the new LGS model and the earlier cavity models as being inconsistent with experiments. We are developing a RPMD method to calculate the partial molar volume of the pseudopotential models.

Our efforts to measure deep UV time resolved resonance Raman (TRRR) spectra of simple inorganic transients in water aims to address both the structure of radicals in water as well as the UV spectral assignments. Attempts to record TRRR spectra of hyponitrite radical ($N_2O_2^-$) and azide radical (N_3) in water were unsuccessful. The preliminary findings suggest that the identity of the transients absorbing at 277nm and 280nm might have been mistakenly assigned to N_3 and $N_2O_2^-$ in the past. In the case of CO_2^- radical anion TRRR measurements confirmed the existing UV spectral assignment. This important intermediate has been extensively studied in rare gas matrices and characterized by infrared spectroscopy. It is reported that even one water molecule is sufficient to prevent auto-detachment of an electron from otherwise metastable bent CO_2^- monomer anion lying 0.6 eV above the linear CO_2 molecule and a free electron. The Raman spectrum of aqueous CO_2^- radical in the range of 800-2800 cm^{-1} consisted of only a single strong band at 1297cm^{-1}. No overtone or combination bands were apparent. No change in the spectrum was observed when CO_2^- radicals ware produced in D_2O. The observed single band can be readily assigned to the fundamental symmetric C-O stretch in CO_2^- as the measured isotopic shift (23 cm^{-1}) for $^{13}CO_2^-$ corresponds very well to the shift predicted by DFT structural calculations that we carried out for $CO_2^-(H_2O)_n$ clusters (for $n \geq 2$). The surprisingly simple aqueous CO_2^- TRRR spectrum implies its structure in bulk water differs considerably from the gas phase or low temperature matrices. The lack of any overtone in the spectrum suggests a very low energy barrier for the electron detachment process. The lack of any bending signatures implies a more linear structure of CO_2^- in the bulk water.

Previous studies of radiation chemistry induced by positive ions have shown that a variety of aromatic compounds have a significant increase in H_2 yields with increasing LET. Recent research focused on examining the H_2 yields with combinations of aliphatic and aromatic compounds or entities. The production of H_2 increases with chain length in the gamma radiolysis of benzene, toluene, ethylbenzene, butylbenzene and hexyl benzene. Increasing the chain length means a larger fraction of the molecule is aliphatic, and aliphatic compounds can have H_2 yields that are orders of magnitude greater than benzene. However, variation of the type of radiation from gamma rays to helium ions shows the same characteristic increase in H_2 for all these compounds. Clearly, the aromatic entity is the dominant factor in the production of H_2 from high

LET irradiation. Further experiments will try to discern the initial energy deposition processes by examining deuterated compounds and examining the isotopic hydrogen production. One of the goals is to determine if energy transfer is predominantly intermolecular or intramolecular.

The main focus of recent plasma investigations was on maximizing the catalytic effect of an atmospheric pressure plasma jet (APPJ), a new low-energy radiation source. Two different materials, semiconductors (e.g., Si) and bio-macromolecules (e.g., deoxyribonucleic acid) were exposed to plasma species in order to probe the efficiency and reactivity of a helium APPJ. To characterize the reactive plasma species generated in the APPJ, optical emission spectra were taken along the APPJ axis. The emission bands recorded for the helium APPJ launched in the open air showed contributions from several species with excited molecular nitrogen and ionic nitrogen bands being the most dominant bands. The presence of these nitrogen-containing species is caused by high-energy states of molecular or ionized nitrogen molecules, excited by discharging electrons, interacting with the surrounding air. A hydroxyl radical emission band, atomic oxygen and the excited singlet state of molecular oxygen were also detected and these are the key reactive species involved during treatment of different materials. Additionally, in some APPJ treatments, a helium admixture with nitrogen-based gas (e.g., N_2, NO, N_2O and NH_3) was employed. When the APPJ was used for silicon wafer surface treatment, the growth of ultra-thin films of $Si_xO_yN_z$ was monitored by recording core-level photoelectron spectra by X-ray Photoelectron Spectroscopy. A short duration APPJ treatment was sufficient to fabricate SiO_xN_y films with a few nanometer thickness even at room temperature. A Si substrate exposed to an APPJ generated in a mixture of He/NH_3 resulted in the most efficient growth of SiO_xN_y films, indicated by the presence of the strongest N 1s XPS signal among all studied gas mixtures. Moreover, the N 1s spectra exhibited two major characteristics of chemical bonding structures attributable to nitrogen bonded to three silicon surface atoms, $N–(Si)_3$, and nitrogen bonded to two silicon surface atoms and one oxygen atom, $(Si)_2–N–O$. When the APPJ was used on bio-macromolecules, different conformers were detected by agarose gel electrophoresis. The appearance and amount of these conformers indicated different levels and type of damage induced to biomolecules mainly by reactive oxygen species.

ODEPR and MARY spectroscopies, originally developed in Novosibirsk in the 1980s, are spin-sensitive techniques based on magnetically sensitive fluorescence from the recombination of geminate radical ion pairs in irradiated solutions. Using state-of-the art components, a new version of an ODEPR/MARY spectrometer has been designed and built at the NDRL, producing a greatly improved signal-to-noise ratio. This apparatus has allowed us to obtain previously-inaccessible, room-temperature, liquid-phase EPR and MARY spectra for a large number of synthetically-important fluoroalkylarene radical anions. Supporting quantum chemical calculations show that these systems exhibit a wide range of radical anion stabilities, often exhibiting unusual electronic structures (pseudo Jahn-Teller effects) and geometries (structural nonrigidity and pseudorotation).

PUBLICATIONS WITH BES SUPPORT SINCE 2012

do Couto P.C.; Chipman D.M. *J. Chem. Phys.* **2012**, **137**, 184301 Insights into the ultraviolet spectrum of liquid water from model calculations: the different roles of donor and acceptor hydrogen bonds in water pentamers.

El Omar A.K.; Schmidhammer U.; Rousseau B.; Laverne J.A.; Mostafavi M. *J. Phys. Chem. A* **2012**, **116**, 11509-18 Competition reactions of $H_2O^{\bullet+}$ radical in concentrated Cl^- aqueous solutions: picosecond pulse radiolysis study.

Jheeta S.; Ptasinska S.; Sivaraman B.; Mason N.J. *Chem. Phys. Lett.* **2012**, **543**, 208-12 The irradiation of 1:1 mixture of ammonia:carbon dioxide ice at 30 K using 1 keV electrons.

LaVerne J.; Baidak A. *Radiat. Phys. Chem.* **2012**, **81**, 1287-90 Track effects in the radiolysis of aromatic liquids.

Patterson L.K.; Mazière J.-C.; Bartels D.M.; Hug G.L.; Santus R.; Morlière P. *Amino Acids* **2012**, **42**, 1269-75 Evidence for a slow and oxygen-insensitive intra-molecular long range electron transfer from tyrosine residues to the semi-oxidized tryptophan 214 in human serum albumin: Its inhibition by bound copper(II).

Chipman D.M. *J. Phys. Chem. B* **2013**, **117**, 5148-55 Water from ambient to supercritical conditions with the AMOEBA model.

El Omar A.K.; Schmidhammer U.; Balcerzyk A.; LaVerne J.; Mostafavi M. *J. Phys Chem. A.* **2013**, **117**, 2287-93 Spur reactions observed by picosecond pulse radiolysis in highly concentrated bromide aqueous solutions.

Janik I.; Marin T.W. *Nucl. Instr. Meth. Phys. Res. A* **2013**, **698**, 44-8 A vacuum ultraviolet filtering monochromator for synchrotron-based spectroscopy.

Janik I.; Tripathi G.N.R. *J. Chem. Phys* **2013**, **139**, 014302 The nature of the superoxide radical anion in water.

Janik I.; Tripathi G.N.R. *J. Chem. Phys* **2013**, **138**, 44506. The early events in the OH radical oxidation of dimethyl sulfide in water.

Jheeta S.; Domaracka A.; Ptasinska S.; Sivaraman B.; Mason N.J. *Chem. Phys. Lett.* **2013**, **556**, 359-64 The irradiation of pure CH_3OH and 1:1 mixture of NH_3:CH_3OH ices at 30 K using low energy electrons.

Klas M.; Ptasinska S. *Plasma Sources Sci. Technol.* **2013**, **22**, 025013 Characteristics of N_2 and N_2/O_2 atmospheric pressure glow discharges.

Mozumder A.; Wojcik M. *Radiat. Phys. Chem.* **2013**, **85**, 167-72 Initial electron-ion distance distribution in irradiated high-mobility liquids: Application of the metropolis method.

Nuzhdin K.; Bartels D.M. *J. Chem. Phys* **2013**, **138**, 124503-1-8 Hyperfine coupling of the hydrogen atom in high temperature water.

Kosno K.; Janik I.; Celuch M.; Mirkowski J.; Kisała, J.; Pogocki, D. *Isr. J. Chem.* **2014**, **54**, 302-315 The role of pH in the mechanism of •OH radical induced oxidation of nicotine.

Han X., Cantrell W.A., Escobar E.E., Ptasinska S. *Eur. Phys. J **2014, D68,** 46.* Plasmid DNA Damage Induced by Helium Atmospheric Pressure Plasma Jet.

Zhang X. , Ptasinska S. . *J. Phys. D.* **2014**, **47,** 145202. Growth of Silicon Oxynitride Films by Atmospheric Pressure Plasma Jet.

SOFT X-RAY SPECTROSCOPY AND MICROSCOPY OF INTERFACES UNDER *IN SITU* CONDITIONS

Hendrik Bluhm, Mary K. Gilles, David K. Shuh,
Chemical Sciences Division, Lawrence Berkeley National Laboratory, Berkeley, CA 94720
HBluhm@lbl.gov; MKGilles@lbl.gov; DKShuh@lbl.gov

I. Program Scope

The scientific program at the Molecular Environmental Sciences Beamline focuses on the molecular level investigation of interfaces under operating conditions, which are essential for a fundamental understanding of heterogeneous reactions at solid/vapor, solid/liquid, and liquid vapor interfaces. The high surface sensitivity of ambient pressure X-ray photoelectron spectroscopy (APXPS), combined with tailored *in situ* cells, allows the correlation of the surface chemistry of a solid or liquid with other reaction parameters (e.g., yield, conversion) for a wide variety of pressing problems, such as ion segregation at liquid surfaces (John Hemminger, U.C. Irvine), the heterogeneous chemistry of fuel cell electrodes (Anthony McDaniel, Sandia), and ultrafast charge transfer across interfaces (Oliver Gessner, CSD). The scanning transmission X-ray microscope (STXM) provides spatially resolved molecular information on materials important for energy sciences and complements the APXPS investigations by expanding the probe depth and pressure range. These unique capabilities enable cutting-edge research on *in operando* interfacial chemistry across a wide range of areas of research, from alternative energy devices to aerosol chemistry.

II. Recent Progress

A. Carbon Monoxide Surface Chemistry at Metal, Metal Alloy, and 2-D Film Interfaces

The interaction of CO with surfaces and interfaces is central to many processes in energy science and catalysis, including Fischer-Tropsch synthesis, automotive exhaust stream processing, and the coking of fuel cell electrodes. The reaction of CO was investigated (using APXPS) on three different surfaces with increasing complexity: pure metal single crystal surfaces, surface alloys, and a 2-dimensional BN film grown onto a metal surface, to understand the molecular mechanisms of CO binding, decomposition, and - in the case of BN/Rh(111) - trapping of CO at an interface under realistic CO partial pressure conditions, comparable to those in technical applications.

The first study examined the adsorption and dissociation of CO on Ru(0001). Increasing the CO pressure above ~ 10^{-7} Torr yielded a CO coverage beyond that observed under UHV conditions. The additionally adsorbed CO is located in previously unobserved bridge sites on Ru(0001). APXPS acquired while heating Ru(0001) in 0.04 Torr CO shows that bridge-bonded CO is stable up to ~ 350 K and desorbs entirely by ~ 400 K, with additional CO desorbing over temperatures up to ~ 485 K. Above 520 K the dissociation of CO leads to a carbon built-up of ~ 4 monolayers. These findings have direct implications for Fischer-Tropsch synthesis using Ru catalysts. We expanded on this study and investigated the adsorption of CO on PtRu/Ru(0001) near surface alloys, where we observed differences in the fraction of Pt covered by adsorbed CO with changing Pt concentrations in the near surface alloy. These findings are consistent with a decrease in the local adsorption energy of CO on Pt sites in alloy surfaces compared to pure Pt(111). The observed correlation between the fraction of Pt covered by CO with the binding energy of the Pt $4f_{7/2}$ core level may provide a straightforward test for CO tolerance of PtRu catalysts used in polymer electrolyte fuel cells. The third study examined the interaction of CO with hexagonal BN grown on Rh(111). Such two-dimensional films are promising candidates as tunable catalytic materials or protective coatings of reactive surfaces. We demonstrated the reversible intercalation of CO between a BN monolayer and a Rh(111) substrate above a threshold CO pressure of 0.01 mbar at 300 K. The pristine BN film can be reinstated by heating to > 625 K. These observations could lead to reversible tuning of the electronic properties of monolayer BN films, and point the way towards technical applications in gas sensors, as well as protective coatings for metal surfaces.

B. Competition between NO and H_2O for Bonding Sites in Porous Materials

One obstacle to using porous materials for gas separation is that H_2O binds more strongly to open metal centers than the gases being separated. $Cu_3(btc)_2$ is composed of Cu^{2+} paddle wheel type

nodes (Cu^{2+}-dimers) connected by 1,3,5-benzenetricarboxylate (btc) linkers to form large interconnecting channels surrounded by small tetrahedral pockets. For $Cu_3(btc)_2$, the binding energy of H_2O is 50% higher than that of CO_2. Hence, enhancing the binding of gases (i.e., CO_2, NO, and SO_2) over water, is crucial for gas separation applications. We presented (with S. R. Leone) the first evidence for an enhanced interaction of NO (compared to water) with Cu^{1+} sites in $Cu_3(btc)_2$. Soft X-rays were used to controllably reduce Cu^{2+} to Cu^{1+} (such sites are also produced during activation by heating). The interaction of NO with $Cu_3(btc)_2$ was probed with photoelectron and NEXAFS spectra using APXPS. In the absence of H_2O, two distinct nitrogen species are observed in the N 1s region: 403.5 (NO adsorbed at Cu^{2+}), and 406 eV (NO adsorbed at newly formed Cu^{1+}). Increasing irradiation increases the number of Cu^{1+} sites and enhanced absorption of NO at 406 eV is observed. With increasing H_2O, NO at the Cu^{2+} site decreases. At ratio of 10:1 (H_2O:NO), NO remains absorbed at the Cu^{1+} site but not at the Cu^{2+} metal center. This indicates that Cu^{1+} sites selectively adsorb NO in the presence of water, and that Cu^{1+} has a higher binding strength for NO than for H_2O. This pioneering work demonstrates the potential use of porous materials with lower oxidation (Cu^{2+} vs Cu^{1+}) metal centers for gas separation.

C. Atmospheric Chemistry of Aerosols

Current models assume that atmospheric aerosols composed of low volatility gas phase products, secondary organic aerosols (SOA), are liquid, with diffusion rates fast enough to maintain equilibrium with the gas phase. A range of SOA surrogates were generated in the laboratory via reactions of ozone with isoprene, α-pinene, and limonene with UV-B broadband irradiation (collaboration with S. Nizkorodov, UC Irvine and A. Laskin, PNNL). Aerosols impacted onto substrates were imaged using STXM. During impaction aerosols were either found to deform and flatten (liquid state) or retain a spherical shape (as solids or semi-solids). From the dependence of the plot of total carbon absorption vs. aerosol diameter, information on the particle shape and phase is obtained. These measurements indicate that the laboratory surrogates are more liquid-like than reported field-collected samples. These results also indicate that the faster diffusion rates for products and reactants in the laboratory SOA surrogates are not valid for field samples.

D. Electronic Structure and Solution Chemistry of Metal Ion Complexes

Progress was made to understand aspects of electron donation and withdrawal to metal ion centers by ligands, both simple and complex, in relevant solid-state materials. This will form the pre-requisite knowledge base to interpret soft X-ray spectra (charge donation, coordination) for future liquid phase experiments. Some solid-state studies have been conducted on selected molecular species including preliminary measurements of the tetramethyl-3-oxaglutaramide ligand and complexes with multiple charge states. This ligand binds to metal ions through three oxygen atoms resulting in sufficiently strong binding such that solution complexation is efficient.

III. Future Plans

A. Investigation of the Liquid/Solid Interfaces with Spatial and Chemical Resolution

Liquid/solid interfaces play a major role in reactions in energy generation, electrochemistry, corrosion, and environmental science. A detailed characterization of the liquid/solid interface is essential for the understanding of, e.g., specific and non-specific adsorption of ions at, as well as charge-transfer processes across, interfaces. Standing Wave Ambient Pressure Photoelectron Spectroscopy (SWAPPS) is a novel technique for investigating heterogeneous interfacial processes at liquid/solid interfaces under *in operando* conditions and with chemical and spatial sensitivity on the molecular scale. A complete study requires measuring the chemical composition

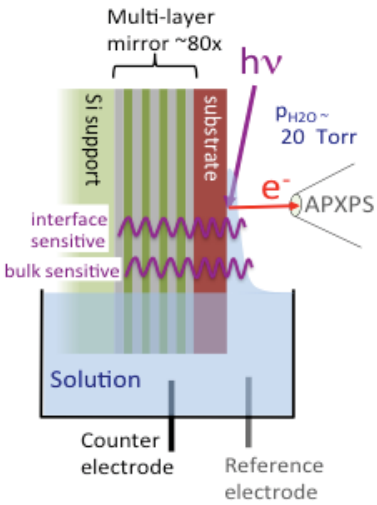

Figure 1 Schematic for measuring solid/liquid interfaces using SWAPPS.

of four distinct regions: (1) bulk liquid, (2) electrical double layer at the interface, (3) solid interface in contact with the liquid, and (4) the sub-surface region of the solid. A major obstacle is enhancing the signal from the narrow interfacial region (2,3) over that originating from the bulk of the liquid layer and solid substrate (1,4). Our proposed method (see Fig. 1) addresses this challenge and will provide detailed chemical information on all four components of the system, and the spatial arrangement of chemical species (bulk and interface constituents) along the direction perpendicular to the interface.

B. Atmospheric Aerosol Related Research

Aerosols in the atmosphere encounter a range of relative humidities, which can alter surface chemical composition, viscosity, and in-particle diffusion. Predicting the aerosols physical properties requires a fundamental, molecular-level characterization of aerosols at realistic relative humidities. These experiments will combine a quartz crystal microbalance with dissipation monitoring (QCM-D) with APXPS. Changes in the photoelectron spectra of organics (sugars, levoglucosan, & dicarboxylic acids) will be measured during hydration/dehydration cycles as a function of depth while monitoring changes in viscosity. Potential chemical changes that occur as the water permeates into the organic (during monolayer, multilayer absorption changes in equilibrium for example, keto-enol tautomerization for dicarboxylic acids or the breaking of disaccharide bond i.e. sucrose into glucose and fructose constituents, and finally phase change from solid to liquid). Any simultaneous changes in viscosity will influence diffusion rates within the aerosol.

C. Electronic Structure and Solution Chemistry of Metal Ion Complexes

We aim to understand the electronic structure and bonding of light atoms to metal ions in solution by x-ray absorption spectroscopy (XAS). Strongly bonded complexes in solutions and metal ion solution chemistry, without containing interfering atoms, will be probed employing *in situ* cells. This bridge into solution chemistry will yield new information on the nature of chemical bonding in metal ion solution species and interfacial solvent effects, while establishing a foundation for probing the electronic structure and chemistry of specifically-selected molecular species originating from solution. Because the metal ion-tetramethyl-3-oxaglutaramide complexes are soluble in acetonitrile, CH_3CN, O K-edge can be studied without interference from the solvent. The initial metal ion species systems include selected symmetric metal (Ti, Cr, Al, Si, Hf) alkoxide species $[M(OR)_x(R')_y]$. These are model solution coordination complexes for probing metal-ligand interactions, and can be transferred from solution to gas for VUV spectroscopy, and ultimately gas-phase XAS. A key aspect of this joint solution/gas-phase approach is to demonstrate the utility of XAS to acquire electronic and bonding information for metal ion complexes in solution and the ability to transfer these same complexes from solution to gas by electrospray ionization, where they can be probed in a rarified environment unperturbed by solvent molecules.

Selected Recent Beamline Publications 2013-2014 (supported by or in part by the Director, Office of Science, Office of Basic Energy Sciences, Division of CSGB and/or the CPIMS program of the CSGB. An additional nine publications (not listed) are accepted and in press.

T. Bartels-Rausch, et al., *A review of air–ice chemical and physical interactions (AICI): liquids, quasi-liquids, and solids in snow*, Atmos. Chem. Phys. Discuss. **14**, 1 (2014).

X. Du, B.T. Flynn, J.R. Motley, W.F. Stickle, H. Bluhm, G.S. Herman, *Role of Self-Assembled Monolayers on Improved Electrical Stability of Amorphous In-Ga-Zn-O Thin-Film Transistors*, accepted ECS J. Sol. State Sci. & Technol. (2014).

L. Jin, Q. Fu, A. Dong, Y. Ning, Z. Wang, H. Bluhm, X. Bao, *Surface chemistry of CO on Ru(0001) under the confinement of graphene cover*, J. Phys. Chem. C **118**, 12391 (2014).

D.J. Miller, H. Sanchez Casalongue, H. Bluhm, H. Ogasawara, A. Nilsson, S. Kaya, *Different reactivity of the various platinum oxides and chemisorbed oxygen in CO oxidation on Pt(111)*, J. Am. Chem. Soc. **136**, 6340 (2014).

R.E. O'Brien, A. Neu, S.A. Epstein, A. MacMillan, S. Nizkorodov, A. Laskin, R.C. Moffet, M.K. Gilles, *Phase State of Ambient and Laboratory Generated Secondary Organic Aerosol.* Geo. Res. Lett., accepted (2014).

N. Nijem, H. Bluhm, M.L. Ng, M. Kunz, S.R. Leone, M.K. Gilles, *Selective gas adsorption in the presence of water in reduced oxidation state unsaturated metal center HKUST-1*. Chem Mat., accepted (2014).

A. Shavorskiy, O. Karslioglu, I. Zegkinoglou, H. Bluhm, *Synchrotron-based ambient pressure X-ray photoelectron spectroscopy*, Synchrotron Radiation News **27**, 14 (2014).

K.R. Siefermann, et al., *Atomic scale perspective of ultrafast charge transfer at a dye-semiconductor interface*, J. Phys. Chem. Lett. **5**, 2753 (2014).

E.J. Crumlin, E. Mutoro, Z. Liu, M.D. Biegalski, W.T. Hong, H.M. Christen, H. Bluhm, Y. Shao-Horn, *In situ ambient pressure X-ray photoelectron spectroscopy of cobalt perovskite surfaces under cathodic polarization at high temperatures*, J. Phys. Chem. C **117**, 16087 (2013).

E.J. Crumlin, H. Bluhm, Z. Liu, *In situ investigation of electrochemical devices using ambient pressure photoelectron spectroscopy*, J. Electr. Spectrosc. Rel. Phenom. **190**, 84 (2013).

Z. Feng, E.J. Crumlin, W.T. Hong, D. Lee, E. Mutoro, M.D. Biegalski, H. Zhou, H. Bluhm, H.M. Christen, Y. Shao-Horn, *In Situ Studies of Temperature-Dependent Surface Structure and Chemistry of Single-Crystalline (001)-Oriented $La_{1-x}Sr_xCoO_{3-\delta}$ Perovskite Thin Films*, J. Phys. Chem. Lett. **4**, 1512 (2013).

S. Carenco, A. Tuxen, M. Chintapalli, E. Pach, C. Escudero, T.D. Ewers, P. Jiang, F. Borondics, G. Thornton, A.P. Alivisatos, H. Bluhm,. Liu, J. Guo, M. Salmeron, *De-alloying of Cobalt from CuCo Nanoparticles under Syngas Exposure*, J. Phys. Chem. C **117**, 6259 (2013).

F. El Gabaly, K.F. McCarty, H. Bluhm, A.H. McDaniel, *Oxidation stages of Ni electrodes in solid oxide fuel cell environments*, Phys. Chem. Chem. Phys. **15**, 8334 (2013).

P. Jiang, D. Prendergast, F. Borondics, S. Porsgaard, L. Giovanetti, E. Pach, J.T. Newberg, H. Bluhm, F. Besenbacher, M. Salmeron, *Experimental and theoretical investigation of the electronic structure of Cu_2O and CuO thin films on Cu(110) using x-ray photoelectron and absorption spectroscopy*, J. Chem. Phys. **138**, 024704 (2013).

S. Kaya, S. Yamamoto, J.T. Newberg, H. Bluhm, H. Ogasawara, T. Kendelewicz, G.E. Brown, Jr., L.G.M. Pettersson, A. Nilsson, *High density liquid like structures in thin water films on $BaF_2(111)$ under ambient conditions*, Sci. Rep. **3**, 1074 (2013).

S.T. Kelly, P. Nigge, S. Prakash, A. Laskin, B. Wang, T. Tyliszczak, S.R. Leone, M.K. Gilles, *An environmental sample chamber for reliable scanning transmission x-ray microscopy measurements under water vapor*. Rev. Sci. Instrum. **84**, 073708 (2013).

T. Kendelewicz, S. Kaya, J.T. Newberg, H. Bluhm, N. Mulakaluri, W. Moritz, M. Scheffler, A. Nilsson, R. Pentcheva, G.E. Brown, Jr., *X-ray photoemission and density functional theory study of the interaction of water vapor with the $Fe_3O_4(001)$ surface at near-ambient conditions*, J. Phys. Chem. C **117**, 2719 (2013).

A. Krepelová, Th. Bartels-Rausch, M.A. Brown, H. Bluhm, M. Ammann, *The adsorption of acetic acid on ice studied by ambient pressure XPS and partial electron yield NEXAFS at 230-240 K*, J. Phys. Chem. A **117**, 401 (2013).

M. Lampimäki, V. Zelenay, A. Křepelová, Z. Liu, R. Chang, H. Bluhm, M. Ammann, *Ozone induced band bending on metal oxide surfaces studied under environmental conditions*, ChemPhysChem. **14**, 2419 (2013).

N. Lundt, S.T. Kelly, T. Roedel, B. Remez, A.M. Schwartzberg, A. Ceballos, C. Baldasseroni, P.A.F. Anastasi, M. Cox, F. Hellman, S.R. Leone, M.K. Gilles, *High spatial resolution Raman thermometry analysis of TiO_2 microparticles*. Rev. Sci. Instrum. **84**, 104906 (2013).

A.H. McDaniel, W.C. Chueh, A. Shavorskiy, T. Tyliszczak, H. Bluhm, K.F. McCarty, F. El Gabaly, *Probing surface and bulk states of cathode materials with synchrotron-based soft X-rays in a functioning solid oxide fuel cell*, Electrochem. Soc. Trans. **58**, 47 (2013).

O. Rosseler, M. Sleiman, V. Nahuel Montesinos, A. Shavorskiy, V. Keller, N. Keller, M.I. Litter, H. Bluhm, e, *Chemistry of NOx on TiO_2 surfaces studied by ambient pressure XPS: products, effect of UV irradiation, water and coadsorbed potassium*, J. Phys. Chem. Lett. **4**, 536 (2013).

A. Shavorskiy, T. Eralp, K. Schulte, H. Bluhm, G. Held, *Surface chemistry of glycine on Pt(111) in different aqueous environments*, Surf. Sci. **607**, 10 (2013).

D.E. Starr, Z. Liu, M. Hävecker, A. Knop-Gericke, H. Bluhm, *Investigation of solid/vapor interfaces using ambient pressure X-ray photoelectron spectroscopy*, Chem. Soc. Rev. **42**, 5833 (2013).

A. Shavorskiy, H. Bluhm, *Ambient pressure X-ray photoelectron spectroscopy*, In: "Handbook of Heterogeneous Catalysts for Clean Technology - Design, Analysis and Application", K. Wilson, A. Lee (Eds.), Wiley - VCH, Weinheim, Germany (2013), pp. 435-466.

D.E. Starr, H. Bluhm, *CO adsorption and dissociation on Ru(0001) at elevated pressures*, Surf. Sci. **608**, 241 (2013).

D.E. Starr, H. Bluhm, Z. Liu, A. Knop-Gericke, M. Hävecker, *Application of Ambient Pressure X-ray Photoelectron Spectroscopy for the In-situ Investigation of Heterogeneous Catalytic Reactions*, In: "*In-situ* Characterization of Heterogeneous Catalysts", J.A. Rodriguez, et al. (Eds.), John Wiley & Sons, Inc., NY, pp. 315 (2013).

C. Zhang, M.E. Grass, Y. Yu, C. Dejoie, W. Ding, K. Gaskell, N. Jabeen, Y.P. Hong, A. Shavorskiy, H. Bluhm, W.-X. Li, G.S. Jackson, Z. Hussain, Z. Liu, B.W. Eichhorn, *Mechanistic Studies of Water Electrolysis and Hydrogen Electro-Oxidation on High Temperature Ceria-Based Solid Oxide Electrochemical Cells*, J. Am. Chem. Soc. **135,** 11572 (2013).

Surface Chemical Dynamics

N. Camillone III and M. G. White
Brookhaven National Laboratory, Chemistry Department, Building 555, Upton, NY 11973
(nicholas@bnl.gov, mgwhite@bnl.gov)

1. Program Scope

This program focuses on fundamental investigations of the dynamics, energetics and morphology-dependence of thermal and photoinduced reactions on planar and nanostructured surfaces that play key roles in energy-related catalysis and photocatalysis. Laser pump-probe methods are used to investigate the dynamics of interfacial charge and energy transfer that lead to adsorbate reaction on metal and metal oxide surfaces. State- and energy-resolved measurements of the gas-phase products are used to infer the dynamics of product formation and desorption. Time-resolved correlation techniques follow surface reactions in real time and are used to infer the dynamics of adsorbate–substrate energy transfer. Measurement of the interfacial electronic structure is used to investigate the impact of adsorbate-surface and cluster-support interactions on the activity of thermal and photoinduced reactions. Capabilities to synthesize and investigate the surface chemical dynamics of arrays of supported metal nanoparticles (NPs) on oxide surfaces include the deposition of size-selected gas-phase clusters as well as solution-phase synthesis and deposition of narrow-size-distribution nanometer-scale particles.

2. Recent Progress

Ultrafast Surface Chemical Dynamics. The ultimate goal here is to follow surface chemical processes in real time. We investigate the dynamics of substrate–adsorbate energy transfer by injecting energy with ~100-fs near-IR (NIR) laser pulses to initiate surface reactions by substrate-mediated processes such as DIMET (desorption induced by multiple electronic transitions) and heating via electronic friction. Time-resolved monitoring is achieved by a two-pulse correlation (2PC) method wherein the surface is excited by a “pump” pulse and a time-delayed “probe,” and the delay-dependence of the product yield reports on the energy transfer rate.

Our current interest is in the impact of confining the photoexcitation to the nanometer scale. Our model systems for these studies are atoms and small molecules (O, O_2, CO) adsorbed on palladium NPs supported on single crystal TiO_2(110). Because the NPs are photoexcited much more efficiently than the oxide by the NIR pulses, our approach enables probing the rate of energy transfer from the NP to the support and to adsorbates on the NP surfaces. These systems provide not only the opportunity to explore the size-dependence of the dynamics in the metal-to-nonmetal transition size regime, but also serve as more realistic model catalysts for time-resolved surface dynamics studies.

We prepare well-defined supported Pd NP assemblies by an inverse micelle synthesis method wherein a metal salt [$Pd(OAc)_2$] is introduced into a suspension of amphiphilic diblock copolymer inverse micelles. The metal salt spontaneously segregates to the hydrophilic micelle core, and the resultant Pd-loaded micelles are spin coated onto solid supports. The challenge is to develop protocols that result in size-controlled monodisperse arrays of well-separated, chemically pure, reduced metal NPs. Recently we have identified some specific copolymer blocks and $Pd(OAc)_2$ loadings that provide good size control in the few-nm size range. Specifically, we are able to tune the mean particle size to be ~3, ~4, ~7 or ~8 nm, whilst maintaining an interparticle distance of ~35 nm (Fig. 1).

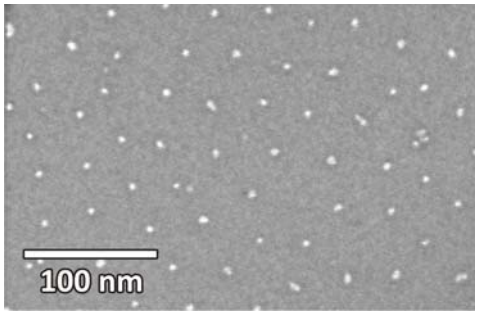

FIG. 1. An example SEM image of Pd NPs supported on a SiO_2/Si(100) (used for NP synthesis optimization purposes) after oxygen plasma cleaning. The mean particle size is ~4 nm.

Initial survey work has indicated that some aspects of the NP thermal and photoinduced chemistry are similar to those of the bulk single crystal surface, while others are clearly distinct. Thus far, the thermal chemistry of O_2 and CO indicates that the NPs expose largely clean Pd surfaces. The molecular adsorption of CO and O_2 are quite similar to that seen on Pd(111). Differences observed in the thermal oxidation of CO suggest that edge/defect sites and limited terrace sizes play important roles in the reaction kinetics.

The cross sections for photoinduced desorption appear to be orders of magnitude larger on the NPs than on the single crystal surfaces. (We are currently in the process of quantifying the enhancement factor.) Both photodesorption and photooxidation show a weaker degree of nonlinearity with respect to photon fluence than on the single crystal, indicating a more efficient conversion of photon energy. The timescales for energy flow are generally longer on the NPs compared to the single crystal, suggesting that the excitation is confined to the NP to some degree, as compared to the single crystal where thermal diffusion via electron–electron scattering more efficiently transports energy into the bulk.

We are continuing to address challenges in the preparation of clean and well-ordered NP arrays. In particular, complete removal of the polymer and counterion has proved difficult. We have realized that in situ cleaning and subsequent chemical and morphological characterization are necessary to maintain surface integrity. Consequently we are modifying our instrument to provide for in situ cleaning (oxygen plasma treatment) and characterization (x-ray photoelectron spectroscopic) in the same chamber in which the thermal and photoinduced chemistry studies are performed. Once completed, the new setup will enable the final stages of NP array preparation to be accomplished without exposure to ambient, as well as the capability to track the dependence of the chemistry on the metal's oxidation state.

We are also extending earlier investigations on single crystal Pd(111) surfaces for the purpose of comparison with dynamics on the NP surfaces. We recently observed a dramatic coverage dependence in the photoinduced desorption cross section for CO from Pd(111) near saturation coverages. Interestingly, the presence of O atoms further enhances this cross section (Fig. 2). We are in the process of quantifying these effects so that we can compare them with similar effects observed on NP surfaces.

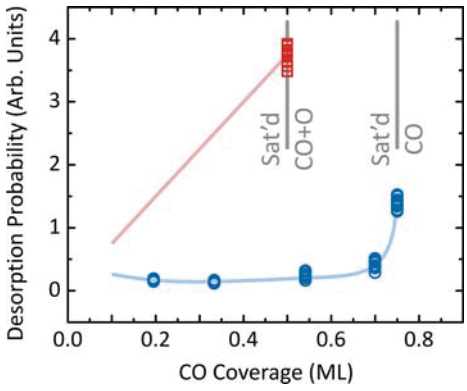

FIG. 2. Single-pulse photodesorption yield normalized to CO coverage vs. CO coverage (θ) for clean Pd(111) (circles) and (2×2) O/Pd(111) (squares) surfaces. For the CO only case, the probability increases a factor of 3.5 between θ = 0.7 and 0.75. At CO saturation, the presence of O atoms enhances this an additional 2.7 times. Lines are a guide to the eye (for the CO + O case, the line is based on preliminary data not shown).

Pump-Probe Studies of Photodesorption and Photooxidation on TiO_2(110) Surfaces. Measurements of the final state properties of gas-phase products are being used as a probe of the mechanism and dynamics of photodesorption and photooxidation on well-characterized TiO_2(110) surfaces. Recent studies have focused on the photooxidation of $R(CO)CH_3$ molecules (R = H, CH_3, C_2H_5, C_6H_5) co-adsorbed with oxygen on a reduced TiO_2(110) surface. Laser pump-probe measurements show that the kinetic energy distributions for the methyl radical fragments ($CH_3^{\bullet}$) from all four molecules are very similar, with "slow" and "fast" components. The "fast" methyl dissociation channel is attributed to a prompt fragmentation process involving an excited intermediate which is formed by charge transfer at the TiO_2(110) surface following UV photoexcitation. More recent work using state-resolved REMPI detection has shown that the ro-vibrational distributions for "fast" methyl radical products from acetone photooxidation have average energies which are significantly smaller than the average translational energy and much lower than that observed from gas-phase acetone photodissociation. These results suggest that methyl ejection

from the acetone-oxygen surface complex proceeds via a late transition state resulting in little vibrational excitation.

In the case of 2-butanone photooxidation, where both methyl and ethyl radical ejection are possible, the kinetic energy distributions are still both bimodal but with very different average energies ($\langle E_{methyl} \rangle$ = 0.20 eV, $\langle E_{ethyl} \rangle$ = 0.05 eV) and fast-to-slow branching ratios (see Figure 3). In agreement with previous studies by Henderson and co-workers, the ethyl radical is also found to be the dominant fragment. The observed product yields and differences in final state distributions are likely the result of fragmentation dynamics and not energetics, as the α-carbon bond energies to the methyl and ethyl groups are essentially identical. Through a combination of tunable VUV ionization detection and velocity map imaging, we have also recently shown that all $C_2H_x^+$ (x = 3, 4, 5) fragments appearing in the product mass spectra from butanone photooxidation originate from the nascent ethyl radical and not from secondary reactions as previously suggested.

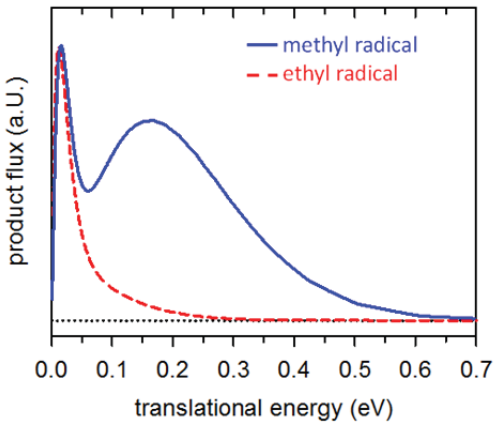

FIG. 3. Comparison of translational energy distributions for methyl (solid) and ethyl (dashed) radicals produced by UV photooxidation of 2-butanone on TiO_2(110).

Current work is focused on understanding the role of co-adsorbed oxygen which is thought to form a photoactive diolate surface complex, whereas the adsorbed ketone (without oxygen) and the final acetate surface photoproduct are inactive. Here we are using a combination of UPS and UV-induced photoproduct yields with different co-adsorbates to investigate the importance of surface charge (band bending), oxygen interactions and adsorbate energy level alignment on photooxidation activity.

Interfacial Electronic Structure of Supported Clusters. The unique catalytic activity of supported nanoparticles versus their bulk counterparts is often attributed to electronic interactions with the support that result in "activating" the particle through charge transfer, structural changes or creation of new active sites at the particle-support interface. One measure of particle-support interactions is the amount and direction of charge transfer, which strongly affects the electronic structure and reactivity of the supported particle. Recently, we have shown that two-photon photoemission (2PPE) can be used to probe interfacial charge transfer at the cluster-support interface via local work function measurements. In these experiments, model supported catalysts are prepared by depositing mass-selected clusters onto a metal oxide film or metallic support, with a surface coverage that varies smoothly from the center to the edges of the substrate. The small laser focus (~200 μm) allows us to obtain 2PPE spectra as a function of cluster coverage by rastering the laser across the surface. Hence, we can map out the change in work function (relative to the bare surface) as a function of cluster coverage over the range 0.05-1 ML for a *single* deposition experiment. These data can be used to derive an intrinsic surface dipole which is specific to cluster and support combination. Comparison with theory for a wide range of small metal oxide nanoclusters (M_xO_y; M = W, Mo, Ti, Nb) supported on Cu(111) and Cu_2O/Cu(111) show that the surface dipole is sensitive to charge transfer as well as the cluster dipole moment which is structure dependent. As O-vacancies can play an important role for reactivity on oxide surfaces, both stoichiometric and sub-stoichoimetric oxide clusters, e.g., Nb_4O_{10} and Nb_4O_7 clusters, are being studied. The ability to prepare well-defined "reduced" surface oxides by controlling the stoichiometry of the clusters rather than by post-deposition heating or chemical treatments highlights a unique capability of cluster deposition.

3. Future Plans

Our planned wok develops three interlinked themes: (i) the chemistry of supported NPs and nanoclusters (NCs), (ii) the exploration of chemical dynamics on ultrafast timescales, and (iii) the photoinduced chemistry of molecular adsorbates. The investigations are motivated by the fundamental need to connect chemical reactivity to chemical dynamics in systems of relevance to catalytic processes—in particular metal and metal-compound NPs and NCs supported on oxide substrates. They are also motivated by fundamental questions of physical changes in the electronic and phonon structure of NPs and their coupling to adsorbates and to the nonmetallic support that may alter dynamics associated with energy flow and reactive processes.

Future work on ultrafast photoinduced reactions will involve modeling of the energy transfer rates to elucidate the novel dynamics we have observed. In addition, further experiments on progressively smaller nanoparticles (towards sub-nm) will be pursued to further explore fundamental changes in surface reaction kinetics and dynamics as the size of the metal substrate material is reduced from macroscopic (planar bulk surfaces) to the nanoscale. Future work in surface photochemistry using pump-probe techniques will continue to explore mechanistic aspects of semiconductor photoreactions, including the development of new instrumentation for time-resolved studies using ultrafast lasers. New studies in size-selected clusters will focus on mixed metal oxides for which oxide nanoclusters are deposited onto single crystal (e.g., TiO_2(110)) and thin film metal oxide (e.g., Cu_2O, MgO) supports to explore cluster-support electronic interactions that can provide a basis for understanding and "tuning" their reactivity.

DOE-Sponsored Research Publications (2012–2014)

Surface Dipoles and Electron Transfer at the Metal Oxide-Metal Interface: A 2PPE Study of Size-Selected Metal Oxide Clusters Supported on Cu(111), Y. Yang, J. Zhou, M. Nakayama, L. Nie, P. Liu and M. G. White, *J. Phys. Chem. C*, **118**, 13697−13706 (2014).

Photooxidation of Ethanol and 2-Propanol on TiO_2(110): Evidence for Methyl Radical Ejection, M. D. Kershis and M. G. White, *Phys. Chem. Chem. Phys.* **15**, 17976-17982 (2013).

Exploring Gas-Surface Photoreaction Dynamics using Pixel Imaging Mass Spectrometry (PImMS), M. D. Kershis, D. P. Wilson, M. G. White, J.J. John, A. Nomerotski, M. Brouard, J. Lee, C. Vallance, R. Turchetta, *J. Chem. Phys*. **138**, 204703 (2013).

Dynamics of Acetone Photooxidation on TiO_2(110): State-resolved Measurements of Methyl Photoproducts, M. D. Kershis, D. P. Wilson, M. G. White, *J. Chem. Phys*., **138**, 204703 (2013).

Final State Distributions of the Radical Photoproducts from the UV Photooxidation of 2-Butanone on TiO_2(110), D. P. Wilson, D. P. Sporleder, M. G. White, *J. Phys. Chem. C*, **117**, 9290–9300 **(**2013**).**

Photocatalytic Activity of Hydrogen Evolution Over Rh doped $SrTiO_3$ Prepared by Polymerized Complex Method, P. Shen, J. C. Lofaro, Jr., W. Worner, M. G. White and A. Orlov, *Chem. Eng. J.*, **223**, 200–208 (2013).

Final State Distributions of Radical Photoproducts from the Photooxidation of Acetone on TiO_2(110), D. P. Wilson, D. Sporleder and M. G. White, *J. Phys. Chem. C*, **116**, 16541–16552 (2012).

Local Work Function of Size-Selected Mo_xS_y Clusters on Al_2O_3/NiAl(110), J. Zhou, J. Zhou, N. Camillone III and M. G. White, *Phys. Chem. Chem. Phys***., 14,** 8105–8110 (2012).

Theory of Dynamics of Complex Systems

David Chandler

Chemical Sciences Division, Lawrence Berkeley National Laboratory
and
Department of Chemistry, University of California, Berkeley CA 94720

chandler@berkeley.edu

DOE funded research in our group concerns the theory of dynamics in systems involving large numbers of correlated particles. Glassy dynamics is a quintessential example. Here, dense molecular packing severely constrains the allowed pathways by which a system can rearrange and relax. The majority of molecular motions that exist in a structural glass former are trivial small amplitude vibrations that couple only weakly to surrounding degrees of freedom. In contrast, motions that produce significant structural relaxation take place in concerted steps involving many particles, and as such, dynamics is characterized by significant heterogeneity in space and time. Our recent contributions to this topic have established that these heterogeneities are precursors to a non-equilibrium phase transition, and that this transition underlies the glass transition observed in laboratory experiments [2,6,10].[1] We have also shown that relaxation leading up to this transition exhibits a surprising degree of universality, even applying to supercooled water [3,9,10].

Liquid interfacial dynamics is another important example, and here too our Group has made several new contributions. Much of this latest work is based upon two advances: i. our general and efficient procedure for identifying instantaneous interfaces from molecular coordinates (see, for example, Ref. [5]), and ii. our generalization of umbrella sampling methods for collecting statistics on rare but important density fluctuations. We have used these methods to examine pathways of water evaporation [5] (an example of which is illustrated in the top panel of the Figure 1), the structure and dynamics of water at a Pt surface [4,7] (lower-right panel), and the structure and dynamics of water at oily surfaces [1,13] (lower-left panel). Related work examining charge fluctuations in non-aqueous nano-scale capacitors [11] promised an understanding of super capacitance relevant for new classes of energy storage devices. And indeed, this promise has turned to fruition in our detailing a surprising two-dimensional phase transition in ionic melts contacting metal electrodes [12].

An insightful perspective on the nature of hydrophobic effects, created in our Group's work over the last decade, focuses on the role of interfacial fluctuations in dynamics and forces of assembly. Quantitative detail on this perspective is found in our recent

[1] Numbers in square brackets refer to papers in the list of Recent DOE Supported Research Publications.

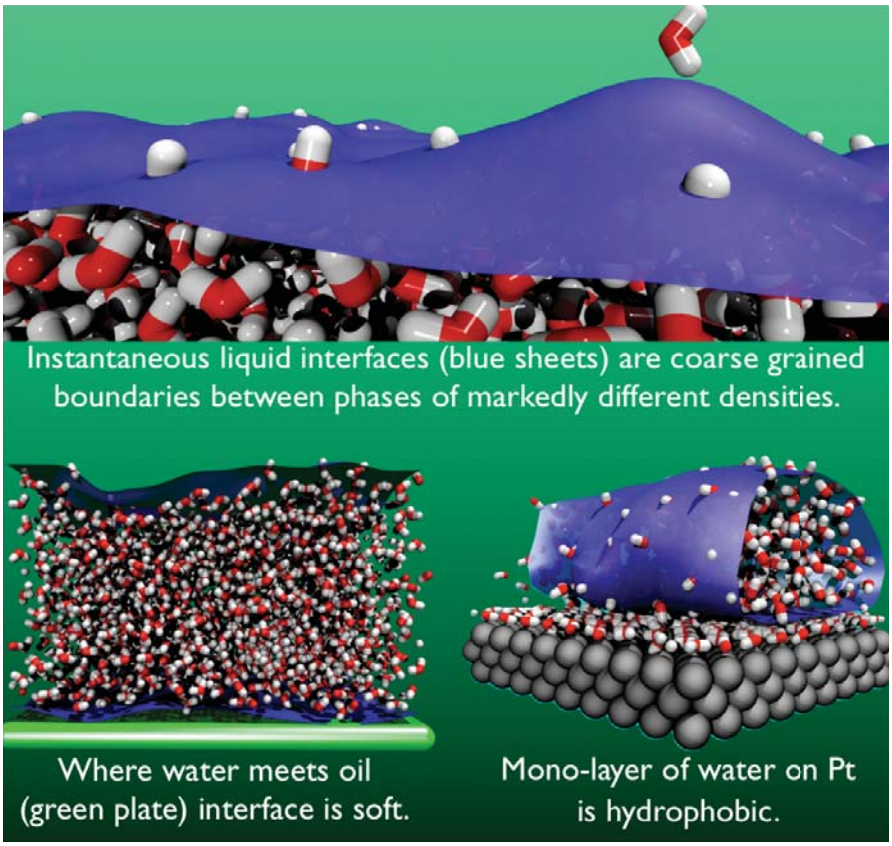

Figure 1: Snap shots from molecular dynamics trajectories showing some of the systems examined by the Chandler research group in their DOE funded studies of liquid interfaces.

advances [1, 13]. The principal effects of interfacial fluctuations can be captured with coarse-grained modeling. This understanding can be used to formulate a quantitatively accurate and computationally convenient theory of solvation and hydrophobic effects.

Finally, we have embarked upon a program of understanding the properties of liquid and solid water at conditions far from bulk equilibrium. Just as hydrophobicity is controlled by interfaces because of the proximity of liquid-vapor coexistence, the behaviors of cold water in bulk, in confinement and in non-equilibrium, depend upon interfaces because of the proximity of crystal-liquid coexistence. Figure 2 illustrates some of our recent results on this topic [3,10]. H. E. Stanley and his many coworkers and followers have widely written on how properties of cold and supercooled liquid water might reflect a metaphysical liquid-liquid transition and critical point. The need for such an unseemly explanation is no longer, as all these properties are now shown to actually reflect easily observed water-ice coexistence and associated pre-melting phenomena [3,8,9,15]. Our studies on thus topic have given us a deep and useful understanding of glass

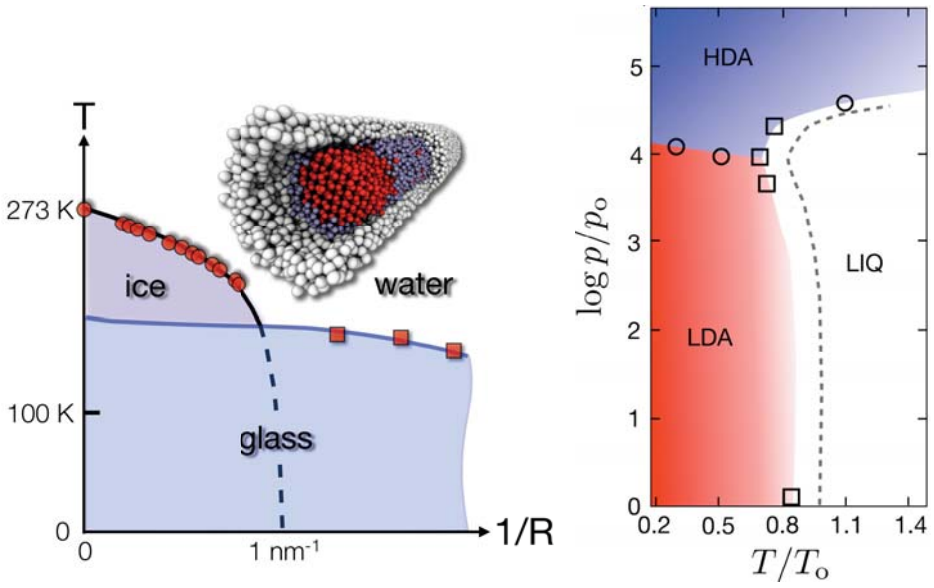

Figure 2: **Left**. Low pressure phase diagram for water confined to a disordered hydrophilic nano-pore of radius R. [Adapted from Ref. 11.] Lines are theoretical curves derived from effects of the interfaces present as the result of confinement (there are no adjustable parameters, only measured bulk transport properties, thermodynamics and liquid-ice interfacial tension enter the theoretical analysis). Experimental data points are from calorimetric observations of the water-ice and water-glass transitions. **Right.** Non-equilibrium phase diagram in corresponding states units for pressure (p_o=1 atm) and temperature (T_o= 277 K). The diagram, computed through application of the s-ensemble method to one of the standard atomistic models of water, is illustrates the first systematic simulation of the far-from-equilibrium high-density and low-density amorphous solids of water, HDA and LDA, respectively. [Adapted from Ref. 18.]

transitions [2,18] and premelting [3,14], applicable to systems beyond aqueous systems. Moreover, now being able to treat confined cold water, this work sets the stage for interpreting crystal, liquid and amorphous-solid phase behaviors of aerosols, a topic of significant importance to climate science, and a topic we plan to examine in the near future.

Recent DOE Supported Research Publications

1. Patel A. J., P. Varilly, S. N. Jamadagni, M. Hagan, D. Chandler and S. Garde, "Sitting at the edge: How biomolecules use hydrophobicity to tune their interactions and function" *J. Phys. Chem. B* **116**, 2498-2503 (2012).

2. Speck, T., and D. Chandler, "Constrained dynamics of localized excitations causes a non-equilibrium phase transition in an atomistic model of glass formers" *J. Chem. Phys*. **136**, 184509.1-9 (2012).

3. Limmer, D. T., and D. Chandler, "Phase diagram of supercooled water confined to hydrophilic nanopores," *J. Chem. Phys.* **137**, 045509.1-11 (2012).

4. Limmer, D. T., A. P. Willard, P. A. Madden and D. Chandler, "Hydration of metal surfaces can be dynamically heterogeneous and hydrophobic," *Proc. Natl. Acad. Sci. USA* **110**, 4200-4205 (2013).

5. Varilly, P., and D. Chandler, "Water evaporation: a transition path sampling study," *J. Phys. Chem. B* **117**, 1419-1428 (2013).

6. Keys, A. S., J. P. Garrahan, and D. Chandler, "Calorimetric glass transition explained by hierarchical dynamic facilitation," *Proc. Natl. Acad. Sci. USA* **110**, 4482-4487 (2013).

7.Willard, A. P., D. T. Limmer, P. A. Madden and D. Chandler, "Characterizing heterogeneous dynamics at hydrated electrode surfaces," *J. Chem. Phys.* **138**, 184702 (2013)

8. Limmer, D. T., and D. Chandler, "The putative liquid-liquid transition is a liquid-solid transition in atomistic models of water, Part II, *J. Chem. Phys.***138**, 214504.1-15 (2013).

9. Limmer, D. T., and D. Chandler, "Corresponding states for mesostructure and dynamics of supercooled water," *Faraday Discuss.* **167**, 485-498 (2013)

10. Limmer, D.T., and D. Chandler, "Theory of amorphous ices," *Proc. Natl. Acad. Sci. USA* **111**, 9413-9418 (2014).

11. Limmer, D.T., C. Merlet, M. Salanne, D. Chandler, P.A. Madden, R. van Roij, B. Rotenberg, "Charge fluctuations in nano-scale capacitors," *Phys. Rev. Lett*. **111**, 106102.1-5 (2013).

12. Merlet, C., D. T. Limmer, M. Salanne, R. Van Roij, P. A. Madden, D. Chandler and B. Rotenberg, "The electric double layer has a life of its own," *J. Phys. Chem. C* **118**, 18291-18298 (2014).

13. Willard, A. P., and D. Chandler, "The molecular structure of the interface between water and a hydrophobic substrate is liquid-vapor like," arXiv:1407.4365. To appear in *Journal of Chemical Physics*.

14. Limmer, D. T., and D. Chandler, "Premelting, fluctuations and coarse-graining of water-ice interfaces," arXiv:1407.3514. To appear in *Journal of Chemical Physics.*

15. Limmer, D.T., and D. Chandler, "Comment on 'Spontaneous liquid-liquid phase separation of water' by T. Yagasaki, M. Matsumoto and H. Tanaka, Phys. Rev. E 89, 020301 (2014)", arXiv:1406.2651. Under review in *Physical Review E*.

Kinetics of charge transfer in a heterogeneous catalyst-reactant system: the interplay of solid state and molecular properties

Tanja Cuk
D46 Hildebrand Hall, Chemistry Department, University of California, Berkeley 94720
tanjacuk@berkeley.edu

I. Program Scope

One of the greatest challenges in the design of efficient and selective catalysis technologies is the limited fundamental understanding of how interfacial properties at solid state/reactant interfaces guide catalytic reactions. The central research question is to determine how molecular properties of reactants influence charge dynamics in solid state catalysts, and conversely, how these charge dynamics induce molecular changes; likely, it is this synergy that results in catalytic efficiency and high turnover rates. There are two perspectives on the solid state catalyst/reactant interface. From the solid state perspective, interfacial properties are described by band alignment and Fermi levels; from the molecular perspective, interfacial properties are described by oxidation states and reactant adsorption. The characterization of catalytic materials has either focused on molecular changes such as adsorption, dissociation, and new bond formations occurring on the reactant side of the interface or the changes in interfacial band alignment and passivation of surface states on the solid state side. While these properties are useful for understanding catalytic performance, a causal link between the changes observed on each side of the interface is lacking. What is needed is to directly follow the trajectory of how charge carriers in solid state catalysts initiate interfacial charge capture by reactant molecules—from the creation of the charge carrier in the bulk, to its accumulation at the interface, and to the moment at which a reactant molecule transforms and, in the process, consumes the charge carrier. It is a goal of this program to develop these approaches. In photoinitated heterogenous catalysis, the charge carrier is injected via a photodiode, photovoltaic, or Schottky junction. Rather than focusing on the excitonic features of an electron-hole pair, this proposal concentrates on the already well-separated charges to understand the detailed balance between the flow of charge carriers to catalyst-reactant interfaces and the dynamics of interfacial charge capture by reactant molecules. Understanding these interfacial dynamics from both the chemical and solid state perspective will reveal the interplay between molecular changes and the heterogeneous catalyst surface, leading to both better catalyst design and more intelligent control of the catalytic environment.

II. Recent Progress

Recent progress uses surface sensitive, *in-situ* transient optical spectroscopy to measure the rate of interfacial charge transfer by monitoring holes generated within the transition metal oxide that drive the water oxidation reaction at the catalyst/reactant interface. These experiments aim to resolve whether the initial, ultrafast steps of the reaction differentiate between the turnover rates in an high overpotential catalyst (~2V, 1000 O_2/site-s) and low over potential catalyst (0.3V, 1 O_2/site-s). Overpotential simply means the free energy difference (with respect to the thermodynamic equilibrium potential of OH^-/O_2) applied to the reaction.

Interfacial Charge Transfer at the n-$SrTiO_3$/H_2O Interface

A measurement that distinguishes the interfacial charge transfer rate from recombination kinetics and drift within the material requires a sample with a high quantum efficiency for separating electron-hole pairs and an experimental configuration with sufficient surface sensitivity. An n-type semiconductor/liquid interface is well described by a Schottky barrier that separates

electron-hole pairs generated with the depletion layer of the semiconductor with efficiency approaching unity. The UV driven water oxidation catalyst, n-$SrTiO_3$, has a quantum efficiency for O_2 evolution approaching 70% for 300 nm excitation. This high quantum efficiency comes from the fact that at 300nm, the depletion width of the electric field matches the penetration depth of the UV light. The surface sensitivity in our configuration comes simply from the fact that we measure the transient signal in reflectance. The effective probe depth of a reflectance measurement is guided by the real, rather than the imaginary, part of the index of refraction, $\alpha_{Reflectance} = \lambda/4\pi n$. In a setup probing the reflectance at the n-$SrTiO_3$/H_2O interface, the three parameters—the depletion width, the penetration depth of the exciting light, and the penetration depth of the probe light are all equal to ~25 nm. Essentially, this is what allows for us to distinguish interfacial charge transfer from recombination and drift using transient optical spectroscopy.

While high intensity, high peak power laser excitation can in principle change this picture, we maintain a high quantum efficiency with ~150 fs, 0.1 mJ/cm^2 excitation due to the high rate of drift in the depletion region and the well matched excitation wavelength. High intensity laser excitation, combined with the high quantum efficiency also creates a large bath of holes at the interface within the ~150 fs pulse— 10^{19}/cm^2, much higher than the number of sites available for catalysis (10^{15}/cm^2). If these holes are not consumed by the water oxidation reaction fast enough, they can lead to other side reactions that damage the catalyst surface. While we have observed damage to the catalyst surface under our excitation conditions, we have been able to control it enough to take reproducible data by taking the data at fresh sample spots and alternating between open and closed circuit conditions in the electrochemical cell.

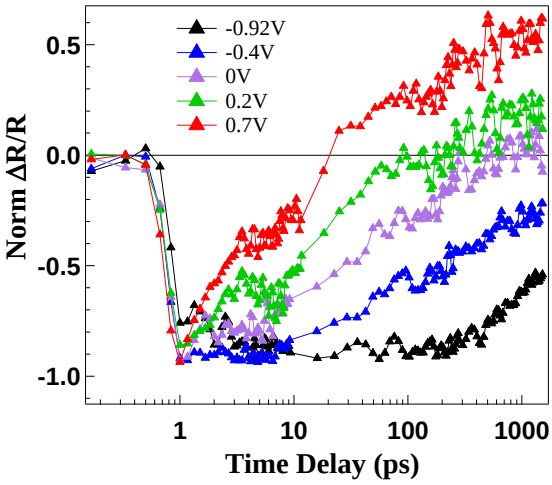

Figure 1: Kinetics of hole decay at n-$SrTiO_3$/H_2O interface upon 300nm excitation for several different voltages applied to the cell.

The transient reflectance results on n-$SrTiO_3$ in an in-situ electrochemical cell, shown in Figure 1, exhibit a marked change in kinetics as a function of voltage applied on the electrochemical cell. The kinetics speed up with applied voltage in a voltage region that does not change the quantum efficiency of the reaction, showing that the measured kinetics reflect interfacial charge transfer rather than the competition between drift and recombination. Given that holes are transferred in oxidative conditions, we can attribute the kinetics to holes that accumulate at the interface and then decay as a result of charge transfer to adsorbed water species. Further, the voltage dependence of the kinetics suggests that the applied voltage in the cell changes the potential of holes at the interface, leading to a larger over-potential for the reaction. In a usual Schottky barrier model of the n-type semiconductor/liquid interface, the VB and CB are pinned at the interface and the applied voltage only changes the band-bending in the semiconductor. However, under the high charge injection conditions that we have here due to both voltage applied and the laser pulse, the band edges at the interface can move approximately linearly with the applied voltage. We were able to quantitatively describe how the potential at the interfacial holes relates to the applied voltage using electrochemical measurements at equilibrium and Poisson's equations [1].

In a manuscript recently published in JACS [1], we ascribe the potential dependent hole kinetics to mapping out the activation barrier of the initial hole transfer of the water oxidation reaction, [h+] + [OH-] → [OH*], where OH* is a neutral, OH radical. In particular, we quantify how much a change in the potential of interfacial holes reduces the activation barrier through a coefficient α (=0.2, or 20% of the applied potential goes to reducing the activation barrier). We also find the kinetics of charge transfer at the equilibrium thermodynamic potential of the reaction (reported as k_0). The values are within expectations for a simple, one hole transfer reaction, as can determined by electrochemistry for such reactions using steady state current flow. Steady state current however cannot follow multi-component reactions accurately and without extensive modeling. The new finding here is we have been able to both separately follow and quantify a single hole transfer step from a multi hole transfer reaction using transient spectroscopy. The physical picture is that we have quantified the initial step to transferring a hole over from a delocalized valence band edge of O 2p orbitals in the solid state catalyst into a molecular oxygen bond at the interface.

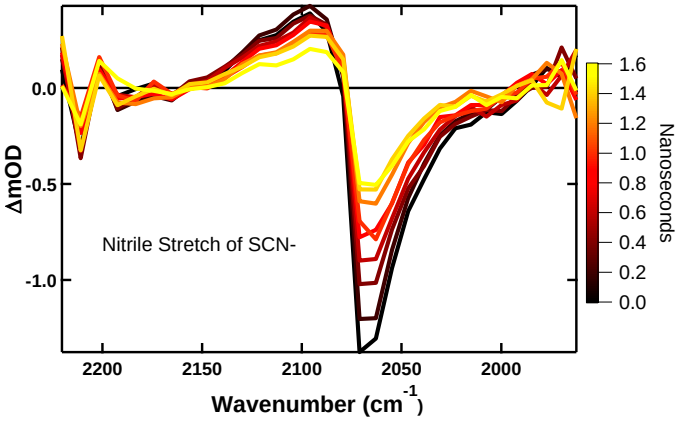

Figure 2: Nitrile stretch of SCN- at the n-$SrTiO_3$ /electrolyte interface at ultrafast time scales.

Ultrafast Infrared Spectroscopy at the n-$SrTiO_3$/H_2O Interface

We are now actively pursuing signatures of hole acceptors on the electrolyte side of the interface. Shown in Figure 2 is the nitrile stretch in SCN^- after a laser pulse initiates hole transfer at the n-$SrTiO_3$/ SCN- electrolyte interface. The experiments are conducted in a full electrochemical cell, where the infrared probe beam is reflected off of the surface of a sample pressed to a CaF_2 window allowing for a short ~um probe path length of the infrared beam through the electrolyte. Figure 2 reports the ultrafast changes to the nitrile stretch when holes are dumped at the interface with the cell at open circuit. Of primary interest in the basic water electrolyte are the effects on the OH stretch region, the H_2O bend region, and possible more stable intermediates of the water oxidation reaction, such as the surface bound oxo (=O). In the transient optical kinetics reported above, we also observe a second, much longer time scale which may be associated with a more stable intermediate than the OH* radical (see [1]).

Investigating low overpotential catalysts with n-p GaAs/catalyst heterojunctions

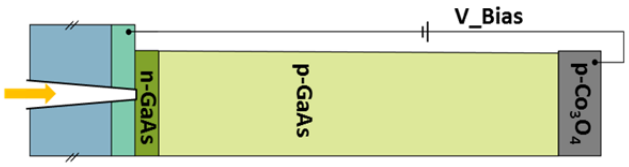

Figure 3: n-p GaAs/Co_3O_4 design.

In order to investigate the interfacial charge transfer kinetics defining low overpotential, lower turnover rate (~1's O_2/site-s) catalysts, we have created a layered device where an underlying n-p GaAs junction is used as a photodiode to inject charges into a Co_3O_4 overlayer. For these initial studies, we have chosen Co_3O_4—an earth abundant catalyst with low over potential for the water oxidation reaction (~0.1-0.3V vs. Ag/AgCl) and reasonable turnover rates (0.1 O_2/site-s).

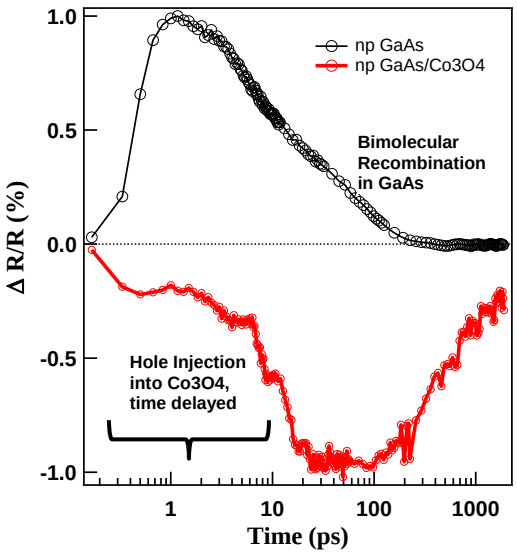

Figure 4: np GaAs diode pumped with 800 nm, and probed in reflectance with 800 nm. np GaAs/Co3O4 diode pumped with 800 nm, and probed in reflectance with 400 nm. Normalized to the maximum signal in each trace.

Figure 3 shows the design of the device. The n-p GaAs photodiode is designed such that the penetration depth of the exciting light matches the depletion width of the electric field. This leads to kinetics defined by drift rather than diffusion, such that the holes are injected into the catalyst over-layer at ultrafast time scales. Further, the biggest electric field is dropped at the back of the device, spatially separating the charge separation step from the hole injection at the front of the device.

In conjunction with this device design, we implement a pump-probe geometry for the transient spectroscopy that maximizes surface sensitivity to the hole injection. In particular, we excite carriers from the back of the device, and probe in reflectance the holes injected into the catalyst over-layer. Figure 4 shows the kinetics that result from the device, with and without the catalyst over-layer. The distinctly different kinetics and their fluence dependence can be ascribed to bimolecular recombination in GaAs (without Co_3O_4) and hole injection and trapping in Co_3O_4 (with Co_3O_4). In particular, we see a rise time associated with hole injection that is about ~10 ps which is the time required for holes to drift through the ~800 nm GaAs p-type layer.

We are in the process of seeing how the hole kinetics change at an electrolyte vs. air interface and as a function of the Helmholtz double layer potential drop at the interface. In the future we would like to study charge transfer during steady state current flow, similar to what was done for n-$SrTiO_3$. This requires more stable heterojunctions under operational conditions, and we are working on that.

III. Future Plans

Ultrafast Infrared Transient Spectroscopy of the n-$SrTiO_3$/H_2O Interface Future plans aim to correlate the ultrafast kinetics of holes observed on the solid state side of the n-$SrTiO_3$/H_2O interface with changes in the molecular bonding of adsorbates on the liquid side of the interface. In order to do this, we are applying ultrafast infrared spectroscopy in a photoelectrochemical cell in reflectance, as described above. These experiments will be the first that investigate ultrafast kinetics of bond changes at the catalyst surface that are initiated by direct charge transfer, rather than heating.

Diffusion kinetics at transition metal oxide/electrolyte interfaces We have set up transient grating diffraction spectroscopy with heterodyne detection to measure hole diffusivity both at the n-$SrTiO_3$/electrolyte interface and at other transition metal oxide/electrolyte interfaces using the n-p GaAs photodiodes. In particular, we will be investigating how the Helmholtz double layer influences hole diffusion in transition metal oxides.

[1] M.M. Waegele, X. Chen, D.M. Herlihy, and **T. Cuk**, *J. Am. Chem. Soc.* **2014** Article ASAP.
[2] M.M. Waegele, H.Q. Doan, and **T. Cuk**, *J. Phys. Chem. C.* **2014**, 118, 3426.

Understanding the Rates and Molecular Mechanism of Water-Exchange around Aqueous Ions using Molecular Simulations. Recent Progress and Future Plans

Liem X. Dang
Physical Sciences Division
Pacific Northwest National Laboratory
Richland, WA 93352
liem.dang@pnnl.gov

Background and Significance

The study of thermodynamic and kinetic properties of ions in water using statistical mechanics or computer simulation techniques has provided molecular-level details that have advanced our understanding of the chemistry and physics of solvation. Because of the roles of kinetics and thermodynamics of water exchange around aqueous ions in electrochemical and biological processes, these properties specifically have been subjects of considerable theoretical, computational, and experimental interest in recent years. Minor differences in ion properties could cause major changes in their role in biological processes. So far, many of the ion-solvation research studies related have focused on the thermodynamics of ion solvation and the hydration structure. Information about the dynamics of ion solvation, particularly the kinetics and mechanism of solvent-exchange process, is scarce. The reactivity of ions in solutions requires rearrangement of the hydration shell, which involves the replacement of the water molecule from first hydration shell. This process, also known as a solvent-exchange reaction, is believed to be associated with activation volume ($\Delta V^{\ddagger}$), which is the key indicator of the water-exchange mechanism. For example, the exchange process is an associative mechanism when the activation volume is negative and a dissociative mechanism when the activation volume is positive.

In this report, we summarize of our recent studies of the dynamics of the ion-solvation process. We used the rate theory approach to determine the solvent-exchange rates. Also, analogous to experimental procedures, we computed pressure-dependent rates to determine the activation volume. Mechanistic properties associated with the water-exchange process, such as potential of mean force (PMF), time-dependent transmission coefficients, and the corresponding rate constants, were examined using transition state theory (TST), the reactive flux (RF) method, and Grote-Hynes (GH) treatments of the dynamic response of the solvent. Characterization of the dynamical effects of the solvent on the rate results and $\Delta V^{\ddagger}$ is the primary focus of this work. We performed a systematic study using four systems: 1) a pure solvent (water), 2) a cation (Li^+), 3) anions (halides), and 4) an ion-pair (Na^+–Cl^-) dissociation process. We also computed pressure-dependent rate constants using the RF and GH methods, which takes into account recrossings induced by solvent dynamics. Future research effort will focus on understanding the influence of nuclear quantum mechanical effects on the kinetics properties of ions in aqueous solution. Also, we are interested in expanding our current methodology to studies of ion-solvation processes at interfaces due to their ability to respond to the local, nonhomogeneous environment; we expect a different behavior for these processes.

1. Water Exchange in Pure Water

In Figure 1a, we present the PMFs for an H_2O-H_2O pair in aqueous solution at three different pressures. Although the free energy profiles are similar at different pressures, the decreasing trend in barrier heights with pressure is noticeable. As expected, because of the decrease in barrier heights, we notice an increasing trend in k^{TST} as pressure increases. The computed activation volume is -2.1 cm^3/mol. As discussed earlier, the negative activation volume resulting from the increase in rate constant values as pressure increases is indicative if an associative mechanism for the exchange of water molecule from the first solvation shell. In Figure 1b, we present the time-dependent transmission coefficient computed using RF method at various pressures. To compute *k(t)*, a 10-ns simulation was carried out by constraining the reaction coordinate at the transition state. Simulation snapshots were saved every 4 ps. Using each of these configurations, molecular dynamics (MD) simulations were run both forward and backward for 2 ps with no constraints. The initial velocities were sampled through a

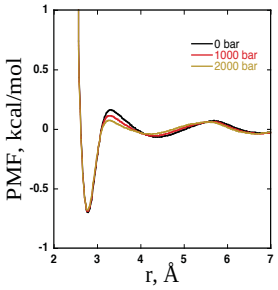

Figure 1a. Computed PMFs for H_2O-H_2O pair.

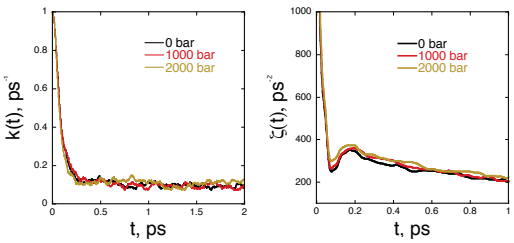

Figure 1b and 1c. (b) Time-dependent transmission coefficients of H_2O-H_2O pair from RF method (c) Time dependence friction kernels for H_2O-H_2O pair computed from GH theory.

Boltzmann distribution. The value of k_{RF} was determined by averaging $k(t)$ over the last 0.5 ps. Transmission coefficients are very low, indicating the existence of significant recrossing events induced by the solvent dynamics. The value of k_{RF} slightly increases as pressure increases. The activation volume obtained from the RF-method rate constants is -6.7 cm^3/mol. In Figure 1c, we present the time-dependent friction kernels $\zeta(t)$ at different pressures computed using GH theory. All friction kernels show two decay time scales. We also notice that the transmission coefficients computed from GH theory decrease as pressure increases, and also, the rate constants determined from GH theory show a decreasing trend with pressure. This observation is counter to the trend noticed when the RF method is used. A similar counter trend in rate constants for GH theory has been noticed previously in the solvent-exchange studies of Li^+.

2. Water Exchange around Aqueous Li^+

In Figure 2a, we present the PMFs for Li^+ at three different pressures 0 MPa, 150 MPa, and 300 MPa. All the free energy profiles are very similar. There are noticeable differences in the barrier heights. As the pressure increases, the barrier height decreases from 4.07 kcal/mol at 0 MPa to 3.77 kcal/mol at 300 MPa. Also, with the increase in pressure, a slight left shift is noticed in the center of mass separation distance corresponding to the transition state (from 2.67 Å to 2.57 Å). The minor differences in the barrier heights could be attributed to the difference in force fields that describe the ion-water interaction. The computed k^{TST} values increase as pressure increases, which are a direct consequence of the barrier height. According to TST, the higher the barrier, the lower the rate constant. The activation volume obtained using the TST rate constants is -3.2 cm^3/mol. As discussed earlier, the negative activation volume obtained from TST indicates an associative mechanism for the exchange process.

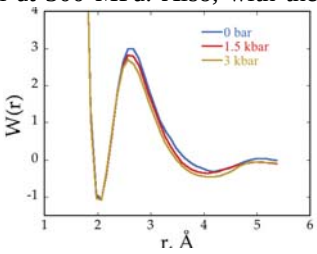

Figure 2a. Pressure dependence of the PMFs of Li^+-H_2O systems.

In Figure 2b, we show the time-dependent transmission coefficient, $k(t)$. As pressure increases, the values of κ_{RF} also increase, implying that pressure have considerable effect on the transmission coefficient. The activation volume computed using the rate constants from the RF method, $\kappa_{RF}k^{TST}$ is -4.1 cm^3/mol. This value is more negative than the activation volume obtained from TST; therefore, the pressure dependence of both the barrier height and the transmission coefficient contribute to the activation volume. The plots shown in Figure 2c correspond to the time-dependent friction kernels $\zeta(t)$ at different pressures. In all cases, there are two distinct decay time scales that show initial rapid sub-picosecond decay and then a longer time decay that lasts for few picoseconds. This oscillating $\zeta(t)$ reflects strong interaction between Li^+ and H_2O, which also is evident from the barrier heights of the computed PMFs. We noticed a decrease in barrier frequency with the increase in pressure. These values are in contrast to the actual transmission coefficients computed using the RF method. From these results, it appears that GH theory does not provide a good approximation of transmission coefficients at high pressures. Spangberg and coworkers also observed poor performance in their solvent-exchange studies on Li^+. They attributed this poor performance of GH theory to the to the recrossing trajectories that make large excursions from $r*$, which violates the assumptions of GH theory. Our computed residence times from RF method are 191, 140, and 120 ps at 0, 150, and 300 MPa, respectively.

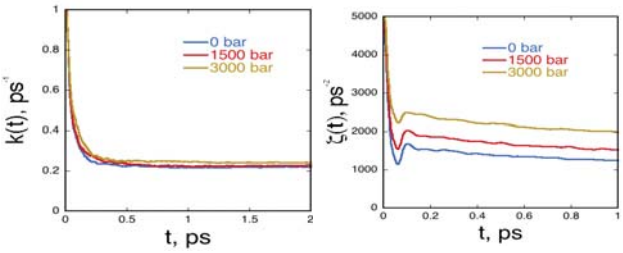

Figure 2b and 2c. (b).Pressure dependence of the time dependence friction kernels of Li^+-H_2O systems. (c) Pressure dependence of the transmission coefficients of Li^+-H_2O systems.

3. Water Exchange in Aqueous Halide Ions

In Figure 3, we show the pressure dependence of PMFs, W(r), for three different anions (chloride, bromide, and iodide). The PMFs were computed at three different pressures: 0 MPa, 100 MPa, and 200 MPa. By comparing all three plots, one observes that, as would be expected, barrier height decreases as ion size increases. Similar to Li^+, PMFs of all halide ions also exhibit a decreasing trend in barrier heights as pressure increases. The decrease in barrier height is 0.15 kcal/mol for chloride, 0.10 kcal/mol for bromide, and 0.09 kcal/mol for iodide. From these values, one observes that the pressure dependence of the barrier height is more prominent for chloride and decreases as the ion size increases. With the increase in pressure, the k^{TST} increases for all the anions. The pressure dependence of k^{TST} is similar in the case of Li^+ as well as for halides. The values are negative for all the anions, thus indicating an associative mechanism for all anions. Similar to the Li^+ and pure water cases, we also computed the actual solvent-exchange rate constants using the RF method for all the anions. We used the same protocol described earlier to compute the time-dependent transmission coefficient *k(t)*. In Figure 4, we show the computed *k(t)* for all the anions at different pressures. It can be seen that k_{RF} decreases as pressure increases. The activation volumes are positive for all the anions, indicating a dissociative mechanism. This is contrary to the TST result. The rate constants from TST increase as pressure increases, whereas the actual rate constants obtained using the RF method decrease as pressure increases for all the anion cases. This result emphasizes the importance of dynamical effects in determining the rates and mechanism of the solvent-exchange process. We also computed the time-dependent friction kernels for all the anions at various pressures. Similar to the previous cases, all the plots show similar behaviors with two decay time scales. Similar to the results obtained using the RF method, the transmission coefficients decrease as pressure increases.

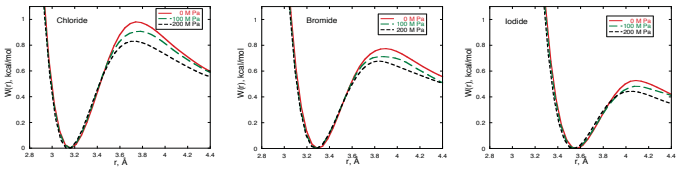

Figure 3. Pressure dependence of the PMFs for a) Cl^--H_2O, b) Br^--H_2O and

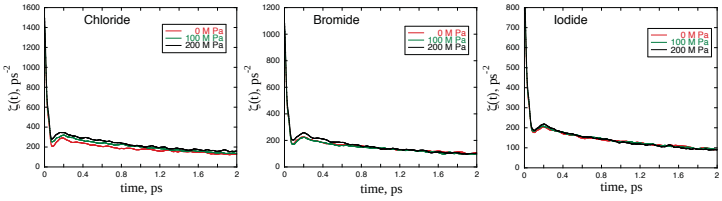

Figure 4. Computed ζ(t) for Cl^--H_2O, Br^--H_2O and I^--H_2O systems.

4. Pressure-Dependent Rate Studies on Na^+–Cl^- Ion-Pair Dissociation in Water

After studying the solvent-exchange rates and mechanisms occurring around aqueous ions, we performed analogous pressure-dependent rate studies on the Na^+–Cl^- ion-pair dissociation reaction in water. In Figure 5, we show the PMFs for Na^+–Cl^- ion pair in water at three different pressures. Similar to the trend observed for Li^+ and the halides, PMFs for the Na^+–Cl^- pair also exhibit decreasing barrier heights as pressure increases, resulting in an increase of the value of rate constants as the pressure increases. Using TST rate constants, we obtained an activation volume of −2.4 cm^3/mol. In Figure 6, we present the time-dependent transmission coefficient $\kappa(t)$ for a Na^+–Cl^- pair in water at different pressures. It can be seen that the transmission coefficients decrease as the pressure increases. This trend is similar to the trend observed for halides and opposite to that observed for Li^+. The actual rate constants from the RF method show a decreasing trend with increasing pressure. We computed the relaxation times $t_{RF} = (\kappa_{RF} k^{TST})^{-1}$ using rate constants obtained using the RF method. The relaxation time for the ion-pair dissociation at 0 MPa obtained from our simulation is 22.5 ps, which is comparable to 20 ps reported by Chandler and coworkers. The activation volume computed from the rate constants of the RF method is

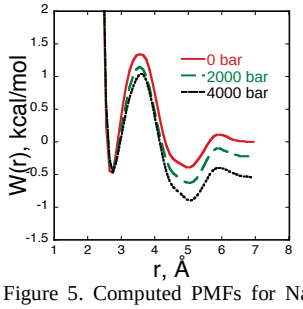

Figure 5. Computed PMFs for Na^+-Cl^- pairs in water.

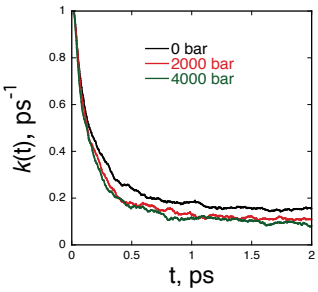

Figure 6. Computed *k(t)* of Na^+-Cl^- systems from RF method

1.58 cm^3/mol. By applying the same mechanistic interpretation of activation volume to the ion-pair dissociation reaction, it appears that the Na^+–Cl^- pair in water exhibits an S_N1 type, or dissociative, mechanism according the RF method. This means that, at the transition state, bond breaking dominates; that is, the chloride ion leaves the first solvation shell of Na^+, followed by a water molecule entering the first solvation shell. For comparison, we also computed the time-dependent friction kernels shown in Figure 7. The transmission coefficient does not change significantly with pressure. There, the rate constants obtained using GH theory, $\kappa_{GH} k^{TST}$ follow the same trend as TST rate constants.

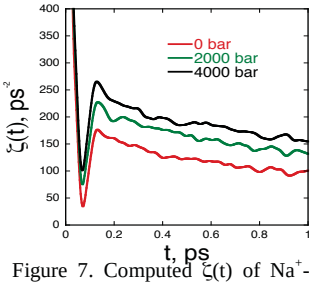

Figure 7. Computed ζ(t) of Na^+-Cl^- systems computed from GH theory

5. Conclusions and Outlook

We present a summary of our recent studies of the dynamics of the ion-solvation process. We used the rate theory approach to determine the solvent-exchange rates. Also, analogous to experimental procedures, we computed pressure-dependent rates to determine the activation volume, which is a key indicator for the solvent-exchange mechanism. We performed a systematic study using four systems: 1) a pure solvent, 2) a cation (Li^+), 3) anions (halides), and 4) an ion-pair (Na^+–Cl^-) dissociation process. From our results, we notice that, because of the decrease in barrier heights, TST rate constants increase as pressure increases for all the cases. Therefore, TST results for all the cases give a negative activation volume, which is indicative of an associative mechanism. We also computed pressure-dependent rate constants using the RF method, which takes in to account recrossings induced by solvent dynamics. We are interested in expanding our current study/method into studies of ion solvation at the interfaces. Our future research effort will focus on understanding the influence of nuclear quantum mechanical effects on the properties of ions in aqueous solution such as the water-exchange rate and the corresponding transmission coefficients using ring-polymer MD techniques. Ring-polymer MD rate theory is a straightforward quantum generalization of the Bennett-Chandler method that we have used to calculate the correct classical transmission coefficient (i.e., the RF method); therefore, we will simply use this method.

References to publications of DOE sponsored research (2013-Present)

1. Understanding Ion-Ion Interactions in Bulk and Aqueous Interfaces using Molecular Simulations. L. X. Dang, Sun, Xiuquan; Ginovska-Pangovska, Bojana; et al. Faraday Discussions 160, 151 (**2013**).

2. Pairing Mechanism among Ionic Liquid Ions in Aqueous Solutions. A Molecular Dynamics Study, Harsha V. R. Annapureddy and L. X. Dang, *J. Phys. Chem. B*, 117, 8555 *(***2013**).

3. Computational Studies of Water Exchange around Aqueous Li^+ with Polarizable Potential Models. L. X. Dang and H.V. R. Annapureddy, *J. Chem. Phys.139*, 084506 (**2013).**

4. Water Exchange Rates and Molecular Mechanism around Aqueous Halide Ions. Annapureddy, H. V. R. and L. X. Dang. *Phys. Chem. B, 118*, 7886 (**2014**).

5. Understanding the Rates and Molecular Mechanism of Water-Exchange around Aqueous Ions Using Molecular Simulations. Annapureddy, H. V. R. and L. X. Dang *J. Phys. Chem. B, 118*, 8917 (**2014**).

6. Computational Studies of Water-Exchange Rates around Aqueous Mg^{2+} and Be^{2+}. L. X. Dang, *J. Phys. Chem. B***, DOI:** 10.1021/jp503243x (**2014**).

7. Fluorocarbon Adsorption in Hierarchical Porous Frameworks. Motkuri RK, HVR Annapureddy, M Vijaykumar, HT Schaef, PF Martin, BP McGrail, L. X. Dang, R Krishna, and PK Thallapally. **2014. Nature Communications** 5:4368. DOI: 10.1038/ncomms5368.

8. A Comparative Study of the Adsorption of Water and Methanol in Zeolite BEA: A Molecular Simulation Study. Van T. Nguyen, Phuong T. M. Nguyen, L. X. Dang, Donghai Mei, Collin D. Wick and Duong D. Do, Molecular Simulation. DOI:10.1080/08927022.2013.848280. Published online: 09 Jan **2014**.

9. Computational Studies of [Bmim][PF_6]/n-Alcohol Interfaces with Many-Body Potentials. Chang, Tsun-Mei and L. X. Dang, *J. Phys. Chem.* A (**2014**). **DOI:** 10.1021/jp405910k.

Transition Metal-Molecular Interactions Studied with Cluster Ion Infrared Spectroscopy

DE-FG02-96ER14658

Michael A. Duncan

Department of Chemistry, University of Georgia, Athens, GA 30602

maduncan@uga.edu

Program Scope

Our research program investigates gas phase metal clusters and metal cation-molecular complexes as models for heterogeneous catalysis, metal-ligand bonding and metal ion solvation. The clusters studied are molecular sized aggregates of metal or metal oxides. We focus on metal-ligand interactions with species such as benzene or carbon monoxide, and on solvation interactions exemplified by complexes with water, acetonitrile, etc. These studies investigate the nature of the metal-molecular interactions and how they vary with metal composition and cluster size. To obtain size-specific information, we focus on ionized complexes that can be mass selected. Infrared photodissociation spectroscopy is employed to measure the vibrational spectroscopy of these ionized complexes. The vibrational frequencies measured are compared to those for the corresponding free molecular ligands and with the predictions of theory to elucidate the electronic state and geometric structure of the system. Experimental measurements are supplemented with calculations using density functional theory (DFT) with standard functionals such as B3LYP. In new experiments photofragment imaging methods are employed as a new way to probe low frequency vibrations and metal-molecular bond energies.

Recent Progress

The main focus of our recent work has been infrared spectroscopy of transition metal cation-molecular complexes with carbon monoxide, water and benzene. These species are produced by laser vaporization in a pulsed-nozzle cluster source, size-selected with a specially designed reflectron time-of-flight mass spectrometer and studied with infrared photodissociation spectroscopy using an IR optical parametric oscillator laser system (OPO). In studies on complexes of a variety of transition metals, we examine the shift in the frequency for selected vibrational modes in the adsorbate/ligand/solvent molecule that occur upon binding to the metal. The number and frequencies of IR-active modes reveal the structures of these systems, while sudden changes in spectra or dissociation yields reveal the coordination number for the metal ion. In some systems, new bands are found at a certain complex size corresponding to intra-cluster reaction products. In small complexes with strong bonding, we use the method of rare gas "tagging" with argon or neon to enhance dissociation yields. In all of these systems, we employ a close interaction with theory to investigate the details of the metal-molecular interactions that best explain the spectroscopy. We perform density functional theory (DFT) calculations (using Gaussian 03W or GAMESS) and when higher level methods are required, we collaborate with theorists. Our infrared data on these metal

ion-molecule complexes provide many examples of unanticipated structural and dynamical information. A crucial aspect of these studies is the infrared laser system, which is an infrared optical parametric oscillator/amplifier system (OPO/OPA; Laser Vision). This system covers the infrared region of 600-4500 cm^{-1} with a linewidth of ~1.0 cm^{-1}. In new work, we have added a photofragment imaging instrument to our existing molecular beam machine for the study of the dissociation dynamics of mass-selected metal-molecular ions. This new methodology makes it possible to investigate metal-ligand vibrations at lower frequencies and to determine bond energies for hard-to-study cation-molecular complexes.

Transition metal carbonyls provide classic examples of metal-ligand bonding, and carbon monoxide is the classic probe molecule for surface science and catalysis. We have investigated transition metal *cation* carbonyls to compare these to corresponding neutral carbonyls known to be stable. The stability of these systems is conveniently explained with the 18-electron rule, and this is a guiding principle for our cation work. We studied the $Co^+(CO)_n$, $Mn^+(CO)_n$ and $Cu^+(CO)_n$ complexes, which formed complexes isoelectronic to neutral $Fe(CO)_5$, $Cr(CO)_6$ and $Ni(CO)_4$, respectively. The cation complexes had a filled coordination at the expected sizes, and they had the same structures as the corresponding neutrals (trigonal pyramid, octahedral, tetrahedral). However, the frequencies of the CO stretch vibrations, which are strongly red-shifted in the neutrals, were hardly shifted at all for the cations. This trend was attributed to the reduced π back-bonding in the cation systems.

A longstanding goal in inorganic chemistry has been to test the limits of the 18-electron rule in situations requiring unusual coordination numbers. Newer studies have extended this work to the early transition metals, which have fewer d electrons and require more CO ligands to achieve an 18-electron configuration. In studies of titanium, zirconium and hafnium cation carbonyls, we found that each of these complexes form six-coordinate complexes with octahedral structures. The red shifts of the C–O stretches were among the largest yet seen, and these increased for the heavier metals. The group III metals scandium and yttrium have fewer-still electrons, and would form 18-electron complexes if they have eight carbonyl ligands. We found that the coordination of the scandium complexes was only seven, but that yttrium did indeed form the unusual eight-coordinate carbonyls. Although rhodium is isoelectronic to cobalt, its primary coordination was four, with a 16-electron square-planar structure for the $Rh^+(CO)_4$ complex. We found the same structure and coordination for the nitrogen complexes of rhodium. In both cases, the bonding has a large component of electrostatics, which yields a blue-shifted carbonyl stretch, but a red-shifted N–N stretch. Extending the metal carbonyl work, we examined metal *dimer* carbonyls of vanadium, copper and cobalt. The carbonyl coordination of Cu_2 was found to be six, while that of V_2 was found to be seven. However, computational studies on these dimer systems were found to be much more difficult than their atomic metal counterparts.

In a study of metal-benzene complexes, we investigate aluminum-benzene cations with up to four benzenes. Spectra in the fingerprint region reveal the nature of benzene ring vibrations and how they are affected by metal complexation. Computational studies and IR spectra indicate that aluminum forms a tri-benzene complex rather than a di-benzene sandwich as its completed coordination. Spectra in the fingerprint region for vanadium-benzene and vanadium-dibenzene found evidence for distortion of the benzene ring in a "buckling" configuration.

Metal ion-water studies focused on titanium-, vanadium- and niobium-water systems. Rotationally resolved spectra were obtained for $Ti^+(H_2O)$ and $Nb^+(H_2O)$, but the

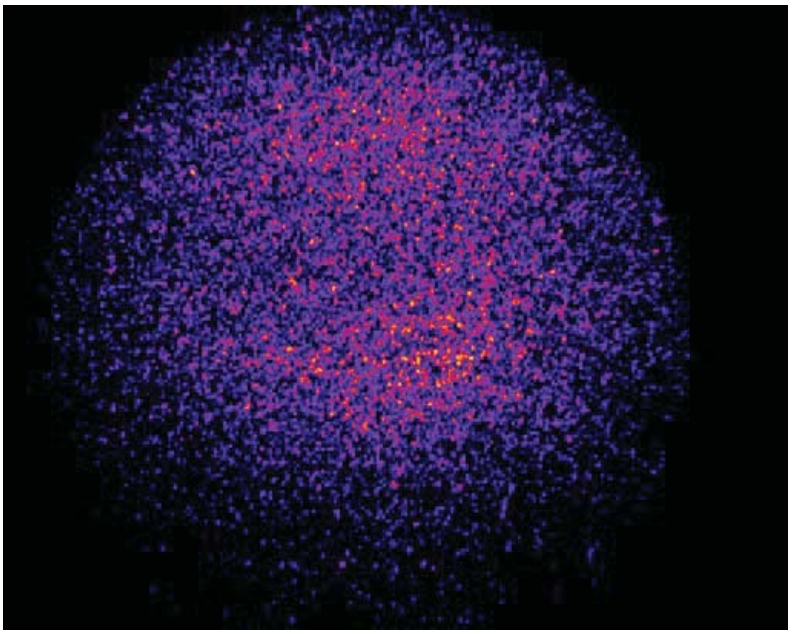

Figure 1. The photofragment image of the benzene cation from the charge-transfer dissociation of Ag^+-benzene.

spectra obtained did not agree with the predictions of density functional theory for these complexes. Theory indicates planar C_{2v} structures, consistent with expectations for charge-dipole bonding, but the rotational patterns indicate non-planar structures. Improved computational work on these systems is in progress.

Significant progress has been made in the last few month in bringing our new photofragment imaging experiment on-line. Initial experiments obtained images for the charge-transfer dissociation of Ag^+-benzene (Figure 1), finding evidence for a bond energy ($\leq$30.6 kcal/mol) lower than previous estimates.

Future Plans

Our work in the immediate future will continue theory on metal-water complexes of titanium and niobium, continue the ongoing experiments on vanadium-benzene complexes, and focus on the continued development of photofragment imaging experiments. We are particularly interested in applying this method to the photodissociation of dication-water complexes to obtain improved information about the bond energies in these systems, which are difficult to measure by other methods.

Publications (1/2012–present) for this Project

1. A. D. Brathwaite and M. A. Duncan, "Infrared spectroscopy of $Si(CO)_n^+$ complexes: Evidence for asymmetric coordination," *J. Phys. Chem. A* **116**, 1375–1382 (2012). **DOI:** 10.1021/jp211578t.

2. R. Garza-Galindo, M. Castro and M. A. Duncan, "Theoretical study of nascent hydration in the $Fe^{+}(H_2O)_n$ system," *J. Phys. Chem. A* **116**, 1906–1913 (2012). **DOI:** 10.1021/jp2117533l.

3. B. Bandyopadhyay and M. A. Duncan, "Infrared spectroscopy of $V^{2+}(H_2O)$ complexes," *Chem. Phys. Lett.* **530**, 10–15 (2012). **DOI:** 10.1016/j.cplett.2012.01.048.

4. M. A. Duncan, "Laser Vaporization Cluster Sources," *Rev. Sci. Instrum.* **83**, 041101/1–19 (2012)(invited review). **DOI:** 10.1063/1.3697599. Selected for April 23, 2012 issue of *Virtual Journal of Nanoscale Science & Technology*, published by AIP.

5. A. M. Ricks, A. D. Brathwaite, M. A. Duncan, "Coordination and spin states of $V^{+}(CO)_n$ clusters revealed by IR spectroscopy," *J. Phys. Chem. A* **117**, 1001–1010 (2013). (Peter Armentrout Festschrift) **DOI:** 10.1021/jp301679m.

6. B. Bandyopadhyay, K. N. Reishus, M. A. Duncan, " Infrared spectroscopy of solvation in small $Zn^{+}(H_2O)_n$ Complexes," *J. Phys. Chem. A* **117**, 7794−7803 (2013). **DOI:** 10.1021/jp4046676.

7. A. M. Ricks, A. D. Brathwaite, M. A. Duncan, "IR spectroscopy of $V^{+}(CO_2)_n$ clusters: Solvation-induced electron transfer and activation of CO_2," *J. Phys. Chem. A* **117**, 11490–11498 (2013). **DOI:** 10.1021/jp4089035.

8. A. D. Brathwaite, M. A. Duncan, " Infrared photodissociation spectroscopy of saturated group IV (Ti, Zr, Hf) metal carbonyl cations," *J. Phys. Chem. A* **117**, 11695–11703 (2013)**.** (Curt Wittig Festschrift). **DOI:** 10.1021/jp400793h.

9. M. Castro, R. Flores, M. A. Duncan, "Theoretical study of nascent solvation in $Ni^{+}(benzene)_m$, m=3 and 4, clusters," *J. Phys. Chem. A* **117**, 12546−12559 (2013). **DOI:** 10.1021/jp406581m.

10. A. D. Brathwaite, A. M. Ricks, M. A. Duncan, "Infrared spectroscopy of vanadium oxide carbonyl cations," *J. Phys. Chem. A* **117**, 13435−13442 (2013). (Terry Miller festschrift) **DOI:** 10.1021/jp4068697.

11. A. D. Brathwaite, J. A. Maner, M. A. Duncan, "Testing the limits of the 18-electron rule: The gas phase carbonyls of Sc^{+} and Y^{+}," *Inorg. Chem.* **53**, 1166–1169 (2014). **DOI:** 10.1021/ic402729g.

12. K. N. Reishus, A. D. Brathwaite, J. D. Mosley, M. A. Duncan, "Infrared spectroscopy of coordination versus solvation in $Al^{+}(benzene)_{1-4}$ complexes," *J. Phys. Chem. A*, in press (Ken Jordan festschrift). **DOI:** 10.1021/jp500778w.

Statistical Mechanical and Mesoscale Modeling of Catalytic Reactions

Jim Evans (PI) and Da-Jiang Liu
Ames Laboratory – USDOE and Departments of Physics & Astronomy and Mathematics,
Iowa State University, Ames, IA 50011
evans@ameslab.gov

PROGRAM SCOPE:

This theoretical Chemical Physics project at Ames Laboratory pursues molecular-level modeling of **heterogeneous catalysis and other complex reaction phenomena** at surfaces and in mesoporous materials. The effort incorporates: *electronic structure analysis; non-equilibrium statistical mechanics; coarse-grained meso- or multi-scale modeling*. The *electronic structure* component includes DFT-VASP analysis of chemisorption and reaction energetics on metal surfaces, and *ab-initio* QM studies in collaboration with Mark Gordon. The *non-equilibrium statistical mechanical and related studies* of reaction-diffusion phenomena include Kinetic Monte Carlo (KMC) simulation of atomistic models, coarse-graining, and heterogeneous multi-scale formulations. We explore: (i) the interplay between anomalous transport and catalytic reaction in functionalized mesoporous materials in collaboration with Ames Lab experimentalists; (ii) chemisorption and heterogeneous catalysis on metal surfaces including: bifurcations in reactive steady-states; TPR and titration kinetics; connecting atomistic to spatiotemporal mesoscale behavior; (iii) statistical mechanics of reaction-diffusion processes exhibiting non-equilibrium phase transitions, metastability, critical phenomena, etc.. (iv) other surface phenomena: complex formation; surface dynamics; reaction on non-conducting surfaces.

RECENT PROGRESS:

CATALYTIC REACTIONS IN FUNCTIONALIZED NANOPOROUS MATERIALS

Recent efforts have considered catalytic conversion reactions occurring inside linear nanopores of zeolites or functionalized mesoporous silica nanospheres (MSN) with inhibited passing of reactants and products [3,5,7,11,15]. These studies are motivated by experiments at Ames Laboratory, e.g., conversion of PNB to an aldol compound, and esterification reactions, in MSN [7,15]. Extensive previous analyses of such systems (mostly for catalysis in zeolites) had produced only partial understanding of such basic issues such as limited reactant penetration into pores (resulting in low reactivity). We showed that mean-field reaction-diffusion equation (RDE) treatments fail to describe behavior, as do "hydrodynamic" treatments. For similar mobility of reactants and products, we developed a successful "generalized hydrodynamic" treatment incorporating fluctuation effects near pore openings [5]. This theory exploited: (i) a relation between chemical diffusion fluxes appearing in the RDE and tracer diffusivity; and (ii) a generalized tracer diffusion coefficient, D_{tr} which is enhanced near pore openings. We have continued analysis of the strong spatial correlations generated by reaction subject to single-file diffusion, noting that these can impact reaction kinetics. We are exploring extensions of the theory to unequal mobilities of reactants and products, and alternative analyses of the generalized D_{tr} from concentration profiles for so-called counter-diffusion modes.

Reactivity increases strongly with the propensity, P, of reactants and products to pass each other inside narrow pores. Only one previous study analyzed P based on the effective free energy versus separation along the pore, applying transition state theory (TST). We performed detailed Langevin simulations of reactant-product pairs, and characterized the vanishing of P

approaching pore diameter where passing is blocked by steric effects [11]. TST fails in this regime. Actual behavior was explained by analysis of the appropriate Fokker-Planck equations (a diffusion equation in high dimension) [11]. Judicious approximation reduced the problem to a 2D diffusion equation where conformal mapping ideas further elucidated behavior.

CHEMISORPTION AND HETEROGENEOUS CATALYSIS ON METAL SURFACES

Realistic multi-site lattice-gas (msLG) modeling of catalytic reaction processes. A long-standing goal for theoretical surface science has been to develop realistic molecular-level models for catalytic reaction processes on metal surfaces (incorporating adsorption, desorption, diffusion, and reaction). We have continued development and application of msLG models and efficient KMC simulation algorithms to describe oxidation reactions on unreconstructed metal surfaces. Reactive steady-states are impacted not only by adlayer thermodynamics, but also by kinetics. Thus, we have developed more realistic models for dissociative adsorption of oxygen on mixed reactant adlayers on metal(100) surfaces. DFT analysis shows that the traditional Langmuir picture of dissociation onto nearest-neighbor (NN) sites, and also the Brundle-Behm-Barker model for constrained dissociation on diagonal NN sites, do not apply. Instead dissociation typically prefers a pathway via neighboring vicinal br sites [9]. This picture was used to develop tailored models where analytic treatment is possible to assess sticking behavior [10]. We also developed realistic CO-adsorption models including steering and funneling.

Extensive DFT analysis has been performed to determine adspecies interactions for CO+O on unreconstructed (100) surfaces of Pd, Rh, Ir, and Pt [8]. These interactions, together with the above refined adsorption models, were incorporated into msLG CO-oxidation models. These models refined our previous models for Pd and Rh, and constituted the first detailed models for Ir and Pt (where O-ordering is quite distinct). The models were used to assess: sticking, adsorption energetics, TPD for separately for CO and O; bifurcations of reactive steady-states, titration and TPR kinetics [8]. Extensive comparison was made with experiment [8].

Chemisorption, complex formation, self-assembly. Detailed and precise characterization of chemisorption processes is key for modeling of catalytic reactions, e.g., to describe reactant ordering, possible chemisorption-induced restructuring and dynamics of metal surfaces, and poisoning and/or promotion by impurities such as sulfur (S). Our previous DFT analyses explored formation of “small” Ag-S complexes on Ag surfaces and related enhanced decay of Ag nanoclusters [6]. These studies were extended to Cu (and also Au) surfaces confirming the existence of a stable Cu_2S_3 complex on Cu(111). Recently, and extensive DFT analysis was also performed to assess viable structure models for S-induced reconstructions on Cu [14]. Finally, for a metal-on-metal system, Liu provided key DFT energetics enabling modeling of far-from-equilibrium self-assembly of bimetallic 2D epitaxial Au-Ag nanoclusters on Ag(100) [12].

FUNDAMENTAL PHENOMENA IN FAR-FROM-EQUILIBRIUM REACTION SYSTEMS

An understanding of discontinuous non-equilibrium phase transitions (such as catalytic poisoning transitions) and associated metastability and criticality at a level comparable to that for equilibrium systems constitutes a ***BESAC Science Grand Challenges*** *(Cardinal Principles of Behavior beyond Equilibrium)*. We continue statistical mechanical studies of Schloegl type models for autocatalysis which exhibit discontinuous transitions between reactive and poisoned states [1,2]. We find “generic two-phase coexistence” distinct from thermodynamic systems, but similar metastablity and nucleation phenomena. We attempt to address a central challenge of developing a theory for the nucleation rate for these non-equilibrium systems in the absence of

the usual free-energy framework (by instead assuming the existence of a free-energy type Lyapunov functional governing evolution) [8]. Predicted behavior is consistent with simulation studies of nucleation kinetics. Other on-going work has focused on mean-field type treatments of critical droplet behavior based on discrete reaction-diffusion equations.

FUTURE PLANS:

CATALYTIC REACTIONS IN FUNCTIONALIZED MESOPOROUS MATERIALS

A key goal is the development of system-specific models for catalytic conversion reactions in mesoporous materials including MSN. One key component is determination of the passing propensity, P, for appropriately-shaped reactant and product molecules versus pore diameter, d_p, as reactivity is strongly dependent on P and d_p (as observed at Ames Lab for PNB conversion to an aldol). Our Langevin modeling will be extended to account for rotational diffusivity of non-spherical molecules. We will assess the utility of approximate reduced-dimensional Fokker-Planck formulations. Also, we will continue efforts to extend of our generalized hydrodynamic treatment, e.g., to describe greatly differing reactant/product mobilities, cooperativity in reaction kinetics (e.g., concentration-dependence of diasteroselective reactions studied at Ames Lab), etc.

CHEMISORPTION AND HETEROGENEOUS CATALYSIS ON METAL SURFACES

We will continue development of realistic and predictive atomistic-level models and KMC simulation algorithms for **catalytic reactions** on various metal (111) and (100) surfaces. Characterization of catalytic ignition for oxidation reactions, and also reaction front propagation, is provided by recent PEEM studies by Rupprechter *et al.* Our models are uniquely positioned to elucidate this behavior. Also of interest are: the development of analytic rate equation treatment for realistic reaction models (providing more insight than KMC simulation); analysis of more complex adlayer ordering and reaction kinetics (e.g., multistability) for higher pressures. There are also multiscale modeling challenges, e.g., concentration variations across polycrystalline catalysts surface as used in recent PEEM studies, which can be studied utilizing our HCLG multiscale modeling approach [8]. For more general **chemisorption systems**, we are interested in exploring ordering and diffusive dynamics in chemisorbed layers (including high-density O adlayers on Pt(111) in EPOC studies by Imbihl), formation of metal complexes and metal surface dynamics (e.g., for chalcogens and halogens of various noble metal surfaces with Thiel).

OTHER STUDIES OF SURFACE ADSORPTION, DIFFUSION AND REACTION

We have initiated comparative ab-initio QM and DFT analysis with the Gordon group of chemisorption energetics on small metal clusters to assess the DFT error. Then, suitable extrapolation should yield more precise energetics for extended metal surfaces, correcting the well-known shortcomings of DFT in predicting site-specific adsorption energies and diffusion barriers. This continues our high-level QM and QM/MM analysis with Gordon of key surface diffusion and reaction processes (to provide input to molecular-level KMC and coarse-grained modeling). Another new effort will consider catalytic reaction in the high-pressure regime where metal surfaces can be oxidized. In this regime, surface mobility is highly limited, so behavior can be controlled by strong correlations and fluctuations (similar to behavior in the models below).

FUNDAMENTAL PHENOMENA IN FAR-FROM-EQUILIBRIUM REACTION SYSTEMS

Analysis will continue of non-equilibrium 1^{st}-order phase transitions, especially issues of metstability and nucleation, in a variety of statistical mechanical reaction-diffusion models. We

are extending these analyses to various ZGB-type surface reaction models, which although too simplistic to describe standard low-pressure reaction behavior, may provide a valuable paradigm for high-pressure high-coverage low-effective-surface-mobility fluctuation-dominated reactions.

PUBLICATIONS WITH BES CPIMS SUPPORT FOR 2012-PRESENT: *Partial BES support.

[1] *Tricriticality in generalized Schloegl models for autocatalysis: Lattice-gas realization with particle diffusion*, X. Guo, D.K. Unruh, D.-J. Liu, J.W. Evans, Physica A **391**, 633 (2012).

[2] *Schloegl's second model for autocatalysis on hypercubic lattices: Dimension-dependence of generic two-phase coexistence*, C.-J. Wang, D.-J. Liu, J.W. Evans, Phys. Rev. E, **85**, 041109 (2012).

[3] *Conversion reactions in surface-functionalized mesoporous materials*, J. Wang, D. Ackerman, K. Kandel, I.I. Slowing, M. Pruski, J.W. Evans, MRS Proc. Symp. RR Fall 2011 (MRS, Pittsburgh, 2012).

[4] *Morphological evolution during growth and erosion on vicinal Si(100) surfaces: From electronic structure to atomistic and coarse-grained modeling*, D.-J. Liu, D.M. Ackerman, X. Guo, M.A. Albao, L. Roskop, M.S. Gordon, J.W. Evans, MRS Proc. Symp. EE Fall 2011 (MRS, Pittsburgh, 2012).

[5] *Generalized hydrodynamic treatment of interplay between restricted transport & catalytic reactions in nanoporous materials*, D.M. Ackerman, J. Wang, J.W. Evans, Phys. Rev. Lett., **108**, 228301 (2012).

[6] *Structure, Formation, and Equilibration of Ensembles of Ag-S Complexes on an Ag Surface*, S. Russell, Y. Kim, D.-J. Liu, J.W. Evans, P.A. Thiel, J. Chem. Phys., **138**, 071101 (2013). (Journal Cover)*

[7] *Controlling reactivity in nanoporous catalysts by tuning reaction product – pore interior interactions: statistical mechanical modeling*, J. Wang, D.M. Ackerman, V.S.-Y. Lin, M. Pruski, J.W. Evans, J. Chem. Phys. **138**, 134705 (2013).

[8] *Realistic multisite lattice-gas modeling and KMC simulation of catalytic surface reactions: Kinetics and multiscale spatial behavior for CO-oxidation on metal(100) surfaces,* D.-J. Liu, J.W. Evans, Progress in Surface Science, **88**, 393-521 (2013).

[9] *Dissociative adsorption of O2 on unreconstructed metal(100) surfaces: Pathways, energetics, and sticking kinetics*, D.-J. Liu, J.W. Evans, Phys. Rev. B **89**, 205406 (2014)

[10] *Statistical mechanical models for dissociative adsorption of O2 on metal(100) surfaces with blocking, steering, and funneling*, J.W. Evans, D.-J. Liu, J. Chem. Phys . **140**, 194704 (2014).

[11] *Langevin and Fokker-Planck analyses of inhibited molecular passing processes controlling transport and reactivity in nanoporous materials*, D.M. Ackerman, C.-J. Wang, I.I. Slowing, J.W. Evans, Phys. Rev. Lett. **113**, 038301 (2014)

[12] *Real-time ab-initio KMC simulation of the self-assembly and sintering of bimetallic nanoclusters on fcc(100) surfaces: Au+Ag on Ag(100),* Y. Han, D.-J. Liu, J.W. Evans, Nano Letters, **14**, 4646 (2014).*

[13] *Transition and Noble Metals on the (0001) Surface of Graphite: Fundamental Aspects of Adsorption, Diffusion, and Morphology*, D. Appy, H. Lei, C.-Z. Wang, M.C. Tringides, D.-J. Liu, J.W. Evans, and P.A. Thiel, Progress in Surface Science, in press (2014).*

[14] *A search for the structure of sulfur-induced reconstruction on Cu(111)*, D.-J. Liu, H. Walen, J. Oh, H. Lim, J.W. Evans, Y. Kim, P.A. Thiel, J. Phys. Chem. C, in press (2014).*

[15] *Multi-functionalization of nanoporous catalytic materials to enhance reaction yield: Statistical mechanical modeling for conversion reactions with restricted diffusive transport*, J. Wang, A. Garcia, D.M. Ackerman, M.S. Gordon, I.I. Slowing, T. Kobayashi, M. Pruski, J.W. Evans, MRS Proc. Symp. AA Fall 2013 (MRS, Pittsburgh, 2014).

Confinement, Interfaces, and Ions: Dynamics and Interactions in Water, Proton Transfer, and Room Temperature Ionic Liquid Systems (DE-FG03-84ER13251)

Michael D. Fayer
Department of Chemistry, Stanford University, Stanford, CA 94305
fayer@stanford.edu

Organized surfactants play an important role in many chemical and biological processes. One example is reverse micelles, in which a surfactant encloses a nanoscopic size pool of water. In the past, we have done extensive studies on the dynamics of water in reverse micelles. Another important class of organized surfactants is bilayers, in which there are two surfactant "leaflets" that compose the bilayer. These surfactants organize such that charged head groups are on the surface of the bilayer in contact with water and organic chains form the interior of the bilayers. We have studied the dynamics of water at the surface of AOT bilayers in the form of lamellar structures. Very recently we made the first measurements of ultrafast dynamics inside of AOT bilayers using two dimensional infrared (2D IR) spectroscopy of a vibrational dynamics probe that locates in the organic interior of the bilayers. We have now greatly extended these studies to a very important class of surfactants, phospholipids.

The ultrafast dynamics in the interior of planar aligned multibilayers of 1,2-Dilauroyl-*sn*-glycero-3-phosphocholine (Dilauroylphosphatidylcholine, DLPC) were investigated using 2D IR vibrational echo spectroscopy.[11] The non-polar and water insoluble vibrational dynamics probe, tungsten hexacarbonyl ($W(CO)_6$), locates in the alkane interior of the membranes. The 2D IR experiments were conducted on the antisymmetric CO stretching mode of $W(CO)_6$ to measure spectral diffusion caused by the structural dynamics of the membrane from ~200 fs to ~200 ps as a function of the number of water molecules hydrating the head groups and as a function of cholesterol content for a fixed hydration level.

Because the samples tend to scatter light to a significant extent, the methodology of IR pulse shaping was used to perform the 2D IR experiments. The mid-infrared pulse, generated with a Ti:Sapphire pumped optical parametric amplifier, was split into a weaker probe pulse and a stronger pulse. The weak pulse is routed through a mechanical delay line, which is used to set the waiting time T_w (see below). The strong pulse was sent to a mid-infrared Fourier-domain pulse-shaper. The output from the pulse shaper, which produces pulses 1 and 2 in the vibrational echo pulse sequence, was crossed in the sample with the weak probe pulse. The probe is sent into a spectrograph equipped with a 32 element HgCdTe infrared array detector.

In a 2D IR vibration echo experiment, τ (the time between pulses 1 and 2) is scanned for a fixed T_w (delay between pulse 2 and 3), which produces a probe pulse temporal interferogram at each wavelength measured by the spectrograph. Fourier transforming the interferograms gives the horizontal axis and the spectrograph output gives the vertical axis of the 2D IR spectrum. Then T_w is changed, and τ is scanned to obtain another 2D spectrum. A series of such spectra was recorded for various T_w . The desired information is contained in the T_w dependence of shapes of the bands in the 2D spectrum (spectral diffusion). The advantages of doing the experiments with the pulse shaping 2D IR spectrometer involve the ability to control the relative phases of the pulses in the sequence and to change the phase of the radiation field across each pulse. By controlling the relative phase, it was possible to use a phased cycled sequence of pulses that greatly reduces the deleterious effects of scattered light. In addition, control of the phase across the bandwidth of the IR pulse permits the experiments to be conducted in a partially rotating frame. In the partially rotating frame, there is a great reduction in the number of time points that must be acquired to obtain an interferogram. This allows more signal averaging in a greatly reduce experimental time.

FT-IR studies of the lipid bilayers and the model liquids, hexadecane and bis(2-ethylhexyl) succinate, demonstrated that as the number of hydrating water molecules increases from 2 to 16, there are structural changes in the membrane that partition some of the $W(CO)_6$ into the ester region of DLPC. However, the 2D IR measurements, which are made solely on the $W(CO)_6$ in the alkane regions, show that the level of hydration had no observable impact on the interior membrane dynamics. FT-IR spectra and 2D IR experiments on partially hydrated (8 water molecules per head group) planar bilayers with cholesterol concentrations from 0% to 60% demonstrated that there was a change in the membrane structure and an abrupt change in dynamics at 35% cholesterol. The dynamics are independent of cholesterol content from 10% to 35%. At 35%, the dynamics become slower and remain unchanged from 35% to 60% cholesterol. Thus, the addition of cholesterol induces a phase transition the causes a decrease in the ultrafast dynamics in the interior of the bilayers.

The question arises as to the influence of curvature on bilayer dynamics. To address this question we studied a series of phospholipid vesicles with well defined sizes.[12] The ultrafast structural dynamics inside the bilayers of DLPC and dipalmitoylphosphatidylcholine (DPPC) vesicles with 70 nm, 90 m and 125 nm diameters were directly measured with 2D IR vibrational echo spectroscopy again using the antisymmetric CO stretch of $W(CO)_6$ as a vibrational probe to measure spectral diffusion (structural dynamics) in the alkyl region of the bilayers. Although the CO stretch absorption spectra remained the same, the interior structural dynamics were observed to be faster as the size of the vesicles was decreased, with the size dependence greater for DPPC than for DLPC. As DLPC vesicles become larger, the interior dynamics approach those of the planar DLPC bilayers. In many biological processes and chemical applications, the interior of bilayers serve as the solvent bath for the chemical processes. As in any chemical process in a solvent, the structural fluctuation of the solvent can play an important role in the chemistry, for example, taking reactants to the transition state. The comparisons of the structural dynamics of different size vesicles with those of planar bilayers show that the radius of curvature has a significant effect on the time scales of the structural dynamics. Eukaryotic cells range in size from 10 μm to 30 μm. The cell membranes are close to planar, having negligible radius of curvature. This is in contrast to vesicles, which are relatively small and have significant radii of curvature. The 2D IR results show that the choice of the type of bilayer used in model studies needs to be considered because of the curvature dependence of the dynamics. In the 2D IR measurements of structural evolution by observing and quantifying the spectral diffusion, it was found that the data were well described by two time constants. As an example of the influence of curvature on dynamics, the time constants for DLPC 70 nm vesicles were found to be 4 ps and 26 ps, while the time constants for planar DLPC bilayers are 8 ps and 35 ps.

The influence of cholesterol concentration was also studied in vesicles.[13] Samples were studied in which the cholesterol concentration was varied from 0% to 40% in both 70 nm diameter vesicles and fully hydrated (16 water molecules per head group) planar bilayers. It was found that at all cholesterol concentrations, the structural dynamics were faster in the curved vesicle bilayers than in the planar bilayers. As the cholesterol concentration was increased, as discussed above, at a certain concentration there is a sudden change in the dynamics, that is, the dynamics abruptly slow down. However, this change occurs at a lower concentration in the vesicles (between 10% and 15% cholesterol) than in the planar bilayers (between 25% and 30% cholesterol for the fully hydrated bilayers). The sudden change in the dynamics, in addition to other IR observables, indicates a structural transition. The results show that the cholesterol concentration at which the transition occurs is influenced by the curvature of the bilayers.

Room temperature ionic liquids (RTILs), salts with a melting point near or below room temperature, have garnered much interest in the past decade due to their very low volatility,

enormous variability, and good thermal stability. They are often composed of an inorganic anion paired with an asymmetric organic cation that contains one or more pendant alkyl chains. The asymmetry of the cation frustrates crystallization, causing the salt's melting point to drop significantly. RTILs have applications in electrochemistry, separation processes, and organic synthesis, among others. The presence of ionic groups and alkyl chains leads to a nanoscopic structure in which there are ionic and organic regions. The nature of this structure and the role it plays in RTIL properties and processes, such as reaction or redox chemistry, are important areas of research. Most RTILs are highly hygroscopic. Therefore, understanding the nature of water in RTILs is also important. In addition, RTILs provide a path to the study of water interacting with ions. In normal aqueous salt solutions, such as those formed with KBr or $MgSO_4$, there is always a large amount of water. So water-ion interactions compete with water-water interactions, which cannot be avoided. If the amount of water is reduced too much, the salt crystallizes out of solution. However, RTILs are liquids in which extremely small amounts of water or other co-solvents can be dissolved and the system still remains a liquid.

We have used 2D IR and polarization selective IR pump-probe experiments to study the interactions of RTILs with water, methanol, and ethanol.[14] For each of these, the concentration is so low that the solute only interacts with the RTIL, which is ethylmethylimidazolium bistriflimide (bis(trifluoromethylsulfonyl)imide). In the experiments we study the OD stretching mode of HOD rather than H_2O to have a single local mode to compare to the OD stretches of methanol-OD and ethanol-OD. All three of these molecules are located in the ionic regions of the RTIL, and the hydroxyls hydrogen bond to the bistriflimide anion. FT-IR spectra show very similar OD stretch absorption spectra with HOD, MeOD, and EtOD absorption maxima at 2645.7 cm^{-1}, 2642.4 cm^{-1}, and 2635.5 cm^{-1}, respectively. For comparison, the OD stretch of HOD in bulk water absorbs at 2509 cm^{-1}. The blue shift of the spectra indicates much weaker hydrogen bonding than in bulk water, and the small shifts to the red in going from HOD to the alcohols indicate that the alcohols have slightly stronger hydrogen bonds to the bistriflimide anions. The line widths are 40 cm^{-1} compared to a width of 170 cm^{-1} for HOD in bulk water. The narrower linewidths indicates a smaller range of hydrogen bonding environments than found for HOD in bulk water.

The 2D IR experiments measure spectral diffusion as discussed above. The IR pump-probe experiments measure orientational relaxation. In contrast to the OD stretch of HOD in bulk water, which has a vibrational lifetime of 1.8 ps, in the RTIL the lifetime is 20 ps. The longer lifetime enables us to perform the experiments out to 60 ps, which is sufficiently long to observe the full range of dynamics in the RTIL. The 2D IR experiments give multi-time scales for the structural dynamics that contribute to the inhomogeneously broadened lines. The fastest components for the three solutes are very similar and, in analogy to bulk water, reflect very local hydrogen bond fluctuations. The slowest component of the spectral diffusion arises from the complete randomization of the environments that interact with the hydroxyl stretch of each solute. For the OD stretches of HOD, MeOD, and EtOD the time constants are 23 ps, 28 ps, and 34 ps, respectively. While there is a progression to slower times as the solute gets larger, the change is rather mild given that the mass and volume of the molecules change substantially. The small changes with solute lead us to the conclusion that the dynamic interactions of the solutes with their environments occur through motions of the surrounding ions rather than motions of the solutes themselves. As the solute becomes larger, the hydroxyls are somewhat screened from close interactions with the surrounding ions. This screening may account for the slowing of the dynamics as the solute gets larger.

The polarization selective IR pump-probe experiments were used to measure orientational relaxation of the solutes as a function of wavelength. All of the decays for the three solutes are biexponential, which reflects wobbling-in-a-cone motions followed by complete orientational

relaxation. Wobbling describes the motions on a fast time scale (a few ps depending on the molecule and the wavelength) in which the solute samples a limited range of angles. Then on a much longer time scale (tens of ps), complete orientational relaxation occurs. For the three solutes, the rate of orientational relaxation slows as the molecule gets bigger. The wavelength dependence is particularly interesting. A shift to the red is interpreted in hydrogen bonding systems as arising from stronger hydrogen bonds. We find that as the wavelength shifts to the red, the cone angles become smaller and the both the wobbling and the complete orientational diffusion constants become smaller (orientational motions slow). The changes are substantial, with the slowing going from the blue side to the red side of the absorption lines being factor of approximately two. This is consistent with significantly stronger hydrogen bonding on the red sides of the lines.

Publication from DOE Sponsored Research Last Two Years

1. "Investigation of Nanostructure in Room Temperature Ionic Liquids using Electronic Excitation Transfer," Kendall Fruchey and M. D. Fayer J. Phys. Chem. B 116, 3054-3064 (2012).
2. "Dynamics of Water Interacting with Interfaces, Molecules, and Ions," M. D. Fayer Acc. of Chem. Res. 45, 3-14 (2012).
3. "Orientational Dynamics of Room Temperature Ionic Liquid/Water Mixtures: Evidence for Water-Induced Structure and Anisotropic Cation Solvation," Adam L. Sturlaugson, Kendall S. Fruchey, and M. D. Fayer J. Phys. Chem. B 116, 17**77-1787** (2012).
4. "Water Dynamics in Water/DMSO Binary Mixtures," Daryl B. Wong, Kathleen P. Sokolowsky, Musa I. El-Barghouthi, Emily E. Fenn, Chiara H. Giammanco, Adam L. Sturlaugson, and Michael D. Fayer J. Phys. Chem. B 116, 5479-5490 (2012).
5. "Dynamics of Functionalized Surface Molecular Monolayers Studied with Ultrafast Infrared Spectroscopy," Daniel E. Rosenfeld, Jun Nishida, Chang Yan, Zsolt Gengeliczki, Brian J. Smith, and Michael D. Fayer J. Chem. Phys. C 116, 23428-23440 (2012).
6. "Comparisons of 2D IR Measured Spectral Diffusion in Rotating Frames Using Pulse Shaping and in the Stationary Frame Using the Standard Method," S. K. Karthick Kumar, A. Tamimi, and M. D. Fayer J. Chem. Phys. 137, 184201 (2012).
7. "Water Dynamics in Divalent and Monovalent Concentrated Salt Solutions," Chiara H. Giammanco, Daryl B. Wong, and Michael D. Fayer J. Phys. Chem. B 116, 13781-13792 (2012).
8. "The Dynamics of Isolated Water Molecules in a Sea of Ions
in a Room Temperature Ionic Liquid," Daryl B. Wong, Chiara H. Giammanco, Emily E. Fenn, Michael D. Fayer J. Phys. Chem. B 117, 623-635 (2013).
9. "Structural Dynamics at Monolayer-Liquid Interfaces Probed by 2D IR Spectroscopy," Daniel E. Rosenfeld, Jun Nishida, Chang Yan, S. K. Karthick Kumar, Amr Tamimi, and Michael D. Fayer J. Phys. Chem. C 117, 1409-1420 (2013).
10. "Dynamics in the Interior of AOT Lamellae Investigated with 2D IR Spectroscopy," S. K. Karthick Kumar, A. Tamimi, and Michael D. Fayer J. Am. Chem. Soc. 135, 5118-5126 (2013).
11. "Ultrafast Structural Dynamics inside Planer Phospholipid Multibilayer Model Cell Membranes Measured with 2D IR Spectroscopy," Oksana Kel, Amr Tamimi, Megan C. Thielges, and Michael D. Fayer J. Am. Chem. Soc. 135, 11063-11074 (2013).
12. "Size Dependent Ultrafast Structural Dynamics inside Phospholipid Vesicle Bilayers Measured with 2D IR Vibrational Echo Spectroscopy," Oksana Kel, Amr Tamimi, and Michael D Fayer Proc. Nat. Acad. Sci. U.S.A. 111, 918-923 (2014).
13. "The Influence of Cholesterol on Fast Dynamics Inside of Vesicle and Planar Phospholipid Bilayers Measured with 2D IR Spectroscopy," Oksana Kel, Amr Tamimi, and Michael D. Fayer J. Phys. Chem. B ASAP (2014).
14. "Dynamics of Isolated Water and Alcohol Molecules in Room Temperature Ionic Liquids Measured with Ultrafast Infrared Experiments," Patrick Kramer, Chiara Giammanco, and Michael D. Fayer in preparation (2014).

Chemical Kinetics and Dynamics at Interfaces

Fundamentals of Solvation under Extreme Conditions

John L. Fulton

Chemical and Materials Sciences Division
Pacific Northwest National Laboratory
902 Battelle Blvd., Mail Stop K2-57
Richland, WA 99354
john.fulton@pnnl.gov

Collaborators: C. J. Mundy, G. K. Schenter , M. Baer, E. J. Bylaska, N. Govind.

Program Scope

The primary objective of this project is to describe, on a molecular level, the solvent/solute structure and dynamics in fluids such as water under extremely non-ideal conditions. The scope of studies includes solute–solvent interactions, clustering, ion-pair formation, and hydrogen bonding occurring under extremes of temperature, concentration and pH. The effort entails the use of spectroscopic techniques such as x-ray absorption fine structure (XAFS) spectroscopy, high-energy x-ray scattering, coupled with theoretical methods such as molecular dynamics (MD-XAFS), and electronic structure calculations in order to test and refine structural models of these systems. In total, these methods allow for a comprehensive assessment of solvation and the chemical state of an ion or solute under any condition. The research is answering major scientific questions in areas related to geochemistry, biochemistry, hydrogen storage and sustainable nuclear energy (aqueous ion chemistry and corrosion). This program provides the structural information that is the scientific basis for the chemical thermodynamic data and models in these systems under non-ideal conditions.

Recent Progress

Measuring cation-anion interactions of the light elements (Na^+, Mg^{2+}, Al^{3+} and Cl^-). The hydration and ion-ion interactions of aqueous Na^+, Mg^{2+}, Al^{3+} and Cl^- play major roles in the areas of biochemistry, geochemistry and atmospheric chemistry. The electrostatic attractive interactions between counter ions are modulated by a delicate balance of different hydration effects that are not yet fully understood. In the past, x-ray and neutron diffraction were the only available methods to probe aqueous structure of these ions, providing rather limited information since scattering intensities are quite weak. The method of extended x-ray absorption fine structure (EXAFS) provides detailed molecular structure information including bond distances, bond disorder, coordination symmetry and the chemical identities of coordination species. Recently we have elucidated the contact ion pair structure[6] between Cl- and hydronium (H_3O^+) using this method for aqueous light-element ions. Our objective has been to push the limits of the EXAFS technique to open up this method for studies of other light elements. At the same time we are continuing to use the EXAFS results to benchmark DFT-based molecular dynamics simulations. The molecular dynamics-EXAFS (MD-EXAFS) spectrum[1] is generated from the dynamic representation of the ion solvation environment. The spectrum is generated from an ab initio procedure that calculates the photoelectron single- and multiple-scattering pathways (~10^6 paths) out to about 6 Å without the need for any adjustable parameters.

The *extended*-XAFS (the region from 50 to 1000 eV above the absorption edge) has not previously been quantitatively evaluated for these light elements because of the many factors limiting the data quality during acquisition of EXAFS spectra at low X-ray energies (1 to 3 keV). These include achieving constant high x-ray flux at the sample, stable beam position, harmonic-free beam, stable sample detectors and finally properly accounting for the strong X-ray absorption by the sample. The combination of a very high-flux, low-energy undulator source, an improved X-ray monochromator, as well as an improved detector has allowed the acquisition of high-quality EXAFS spectra sufficient for a quantitative treatment of the higher-order scattering paths that are required to determine the aqueous structure. The method also involves using a low-Z EXAFS cell that incorporates 200 nm thick Si_3N_4 x-ray transmission windows to contain the flowing liquid.[3]

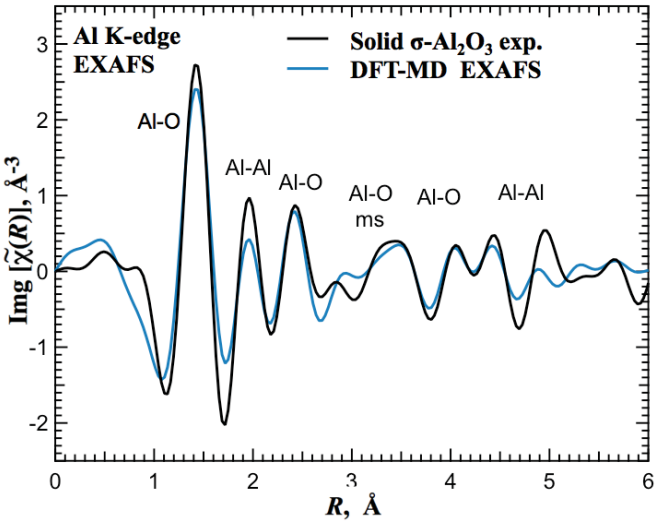

Figure 1. Al K-edge EXAFS spectra for the solid standard of σ-Al_2O_3 compared to full ab initio calculation using the DFT-MD method. Locations of the photoelectron single and multiple (ms) peaks are indicated

In order to verify the feasibility of using EXAFS for Al species, the crystal compound, σ-Al_2O_3 was evaluated. Figure 1 shows a comparison of the measured EXAF spectrum with the spectrum calculated from the first-principles method of DFT-MD (using only the crystallographic structure as input). Remarkably, in Figure 1, the experimental and MD-EXAFS calculation are in agreement for all the relevant features in EXAFS spectrum including an excellent job of reproducing the position and amplitudes of the peaks over the full range from 1 to about 5 Å. (JACS, 2014, 136, 8296) Thus the application of the method to the aqueous systems is fully justified.

The hydrated structure of Al^{3+}: EXAFS and ab initio MD Simulations. The hydrated structure of Al^{3+} has not previously been measured by EXAFS because of the challenges of working at low x-ray energies. We have again utilized the special low-Z x-ray cell to determine the hydration structure of this ion and to evaluate the reported existence of the Al^{3+} - Cl^- contact ion pair. Figure 2 compares the experimentally measured EXAFS spectrum with the DFT-MD spectrum generated from the QM/MM PBE method. The first-shell water structures represented by the peak at about 1.5 Å are in good agreement. In addition, the features at distances greater than 2Å, that includes first-shell multiple scattering as well as contributions from the second shell, are in good agreement.

The experimental EXAFS and XRD (from HEXS) results show Al^{3+}-H_2O bond distances of 1.87 and 1.89 Å, respectively. These distances can be compared to DFT-MD distances of 1.93 and 1.90 Å from PBE and PBE0, respectively. Thus, we found that only the more computationally-demanding version of DFT using exact exchange (PBE0) better predicts the bond length that is measured experimentally.

In a related study, very recent DFT-MD results point to the formation of a contact ion pair between Al^{3+} and Cl^- (InorgChem 51, 10856, 2012). We embarked upon very extensive effort to confirm this structural species however results from Cl and Al EXAFS (and from HEXS) have definitively shown that a contact ion pair of Al^{3+}-Cl^- does not form up to the saturation concentration. In contrast, our results for Al^{3+} are consistent with the structure illustrated in Figure 3 in which solvent-separated ion pairs(SSIP) are formed. The challenge for the DFT-MD methods then appears to be achieving the cation/anion/water equilibrium for a system in which the first-shell ligands have very long lifetimes. Improvements to the simulated equilibrated structure are being explored that include various types of free-energy optimizations. (E. Bylaska) The implications of these findings have far reaching consequences on how DFT-MD is employed in describing aqueous ions in chemistry.

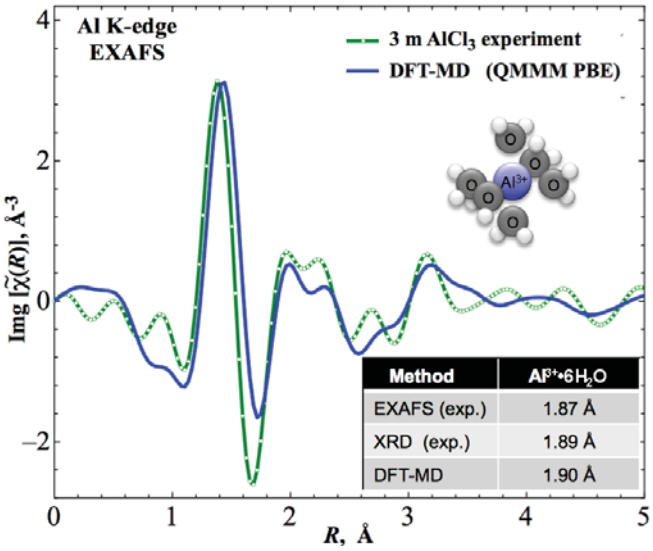

Figure 2. EXAFS spectra for aqueous Al^{3+} and the calculated spectra from DFT-MD simulation. Inset shows the first-shell water distance from measurement (EXAFS and XRD) and simulation.

Another interesting feature from the HEXS spectra in Figure 3 is the $g(r)_{O\text{-}O}$ peak at 2.67 Å that represents the structure of water in the concentrated electrolyte. For comparison the $g(r)_{O\text{-}O}$ structure of pure water is included in Figure 3. The peak at about 2.67 Å is significantly contracted from that of bulk water (2.79 Å) due to the electrostriction of water about Al^{3+} that significantly affects the water-water structure of the both the first- and second shells about the Al^{3+}.

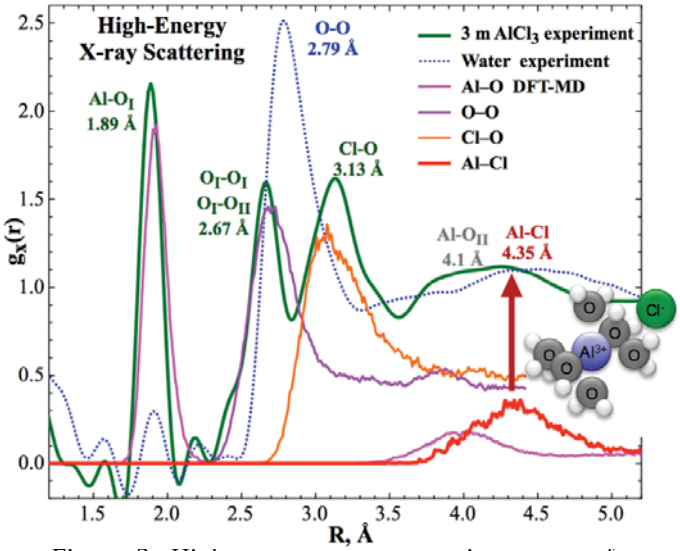

Figure 3. High energy x-ray scattering spectra for concentrated Al^{3+} solution. The various pair distribution functions from the DFT-MD simulations are shown for comparison. The position of the calculated (DFT-MD) solvent-separated (SSIP) ion pair is compared to experimentally measured position.

Future Plans

As a part of our future EXAFS studies we are in the process of measuring the detailed structure of aqueous ion pairs of (i) Mg^{2+} with CO_3^{2-} and HCO_3^- (ii) $MgHCO_3^+$ with Cl^- and (iii) the aqueous structure of $Al(OH)_4^-$ and its ion pairing with Na^+. In a decades-long quest, the structure and in some cases, even the existence of these species, has not been directly experimentally determined. The existence of the Mg^{2+} /HCO_3^- ion pair

has been the subject of continuing debate for almost 50 years (J.Phys.Chem. Ref.Data 2012, 41, No. 1). This ion pair is particularly relevant to the chemistry of $MgCO_3$ that is important for the capture and storage of carbon dioxide in deep geologic formations. Likewise, the structure and chemistry of $Al(OH)_4^-$ is of industrial and geological importance, and is among the most intensely investigated species in the chemistry of aluminum over the last 120 years (J. Mole. Liquids 2009, 146, 1). A dimer of $Al(OH)_4^-$ has been proposed from Raman spectra. Our development of EXAFS methods for the light element opens the possibility to answer these questions for the first time. Our analysis protocol will include comparison of the experimental spectra to EXAFS spectra generated from density functional theory-molecular dynamics simulations (DFT-MD) of these species.

References to publications of DOE sponsored research (2012 - present)

1. J. L. Fulton, E. J. Bylaska, S. Bogatko, M. Balasubramanian, E. Cauët, G. K. Schenter, J. H. Weare, "Near quantitative agreement of model free DFT- MD predictions with XAFS observations of the hydration structure of highly charged transition metal ions." **J. Phys. Chem. Lett.**, 3, 2588–2593 (2012)
2. V.-T. Pham, J. L. Fulton, "Ion-pairing in aqueous $CaCl_2$ and RbBr solutions: simultaneous structural refinement of XAFS and XRD data.", **J. Chem. Phys.**, 138, 044201, (2013)
3. J. Fulton, M. Balasubramanian, V.-T. Pham, G. S. Deverman, "A variable, ultra-short pathlength solution cell for XAFS transmission spectroscopy of the light elements", **J. Synchrotron Radiation**, 19, 949,(2012)
4. S. Bogatko, E. Cauet, E. Bylaska, G. K. Schenter, J. L. Fulton, J. H. Weare, "Hydration Structure and Dynamics of Aqueous Ca^{2+} using Ab Initio Molecular Dynamics: Comparison with Zn^{2+}, Fe^{3+}, and Al^{3+}." **Chemistry: A European Journal**, 19, 3047, (2013)
5. "The Aerobic Oxidation of Bromide to Dibromine Catalyzed by Homogeneous Oxidation Catalysts and Initiated by Nitrate in Acetic Acid." Partenheimer W, John L. Fulton, Christine M. Sorensen, Van-Thai Pham, and Yongsheng Chen. **Advanced Synthesis & Catalysis** 387, 130-137, (2014).
6. "Persistent ion pairing in aqueous hydrochloric acid" Marcel D. Baer, John L. Fulton, Mahalingam Balasubramanian, Gregory K. Schenter, and Christopher J. Mundy, **J. Phys. Chem. B,** 118, 7211 (2014) (Feature Article)

Probing Chromophore Energetics and Couplings for Singlet Fission in Solar Cell Applications

DE-FG02-13ER16393

Etienne Garand

Department of Chemistry, University of Wisconsin-Madison, Madison, WI 53706
egarand@chem.wisc.edu

Program scope

The goal of this project is to provide a molecular-level understanding of processes that can improve efficiencies of alternative sources of energy, such as dye-sensitized solar cells. In particular, the mechanisms and molecular requirements for efficient exciton multiplication through singlet fission are explored using high-resolution anion photoelectron (PE) spectroscopy. The experiments are capable of observing directly the singlet, triplet, and charge transfer states involved in singlet fission and determining precisely their energetics, vibrational structures and couplings. More specific aims are (1) to probe the evolution of the electronic structure as a function of cluster size in order to understand singlet fission in crystals, (2) to explore the relationship between the nature of linkers and the electronic structure in covalently-bonded chromophore dimers, and (3) to highlight the differences, including exciton delocalization and the effects of solvent interactions, between the crystalline species and the isolated covalently-bonded dimers.

The electronic states of organic chromophore clusters and covalently-bonded dimers will be probed via PE spectroscopy of mass-selected anion precursors. Starting from the radical anion with a doublet ground state, all the low-lying singlet and triplet states of the neutral molecule that involve removal of a single electron can be accessed in one-photon photodetachment. Therefore, with the exception of the doubly excited state, all the electronic states relevant to singlet fission are accessible in our experiments. Using anions also provide the added advantage of mass selection, which is crucial for studying the behavior of singlet fission as a function of cluster size. To extract precise information about the electronic state energies and couplings, it is important to obtain well-resolved PE spectra. This can be achieved by using the slow electron velocity-map imaging (SEVI) technique which combines velocity-map imaging (VMI) detection with tunable lasers to yield PE spectrum with sub-meV resolution. We can also avoid temperature related resolution limitations by collisionally cooling the anions to ~10 K in a cryogenic radio-frequency ion trap prior to laser photodetachment.

Progress

Since the start of this program in July 2013, we began designing and building the cryogenic SEVI apparatus shown schematically in Figure 1. The experimental setup will be equipped with both a heated oven supersonic expansion discharge source and an electrospray ionization source. The anions generated by either method are sent into a cryogenic ion trap using ion guides. In the quadrupole ion trap, held at 10 K, the anions are cooled via collisions with helium buffer gas. Residence time inside the trap is typically 50-90 ms to ensure temperature equilibrium before the anions are gently extracted into a time-of-flight mass spectrometer. A mass-gate allows only anions with a specific mass into the VMI region where they intersect the gently focused output of a tunable pulsed UV-Vis laser. Photoelectrons will be mapped onto a detector assembly consisting of imaging quality micro-channel plates and a phosphor screen. The resulting images will be captured by a high resolution camera connected to a computer, and will provide both the conventional PE spectra via angular integration, as well as anisotropy information on the individual vibronic transitions. The SEVI instrument will also have capabilities to acquire infrared spectra of the anions via cryogenic infrared vibrational predissociation spectroscopy. A reflectron will be installed to allow facile switching between the two spectroscopic methods.

Currently, the electrospray ionization and oven discharge sources, the ion guides, the main quadrupole ion trap, and the time-of-flight mass spectrometer has been built, and the assembly process is almost complete. At the same time, simulations and designing of the VMI stage is being carried out to achieve optimal signal-to-noise ratio and energy resolution. Conventional VMI setup has two main issues that are amplified when the method is applied to low energy electrons. First, at a given set of VMI voltages, electrons with different kinetic energies have different focal lengths which can considerably degrade the achievable resolution across the image. Another issue is the "noise" electrons ejected from VMI electrodes when high energy (> ~4.4 eV, the work function of stainless steel) photons are used. This is particularly relevant for our experiments because we are interested in studying not only the ground states of

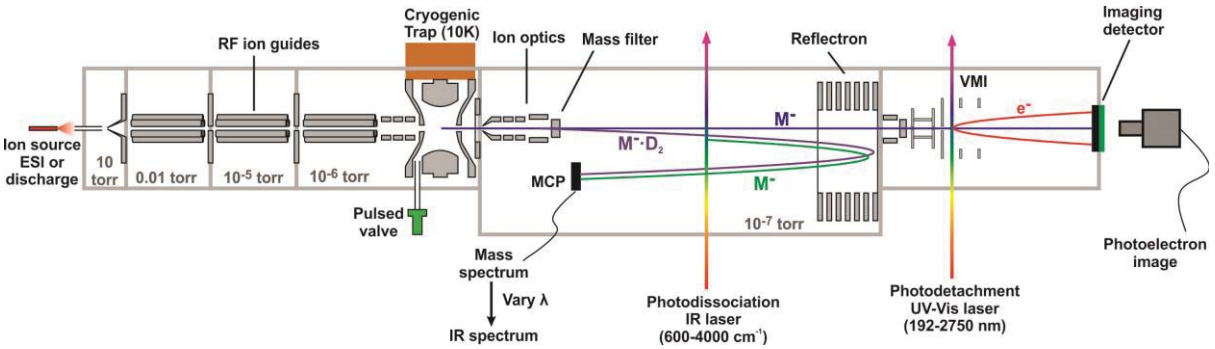

Figure 1. Schematic of the experimental setup in construction, which includes two different anion sources, a cryogenic ion trap for cooling and tagging, a two stage TOF mass-spectrometer for mass-selection and CIVS, and a slow photoelectron VMI detector.

the neutral chromophores, but also the excited states. Because SEVI VMI is designed to efficiently collect low energy electrons, these photo-ejected electrons can easily overwhelm the actual signal. In addition, SEVI necessitates low kinetic energy photoelectrons, which are very sensitive to any stray fields, electric or magnetic. Much of the difficulty in carrying out SEVI experiments lies in keeping the photoelectrons perfectly unperturbed.

To carry out the proposed experiments, we have redesigned the SEVI VMI setup to allow for better focusing and less noise operations. A schematic of the new design is shown in Figure 2. A series of 40 evenly spaced plates extend the entire VMI region, giving us a well-defined electric field environment. Two layers of mu-metal shielding will encase the setup, providing the necessary magnetic shielding. While there are significantly more electrodes, they are resistively coupled (or grounded) with only three adjustable voltage parameters. V_2 defines the kinetic energy of the electrons, and is a fixed value that dictates the size of the image. VMI focus is determined by V_1 and V_3, where V_1 corrects the energy aberration, and V_3 is adjusted to bring the focal plane onto the detector. Therefore, the day-to-day operation of this VMI is not more difficult than the traditional three-plate VMI.

We found that the best VMI focus is achieved when the photoelectrons are formed on a slightly curved electric field line, which is difficult to obtain against a flat repeller plate. It is possible to machine a repeller to match the curvature needed, but that removes some adjustability of the VMI. Instead, we replaced the repeller plate with the V_1-V_2 region which can provide a smooth gradient to give the right curvature at the interaction region. We also expanded the extraction lens of the traditional VMI into the V_2-V_3 region. The physical width of the laser beam can blur a VMI image simply because the electrons are formed on a sloping electric field. Specifically, those electrons formed closer to the detector have a different focal length than those formed further away from the detector. By stretching out the extraction region, we can provide a much gentler sloping field, and therefore minimize the blurring effect from the laser beam width.

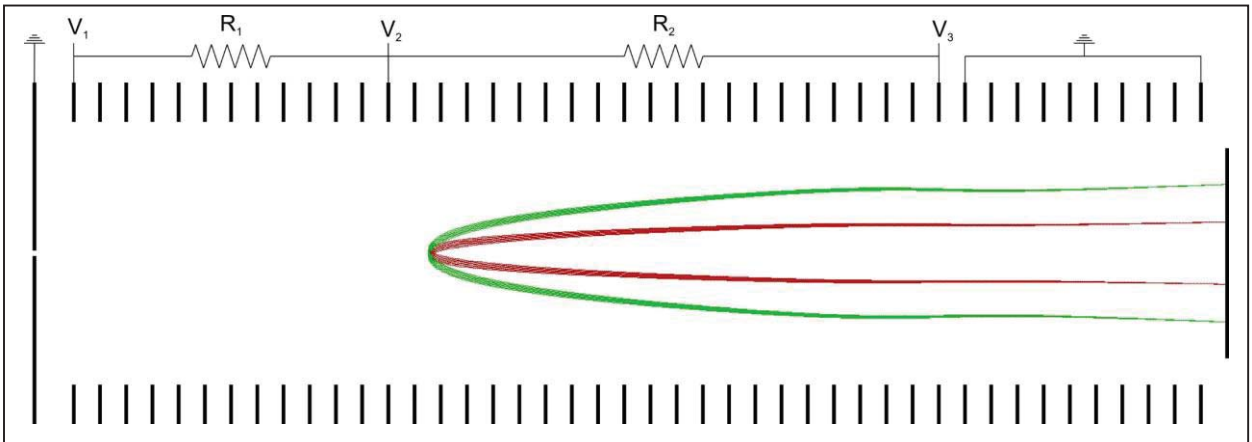

Figure 2: Schematic of the aberration corrected SEVI VMI setup. For the simulated electron flight path, 0.1 eV electrons are shown in red, 0.5 eV electrons are shown in green. V_2 is at -200V.

Lastly, this design also minimizes the "noise" electrons from the electrodes. While there are more electrodes, almost all of them are very open with minimal surface area. The pinhole, necessary for defining the anion molecular beam, has the most surface area, but the field is such that electrons with less than 200 eV will not escape onto the detector. Based on these considerations, we should have significantly less noise from photo-ejected electrons.

Beside instrument designs and constructions, we also began investigating the formation of the polyacene radical anion directly from electrospray ionization using a separate already operational cryogenic ion vibrational spectrometer (CIVS). Three different approaches are being tested. In one method, a strong reducing agent is added to the polyacene solution, where a faint color change can be observed indicating the polyacene has been reduced. Electrospray of the reduced solution has yielded radical anion signals, however source conditions need to be optimized for signal stability. The other method utilizes electrochemistry to controllably reduce the polyacene species, many of which has known redox potentials. We have successfully interfaced an electrochemical flow cell to the electrospray source and obtained oxidative products of reserpine and Ru(bpy(tpy)(H_2O). Finally, we are also building an oven and discharge source, which has a proven record of producing a variety of radical anions.

Future plans

Our immediate plan in the next year is to complete the building and testing of the cryogenic SEVI apparatus. We expect the building of the machine to be completed by the end of the fall. The capabilities of the new VMI setup will be demonstrated and optimized with atomic and simple molecular anions. At the same time, we will continue to use our existing CIVS machine to determine the conditions required for coupling the electrospray source with chemical and electrochemical reduction processes. When we can stably produce the polyacene radical anions, we will use the CIVS instrument to acquire infrared spectrum of polyacene anion clusters. These, in conjunction with DFT calculations, will clarify the structure of the radical anions, a necessary step for interpretation of the PE spectra.

We anticipate to start the SEVI experiments by next spring. Specifically, we aim to acquire the well-resolved PE spectra of anthracene and tetracene anions, as well as the dimers of these species. We will probe the ground states of the neutral species to validate our experimental and theoretical techniques. After which, we will focus our studies on the low-lying excited states that are relevant in the singlet fission process.

Ion Solvation in Nonuniform Aqueous Environments

Principal Investigator
Phillip L. Geissler
Faculty Scientist, Chemical Sciences, Physical Biosciences, and Materials Sciences Divisions

Mailing address of PI:
Lawrence Berkeley National Laboratory
1 Cyclotron Road
Mailstop: HILDEBRAND
Berkeley, CA 94720

Email: plgeissler@lbl.gov

Program Scope

Research in this program applies computational and theoretical tools to determine structural and dynamical features of aqueous salt solutions. It focuses specifically on heterogeneous environments, such as liquid-substrate interfaces and crystalline lattices, that figure prominently in the chemistry of energy conversion. In these situations conventional pictures of ion solvation, though quite accurate for predicting bulk behavior, appear to fail dramatically, e.g., for predicting the spatial distribution of ions near interfaces. We develop, simulate, and analyze reduced models to clarify the chemical physics underlying these anomalies. We also scrutinize the statistical mechanics of intramolecular vibrations in nonuniform aqueous systems, in order to draw concrete connections between spectroscopic observables and evolving intermolecular structure. Together with experimental collaborators we aim to make infrared and Raman spectroscopy a quantitative tool for probing molecular arrangements in these solutions.

Recent Progress

Our past work in this program has revealed that selective ion adsorption at the air-water interface involves as essential ingredients several previously underappreciated microscopic factors, for instance the fluctuating roughness of the liquid's boundary. Recent work has been focused in two complementary areas: (1) construction of an analytically tractable microscopic model for ions at liquid-vapor interfaces that respects the physical understanding we have gained from computer simulations, and (2) further exploring by the molecular underpinnings of adsorption selectivity, e.g., the preferential solvation of anions at the interface.

Long-standing debates over the surface propensities of small ions were reinvigorated in recent years by computer simulations demonstrating that charged model solutes can adsorb strongly to the air-water interface. From the perspective of classic theories of ion solvation in bulk polar solvents, this behavior is quite counterintuitive. Despite a significant amount of experimental and theoretical work in this area, a deep appreciation of the structure and fluctuations that distinguish interfacial solvation from bulk scenarios has remained outstanding. For instance, we have found in molecular simulations that capillary waves (mesoscopic undulations in topography of a soft interface) can be a key contributor to the thermodynamics of ion adsorption. This observation

greatly enriches solvation scenarios at liquid interfaces, but also complicates the task of determining a successful theory.

In the past year, we have made progress towards this goal by establishing the minimal ingredients of a model that captures the basic physics of topographic fluctuations at the air-water interface. We have specifically explored this issue in the context of the hydrophobic effect, whose essential theoretical understanding is more advanced than the case of ion adsorption. The basis for that understanding is a recognition (principally by David Chandler and his coworkers) that solvation of ideally volume-excluding objects in liquid water is controlled exclusively by fluctuations in liquid water's molecular density field, and that these fluctuations can be described quite accurately by simple mathematical descriptions at small and large length scales. At short wavelengths (roughly the scale of a water molecule and below) variations in density obey Gaussian statistics to a striking degree. By contrast, hydrophobic objects extending over a nanometer or more evoke density fluctuations characteristic of the nearby phase coexistence with the vapor phase. A theory that marries these two extremes is a promising way to understand and predict the liquid's response to a variety of hydrophobic perturbations, from the accommodation of small hydrophobes to mediation of the forces between large hydrophobic surfaces. Such a theory has been constructed and explored by Chandler and coworkers, providing much insight into water's role in hydrophobic assembly in general.

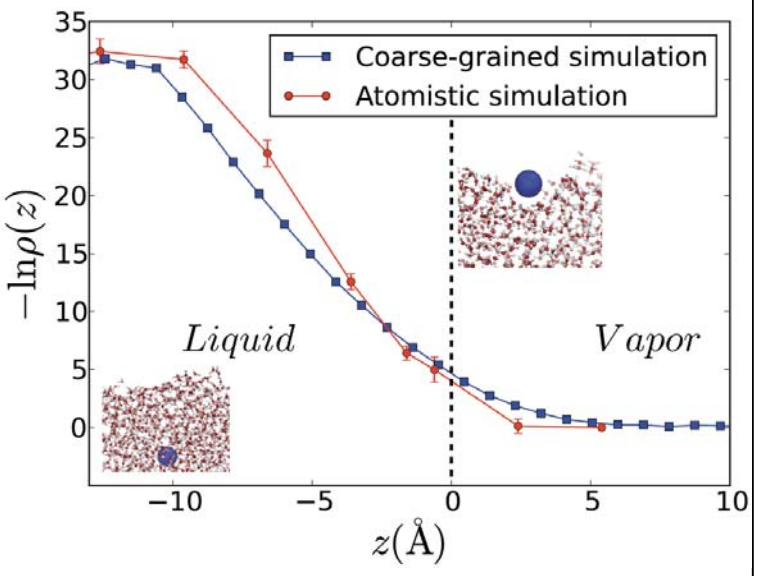

Figure 1. Free energy profile of a hydrophobic solute (5Å in diameter) crossing through the liquid-vapor interface. The influence of capillary fluctuations is strongly evident from variations of the average solute density ρ(*z*) at heights *z* more than twice the solute diameter away from the average position of the interface (*z*=0).

One challenge in creating this theory is the coupling between fields representing density variations at small and large length scales. Some variants include an ad hoc interaction between the two, introducing poorly constrained adjustable parameters; others, which include only the coupling implicit in accommodating constraints on the total density field, have fallen short of quantitative accuracy. A seemingly more straightforward, but in fact subtle, challenge is parameterizing an Ising-like description of the coarse density field, i.e., assigning a lattice spacing and energies for interaction among neighboring lattice cells. We have recently shown that these two challenges can be addressed thoroughly and simply, provided the influence of capillary fluctuations is carefully acknowledged.

Drawing from and extending classical theories of surface roughness, we derived an approximate relationship between the microscopic cohesive energy ε of a lattice gas and its emergent surface tension γ. This connection ($\varepsilon^2 \propto \gamma$) is different in form from the low-temperature result ($\varepsilon \propto \gamma$) previously used to parameterize lattice gas models. This calculation also makes clear that Ising-like models can be faithful to water's distance from criticality at ambient condition, while capturing the roughness at all scales of its interface with vapor, within a very narrow range of parameters. The lattice spacing and nearest-neighbor attraction of a suitable Ising model are then essentially set (at ~1.8Å and ~1.4 $k_B T$, respectively) by the value of surface tension, allowing no freedom of adjustment. With these choices, and the omission of explicit length scale couplings, we have shown that a Chandler-inspired model for hydrophobicity can achieve remarkable quantitative accuracy. Fig. 1 shows a particularly impressive example, predicting the association between a small hydrophobe and the air-water interface, which stringently tests the theory's ability to describe the interplay between short- and long-wavelength physics.

Establishing reduced models for solvation of generic solutes near fluctuating interfaces constitutes a first step towards a predictive understanding for ion adsorption. The *specificity* of this phenomenon, however, has eluded even rudimentary understanding. Experiments and simulations indicate that an ion's affinity for the surface is extremely sensitive to the details of the ion itself. Perhaps the most dramatic example of this selectivity is the asymmetry between anions and cations: Merely switching the sign of the charge of a model ion can modulate its density at the surface by a factor of 100. This behavior (which ultimately originates in the charge asymmetry of water molecules themselves) is often attributed to liquid water's nonzero surface potential. We have recently scrutinized this proposition and found it to be unsatisfactory.

Surface potential is conventionally defined as the electrostatic potential averaged over all points in the liquid (including the interior of solvent molecules). To be a meaningful physical factor in ions' surface propensity, the bias implied by a nonzero surface potential should be insensitive to a solute's size and charge. By sampling very broadly over the electrostatic environments experienced by volume-excluding solutes, we have shown that careful measures of this bias are in fact highly sensitive to such details. We isolate the bias by comparing free energies of hard anions and cations with the same magnitude of charge. The difference in these free energies, per unit charge, should from naïve expectations amount to twice the surface potential. We have found from simulations that this difference varies strongly and nonlinearly with ion size and charge, corresponding to the surface potential only in the limit of an uncharged point solute. For certain ranges of ion parameters, the bias is even reversed, yielding an apparent preference for cations at the interface. Our studies suggest that charge asymmetry in surface propensity instead reflects the flexibility of solvent arrangements in the vicinity of a solute in bulk. Solvation environments that are highly variable tend to be more permissive of structural changes imposed by the interface, facilitating adsorption. Tests of this hypothesis, and efforts to characterize its quantitative effects, are underway.

Future Plans

A major goal for the next few years is to continue constructing a predictive theory for ions' spatial distributions near a liquid-vapor interface. Our previous work has set the stage for this development, pointing to essential physical ingredients missing in previous approaches. With

this knowledge we are poised to formulate a tractable mathematical description of this phenomenon, capable of predicting density profiles, thermodynamic driving forces, and key experimental control parameters.

Among the challenges we face in this goal is extending the lattice model of density fluctuations described above to include as well a description of electrostatic interactions with charged and generally hydrophilic species. In the simplest approach, which is underway, a dielectric continuum representation could be appended to the coarse-grained density field. The resulting model, however, cannot capture adsorption specificity, as it lacks charge asymmetry. More detailed information about local molecular orientations is required; these might be captured by a measure of local tetrahedral order, or else Steinhardt-Nelson order parameters. Further insight from simulations may be required to properly couple essential coarse-grained fields together.

Our focus thus far has been on understanding properties of single ions in solution. In particular, we have aimed to predict free energy profiles in the microscopic vicinity of a liquid-vapor interface. While this quantity is well-defined at infinite dilution, many macroscopic properties require attention to correlations among ions. Energy applications often involve sufficiently high ionic strength that such correlations cannot be neglected. Moreover, SHG studies by Saykally's group indicate that finite-concentration effects on adsorption appear at relatively low concentration. In previous theoretical work Debye-Hückel calculations have been performed in attempt to gauge these effects. As with conventional applications of dielectric continuum theory, however, this approach neglects many aspects of interfacial physics we now know to be important.

We aim to begin characterizing multi-ion correlations in the interfacial environment. The screening effects described by Debye-Hückel theory are of course an important component. But the adsorption mechanisms we have revealed suggest other, rather different consequences of ions' association. For example, the thermodynamics of interfacial pinning could favor clustering of two or more solutes, since one localized interfacial constraint is likely to be less costly than pinning at many dispersed sites. Similar mechanisms of solute aggregation have been discussed in the context of large molecules embedded in an elastic membrane. In addition, it is not clear how the energetics of excluding volume in the interfacial zone will depend upon solutes' spatial arrangement. We plan to explore these behaviors in computer simulations, both of detailed molecular models and of the reduced models we have described.

Recent Publications

D. E. Otten, P. R. Shaffer, P. L. Geissler, and R. J. Saykally, "Elucidating the Mechanism of Selective Ion Adsorption to the Liquid Water Surface," *Proc. Natl. Acad. Sci.,* **109**, 701 (2012).

S. Vaikuntanathan, P. R. Shaffer, and P. L. Geissler, "Adsorption of solutes at liquid-vapor interfaces: insights from lattice gas models," *Faraday Discuss.,* **160**, 63 (2013).

P. L. Geissler, "Water interfaces, solvation, and spectroscopy," *Ann. Rev. Phys. Chem.*, **64**, 317 (2013).

S. Vaikuntanathan and P. L. Geissler, "Putting water on a lattice: The importance of long wavelength density fluctuations in theories of hydrophobic and interfacial phenomena," *Phys. Rev. Lett.*, 112, 020603 (2014).

Program Title: Theoretical Developments and Applications to Surface Science, Heterogeneous Catalysis, and Intermolecular Interactions

Principal Investigator: Mark S. Gordon, 201 Spedding Hall, Iowa Sate University and Ames Laboratory, Ames, IA 50011; mark@si.msg.chem.iastate.edu

Program Scope. Our research effort combines new theory and code developments with applications to a variety of problems in surface science and heterogeneous catalysis, as well as the investigation of intermolecular interactions, including solvent effects in ground and excited electronic states and the liquid-surface interface. Many of the surface science studies are in collaboration with Dr. James Evans. Much of the catalysis effort is also in collaboration with Drs. Evans, Marek Pruski and Igor Slowing.

Recent Progress. Chemical processes on and with the Si(100) surface have been one research focus[5,10]. The diffusion of both Al and Ga on Si(100) was studied using an embedded cluster model and multi-reference electronic structure methods, including CASSCF explorations of the doublet and quartet potential energy surfaces and improved energies with multi-reference perturbation theory. The details of the potential energy surfaces depend critically on the presence of the bulk that is represented by molecular mechanics (MM). Only when edge effects are minimized by embedding the quantum mechanics (QM) region in a much larger MM region, using our SIMOMM method, does a consistently realistic picture emerge. It appears that both Al and Ga can form metal wires on the Si(100) surface. Studies of surface growth are greatly enhanced through collaborations with the Evans group so that the morphology of surface processes can be better understood.

A significant effort involves the development of efficient methods that can be applied to large systems, such as surfaces, nanoparticles and liquids. One such method is the effective fragment potential (EFP) method whose accuracy for intermolecular interactions rivals that of second order perturbation theory (MP2). The EFP method, which is a highly sophisticated model potential, can be combined with essentially any electronic structure method to, for example, provide insights about solvent effects and liquid behavior. Most recently, the EFP method has been combined with nonlinear time-dependent density functional theory to facilitate the investigation of solvent effects on nonlinear optical properties[12]. Because the EFP method is fully implemented only in the GAMESS program, we have used the common component architecture (CCA) approach to make the EFP method available to other codes, such as NWChem[6]. The EFP method has also been combined with our spin-flip TDDFT method to study solvent effects on the location and energy profile of conical intersections, which have a profound effect on excited states, photochemistry and photobiology.

Another (fully quantum) fragmentation approach is the fragment molecular orbital (FMO) method. The FMO method divides a large species into fragments to facilitate accurate QM calculations on very large systems. The FMO method can be used in concert with any electronic structure method in GAMESS. In order to optimize geometries using the FMO method, or to perform molecular dynamics (MD) simulations,

it is necessary to derive and code fully analytic gradients for each method that is combined with the FMo, such as Hartree-Fock (HF) or DFT. Fully analytic FMO/HF and FMO/DFT gradients have been derived and implemented in GAMESS, to enable geometry optimizations and MD simulations. We have shown that one can do FMO/HF MD simulations with periodic boundary conditions and that fully analytic gradients are absolutely essential[7]. A manuscript that describes the fully analytic FMO/DFT gradient development and implementation is under review. Two invited reviews of fragmentation methods have appeared in high impact journals[1,13] The FMO method is also highly scalable, because the calculation for each fragment can be performed on a separate compute node. Advances have also been made in high performance computational chemistry. A prior INCITE grant has enabled us to have access to the BlueGene /P at Argonne, where we have demonstrated that the FMO method allows essentially perfect scaling to the petascale (more than 131,000 processors)[2]. The EFP and FMO methods have both been used to study problems related to biomass conversion to useful energy[4,9].

Another approach to making high-level electronic structure calculations is to use localized molecular orbitals (LMOs), because correlation is local. So, one can design LMO domains or subsystems and only perform the correlation calculation within those domains. Professor Carter (Princeton) has developed a multi-configurational (MR) configuration interaction (CI) code called TigerCI to perform such calculations. In collaboration with the Carter group, a preliminary parallel version of TigerCI code has been implemented[14].The TigerCI code has now been incorporated into GAMESS. A manuscript that describes this effort is in preparation. Another LMO-based fragmentation method, developed by the Piecuch group, called cluster-in-molecule (CIM) has been implemented in GAMESS. The CIM method is primarily intended to work with MP2 and coupled cluster methods, such as CCSD(T) and CR-CC(2,3).

“Composite” methods refer to the use of multiple levels of theory to predict accurate thermodynamic properties of molecules. Most composite methods can predict very accurate thermochemistry, but are not reliable for the prediction of reaction mechanisms, barrier heights and (therefore) kinetics. We have recently developed a new composite method, called ccCA-CC(2,3), based on the Piecuch CR-CC(2,3) method, that can predict both thermodynamics and reaction mechanisms with very high accuracy. We have shown that the ccCA-CC(2,3) method correctly predicts complex mechanisms for important chemical reactions, whereas the usual single reference composite methods fail[3].

Mesoporous silica nanoparticles (MSN) have received increasing attention due to their catalytic capabilities. Because the MSN species are very important for their selective heterogeneous catalytic capability, we have an ongoing effort to model these complex species. Previously, we have implemented the ReaxFF force field into GAMESS. A combined ReaxFF/NMR study, in collaboration with the Pruski group, demonstrated that the ReaxFF method can produce structural data that are consistent with the temperature-dependent NMR data. Similarly, we have demonstrated that the FMO method is capable of studying reactions within MSN. Equally importantly, the HF-D method (HF combined with a dispersion correction) can provide energetics for a benzene molecule moving through a MSN with an accuracy that is comparable with that of MP2. The electronic

structure theory calculations are also combined with the non-equilibrium statistical mechanics methods of the Evans group to provide mesoscale insights.

Current and Future Plans. The main bottleneck of the CIM method is that one must first perform a HF calculation on the entire system of interest, in order to obtain the LMOs. This requirement can force the user to use a smaller basis set that would be desired for the correlation calculation. Therefore, a combined CIM-FMO method has been implemented and is being tested. The combined method allows one to use FMO for the initial step, therefore removing the bottleneck and making the FMO-CIM a true linear scaling method. The FMO-CIM/CR-C(2,3) method will be applied to studies of phenomena on the Si(100) surface, such as more extensive studies of diffusion of Ga and In, and of the MSN systems. Preliminary FMO studies have been performed on model MSN species at the Hartree-Fock level of theory with a small basis set. The agreement with the fully ab initio method is excellent, especially when one used the HF-D method, so we will now apply FMO with higher levels of theory and reliable basis sets to processes that occur within the MSN. A new embedded cluster method SIMOMM-Rx that replaces the Tinker force field with ReaxFF is under development. The EFP-QM exchange repulsion analytic gradients have been derived, and these will now be implemented so that any solvent can be studied.

The FMO method is being used to perform MD simulations on water and on aqueous solvation of ions such as hydronium ion and nitrate. It is apparent that three-body effects are critical for these simulations, so the derivation and implementation of the FMO3 fully analytic gradients is in progress. The more computationally efficient effective fragment molecular orbital (EFMO) method, a merging of EFP and FMO is very appealing for MD simulations that involve water. The derivation and implementation of the fully analytic EFMO gradients is underway.

An interface between the GAMESS electronic structure program and the FMS program from the Martinez group has been implemented. The combined GAMESS-FMS methodology will now be used to study excited state phenomena, such as conical intersections that are ubiquitous in photochemical processes. In order to fully analyze surface crossings and conical intersections, one needs the ability to calculate non-adiabatic coupling matrix elements (NACME) that couple multiple surfaces when they are in close proximity. For large systems, TDDFT and SF-TDDFT are the most efficient methods for exploring excited state phenomena, so the derivation and implementation of TDDFT and SF-TDDFT NACME are in progress.

References to publications of DOE sponsored research 2010-present

1. M.S. Gordon, D.G. Fedorov, S.R Pruitt, and L.V. Slipchenko, "Fragmentation Methods: A Route to Accurate Calculations on Large Systems", Chem. Rev, 112, 632 (2012) (INVITED).

2. G.D. Fletcher, D.G. Fedorov, S.R. Pruitt, T.L. Windus and M.S. Gordon, "Large-Scale MP2 Calculations on the Blue Gene Architecture Using the Fragment Molecular Orbital Method", J. Comp. Theor. Chem., 8, 75 (2012).

3. S. Nedd, N.J. DeYonker, A.K. Wilson, P. Piecuch, and M.S. Gordon, "Incorporating a Completely Renormalized Coupled Cluster Approach into a Composite Method for Thermodynamic Properties and Reaction Paths", J. Chem. Phys., 136, 144109 (2012).
4. S. Markutsya, Y. Kholod, A. Devarajan, T.L. Windus, M.S. Gordon, and M.H. Lamm, "A coarse-grained model for β-D-glucose based on force matching", Theor. Chem. Accts., 131, 1 (2012).
5. D.-J. Liu, D.M. Ackerman, X. Guo, M.A. Albao, L. Roskop, M.S. Gordon, and J.W. Evans, "Morphological Evolution during Growth and Erosion on Vicinal Si(100) Surfaces: From Electronic Structure Analyses to Atomistic and Coarse-Grained Modeling", Mater. Res. Soc. Symp. Proc., 1411 (2012)
6. A. Gaenko, T.L. Windus, M. Sosonkina and M.S. Gordon, "Design and Implementation of Scientific Software Components to Enable Multi-scale Modeling: The Effective Fragment Potential (QM/EFP) Method", J. Chem. Comp. Theory, 9, 222 (2012).
7. K.Brorsen, N. Minezawa, F. Xu, T.L. Windus, and M.S. Gordon, "Fragment molecular orbital dynamics with the fully analytic gradient.", J. Chem. Comp. Theory, 8, 5008 (2012).
8. D. Rios, G. Schoendorff, M.J. Van Stipdonk, M.S. Gordon, T.L. Windus, J.K. Gibson, and W. A. de Jong, "Roles of Acetone and Diacetone Alcohol In Coordination and Dissociation Reactions of Uranyl Complexes", Inorg. Chem., 51, 12768 (2012).
9. A. Devarajan, S. Markutsya, M.H. Lamm, X. Cheng, J.C. Smith, J.Y. Baluyut, Y. Kholod, M.S. Gordon, and T.L. Windus, "Ab Initio Molecular Dynamics Study of Molecular Interactions in a Cellulose Iα Microfiber", J. Phys. Chem. B, 117, 10430(2013)
10. D.-J. Liu, D.M. Ackerman, X. Guo, M.A. Albao, L. Roskop, M.S. Gordon, J.W. Evans, Morphological evolution during growth and erosion on vicinal Si(100) surfaces: From electronic structure to atomistic and coarse-grained modeling, MRS Proc. Symp. EE Fall 2011 (MRS, Pittsburgh, 2012).
11. J. Wang, A. Garcia, D.M. Ackerman, M.S. Gordon, I.I. Slowing, T. Kobayashi, M. Pruski, J.W. Evans, Multi-functionalization of nanoporous catalytic materials to enhance reaction yield: Statistical mechanical modeling for conversion reactions with restricted diffusive transport, MRS Proc. Symp. AA Fall 2013 (MRS, Pittsburgh, 2014).
12. F. Zahariev and M.S. Gordon, "Non-linear Response Time-Dependent Density Functional Theory combined with the Effective Fragment Potential Method", J. Chem. Phys., 140, 18A523 (2014)
13. S.R. Pruitt, C. Bertoni, K. Brorsen, and M.S. Gordon, "Efficient and Accurate Fragmentation Methods", Acc. Chem. Research (INVITED), DOI: 10.1021/ar500097m
14. J. Dieterich, D. Krisiloff, A Gaenko, F.Libisch, T. Windus, M. Gordon, E. Carter, "Shared-memory parallelization of a local correlation multi-reference CI program", Comp. Phys. Comm., in press.

Ultrafast Interfacial Electron Dynamics of Materials

Charles B. Harris P.I.
Chemical Sciences Division
Lawrence Berkeley National Lab
1 Cyclotron Road, Mail Stop Latimer
Berkeley, CA 94720
cbharris@berkeley.edu

Program Scope:

Though bulk properties are the most widely studied, the properties of the interface between two materials can dictate the behavior of devices. In the case of organic photovoltaic cells, the interface between donor and acceptor type materials is believed to drive charge separation. In supercapacitors, charge is stored by molecular reorganization at the metal-solvent interface. Finally, in the case of microelectronics, charges are moved over nanometer length scales where bulk properties have little meaning. The physical phenomena governing the electronic properties of surfaces and interfaces are unique from the bulk solid and remain difficult to directly probe. Our research aims to explore the nature of electronic states and the dynamics of excess electrons at the metal-molecule interface.

We utilize femtosecond time- and angle-resolved two-photon photoemission spectroscopy (TPPE) to probe the energy and momentum of electrons in thin film adlayers on a metal surface. Briefly, a pump pulse excites an electron from below the Fermi level of the substrate into a previously unoccupied state below the vacuum level. After a variable time delay, a probe pulse photoemits the electron into a time-of-flight detector. The low energy electrons generated in this process give TPPE high surface sensitivity and high energy resolution. Angle resolved measurements allow TPPE to collect electronic spectra as a function of momentum. Localization can be determined by the curvature and intensity of the measured momentum dependent band structure. Our work has investigated several cases where delocalized electrons collapse into localized states on the femtosecond timescale.

Broadly, our work can be divided into two distinct areas. The first area concerns the static modification of the interfacial electronic states upon the deposition of films. This was recently explored in experimental and theoretical studies of phthalocyanine monolayer films by examining the modification and hybridization of the metallic surface states by the adlayer. This line of work was extended with studies of the surface potential of graphene on the silicon carbide surface. The second area concerns dynamic processes such as the localization and solvation of electrons in thin films supported by the metal surface; this line of work originated with our pioneering work on polaron formation in alkane thin films, and continues today with studies of the solvation response of room temperature ionic liquids and the trapping of free-electrons in insulating ultrathin films. These studies inform and complement ongoing work which attempts to monitor excitonic states in organic semiconductors.

Recent and Ongoing Work:

Electron Localization in Ultrathin Alkali Halide Films:

The interface between insulators and metals is important for a wide range of technologically relevant devices. Thin films of alkali halides are now commonly incorporated between the metal electrode and photoactive layer of organic electronics and have been shown to improve efficiency. These interfaces are also important for the emerging field of microelectronics where they are used to isolate conducting species and in the field of catalysis where water splitting is studied at the metal/metal-oxide interface. Despite their importance, few studies have examined the excited states and dynamics of electrons at these interfaces.

We have recently studied excess electron dynamics for ultrathin layers of NaCl on Ag(100). We find that free electrons excited into the image potential states localize on the ultrafast time scale due to trapping at neutral defect states existing at the NaCl/vacuum interface. These trap states result in an energetic stabilization much greater than thermal energy (k_BT) relative to free electrons in the n=1 image potential state. We propose that the trap sites reside at step edges, kinks, or NaCl pair vacancies in the NaCl thin film which has not been previously observed for these systems. The trap states observed could

have a potential impact on electron transport in systems where ultrathin layers of insulating layers are used, and have a subsequent impact on device efficiency. We are currently extending our studies to explore the impact of intraband and interband relaxation on the trapping of excess electrons at the NaCl/ metal interface.

Probing Ultrafast Solvation Dynamics at the Room Temperature Ionic Liquid/Electrode Interface:

Room temperature ionic liquids (RTILs) are known to have many interesting and unique properties such as extremely low volatility, high electrochemical stability, and low flammability that distinguish them from traditional, molecular solvents. These characteristics make them an attractive and powerful alternative to traditional solvents in applications ranging from synthetic chemistry to electrochemical energy storage devices. The properties of RTIL's in bulk have been well-studied in recent years, yet the behavior of these compounds at surfaces is still not well documented or understood. Characterizing this interfacial behavior is important given the incorporation of these materials into electrochemical devices, where surfaces and interfaces play a key role in the efficiency and effectiveness of the device.

The goal of this work is to characterize the ultrafast response of an RTIL at an interface to an excess electron. In a recently published study, we characterized films of 1-Butyl-1-methylpyrrolidinium bis(trifluoromethanesulfonyl)imide ($[Bmpyr]^+[NTf_2]^-$) on the Ag(111) surface. Using TPPE, we showed that an electron injected into a film of $[Bmpyr]^+[NTf_2]^-$ solvated (relaxes in energy over time) and that the magnitude of this relaxation is sensitively dependent on the temperature of the film. By monitoring the temperature dependent response of the thin films we observed that the $[Bmpyr]^+[NTf_2]^-$ films undergo a interfacial phase transition around 250 K.

Further angle-dependent TPPE measurements have shown that two states initially exist at the interface, and that one state is delocalized across the film while the other is localized. The delocalized state's binding energy does not change over time, and this state can only be observed <200 fs after the initial injection event. The localized state is observed to relax in energy after being populated. The lifetime of the localized state increases dramatically as a function of thickness, indicating that the film is screening the excess charge from the metal surface. Interestingly, we find that the thickness of the films does not have an effect on the relaxation steps themselves, instead, only the lifetime is affected. These studies are some of the first to characterize the ultrafast behavior of interfacial RTILs. We hope to continue this work in order to better understand the relationship between film structure and dynamics.

The Hybridization of Metallic Surface States and Molecule States:

Metal/organic interfaces are a matter of intense study in numerous fields, many of which are related to energy-sciences. In all of these fields, knowledge of the electronic structure of the metal/organic interface is critical; however, this understanding can be elusive, even in some of the simplest cases. The current understanding of the interfacial electronic structure at metal/organic interfaces relies heavily on models that assume the combined system is a superposition of molecular orbitals and surface bands. Here, we highlight an example that qualitatively departs from this model – a system where a metallic state directly hybridizes with a molecular state, yielding a new interface state.

In this work, we investigate the interaction between the molecular orbitals of the widely-studied phthalocyanine ligand and the Shockley surface state on the Ag(111) surface. We use time- and angle-resolved TPPE spectroscopy to observe an interface state formed at the phthalocyanine/Ag(111) surface. The energetic location, effective mass, and lifetime are compared to plane-wave DFT calculations and previous experimental/theoretical studies, which, reveals that the LUMOs of the phthalocyanine ligand hybridize with metallic surface state. Notably, when combined with the previous literature on the phenomenon, our work suggests that hybridization between extended metallic surface states and molecular orbitals is likely general to planar polycyclic aromatic hydrocarbon/Ag(111) surfaces, and, more generally this highlights that the organic/metal interface can exhibit behavior more complex than simple energy alignment diagrams can explain.

Measuring the Electronic Corrugation at the Phthalocyanine/Ag(111) Interface:

In this work we seek to understand how a self-assembled monolayer of an organic material (in this case the popular phthalocyanine molecules) can modify the interfacial potential both parallel to and perpendicular to the interface. A more detailed understanding of the interfacial potential is important for charge transport and self-assembly processes at the interface and is therefore of fundamental importance.

Here, the interfacial potential is probed using time- and angle-resolved TPPE spectroscopy to measure the band structure of the image potential states. The first few image potential states are highly localized at the metal/molecule interface and thus serve as a sensitive probe of the interfacial potential. By modelling the measured band structure it was possible to determine the corrugation of the interfacial potential due to the phthalocyanine lattice. Interestingly, the analysis revealed that counter to intuition, the metal-free phthalocyanine can cause larger modifications to the interfacial potential than the corresponding cobalt substituted phthalocyanine. These results highlight the power of the TPPE technique to characterize the electronic potential at the metal/molecule interface. Further, they suggest that even for molecules with nearly identical lattice structure, the interfacial potential energy landscape can be significantly different.

The Surface Potential of Graphene on Silicon Carbide:

Graphene has been the topic of innumerable studies due to its unique structural and quantum mechanical properties. Graphene on the silicon carbide (SiC) substrate is particularly interesting because two-dimensional carbon sheets can be grown directly on the semiconducting SiC surface. The initial annealing steps in this process give rise to a carbon-rich buffer layer, further annealing then forms freestanding graphene layers atop the buffer layer. The key difference between the buffer layer and graphene is a strong covalent bonding interaction of the buffer layer with the SiC substrate, which is in contrast with the freestanding nature of the subsequently formed graphene overlayers. The buffer layer has a similar 'honeycomb' structure as freestanding graphene but is corrugated as a result of its interaction with the substrate.

In this study, we use angle-resolved TPPE to examine the image potential states, which serve as sensitive probes of the interfacial potential, to compare the surface potential of the corrugated buffer layer versus that of the freestanding graphene. Until our study, there remained an unanswered question if the buffer layer on SiC could support an IPS series. Angle dependent measurements revealed that the corrugation of the buffer layer had no significant effect on the IPS's, as all three states in the series we observed were similarly delocalized for both the buffer layer and graphene bilayer samples. The lifetime remained similar between equivalent IPS's in the buffer layer and bilayer samples, except in the case of the n = 3 state, which showed a longer lifetime in the bilayer. Our observation that only the n = 3 state's lifetime increases suggests that the graphene is not acting as a simple dielectric screening barrier, but that IPS decay is mediated by the graphene layers through a more involved process. The similarity between the behavior of image states in the buffer layer and bilayer samples shows that a similar surface potential is present in both cases. This similarity is significant given the role of the surface potential in sensors and other devices.

Future Work:

Electron Dynamics and Localization in Crystalline Insulating Ultrathin Films:

Future studies of ultrathin layers of alkali halides on metal substrates will explore changing cation and anion identities and their subsequent impact on electron dynamics and behavior. Initial studies of KCl and NaF have revealed qualitatively similar phenomenon to NaCl, where electrons are excited into IPS and subsequently decay and localize into neutral trap states. We aim to correlate the impact of the alkali halide's electron affinity on the magnitude of energetic trapping of excess electrons and decoupling ability of the insulating material. Results correlating the magnitude of electron trapping with different alkali halides will be important to the emerging field of nanoelectronics where ultrathin insulating layers are used to isolate conducting species.

Monitoring Molecular Excitation in Organic Semiconductors:

One of the exciting properties of ultrathin layers of alkali halides on metal substrates is their ability to decouple molecular properties from bulk material even at bilayer thicknesses. This property has been demonstrated by STM experiments imaging the frontier orbitals of organic semiconductors on bilayer films of NaCl on metal substrates, where the insulating film is thin enough to conduct but still isolate the molecular properties. Future studies will explore the excited state dynamics of organic semiconductors deposited onto ultrathin insulating layers. The molecular excitations of organic semiconductors directly deposited on metal substrates are energetically broadened and quenched by the metal substrate. However, deposition on thin layers of alkali halides can isolate molecular excitations and excitonic levels. These results could have potential impact for the field of microelectronics, where our systems would mimic microelectronic devices and observe the excited state electron dynamics important to device operation and design.

Probing the Solvation Response of Room Temperature Ionic Liquids at Carbon-rich Surfaces:

Incorporating ionic liquids into electrochemical devices is a promising option by which these methods of energy storage can become more efficient, safe, and reliable. Since interfaces play a key role in the operation of these electrochemical devices, it will be necessary to explore processes occurring at the interface between an ionic liquid and an electrode. Our ongoing work focusing on excess charge in films of [Bmpyr]+[NTf2]- on the Ag(111) surface is the first step toward understanding these interfaces, however, more realistic for device applications are carbon-based electrodes. Our objective is to leverage our work on the graphene/SiC surface along with our understanding of the RTIL/Ag(111) interface to begin to probe the processes at the interface between RTILs and a device-relevant carbon electrode.

Tuning the Response of Ionic Liquid Films by Simple Changes in Film Composition:

One powerful characteristic of ionic liquids is the ease by which their bulk properties are tuned by changing the chemical identity of the cation, the anion, or both. For example, an ionic liquid containing an immidzolium cation with a short alkyl chain displays no structural organization, while a simple extension of the alkyl chain has been shown to prompt domain formation on the nanometer scale. Our goal is to demonstrate that the ultrafast behavior and physical structure of an ionic liquid film at an interface can be tuned in a similar way. Preliminary experiments in our group have revealed that replacing the [NTf_2] anion with dicyanamide changes the room temperature surface structure from diffusive and liquid-like to crystalline, and changes the relaxation dynamics of an excess electron in the film as well. We hope to continue this work by studying a series of different cation/anion pairs, and observe how the films' behavior changes with chemical composition. Establishing a set of connections between chemical composition, structure, and ultrafast behavior will be valuable to the electrochemical devices field, as well as to the ionic liquid community as a whole.

Publications Supported by DOE Funding from 2012-present:

[1] "Femtosecond Trapping of Free Electrons in Ultrathin Films of NaCl on Ag(100), " D.E. Suich, B.W. Caplins, A.J. Shearer, and C.B. Harris, J. Phys. Chem. Lett., 5, 3073−3077, (2014).
[2] "Electron Dynamics of the Buffer Layer and Bilayer Graphene on SiC," A.J. Shearer, J.E. Johns, B.W. Caplins, D.E. Suich, C.B. Harris, Appl. Phys. Lett., 104, 231604, (2014).
[3] "Metal/Phthalocyanine Hybrid Interface States on Ag(111)," B.W. Caplins, D.E. Suich, A.J. Shearer, E.A. Muller, C.B. Harris, J. Phys. Chem. Lett., 5, 1679-1684, (2014).
[4] "Measuring the Electronic Corrugation at the Metal/Organic Interface," B.W. Caplins, A.J. Shearer, D.E. Suich, E.A. Muller, C.B. Harris, Phys. Rev. B., 89, 155422, (2014).
[5] "Femtosecond Electron Solvation at the Ionic Liquid/Metal Electrode Interface," E.A. Muller, M.L. Strader, J.E. Johns, A. Yang, B.W. Caplins, A.J. Shearer, D.E. Suich, C.B. Harris. J. Am. Chem. Soc., 135 (29), 10646-10653, (2013).
[6] "Electron Dynamics and Symmetries at the Metal-Molecule Interface Probed by Two-Photon Photoemission," E.A. Muller, LBNL Thesis, (2012).

Program Title: "SISGR: Ultrafast Molecular Scale Chemical Imaging"
(DOE Grant Number: DE-FG02-09ER16109)

PI: Mark C. Hersam, Professor of Materials Science and Engineering, Chemistry, and Medicine; Northwestern University, 2220 Campus Drive, Evanston, IL 60208-3108;
Phone: 847-491-2696; Fax: 847-491-7820; E-mail: m-hersam@northwestern.edu;
WWW: http://www.hersam-group.northwestern.edu/

Co-PIs: Jeffrey R. Guest (Argonne National Lab), Nathan P. Guisinger (Argonne National Lab), Saw Wai Hla (Argonne National Lab), George C. Schatz (Northwestern University), Tamar Seideman (Northwestern University), Richard P. Van Duyne (Northwestern University)

1. Program Overview

This SISGR program utilizes newly developed instrumentation and techniques including integrated ultra-high vacuum tip-enhanced Raman spectroscopy/scanning tunneling microscopy (UHV-TERS/STM) and surface-enhanced femtosecond stimulated Raman scattering (SE-FSRS) to advance the spatial and temporal resolution of chemical imaging for the study of photoinduced dynamics of molecules on plasmonically active surfaces. An accompanying theory program includes modeling of charge transfer processes using constrained density functional theory (DFT) in addition to modeling of SE-FSRS, thereby providing a detailed description of the excited state dynamics. Over the past year, significant experimental and theoretical progress has been made on multiple topics including ultrafast UHV-TERS/STM and chemically modified graphene and silicon on plasmonic substrates.

2. Recent Progress

2.1. Ultrafast UHV-TERS/STM

The SISGR team has reliably demonstrated single molecule detection with TERS. In particular, TERS spectra show significant relative intensity fluctuations over time. No correlation is observed in mode-to-mode intensity fluctuations, indicating that the changes in mode intensities are completely independent. Theoretical calculations provide convincing evidence that the fluctuations are not the result of diffusion, orientation, or local electromagnetic field gradients but rather are the result of subtle variations of the excited-state lifetime, energy, and geometry of the molecule.

In UHV, the first TERS data with liquid helium cooling of the sample was reported, from which the adsorbate-substrate interactions of the rhodamine 6G/Ag(111) system were deduced. The spectra exhibited significant line narrowing up to the instrument-limited response along with new vibrational characteristics of rhodamine 6G. Theoretical analysis of the rhodamine 6G vibrational modes allowed interrogation of the interaction between rhodamine 6G and the Ag(111) surface.

Temporally resolved TERS has also been advanced significantly in the past year. Specifically, TERS using pulsed excitation under atmosphere pressure conditions was demonstrated. TERS data from both crystal violet and malachite green isothiocyanate were observed, and were found to match spectra taken with CW irradiation. The necessarily high peak power during the laser pulses led to a loss in signal, which could be attributed to reactive decay chemistry. To minimize the presence of atmospheric reactants, we have recently incorporated picosecond pulses into our UHV-STM for pulsed-excitation UHV-TERS. We have collected spectra demonstrating UHV-TERS of rhodamine 6G on Ag(111) using picosecond irradiation and, importantly, our results suggest that the UHV environment mitigates signal decay.

2.2. Chemically Modified Graphene and Silicon on Plasmonic Substrates

The SISGR team demonstrated the first growth of graphene on Ag(111), which has been a challenge to the scientific community because of the inert nature of Ag surfaces. Since traditional chemical vapor deposition (CVD) techniques that are typically utilized for graphene growth do not work on Ag substrates, we developed an alternative method based on direct deposition of elemental carbon (i.e., carbon evaporated from a graphite rod in an e-beam heater). The resulting graphene on Ag substrates complement, enhance, and support the aforementioned efforts on chemical imaging utilizing TERS.

In addition to bulk graphene, progress has been made on the growth of graphene nanoribbons on plasmonically active Au(111) surfaces. Specifically, halogenated polycyclic aromatic hydrocarbons allow graphene nanoribbons to be formed via ring-coupling reactions on Au(111). At the initial stage, the molecules self-assemble to form a noncovalently interacting adlayer. However, after annealing the substrate to 500 K, the molecules covalently cross-link via scission of the halogen bonds. Further annealing of the substrate to 750 K finally results in the formation of graphene nanoribbons. The structural and electronic properties of the graphene nanoribbons are then investigated at the single nanoribbon level using STM and scanning tunneling spectroscopy, respectively.

In an effort to diversify the range of surface chemistries on plasmonically active substrates, we have also completed an extensive study that follows the evolution of silicon deposition on Ag(111) from multiple surface alloy phases to the precipitation of two-dimensional sheets of sp^3-bonded silicon. This silicon growth method is compatible with graphene growth on silver, thus allowing the synthesis of both lateral and vertical graphene-silicon heterostructures. These substrates thus allow direct interrogation of the interaction of adsorbates with two contrasting surfaces: highly reactive silicon and relatively inert graphene, which tend to interact with adsorbates in a covalent and noncovalent manner, respectively.

In parallel with the silicon and graphene growth efforts, chemical functionalization methods have been developed and interrogated on these surfaces with UHV STM. For example, perylenetetracarboxylic diimide (PTCDI) and melamine have been co-deposited on graphene to form a spatially periodic two-dimensional nanoporous network architecture with hexagonal symmetry. The resulting adlayer interacts noncovalently with the underlying graphene substrate and possesses a characteristic domain size of 40-50 nm. In addition, ZnO nanoparticle growth has been achieved on graphene following epoxidation with atomic oxygen, while covalent adsorption has been achieved on Si(100) with cyclopentene.

2.3. Theory/Modeling

Due to the complexity of the ongoing experimental work, theory and modeling play a critical role in helping define productive experiments and interpreting freshly gathered data. In the area of plasmonics, the nonlinear optical dynamics of nanomaterials comprised of plasmons interacting with quantum emitters have been investigated using a self-consistent model based on the coupled Maxwell-Liouville-von Neumann equations. It was shown that ultra-short resonant laser pulses can serve to control the optical properties of such hybrid systems. Furthermore, it was illustrated that the energy transfer between interacting molecules and plasmons occurs on a femtosecond time scale and can be tuned with both material and laser parameters.

Theoretical effort has also been devoted to understanding surface chemical reactions such as ZnO nanoparticle growth on epoxidized graphene. As expected, computational models verify that diethyl zinc abstracts an oxygen from graphene epoxide when deposited on the surface. Here, the weak Zn-C bond is replaced with a stronger Zn-O bond. The resulting species then

proceeds to search for a second epoxide group on the surface to replace the remaining Zn-C bond with a second Zn-O bond. Both of these reactions were found to be exothermic from DFT calculations. More recent work has focused on the examination of subsequent reactions that occur when two of these zinc-containing species interact. For example, diethoxy zinc species are prone to oligomerization by forming a four-membered Zn-O-Zn-O ring.

3. Future Plans

In future work, we intend to utilize the knowledge and momentum gained from the aforementioned accomplishments to advance the following project objectives:

(1) *Ultrafast UHV-TERS/STM*: We aim to further our instrumental capabilities while studying molecules and processes with direct applications to energy technologies. For example, we are currently employing UHV-TERS/STM to interrogate the properties of perylene-based chromophores that are commonly used by the solar energy community as light harvesters. Another area of research centers on quantifying the ultimate spatial resolution in TERS. At present, we have demonstrated 4 nm resolution and are continuing efforts to determine if this can be extended to the 1 nm level. In addition, we will work toward picosecond and femtosecond pump-probe experiments in conjunction with UHV-TERS. After determining conditions where femtosecond pulses do not result in substrate or tip damage, we will conduct ground state FSRS experiments.

(2) *Integrating 2D materials and heterostructures with plasmonic substrates*: Over the past year, graphene and two-dimensional silicon have been grown separately and together as heterostructures on plasmonically active Ag(111) in UHV. In future work, we will expand these UHV growth efforts to include other emerging 2D materials such as transition metal dichalcogenides and elemental semiconductors. For example, in preliminary data, we have seen evidence for a 2D phase of boron on Ag(111), which was predicted theoretically but not previously observed experimentally. Heterostructures and alloys (e.g., 2D-SiC) will also be pursued based on these materials since they share the same growth substrate. Furthermore, chemical functionalization will be performed in UHV with gas-phase precursors such as hydrogen, oxygen, and volatile organics.

4. Publications

[1] Md.Z. Hossain, J.E. Johns, K.H. Bevan, H.J. Karmel, Y.T. Liang, S. Yoshimoto, K. Mukai, T. Koitaya, J. Yoshinobu, M. Kawai, A.M. Lear, L.L. Kesmodel, S.L. Tait, M.C. Hersam, *Nature Chemistry*, **4**, 305 (2012).

[2] N. Jiang, E.T. Foley, J.M. Klingsporn, M.D. Sonntag, N.A. Valley, J.A. Dieringer, T. Seideman, G.C. Schatz, M.C. Hersam, R.P. Van Duyne, *Nano. Lett.*, **12**, 5016 (2012).

[3] A. Deshpande, C.-H. Sham, J.M.P. Alaboson, J.M. Mullin, G.C. Schatz, M.C. Hersam, *J. Am. Chem. Soc.*, **134**, 16759 (2012).

[4] J. Cho, J. Smerdon, L. Gao, Ö. Süzer, J.R. Guest, N.P. Guisinger, *Nano Lett.*, **12**, 3018 (2012).

[5] J. Tian, H. Cao, W. Wu, Q. Yu, N.P. Guisinger, Y.P. Chen, *Nano Lett.*, **12**, 3893 (2012).

[6] J.M. Mullin, J. Autschbach, G.C. Schatz, *Comp. Theor. Chem.*, **987**, 32 (2012).

[7] J.M. Mullin, G.C. Schatz, *J. Phys. Chem. A*, **116**, 1931 (2012).

[8] J.M. McMahon, S.K. Gray, G.C. Schatz, *J. Phys. Chem. C*, **114**, 15903 (2012).

[9] M.G. Blaber, A.-I. Henry, J.M. Bingham, G.C. Schatz, R.P. Van Duyne, *J. Phys. Chem. C*, **116**, 393 (2012).

[10] M.D. Sonntag, J.M. Klingsporn, L.K. Garibay, J.M. Roberts, J.M. Dieringer, T. Seideman, K. Scheidt, L. Jensen, G.C. Schatz, R.P. Van Duyne, *J. Phys. Chem. C*, **116**, 478 (2012).
[11] J.M. Mullin, N. Valley, M.G. Blaber, G.C. Schatz, *J. Phys. Chem. A*, **116**, 9574 (2012).
[12] M.G. Reuter, M.C. Hersam, T. Seideman, M.A. Ratner, *Nano Lett.*, **12**, 2243 (2012).
[13] M.G. Reuter, M.A. Ratner, T. Seideman, *Phys.Rev. A*, **86**, 013426 (2012).
[14] Z. Hu, M.A. Ratner, T. Seideman, *J. Chem. Phys.*, **137**, 204111 (2012).
[15] R.R. Frontiera, N.L. Gruenke, R.P. Van Duyne, *Nano. Lett.*, **12**, 5989 (2012).
[16] B. Sharma, R.R. Frontiera, A.-I. Henry, E. Ringe, R.P. Van Duyne, *Materials Today*, **15**, 16 (2012).
[17] E.A. Pozzi, M.D. Sonntag, N. Jiang, J.M. Klingsporn, M.C. Hersam, R.P. Van Duyne, *ACS Nano*, **7**, 885 (2013).
[18] H.J. Karmel, M.C. Hersam, *Appl. Phys. Lett.*, **102**, 243106 (2013).
[19] E.V. Iski, E.N. Yitamben, L. Gao, N.P. Guisinger, *Adv. Funct. Mater.*, **23**, 2554 (2013).
[20] J.A. Smerdon, R.B. Rankin, J.P. Greeley, N.P Guisinger, J.R. Guest, *ACS Nano*, **7**, 3086 (2013).
[21] N. Valley, N. Greeneltch, R.P. Van Duyne and G.C. Schatz, *JPCL*, **4**, 2599 (2013).
[22] B. Fainberg, T. Seideman, *Chem. Phys. Lett.*, **576**, 1 (2013).
[23] S.L. Kleinman, R.R. Frontiera, A.-I. Henry, J.A. Dieringer, R.P. Van Duyne, *Phys. Chem. Chem. Phys.*, **15**, 21 (2013).
[24] M.D. Sonntag, D. Chulhai, T. Seideman, L. Jensen, R. P. Van Duyne, *J. Am. Chem. Soc.*, **135**, 17187 (2013).
[25] A. Natan, M.C. Hersam, T. Seideman, *Nanotechnology*, **24**, 505715 (2013).
[26] Z. Hu, M.A. Ratner, T. Seideman, *Chem. Phys.*, **415**, 14 (2013).
[27] J.E. Johns, J.M.P. Alaboson, S. Patwardhan, C.R. Ryder, G.C. Schatz, M.C. Hersam, *J. Am. Chem. Soc.*, **135**, 18121 (2013).
[28] B. Kiraly, E. V. Iski, A. J. Mannix, M. C. Hersam, N. P. Guisinger, *Nature Comm.*, **4**, 2804 (2013).
[29] J.M.P. Alaboson, C.-H. Sham, S. Kewalramani, J.D. Emery, J.E. Johns, A. Deshpande, T. Chien, M.J. Bedzyk, J.W. Elam, M.J. Pellin, M.C. Hersam, *Nano Lett.*, **13**, 5763 (2013).
[30] J.M. Klingsporn, N. Jiang, E.A. Pozzi, M.D. Sonntag, D. Chulhai, T. Seideman, L. Jensen, M.C. Hersam, R. P. Van Duyne, *J. Am. Chem. Soc.*, **136**, 3881 (2014).
[31] J.M. Klingsporn, M.D. Sonntag, T. Seideman, R.P. Van Duyne, *JPCL*, **5**, 106 (2014).
[32] F.W. Aquino, G. C. Schatz, *J. Phys. Chem. A*, **118**, 517 (2014).
[33] Md. Z. Hossain, M.B.A. Razak, S. Yoshimoto, K. Mukai, T. Koitaya, J. Yoshinobu, H. Sone, S. Hosaka, M.C. Hersam, *J. Phys. Chem. C*, **118**, 1014 (2014).
[34] H.J. Karmel, T. Chien, V. Demers-Carpentier, J.J. Garramone, M.C. Hersam, *JPCL.*, **5**, 270 (2014).
[35] A.J. Shearer, J.E. Johns, B.W. Caplins, D.E. Suich, M.C. Hersam, C.B. Harris, *Appl. Phys. Lett.*, **104**, 231604 (2014).
[36] H.J. Karmel, J.J. Garramone, J.D. Emery, S. Kewalramani, M.J. Bedzyk, M.C. Hersam, *Chem. Comm.*, **50**, 8852 (2014).
[37] E.A. Pozzi, M.D. Sonntag, N. Jiang, N. Chiang, T. Seideman, M.C. Hersam, R.P. Van Duyne, *JPCL*, **5**, 2657 (2014).
[38] A.J. Mannix, B. Kiraly, B.L. Fisher, M.C. Hersam, N.P. Guisinger, *ACS Nano*, **8**, 7538 (2014).
[39] M.D. Sonntag, E.A. Pozzi, N. Jiang, M.C. Hersam, R.P. Van Duyne, *JPCL*, **5**, 3125 (2014).

Chemical Kinetics and Dynamics at Interfaces

Laser induced reactions in solids and at surfaces

Wayne P. Hess (PI) Alan G. Joly and Kenneth Beck

Physical Sciences Division
Pacific Northwest National Laboratory
P.O. Box 999, Mail Stop K8-88,
Richland, WA 99352, USA
wayne.hess@pnnl.gov

Additional collaborators include A.L. Shluger, P.V. Sushko
P.Z. El-Khoury, W.D. Wei, S.J. Peppernick, V.A. Apkarian

Program Scope

The chemistry and physics of electronically excited solids and surfaces is relevant to the fields of photocatalysis, radiation chemistry, and solar energy conversion. Irradiation of solid surfaces by UV, or higher energy photons, produces energetic species such as core holes and free electrons, that relax to form electron-hole pairs, excitons, and other transient species capable of driving surface and bulk reactions. The interaction between light and nanoscale oxide materials is fundamentally important in catalysis, microelectronics, sensor technology, and materials processing. Photostimulated desorption studies, of atoms or molecules, provide a direct window into these important processes and are particularly indicative of electronic excited state dynamics. Greater understanding is gained using a combined experiment/theory approach. We therefore collaborate with leading solid-state theorists who use *ab initio* calculations to model results from our laser desorption and photoemission experiments. The interaction between light and metal nano objects can lead to intense field enhancement and strong optical absorption through excitation of surface plasmon polaritons. Such plasmon excitation can be used for a variety of purposes such as ultrasensitive chemical detection, solar energy generation, or to drive chemical reactions. Large field enhancements can be localized at particular sites by careful design of nanoscale structures. Similar to near field optics, field localization below the diffraction limit can be obtained. The dynamics of plasmonics excitations is complex and we use finite difference time domain calculations to model field enhancements and optical properties of complex structures including substrate couplings or interactions with dielectric materials.

Approach:

We are developing a combined PEEM two-photon photoemission approach to probe plasmonic nanostructures such as solid metal particles or lithographically produced nanostructures such as such as gratings or nanohole arrays. We then correlate PEEM images with scanning electron microscopy or surface enhanced Raman spectroscopy (or the spatially resolved tip-enhanced implementation). Finite difference time domain (FDTD) calculations are used to interpret the field enhancements measured by the electron and optical techniques. The effects of extreme electric field enhancement on Raman spectra is investigated using plasmonic nanostructures constructed from a metal nanoparticles or metal covered atomic force microscopy (AFM) tips on flat metal substrates. The Raman scattering from molecules adhered between these structures show greatly enhanced scattering and often highly perturbed spectra depending on nanogap dimensions or whether a conductive junction is created between tip and substrate. In photodesorption studies, photon energies are chosen to excite specific surface structural features

that lead to particular desorption reactions. The photon energy selective approach takes advantage of energetic differences between surface and bulk exciton states and probes the surface exciton directly. We measure velocities and state distributions of desorbed atoms or molecules from ionic crystals using resonance enhanced multiphoton ionization and time-of-flight mass spectrometry. Application of this approach to controlling the yield and state distributions of desorbed species requires detailed knowledge of the atomic structure, optical properties, and electronic structure. We have demonstrated surface-selective excitation and reaction on alkali halides and generalized our exciton model to oxide materials and shown that desorbed atom product states can be selected by careful choice of laser wavelength, pulse duration, and delay between laser pulses.

Recent Progress

Very intense photoelectron emission has been observed from localized points on nanostructured metal surfaces following UV femtosecond (fs) laser excitation. The regions of intense emission, dubbed 'hot spots', are due to collective charge oscillations, termed localized surface plasmons (LSPs). The intensity of the incident electric field can be amplified several orders of magnitude when resonantly coupled with the LSP mode of the nanostructure. The electromagnetic (EM) field amplification is largely responsible for non-linear phenomena such as surface enhanced Raman scattering (SERS) although SERS intensities are a convolution of both electronic and chemical Raman enhancement factors. While the EM contribution is believed to dominate the overall SERS signal, obtaining a quantitative measure of individual chemical and EM contributions, from a single molecule or hot spot, has proved challenging. It is possible to measure the field enhancement due to a nanoparticle LSP using PEEM. By applying a two-photon excitation scheme, using fs laser pulses, isolated EM enhancements can be examined and photoemission yields can be correlated with detailed structural images from complementary microscopic techniques such as scanning electron microscopy (SEM).

Solid silver nanoparticles (average diameters of 34, 75 and 122 nm) were deposited on an atomically flat mica substrate and covered with a 50 nm Ag thin film. The enhancement in photoelectron yield of single nanoparticles illuminated with femtosecond laser pulses (400 nm, ~3.1 eV) is found to be a factor of 10^2 to 10^3 times greater than that produced by the adjacent flat silver thin film. High-resolution, multi-photon PEEM images of single silver nanoparticles reveal that the greatest enhancement in photoelectron yield is localized at distinct regions of the nanoparticle whose magnitude and spatial extent is dependent on the incident electric field polarization. In conjunction with correlated scanning electron microscopy (SEM), nanoparticles that deviate from nominally spherical shapes are found to exhibit irregular spatial distributions in the multi-photon PEEM images that are correlated with unique particle shape or topology. Furthermore, we determined that Enhancement Factors, within each nanoparticle size range, exhibit a large spread of values indicative of the exact geometry and local environment unique to each individual nanoparticle.

PEEM is a charged particle (photoelectrons) imaging technique and has therefore been applied almost exclusively to conducting materials and in particular metals. We have found, however, that wide-gap semiconductors and even insulating materials, in some cases, yield high quality PEEM images. We have imaged 3 μm diameter polystyrene spheres supported on a thin metal substrate illuminated by 400 nm (~ 3.1 eV) and 800 nm (~ 1.5 eV) femtosecond (fs) laser pulses. Intense photoemission is generated by microspheres even though polystyrene is an insulator and its ionization threshold is well above the photon energies employed. We observe the most intense photoemission from the far side (the side opposite the incident light) of the illuminated microsphere that is attributed to light focusing within the microsphere. The light focused though the microsphere then propagates to the thin film surface where photoemission from the metal substrate can be imaged. For the case of p-polarized, 800 nm fs laser pulses, we observe

photoemission exclusively from the far side of the microsphere and additionally resolve sub-50 nm hot spots in the supporting Pt/Pd thin film that are located only within the focal region of the microsphere. We find that the fs PEEM images at both 400 and 800 nm can be modeled using FDTD electrodynamic simulations. The FDTD calculations predict light focusing in the optically transparent microsphere and subsequent focusing of the transmitted field on the supporting metal surface. The ability to obtain high resolution and high contrast PEEM image from an insulator is attributed to photoinduced conductivity of the polystyrene microspheres.

Future Plans

Time-resolved two-photon PEEM is an experimental method which offers both nanometer spatial and fs time resolution. We have conducted proof-of-principle studies for an initial set of plasmonic nanostructures, specifically, hexagonal and prism shaped gold particles using this technique. These initial studies capture spatially resolved field enhancement, and subsequent decay dynamics, following 800 nm fs laser excitation. Using PEEM we have measured plasmonic enhancement factors, without the presence of a molecular emitter as in surface enhanced Raman scattering (SERS). We now have the tools needed to correlate field enhancement with SERS response and by adding time-resolved PEEM (stabilized using a recently constructed Mach-Zhender interferometer) the path opens to an entirely new set of measurements capable of correlating structure and dynamics of a variety of designer plasmonic hotspots (e.g. the nano-gaps of particle aggregates or in gaps between surface structures drawn by focused ion beam lithography). The inclusion of helium ion lithography into our arsenal, now allows sub 10 nm structures to be fabricated.

Future plans include correlating femtosecond PEEM with transmission electron microscopy (TEM) and tip-enhanced Raman spectroscopy (TERS) to study plasmon resonant photoemission from noble metal nanostructures and time-resolved PEEM to probe dynamics of metal and hybrid (metal:metal-oxide) nanostructures. We will interrogate such metal-insulator systems using a variety of advanced techniques including: x-ray and ultraviolet photoelectron spectroscopy (XPS, UPS) femtosecond 2PPE, PEEM, SERS and the tip enhanced version (TERS) for spatially-resolved Raman spectroscopy. Femtosecond time-resolved PEEM can reveal spatially resolved ultrafast dynamics and is a powerful tool for studying the near-surface electronic states of nanostructures or plasmonic devices. We have recently developed capabilities to perform energy-resolved two-photon photoemission using a hemispherical analyzer XPS instrument. In combination we expect these two techniques will provide spatially-resolved electronic state dynamics of nanostructured metal-insulator materials.

By generalizing the exciton based desorption model to metal oxides, we can pursue selective excitation of specific surface sites, on an atomic scale, for a general class of technologically important materials. We note that the higher valence of oxides requires a more complex mechanism. With the aid of DFT calculations we have developed a “hole plus exciton” mechanism that relies on the combination of a surface exciton with a three-coordinated surface-trapped hole. In analogy to alkali halide thermal desorption, we have considered a bulk-based thermal desorption mechanism involving trapping of two holes at a three-coordinated site (a “two-hole localization” mechanism). Our calculations, however, do not indicate that two-hole localization is likely without invoking a dynamical trapping process. Since extensive calculations have not yielded an enduring theoretical model for thermal desorption we are exploring possible nonthermal mechanisms that yield low kinetic energy particle desorption in the “thermal energy” range. Experiments on CsBr thin films on Cu suggest intriguing possibilities of near-thermal desorption due to surface charging. We will therefore study low energy desorption from thin films of CsBr, CsI, and perhaps RbI grown on insulators and metals. We also plan to grow and study oxide thin films, such as ZrO_2, BaO, and MgO, on well-characterized metal surfaces.

References to publications of DOE BES sponsored research (2012 to present)

1. S.J. Peppernick, A.G. Joly, K.M. Beck, and W.P. Hess "Near-Field Focused Photoemission from Polystyrene Microspheres Studied with Photoemission Electron Microscopy", *J. Chem. Phys.* **137**, 014202 (2012).

2. S.J. Peppernick, A.G. Joly, K.M. Beck and W.P. Hess, J. Wang, Y.C. Wang and W.D. Wei, "Two-Photon Photoemission Microscopy of a Plasmonic Silver Nanoparticle Trimer," *Appl. Phys. A* **112**, 35 (2013).

3. A. Polyakov, C. Senft, K. F. Thompson, J. Feng, S. Cabrini, P. J. Schuck, H. A. Padmore, S. J. Peppernick, and W. P. Hess, "Plasmon enhanced photocathode for high brightness and high repetition rate x-ray sources" Phys. Rev. Lett.**110**, 076802 (2013).

4. P.Z. El-Khoury, S.J. Peppernick, D. Hu, A.G. Joly, and W.P. Hess, "The Origin of Surface-Enhanced Raman Scattering of 4,4'-Biphenyldicarboxylate on Silver Substrates" *J. Phys. Chem. C*, **117**, 7260 (2013).

5. S.J. Peppernick, A.G. Joly, K.M. Beck, and W.P. Hess "Plasmon-Induced Optical Field Enhancement studied by Correlated Scanning and Photoemission Electron Microscopy", *J. Chem. Phys.* **138**, 154701 (2013).

6. P.Z. El-Khoury, D. Hu, V.A. Apkarian and W.P. Hess, "Raman Scattering at Plasmonic Junctions Shorted by Conductive Molecular Bridges" *Nano Lett*. **13**, 1858 (2013).

7. M.T.E. Halliday, A.G. Joly, W.P. Hess, P.V. Sushko and A.L. Shluger, "Photodesorption of Br-atoms from crystalline CsBr thin films grown on LiF and KBr(100)," *J. Phys. Chem. C*, **117**, 1302 (2013).

8. P.Z. El-Khoury, W.P. Hess, "A Theoretical Investigation of Raman from a Single 1,3-Propanedithiol Molecule." *Chem. Phys. Lett*. **581**, 57 (2013).

9. Patrick Z. El-Khoury, Dehong Hu, and Wayne P. Hess, "Junction Plasmon Induced Molecular Reorientation" *J. Phys. Chem. Lett.* **4**, 3435 (2013).

10. Patrick Z. El-Khoury, Eric J. Bylaska, and Wayne P. Hess, "Time Domain Simulations of Chemical Bonding Effects in Surface-Enhanced Spectroscopy." *J. Chem. Phys.* **139**, 174303 (2013).

11. Patrick El-Khoury, Wayne Hess, "Vibronic Raman Scattering at the Quantum Limit of Plasmons" *Nano Lett*. **14**, 4114 (2014).

12. Patrick Z. El-Khoury, Karoliina Honkala, Wayne P. Hess, "Electronic and Vibrational Properties of Meso-Tetraphenylporphyrin on Silver Substrates" in press *J. Phys. Chem. A* (A.W. Castleman Festschrift Issue).

13. Patrick Z. El-Khoury, Tyler W. Ueltschi, Amanda L. Mifflin, Dehong Hu, and Wayne P. Hess "Frequency Resolved Nanoscale Chemical Imaging of4,4′-Dimercaptostilbene on Silver" submitted to *Nano Lett.*

Spectroscopic Imaging of Molecular Functions at Surfaces

Wilson Ho

Department of Physics & Astronomy and of Chemistry
University of California, Irvine
Irvine, CA 92697-4575 USA

wilsonho@uci.edu

Program Scope:

This project is concerned with the experimental challenge of reaching single molecule sensitivity with atomic scale spatial resolution in spectroscopic imaging and the associated understanding of molecular functions. These experiments would lead to an understanding of the inner machinery of single molecules that are not possible with other approaches, including the electronic, vibrational, and structural properties, as well as the relation of these properties to the reactivity, chemical sensing, self-assembly, and other molecular interactions. Results from these studies provide the molecular basis for understanding properties, processes, and phenomena in chemical and physical systems over different length scales from the atomic to macroscopic ensembles. The experiments rely on the unique properties of the scanning tunneling microscope (STM) when operated below 1 K. Results from this project could form the basis for new insights into surface chemistry and catalysis, environmental processes and energy generation, electronic processing and electron transport through molecules.

Recent Progress:

The most recent results obtained during the past year are described in this report, highlighting the spectroscopic imaging of the molecular structure and its relation to molecular functions (in this case, intermolecular interactions pertinent to self-assembly.) The arrangement of atoms in a molecule implicates its physical and chemical properties. The scanning tunneling microscope previously has provided spatially resolved electronic and vibrational signatures of single molecules. However, the spatial distributions of these signatures do not relate directly to the geometric structures of the molecules. When a CO-terminated tip is scanned over a cobalt phthalocyanine (CoPc) molecule, the energy, intensity, and line shape of the lowest energy, hindered translational, soft mode of CO vary over each atom, bond, and lone electron pair in the molecule. These variations in the CO vibration are detected by inelastic electron tunneling spectroscopy (IETS) with the STM. Spatial imaging at a selected energy within the peak of the hindered translational mode of the CO of the CO-terminated tip yields direct visualization of the skeletal structure of the molecule. The combined capabilities of the scanning tunneling microscope suggest the possibility of relating the structure (electronic, vibrational, geometric) and function in chemistry at the single molecule level.

In the August 28, 2009 issue of Science, Leo Gross, Fabian Mohn, Nikolaj Moll, Peter Liljeroth, and Gerhard Meyer at IBM Zürich imaged the molecular structure of pentacene with the atomic force microscope (AFM) with a CO-terminated tip. Since then a few papers have been

published by Meyer's group and others, notably in the June 21, 2013 issue of Science led by the UC Berkeley groups and in the November 1, 2013 issue of Science led by National Center for Nanoscience and Technology in Beijing. Numerous other papers followed. In all these papers the authors note the inability of the scanning tunneling microscope (STM) to achieve structural resolution, e.g. "Structural identification using STM, however, is limited by the microscopic contrast arising from the electronic local density of states (LDOS), which is not always easily related to chemical structure."

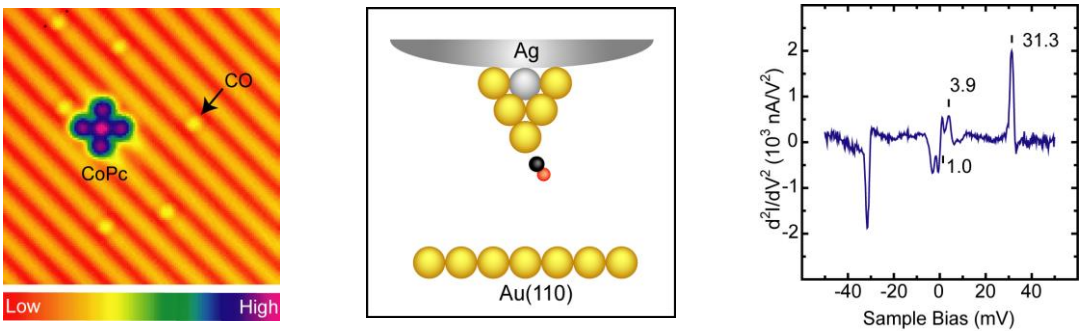

Fig. 1: (Left) Topographic image of CO coadsorbed with cobalt phthalocyanine (CoPc) on Au(110)-1×2 surface, recorded with a bare Au-covered Ag tip. (Middle) Schematic illustrating a CO-terminated tip. (Right) Vibrational spectrum for a single CO molecule on the tip taken by inelastic electron tunneling spectroscopy at 600 mK, revealing hindered translation mode at 3.9 meV and hindered rotational mode at 31.3 mV.

We showed that molecular structures can be imaged by the STM. Specifically individual atoms and bonds, as well as lone electron pairs are resolved. We have developed a new approach by picking up a CO molecule on the tip (Fig. 1) and monitor its low energy (about 4 meV), hindered translational vibrational mode as the CO-terminated tip is scanned over another molecule adsorbed on the surface (Fig. 2). We show that the energy, intensity, and line shape of the CO vibration are sensitive to the atoms, bonds, and lone electron pairs in the adsorbed molecule (cobalt phthalocyanine: 57 atoms, 68 bonds, and 4 lone pairs) (Fig. 3). The CO vibration senses the skeletal structure differently than elsewhere, and is detected by inelastic electron tunneling spectroscopy with the STM (STM-IETS). This inelastic tunneling probe (itProbe) is expected to be generally applicable to other adsorbed molecules.

The CO-terminated tip has proven to be crucial for both the AFM and itProbe to resolve molecular structures. For the AFM, the CO-terminated tip provides a well-defined tip apex structure and the interactions in the tip-molecule junction can be sensed by the macroscopic cantilever with high sensitivity to obtain the required contrast for imaging the molecular structure. The itProbe also benefits from the well-defined tip apex structure provided by the CO. However, in contrast to the AFM, the environmental perturbations to a molecular vibration of the CO are monitored by STM-IETS signals.

The ability of the STM to image molecular structure is an important addition to its previously shown capabilities for manipulation and the determination of the electronic and vibrational properties. The results presented in this manuscript suggest opportunities to relate structure and function in chemistry at the single molecule level.

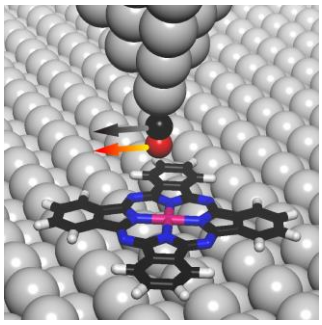

Fig. 2: Schematic of itProbe. A CO-terminated tip is scanned over a cobalt-phthalocyaine (CoPc) molecule adsorbed on Ag(110) at 600 mK. The intensity of the hindered translational mode of CO is monitored and imaged in this inelastic tunneling probe (itProbe).

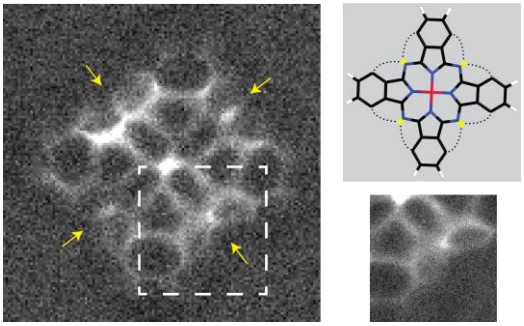

Fig. 3: Image of CoPc skeletal structure. (Left) Spatial distribution of the d^2I/dV^2 signal at 1.7 mV within the hindered translational mode of CO of the CO-terminated tip. Arrows point to the four lone pairs on the imine nitrogen atoms. (Right, Top) Schematic of CoPc showing in curved dash line the interactions of the C-H bonds with the lone pairs. (Right, Bottom) Zoom-in of the area indicated by the dashed box in the Left panel.

Future Plans:

The relationship among the molecular composition, structure, bonding, and reactivity is one of the central dogmatic principles in chemistry. The itProbe images the structure and bonding in single molecules. The determination of the molecular composition by identifying the atoms remains a challenge. The changes that a molecule undergoes are in response to its environment, such as temperature, light, charge, and nearby chemical species. The functions of a molecule could involve a change to a different molecule or an interaction with another molecule without a change in identity, such as in self-assembly or chemical sensing. Future research seeks an understanding of molecular functions by imaging the structure and bonding with a low temperature scanning tunneling microscope, in combination with the electronic and vibrational spectroscopies and manipulation. The focus of the future plans includes the following problems in chemistry: 1. imaging the nature of different bonds: covalent, coordination, hydrogen, and van der Waals, 2. the driving forces in self-assembly, 3. mechanism of tautomerism, and 4. visualization and understanding of valence bond and molecular orbital theories.

References to Publications of DOE Sponsored Research:

[1] "*Rotational and vibrational excitations of a hydrogen molecule trapped within a nanocavity of tunable dimension*", S. Li, A. Yu, F. Toledo, Z. Han, H. Wang, H.Y. He, R. Wu, and W. Ho, Phys. Rev. Lett. **111**, 146102 (2013); DOE supported the experimental work of Li, Yu, Toledo, Han, and Ho; NSF supported the theoretical work of Wang, He, and Wu.

[2] "*Real-space imaging of molecular structure and chemical bonding by single-molecule inelastic tunneling probe*", Chi-lun Chiang, Chen Xu, Zhumin Han, and W. Ho, Science **344**, 885-888 (2014).
Highlighted in: UC Irvine News, Janet Wilson, "*Molecule unmasked*", 23 May 2014; Chemistry World, Simon Hadlington, "*Unusual H-Bond patterns revealed in single molecule image*", 27 May 2014; Microscopy and Analysis, Rebecca Pool, "*STM reveals bonds in single molecule*", 29 May 2014.

THEORY OF THE REACTION DYNAMICS OF SMALL MOLECULES ON METAL SURFACES

Bret E. Jackson

Department of Chemistry
104 LGRT
710 North Pleasant Street
University of Massachusetts
Amherst, MA 01003
jackson@chem.umass.edu

Program Scope

Our objective is to develop realistic theoretical models for molecule-metal interactions important in catalysis and other surface processes. The dissociative adsorption of molecules on metals, Eley-Rideal and Langmuir-Hinshelwood reactions, recombinative desorption and sticking are all of interest. To help elucidate the experiments that study these processes, we examine how the reaction dynamics depend upon the nature of the molecule-metal interaction, as well as experimental variables such as substrate temperature, beam energy, angle of impact, and the internal states of the molecules. Electronic structure methods based on Density Functional Theory (DFT) are used to compute the molecule-metal potential energy surfaces. Both time-dependent quantum scattering techniques and quasi-classical methods are used to examine the reaction dynamics. Effort is directed towards developing improved quantum methods that can accurately describe reactions, as well as include the effects of temperature (lattice vibration) and electronic excitations.

Recent Progress

The dissociative chemisorption of methane on a Ni catalyst is the rate-limiting step in the chief industrial process for H_2 production. This reaction, where a single C-H bond breaks, leaving CH_3 and H fragments bound to the surface, has a high barrier and a correspondingly small dissociative sticking probability that increases exponentially with collision energy below saturation. The reaction has an unusually strong dependence on the temperature of the substrate, and is also enhanced by vibrational excitation of the methane, but in a non-statistical fashion. Most of our recent work has focused on this reaction in an attempt to understand how methane reactivity varies with the temperature of the metal, the translational and vibrational energy in the molecule, and the properties of the metal surface. Initial studies used DFT to locate the transition state on several Ni and Pt surfaces, exploring how the potential energy surface (PES) for this reaction changed due to lattice motion. We found that vibrational motion of the metal atom over which the molecule dissociates causes the height of the barrier to dissociation to change. High dimensional quantum scattering calculations that included several key methane degrees of freedom (DOF) and the motion of this metal atom demonstrated that this effect led to a strong increase in reactivity with temperature. These studies led to the development of sudden models, where quantum calculations were implemented for and averaged over several frozen lattice configurations. These approaches reproduced the results of quantum treatments, and because motion of the heavy metal atom was not explicitly included, several orders of magnitude less computer time were required. These models have proven to be very useful in our more recent studies, and have been adopted by other groups. This early work was summarized in a recent book chapter reviewing the effects of lattice motion on gas-surface reactions [1].

We have developed a fully quantum approach to reactive scattering based on the Reaction Path Hamiltonian (RPH). The PES is harmonic for small displacements away from the reaction (or minimum energy) path, and if we ignore anharmonic terms for larger displacements, we can use DFT to compute a reasonably accurate PES that includes all 15 molecular DOF. We have derived close-coupled equations by expanding the total wavefunction in the adiabatic vibrational states of the molecule. We can then compute full 15-DOF dissociative sticking probabilities for methane dissociation on metals, using sudden models to average over surface impact sites and to introduce the effects of lattice motion. This represents a major breakthrough in our research program; these were the first calculations, based entirely on *ab intio* data, which could be compared directly with experimental studies of methane dissociative adsorption. We studied this reaction on Ni(111), motivated by experiments from the Utz group (Tufts), where they were able to measure dissociative sticking probabilities over a wide range of surface temperatures. This was the first real test of the models we developed for including lattice motion effects in these reactions. Not only did our methods accurately reproduce the observed variation with temperature, they were able to explain why the variation in reactivity with temperature was strong for certain energies and weak for others [2]. In addition, we were able to model and explain the variation in reactivity with nozzle temperature in terms of contributions to sticking from vibrationally excited molecules. Another set of studies focused on Pt(110)-(1x2), where the missing-row reconstruction leads to a very large surface corrugation, making this an excellent model for real (rough) catalysts [3]. Our focus was on comparing the reactivity and the molecule-phonon coupling at the step edges with that on the terrace sites of smooth Pt(111) and Pt(100) surfaces, as well as comparing with experimental work from the Beck group (EPFL). We found that the edge sites were more reactive, as expected, but that the effects of lattice motion were not any larger than on smoother surfaces, even though the phonon coupling was far more complicated, involving the motion of several lattice atoms. This coupling increases the dissociative sticking probability by about an order of magnitude when the surface temperature increases from 400 K to 600 K, in agreement with the experiments [3].

Recent experimental studies of CH_4 dissociation on Pt(111) by the Beck group show that the saturation coverage of CH_3 on the surface increases with both the translational energy and vibrational excitation of the incident molecule. We used DFT to examine how the dissociation barrier is modified by the presence of chemisorbed H and CH_3 fragments, finding that this barrier increases as the surface coverage of reaction products increases [4]. Using these results, we developed kinetic models that were able to reproduce and explain the saturation behavior observed in the experimental uptake curves, publishing a joint paper with the Beck group [4]. In another study, we used a purely classical RPH to examine methane reactions on Ni(100) and Ni(111) [5]. First, we showed that the perturbative assumptions made in our quantum RPH model are valid. Second, we showed that classical trajectory methods based on the RPH could reproduce in a reasonable fashion the behavior observed in the experiments, including differing vibrational efficacies. However, while these classical methods did a good job at describing the reactions of vibrationally excited molecules, they overestimated the reaction probability of molecules in the ground vibrational state. Our studies suggest that this is due to a non-conservation of zero point energy. The amount of vibrational zero point energy in the molecule is large, about 1.2 eV, and in classical mechanics this energy can lead to reactive trajectories at energies below the zero point energy-corrected activation energy [5].

In collaboration with the Kroes group (Leiden) we have used AIMD, *ab initio* molecular dynamics, to study methane dissociation on moving Pt(111) and Ni(111) surfaces. In AIMD, one computes the instantaneous forces on the particles "on the fly", using DFT in our case. This eliminates the need to construct approximate many-dimensional PESs, or make dynamical assumptions (other than the use of classical mechanics). This is part of a broader collaboration

with the Beck and Utz groups, who are performing experiments on these metal surfaces at high energies, where our classical methods should be accurate. The first set of studies on Pt(111) taught us many things [7]. First, it verified that our sudden treatment of molecular motion parallel to the surface was accurate. It also confirmed that reactions at lower energies occurred close to the top sites, where the barriers were lowest. These studies also allowed us to benchmark the accuracy of our DFT-based PES, confirming that the barrier was too low, as suspected. Finally, this work suggested that our treatment of molecular rotation could be improved. We explored methods for doing this in a subsequent paper [8]. In particular, we showed that a sudden treatment of molecular rotation was easily implemented, leading to good results. New AIMD results for Ni(111) were shown to be consistent with our earlier work. We also significantly expanded our basis set and coupling order, demonstrating full convergence for our RPH-based approach [8].

Exciting the vibrational modes of methane can significantly enhance reactivity. This increase, relative to that from putting the same amount of energy into translational motion, the so-called efficacy, is different for different vibrational modes, as well as for the same mode on different metal surfaces. We showed that on Ni(100) the symmetric stretch significantly softens at the transition state and is strongly coupled to the reaction coordinate. As a result there is a large vibrational efficacy for this mode, as observed by two experimental groups. We demonstrated how the efficacies for vibrational enhancement are related to transitions from higher to lower energy vibrationally adiabatic states, or to the ground state, with the excess energy going into motion along the reaction path, which corresponds to bond breaking at the transition state. We have been able to elucidate similar behavior on Ni(111) [2, 8]. Overall, agreement with experiment has been good, in terms of both the magnitude of the reactivity over a broad range of incident energies and temperatures, and the efficacies of the different vibrational modes for promoting reaction. More importantly, our approach made it possible to follow the flow of energy within the molecule as it dissociates, providing a detailed understanding of how translational, vibrational and lattice energy contribute to reactivity. All of our DOE-funded work on methane has been summarized in a invited Feature Article in *J. Phys. Chem.* [10].

In other (minor) work we co-authored a book chapter in a Springer text aimed at a more general audience, focusing on quantum effects in reactions [6]. We also have a brief Comment appearing in *Phys. Rev. Lett.*, regarding an earlier study in that journal that examined H atom trapping and sticking on graphene at very low temperatures [9].

Future Plans

We have recently computed a new, more accurate, PES for methane dissociation on Ni(111), and are close to generating one for Pt(111). The new Ni(111) surface will be used in a set of studies focused on several recent experiments involving the isotopologues of methane, CH_xD_{4-x}. Of particular interest are bond-selective reactions (by vibrational excitation) and the effects of mass, tunneling, and zero point energy on reactivity. We will also explore some improvements to our RPH-based scattering approach, particularly our treatment of molecular rotation. These PESs will also be used in our on-going collaboration with the Beck and Utz groups, who are making new measurements of CD_3H dissociation on Pt(111) and Ni(111), respectively. We have not yet applied our RPH-based approach to Pt(111), and it will be interesting to explore the mode-specific chemistry that has been observed on that metal. Also of interest is the relative reactivity of the Ni(111) and Pt(111) surfaces. Our earlier work found the Pt surface to be more reactive than the Ni, but experiment suggests that the difference is much larger than our study found. The behavior of the methyl group during the dissociation is different on the two metals, and this may play a role.

In a second, relatively new, study we are examining the dissociative chemisorption of H_2O on Ni(111). This is motivated by recent experimental results from the Beck group, who are the very first to measure dissociative sticking probabilities for water on a metal surface. Mode-selective chemistry is also observed, and the effects of lattice motion are more complicated than for methane. We are close to completing the PES study and computing dissociative sticking probabilities. We also have an ongoing project examining H-Ag interactions, motivated by experiments in the Wodtke group (MPI, Göttingen). In particular, we are examining scattering, subsurface penetration and thermal desorption, in collaboration with the Lemoine group in Toulouse, and Sven Nave in Orsay.

DOE-Sponsored Publications (past 2 years)

[1] B. Jackson, "The effects of lattice motion on gas-surface reactions", in *Dynamics of Gas-Surface Interactions, Atomic-level Understanding of Scattering Processes at Surfaces*, Springer Series in Surface Sciences, Vol. 50, pp. 213 – 237, 2013, eds. R. D. Muiño and H. F. Busnengo.

[2] B. Jackson and S. Nave, "The dissociative chemisorption of methane on Ni(111): The effects of molecular vibration and lattice motion" J. Chem. Phys. 138, 174705 (2013).

[3] D. Han, S. Nave and B. Jackson," Dissociative Chemisorption of Methane on Pt(110)-(1x2): Effects of Lattice Motion on Reactions at Step Edges." J. Phys. Chem. A 117, 8651-8659 (2013).

[4] H. Ueta, L. Chen, R. D. Beck, I. Colón-Diaz and B. Jackson, "Quantum state-resolved CH_4 dissociation on Pt(111): Coverage dependent barrier heights from experiment and density functional theory," Phys. Chem. Chem. Phys. 15, 20526 – 20535 (2013).

[5] M. Mastromatteo and B. Jackson, "The dissociative chemisorption of methane on Ni(100) and Ni(111): Classical and quantum studies based on the Reaction Path Hamiltonian, J. Chem. Phys. 139, 194701-1 – 9 (2013).

[6] C, Díaz, A. Gross, B. Jackson and G.-J. Kroes, "Elementary Molecule-Surface Scattering Processes Relevant to Heterogeneous Catalysis: Insights from Quantum Dynamics Calculations," in *Molecular Quantum Dynamics*, Springer Series Physical Chemistry in Action, pp. 31 – 58, 2014, ed. F. Gatti.

[7] F. Nattino, H. Ueta, H. Chadwick, M. van Reijzen, R. D. Beck, B. Jackson, M. C. van Hemert, and G.J. Kroes, "Ab Initio Molecular Dynamics Calculations versus Quantum-State Resolved Experiments on CHD_3 + Pt(111): New Insights into a Prototypical Gas-Surface Reaction," J. Phys. Chem. Lett. 5, 1294-1299 (2014).

[8] B. Jackson, F. Nattino, and G.J. Kroes, "Dissociative chemisorption of methane on metal surfaces: Tests of dynamical assumptions using quantum models and ab initio molecular dynamics," J. Chem. Phys. 141, 054102 (2014).

[9] B. Lepetit and B. Jackson, Reply to "Comment, Phys. Rev. Lett. 113, LTK1078 (2014)," Phys. Rev. Lett. LSK1108 (2014).

[10] S. Nave, A. K. Tiwari and B. Jackson," The Dissociative Chemisorption of Methane on Ni and Pt Surfaces: Mode-specific Chemistry and the Effects of Lattice Motion," J. Phys. Chem. (in press).

DE-FG02-07ER15889: **Probing catalytic activity in defect sites in transition metal oxides and sulfides using cluster models: A combined experimental and theoretical approach**

Caroline Chick Jarrold and Krishnan Raghavachari
Indiana University, Department of Chemistry, 800 East Kirkwood Ave.
Bloomington, IN 47405
cjarrold@indiana.edu, kraghava@indiana.edu

I. Program Scope

Our research program combines experimental and computational methods to study well-defined cluster models of heterogeneous catalytic materials. The focus of our studies has been transition metal oxide and sulfide clusters in non-traditional oxidation states (surface defect models) and their chemical and physical interactions with water, with the goal of modelling and understanding the role of various processes involved in H_2 production from photocatalyic decomposition of water using Group 6 (Mo and W) oxides and sulfides. The experiments and calculations are designed to probe fundamental, cluster-substrate molecular-scale interactions that are governed by charge state, peculiar oxidation states, and unique physical structures.

The general strategy of our studies continues to be as follows: (1) Determine how the molecular and electronic structures of transition metal suboxide and subsulfide clusters evolve as a function of oxidation state by reconciling anion photoelectron spectra of the bare clusters with high-level DFT calculations. Anions are of particular interest because of the propensity of metal oxide and sulfides to accumulate electrons in applied systems. (2) Measure and analyze the kinetics of cluster reactivity with water. (3) Dissect possible reaction mechanisms computationally, to determine whether catalytically relevant interactions are involved. (4) Verify these challenging computational studies by spectroscopic investigation [typically, anion photoelectron (PE) spectroscopy] of observed reactive intermediates. (5) Probe the effect of local electronic excitation on bare clusters and cluster complexes, to evaluate photocatalytic processes. The overarching goal of this project is to identify particular defect structures that balance structural stability with electronic activity, both of which are necessary for a site to be simultaneously robust and catalytically active, and to find trends and patterns in activity that can lead to improvement of existing applied catalytic systems, or the discovery of new systems.

II. Recent Progress

In addition to publishing reports on several ongoing projects, the preliminary results of which were reported in the 2013 abstract (computational studies on Group 6 transition metal sulfide reactions with H_2O, $M_xO_y^-$ + *R*OH reactivity studies), we have made progress on the following studies.

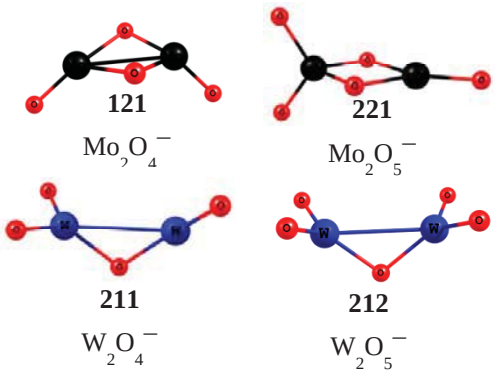

Figure 1. Based on mass spectrometric measurements, these ground state structures of Mo- and W- oxide clusters appear to have identical reactivity toward water; Anion PES and calculations uncover important differences.

A. Resolving the structure-reactivity paradox in $W_xO_y^-$ + H_2O and $Mo_xO_y^-$ + H_2O reactions. We have completed a series of experimental reactivity studies and computational studies on mechanisms and energies for the $M_xO_y^-$ + H_2O (M = Mo, W; x = 2, 3; $y \leq 3x$) reactions, resulting in numerous publications, with additional ongoing submissions. The primary motivation for the combined studies was to learn what governs the molecular scale interactions between water and model defect sites on heterogeneous catalysts for the production of H_2 from water decomposition. The results of these studies underscore the importance of electrostatic interactions, oxygen vacancies, *M*-O bond energies, and subtle differences in barrier heights.

These Group 6 transition metal-oxo clusters provided a unique opportunity to compare, in parallel, $Mo_2O_y^-$ and $W_2O_y^-$ homologs that have different ground state structures but apparently identical product patterns in reactions with water (see Figure 1; structures labeled ***abc*** to indicate the distribution of O-atoms between the two metal centers, O_a–M–O_b–M–O_c), and the $Mo_3O_y^-$ and $W_3O_y^-$ homologs have the same molecular and electronic structures, but exhibit disparate product patterns in reactions with water. Following is a synopsis of what we have learned.

First, most of the more reduced clusters of both $Mo_xO_y^-$ and $W_xO_y^-$ with $y < 2x$ for $x = 2$ and 3 readily reacted with water to form $M_xO_{y+1}^-$ and H_2. The high reactivity of these suboxide clusters is not unanticipated, but the production of H_2, rather than $M_xO_{y+1}H_2^-$ hydroxide complexes may indicate the usefulness of these species as photocatalysts.

Second, while our cluster models carry a negative charge, local dipole-dipole interactions are more important than charge-dipole interactions at reactive distances; dipole-dipole alignment initiates the dissociation of the water. Our most recent computational studies indicate that dissociative addition of water to $Mo_xO_y^-$ clusters is a lower-barrier process than dissociative water addition to $W_xO_y^-$ clusters. The ground state structure of $Mo_2O_5^-$ in particular accommodates less hindered dipole-dipole interactions, so while both $Mo_2O_5^-$ and $W_2O_5^-$ form dihydroxides upon water addition, the differences in rate constants and PE spectra of $Mo_2O_6H_2^-$ and $W_2O_6H_2^-$ can be correlated with their different structures.

Third, dissociative addition of water onto $M_xO_y^-$ clusters does not necessarily lead to H_2 formation. Structural rearrangement of one hydroxide group to form a hydride/hydroxide pair is a prerequisite for H_2 production. Our studies have shown that $W_xO_yH_2^-$ dihydroxide complexes convert to hydride/hydroxide complexes with lower barriers than the same conversion in analogous $Mo_xO_yH_2^-$ clusters, as borne out in the disparate reaction patterns observed in the $Mo_3O_y^-$ versus $W_3O_y^-$ + H_2O reactivity studies, and resolves another component structure-reactivity paradox.

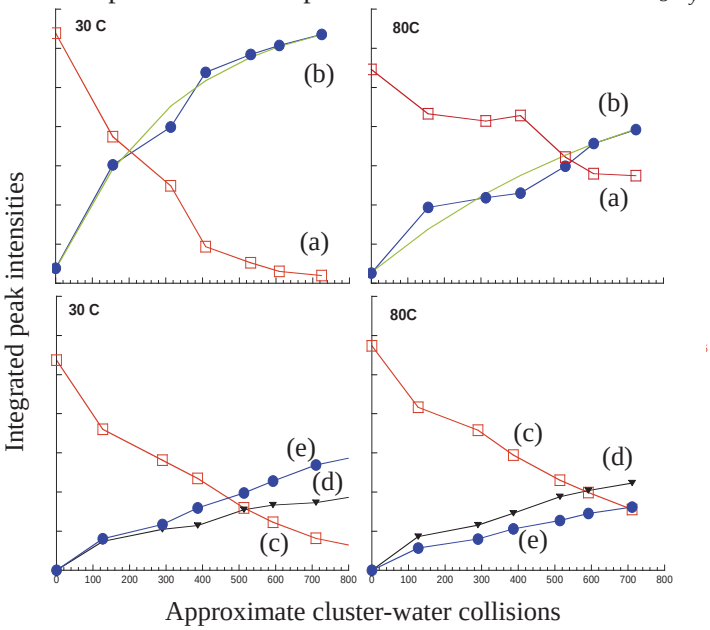

Figure 2. Integrated peak intensities for $M_2O_y^-$ and $M_2O_6H_2^-$ ions as a function of cluster-water collisions. The two top panels show (a) the sum of the $Mo_2O_y^-$ suboxide cluster intensities ($y = 2 – 5$) and (b) the $Mo_2O_6H_2^-$ peak intensity at T = 30°C and 80°C. The two bottom panels show (c) the sum of $W_2O_y^-$ suboxide cluster intensities ($y = 2 – 5$) and the increase in (d) $W_2O_6^-$ and (e) $W_2O_6H_2^-$ peak intensities at T = 30°C and 80°C.

B. Effect of temperature on $M_xO_y^-$ + H_2O reaction rates: *x*- and *y*-dependent Anti-Arrhenius behavior. Calculations on $M_xO_y^-$ + H_2O (M = Mo, W) reactions generally predict a fairly intricate sequence of steps, starting with electrostatic complex formation. Dissociative addition and rearrangement steps lead to $M_xO_{y+1}^-$ + H_2 formation, but initial complex formation tends to be either barrierless, as in the case of $Mo_xO_y^-$ + H_2O, or the barrier is low and arises from entropic factors, as in the case of $W_xO_y^-$ + H_2O. We have recently implemented the ability to control the temperature in the high-pressure fast-flow reactor used in our cluster + H_2O reactivity studies, and have preliminary results on the $M_xO_y^-$ + H_2O (M = Mo, W; $x = 2, 3$; $y \leq 3x$) reactions. Our new results show size-dependent anti-Arrhenius behavior, in addition to new processes not observed in previous studies because of significant improvements in our mass resolution.

With improved mass resolution, we have found that $W_2O_5^-$ + H_2O forms both $W_2O_6H_2^-$ and $W_2O_6^-$ + H_2 products in significant quantities, in contrast to $Mo_2O_5^-$, which reacts with water to exclusively form $Mo_2O_6H_2^-$. This result is shown graphically in Figure 2. $W_2O_6^-$ + H_2 product formation had been explored computationally; the new experimental results confirm the viability of the calculated reaction pathway. The rate of the $Mo_2O_6H_2^-$ terminal product formation has anti-Arrhenius temperature dependence; the overall rate decreases by a factor of more than 2 (individual steps, e.g., $Mo_2O_3^-$ + H_2O → $Mo_2O_4^-$ + H_2, $Mo_2O_4^-$ + H_2O → $Mo_2O_5^-$ + H_2, have unique T-dependence). In contrast, the terminal product for the oxidation of the $W_2O_y^-$ suboxides is partitioned between $W_2O_6^-$ and $W_2O_6H_2^-$; the ratio of the two products is T-dependent, as well. Calculations on activation barriers are method-sensitive, and these studies provide benchmarks for the methods we use.

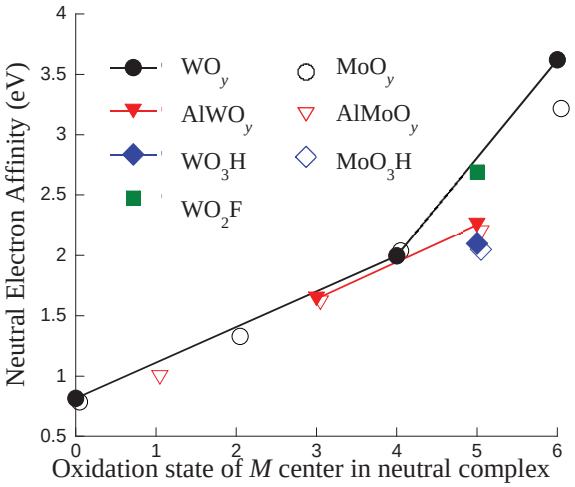

Figure 3. Adiabatic electron affinities (eV) of several W- and Mo-complexes, plotted as a function of the oxidation state of the metal center in the neutral complex.

C. General trends in EA for monometallic complexes- The binding energy of an 'excess' electron in metal-local orbitals in a metal-containing complex reflects or the ease with which a metal center can change between different oxidation states is an important parameter in its catalytic activity. We recently reported a systematic study of the impact of metal center oxidation state on neutral electron affinity (EA) determined by anion PES of a series of Mo- and W-molecular complexes. Since many Mo- and W- based enzymes feature coordination by oxo and hydroxo groups, we varied the oxidation state of MO_xH_y (M = Mo, W; x = 0-3; y = 0, 1) complexes with +1 increments by varying x and y. We also considered complexes in which the more electronegative F ligand replaced an OH ligand. Figure 3 shows a plot of neutral EA as a function of formal oxidation state of the metal center for a series of Mo- and W- complexes. We included points on the plot from previous measurements made by Lineberger et al., Wang et al., our own group, in which the metal center was found to assume the same oxidation state as MO_yH^-. See publication 5 for a complete reference list.

The anion PE spectra also give structural information about both the complex anions and neutrals, and from the spectra of species with different oxidation states, we found an incremental transformation between pyramical and planar structures as the metal center was incrementally reduced. Understanding these structural shifts informs efforts to understand mechanisms of Mo enzymes/catalysts.

D. Reactivity of Metal Sulfides with Water: The electronic structures and chemical reactivity of the mixed metal sulfide cluster anion ($MoWS_4^-$) have been investigated with density functional theory. Our study reveals the presence of two almost isoenergetic structural isomers, both containing two bridging sulfur atoms in a quartet state. However, the arrangement of the terminal sulfur atoms is different in the two isomers. In one isomer, the two metals are in the same oxidation state (each attached to one terminal S). In the second isomer, the two metals are in different oxidation states (with W in the higher oxidation state attached to both terminal S). The reactivity of water with the two lowest energy

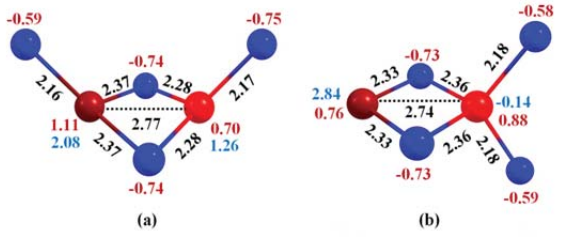

Figure 4. Optimized low-energy structures of $MoWS_4^-$. Brown, red, and blue circles denote Mo, W, ans S, respectively. Bond lengths in Å (black), atomic charges (red), and spin densities on the metal centers (blue) are also shown.

isomers has also been studied, with an emphasis on pathways leading to H_2 release. The reactive behavior of the two isomers is different though the overall barriers in both systems are small. In the first isomer, water reacts primarily through the lower coordinate Mo center since the oxidation state of W is already saturated. However, in the second isomer, W is the most reactive site for H_2 elimination reaction with water. Both kinetic selectivity and thermodynamic gain favor water addition on W-site. In conjunction with our previous work on the reactions of monometallic sulfides ($Mo_2S_n^-$ and $W_2S_n^-$, n=4-6), metal sulfides appear to be promising candidates for hydrogen generation from water.

III. Future Plans

The enduring strength of the research program is the synergistic interplay between theory and experiment. We have been working toward achieving a generalized description of the chemical reactivity of the transition metal oxides and sulfides resulting in H_2 evolution. We will expand on the temperature-dependence studies to new sulfide and heteronuclear cluster model systems. In addition, we have begun experimental and computational studies modeling full-cycle catalysis using sacrificial reagents, collision-induced dissociation and photolysis of trapped intermediate reaction complexes. Our preliminary computational studies of several thermoneutral or slightly endothermic overall reactions that may facilitate H_2 production with simultaneous oxidation of organic molecules have already given insight on potential deep traps formed by the sacrificial reagents and the transition metal oxide cluster anions.

IV. References to publications of DOE sponsored research that have appeared in 2012–present or that have been accepted for publication

1. "Comparative study of water reactions with $Mo_2O_y^-$ and $W_2O_y^-$ clusters: A combined experimental and theoretical investigation," Manisha Ray, Sarah E. Waller, Arjun Saha, Krishnan Raghavachari, and Caroline Chick Jarrold, **Accepted**, *J. Chem. Phys.*, (September, 2014) http://dx.doi.org/10.1063/1.4894760.

2. "Electronic Structures and Water Reactivity of Mixed Metal Sulfide Cluster Anions," Arjun Saha and Krishnan Raghavachari, *J. Chem. Phys.*, **141**, 074305(1-9) (2014); http://dx.doi.org/10.1063/1.4892671.

3. "*R*H and H_2 production in reactions between *R*OH and small molybdenum oxide cluster anions," Sarah E. Waller and Caroline Chick Jarrold, *J. Phys. Chem. A*, http://dx.doi.org/10.1021/jp502021k (2014).

4. "Electrochemical Reduction of 2-chloro-N-phenylacetamides at Carbon and Silver Cathodes in Dimethylformamide", Erick M. Pasciak, Arkajyoti Sengupta, Mohammad S. Mubarak, Krishnan Raghavachari and Dennis G. Peters, *Electrochim. Acta* **127**, 159-166 (2014).

5. "A Simple Relationship Between Oxidation State and Electron Affinity in Gas-Phase Metal-oxo Complexes," Sarah E. Waller, Manisha Ray, Bruce L. Yoder, and Caroline Chick Jarrold, *J. Phys. Chem. A* **117**, 13919-13925 (2013).

6. "Hydrogen Evolution from Water through Metal Sulfide Reactions," Arjun Saha and Krishnan Raghavachari, *J. Chem. Phys.* **139**, 204301(1-12), (2013).

7. "New Insights on Photocatalytic H_2 Liberation from Water using Transition Metal Oxides: Lessons from Cluster Models of Molybdenum and Tungsten Oxides," Raghunath O. Ramabhadran, Jennifer E. Mann, Sarah E. Waller, David W. Rothgeb, Caroline Chick Jarrold and Krishnan Raghavachari, *J. Amer. Chem. Soc.*, **135**, 17039-17051 (2013).

8. "Fluxionality in Chemical Reactions of Transition-Metal Oxide Clusters: The Role of Metal, Spin-state and the Reactant Molecule", Raghunath O. Ramabhadran, Edwin L. Becher III, Arefin Chowdhury and Krishnan Raghavachari, *J. Phys. Chem. A* **116**, 7189-7195 (2012).

9. "Properties of Metal Oxide Clusters in non-Traditional Oxidation States," Jennifer E. Mann, Nicholas J. Mayhall and Caroline Chick Jarrold, *Chem. Phys. Lett.* **525-6**, 1-12 (2012).

Critical evaluation of theoretical models for aqueous chemistry and CO_2 activation in the temperature-controlled cluster regime

RE: DE-FG02-00ER15066 and DE-FG02-06ER15800

Program Managers: Dr. Mark Pederson and Dr. Gregory Fiechtner

K. D. Jordan (jordan@pitt.edu), Dept. of Chemistry, University of Pittsburgh, Pittsburgh, PA 15260

M. A. Johnson (mark.johnson@yale.edu), Dept. of Chemistry, Yale University, New Haven, CT 06520

Program Scope:

Our program exploits size-selected clusters as a medium with which to unravel molecular level pictures of key transient species in condensed phase and interfacial chemistry that are relevant to mediation of radiation damaged systems and the catalytic activation of small molecules (CO_2, H_2O). In the past year, we have made dramatic advances in the integration of a temperature controlled ion trap to allow much better control of water clusters as model systems for aqueous chemistry.

I. Identification of the spectral signature of the excess proton in three dimensional water networks

One of the most important ionic species in nature is the hydrated proton, a phenomenon crucial to a number of physical and biological processes. A decade ago, our joint theory/experiment approach led to a major advance in the elucidation of how water networks accommodate a proton defect using vibrational spectroscopy of size-selected $H^+(H_2O)_n$ clusters. The spectral signature encoding the delocalized nature of the excess charge was clear for the smaller clusters ($n \leq 10$), but a major unsolved mystery since then has been the identification of bands associated with the proton defect in the larger, three dimensional cage-like structures. It was therefore a breakthrough when earlier this year, we succeeded in obtaining a predissociation spectrum of the H_2 tagged, n=21 "magic number" cluster with the result included in

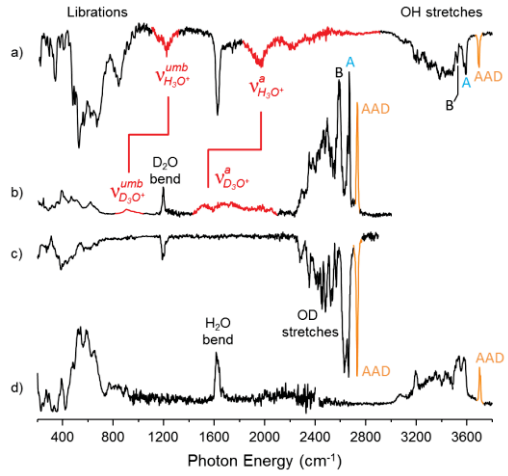

Figure 1: Composite vibrational predissociation spectra of D_2 tagged ions taken with the Berlin FEL (<1000 cm^{-1}) and the Yale table top system (1000 – 3800 cm^{-1}): a) $H_3O^+(H_2O)_{20}$, b) $D_3O^+(D_2O)_{20}$, c) $Cs^+(D_2O)_{20}$, and d) $Cs^+(H_2O)_{20}$. Bands attributed to the hydronium ion in a) and b) are highlighted in red and are clearly absent in the $Cs^+(D_2O)_{20}$ spectrum.

Fig. 1a. The charge defect displays clear bands near 1200 and 1900 cm^{-1} (highlighted in red) that are traced, with the aid of anharmonic vibrational calculations, to the umbrella and OH stretching motions of an H_3O^+ moiety located on the surface of the cage. The first paper [1] describing the results was published earlier this year in *Science* and was immediately highlighted by *Chemistry World*.

Starting in the spring of 2014, we established a collaboration with Prof. Knut Asmis in order to extend the spectral coverage down to 200 cm^{-1}, which gives us a first look at the charge- and size-dependence of the low frequency librational modes associated with water molecules held in the cage by a variety of H-bonding configurations. Together, we now have complete spectra of both H and D isotopologues of the $H_3O^+(H_2O)_{n=2-28}$ clusters. This data set is remarkable in that we can, again with the aid of theory, clearly identify distinct bands in the OH and OD stretching regions that are associated with particular H-bonding sites in the cages. The next paper describing these site-specific spectral signatures has already been submitted to PNAS in late August. The Jordan group is engaged in calculations to identify the isomers at play and to characterize their vibrational spectra theoretically.

II. Local molecular assembly motifs in ionic liquids

We are interested in the structures of complexes invoked to explain the advantages of ionic liquids (IL) as media for CO_2 chemistry. In this period, we have explored the intramolecular distortions suffered by the counterions in the commonly used [EMIM][BF_4]ionic liquid. In that system, there existed a controversy in the literature regarding the role of H-bonding at the $C_{(2)}$ position of the $EMIM^+$ cation (see notation in top right inset in Fig. 2). We exploited site-specific isotopic (H/D) labeling at the $C_{(2)}$ position to establish that, in fact, H-bonding is not significant in this system, (at least that can be characterized by a red-shift in the H-bond donor). This, in turn, supports the conclusion that electrostatics dominate the packing structure. The first report of this work has been published in the *Journal of Chemical Physics* in ref. [2].

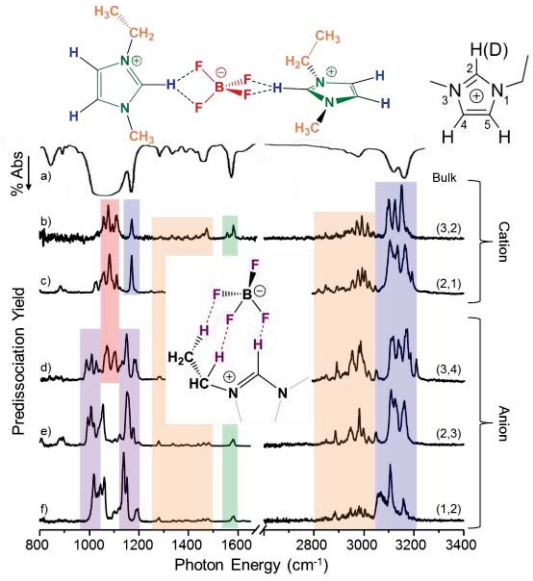

Figure 2. Comparison of size-selected cluster vibrational spectra of the $[EMIM]_n[BF_4]_m$ ions (denoted by (n,m)), with the spectrum of the bulk, room temperature liquid a). Bands traced to specific groups and interactions are color coded to the calculated structure in the top inset.

Understanding the origin of the confusion regarding the role of H-bonding in the [EMIM][BF_4] case naturally led to a study in which the $C_{(2)}$-H was replaced with a methyl group to purposefully quench any H-bonding possibility, which has been

completed and the paper is now being prepared describing the results. A second study has also been completed in which we compare the key $C_{(2)}$-D transition energy for the IL with chloride, and we indeed observe the large red-shift expected for H-bonding in that case.

In an unexpected aspect of the IL study, we noted that the very small $EMIM_2BF_4$ cluster ion already displays the key vibrational features that appear in the bulk spectrum. This suggests that the cationic ternary arrangement is an important structural component at elevated temperatures, such that the liquid effectively self-assembles around this moiety. We are now carrying out finite temperature simulations to characterize the time-dependence of local structural motifs

One of the key aspects of ILs for CO_2 trapping and activation is the role of the anion, and we have therefore extended this work to include other ILs (e.g., Tf_2N^-, PF_6^-, acetate, etc.). We are first establishing the spectral signatures of the assemblies to both elucidate their structures and to identify changes that occur upon CO_2 uptake. An important new feature of the current work is that we are also monitoring the spectra of the neutral ion pairs to complement the data we have taken so far on the charged clusters. The neutral spectra are being taken in collaboration with Martina Havenith's group in Bochum, Germany. They have the capability of capturing neutral ion pairs and studying their vibrational spectra in liquid helium droplets. First results from this joint project on the Butyltrimethylammonium bis(trifluoro-methylsulfonyl)imide system are displayed in Fig. 3. An interesting and unexpected aspect of this preliminary data is that the H_2 tagged ion spectra are considerably sharper than that of the neutral pair despite the fact that the latter was taken at much lower temperature (0.37 K in He droplets vs 15 K for N_2 tagging).

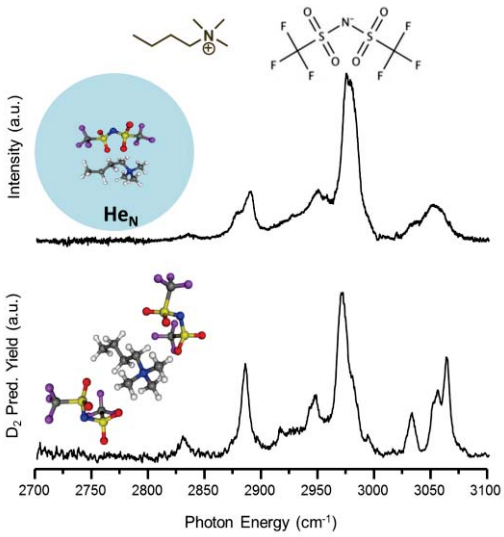

Figure 3. Comparison of the vibrational spectra of the Butyltrimethylammonium bis(trifluoromethylsulfonyl)imide ion pair in He droplets (top trace) with the (1,2) anionic cluster taken with N_2 tagging.

III. Excess electron-induced, water-network mediated intracluster proton transfer

Finally, we are completing a year-long effort to understand how the pyridinium radical ($PyH^{\cdot}$), a potential intermediate in the photoelectrocatalytic activation of CO_2, is formed in an aqueous environment. This was carried out using hydrated electron clusters as the reducing agent, and the transformation to the organic radical was followed through theoretical analysis of the cluster vibrational and photoelectron spectra. The Jordan group has recently completed ab initio molecular dynamics simulations of the $(H_2O)_3^-$·Py system, finding rapid isomerization to $OH^-(H_2O)_2PyH$ upon excitation with energy content consistent with OH stretch excitation. The

trajectories are currently being analyzed to determine whether the dominant process is direct H atom transfer or whether a solvent-stabilized Py^- intermediate is involved.

Plans for the next year

With the observation of distinct spectral features in the usually diffuse OH stretching band of relatively large water clusters, we are now poised to carry out two ground-breaking studies regarding the nature of the vibrational spectrum of condensed phase water (including ice). First, we will exploit our IR-IR photochemical hole burning scheme in conjunction with single isotopically labeled water clusters, [e.g., $D_3O^+(D_2O)_n$ (HDO)], which will create a family of isotopomers according the various sites that can be occupied by the unique hydron. This will establish, for the first time, the degree to which anharmonic coupling complicates the simple expectation that each OH contributes a local fundamental to the spectrum. We will then use our newly demonstrated temperature control capability to systematically warm this ensemble to a finite temperature and record the evolution of the OH stretching pattern in a double resonance mode. The key is that, as sites begin to exchange, we expect to observe the onset of spectral diffusion as the OH oscillator absorbs at more than one frequency in the fluctuating ensemble. Understanding the implications of these data on the microscopic mechanics underlying spectral diffusion will rely heavily on the Jordan theoretical team. This endeavor will present a non-trivial challenge due to the fact that the high temperature ensembles will explore regions of the potential surface (including barriers) that are far from the stationary points we have characterized thus far. We will also be extending our work on the ionic liquids to include their interactions with CO_2 and to elucidate the cluster sizes required to accurately recover the spectra of the bulk systems.

Papers in the past two years under this grant

1. "Spectral signature of the proton defect in a three-dimensional water network through cryogenic vibrational spectroscopy of the "magic" $H^+(H_2O)_{21}$ cluster" Joseph A. Fournier, Christopher J. Johnson, Conrad T. Wolke, Gary H. Weddle, Arron B. Wolk, and Mark A. Johnson, *Science*, 344, 1009 (2014).

2. "Structures and fragmentation pathways of size-selected, D_2-tagged ammonium/methylammonium bisulfate clusters" Christopher J. Johnson and Mark A. Johnson, *J. Phys. Chem. A* 117, 13265, 2013.

3. "Origin of the diffuse vibrational signature of a cyclic intramolecular proton bond: anharmonic analysis of protonated 1,8-disubsituted naphthalene ions" Andrew F. DeBlase, Steven Bloom, Thomas Lectka, Kenneth D. Jordan, Anne B. McCoy, and Mark A. Johnson, *J. Chem. Phys.* 139, 024301, 2013.

4. "Ionic Liquids from the bottom up: Local assembly motifs in [EMIM][BF_4] through cryogenic ion spectroscopy" Christopher J. Johnson, Joseph A. Fournier, Conrad T. Wolke, and Mark A. Johnson, *J. Chem. Phys.* 139, 224305, 2013.

Nucleation Chemical Physics

Shawn M. Kathmann
Physical Sciences Division
Pacific Northwest National Laboratory
902 Battelle Blvd.
Mail Stop K1-83
Richland, WA 99352
shawn.kathmann@pnl.gov

Program Scope

The objective of this work is to develop an understanding of the chemical physics governing nucleation. The thermodynamics and kinetics of the embryos of the nucleating phase are important because they have a strong dependence on size, shape and composition and differ significantly from bulk or isolated molecules. The technological need in these areas is to control chemical transformations to produce specific atomic or molecular products without generating undesired byproducts, or nanoparticles with specific properties. Computing reaction barriers and understanding condensed phase mechanisms is much more complicated than those in the gas phase because the reactants are surrounded by solvent molecules and the configurations, energy flow, quantum and classical electric fields and potentials, and ground and excited state electronic structure of the entire statistical assembly must be considered.

Recent Progress and Future Directions

Charge and Field Fluctuations in Aqueous NaCl

The observations of luminescence during crystallization suggest that the process of crystallization may not be purely classical but also involves an essential electronic structure component. Strong electric field fluctuations may play an important role in this process by providing the necessary driving force for the observed electronic structure changes (see Fig. 1 – top). The importance of electric field fluctuations driving electron transfer has been a topic of intense research since the seminal work of Marcus. The main objective of this work is to provide basic understanding of the fluctuations in charge, electric potentials, and electric fields for concentrated aqueous NaCl electrolytes. Our charge analysis reveals that the water molecules in the 1st solvation shell of the ions serve as a sink for electron density originating on Cl^- (see Fig. 1 – bottom). We find excellent agreement between our simulations solution structure and neutron diffraction measurements. We find that the electric fields inside aqueous electrolytes are extremely large (up to several V/Å – see Fig. 2) and thus may alter the ground and excited electronic states in the condensed phase. Furthermore, our results show that the potential and field distributions are largely independent of concentration. These calculations and analyses provide the first steps toward understanding the magnitude and fluctuations of charge, classical point charge sources of electric potentials and fields in aqueous electrolytes and what role these fields may play in driving charge redistribution/transfer during crystalloluminescence.

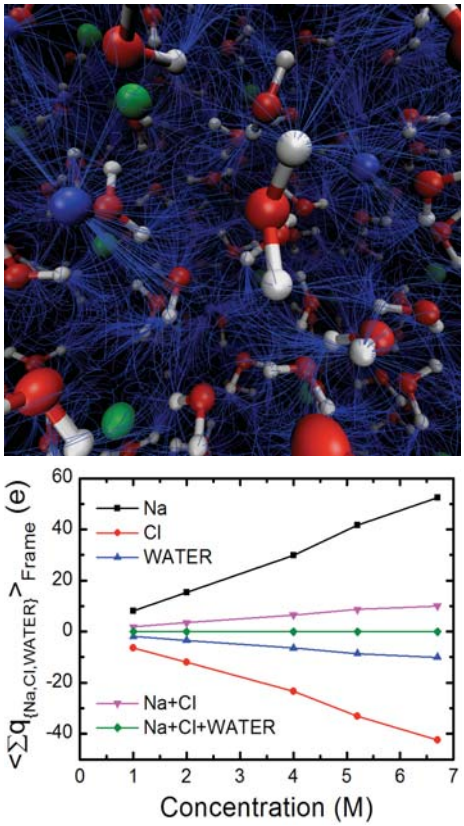

Figure 1. Electric fields in 6.7M NaCl (top), charge redistribution as a function of concentration (bottom).

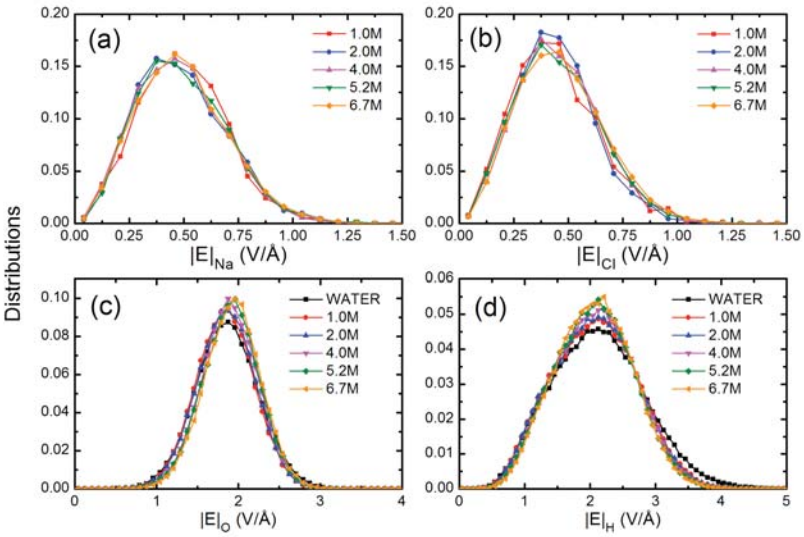

Figure 2. Distributions of the magnitude of the electric field P(E) at the Na^+, Cl^-, O, and H sites. The electric field distributions on Na^+ and Cl^- are nearly concentration independent with the distributions for O and H showing a slight concentration dependence and having larger fields (by a factor of 4) and broader distributions (factor of 2) than those on Na^+ and Cl^-.

Heterogeneous Ice Nucleation on Nanoparticles

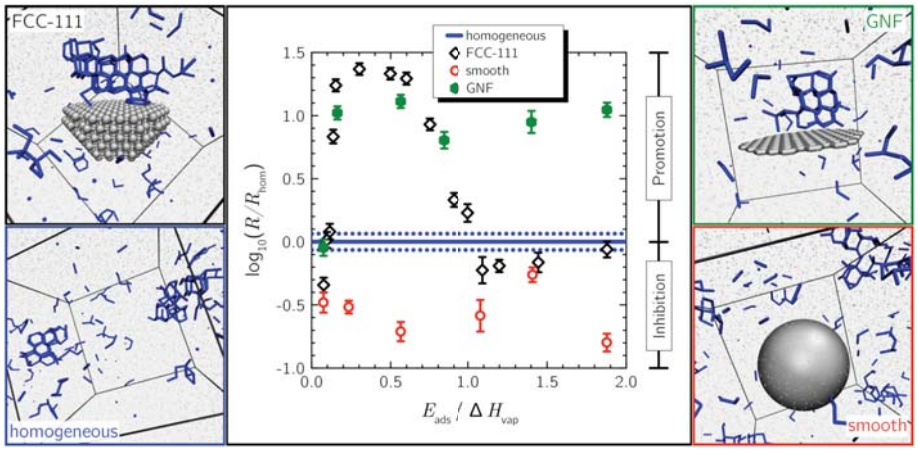

Figure 3. Controlling ice nucleation through surface topography and hydrophilicity. The heterogeneous nucleation rate R (center) depends on the water monomer adsorption energy E_{ads} in the presence of the three NPs. Blue line indicates the homogeneous nucleation R_{hom}. ΔH_{vap} = 10.65 kcal/mol is the enthalpy of vaporization of bulk mW water at 298K.

Ice nucleation is arguably the most common phase transition on the planet and almost always occurs heterogeneously. Despite the importance of ice formation to the climate, medical and geological sciences, food and transport industries, a clear understanding of how the properties of a material affect its ability to nucleate ice has remained elusive. This has prevented the rational design of new materials to either inhibit or promote ice nucleation. Here we present results of molecular dynamics simulations of ice nucleation in the presence of nanoparticles (NPs): FCC-111 (face centered cubic hemisphere with exposed 111 face), GNF (graphene nanoflake), and smooth nanoparticle (see Fig. 3). At very low values of E_{ads}, all of the NPs either inhibit or give rates similar to R_{hom}; this inhibition persists over the full range of E_{ads} for the smooth NP. The FCC-111 NP exhibits a maximum in R at $E_{ads}/\Delta H_{vap} \approx 0.4$ before falling to $R \leq R_{hom}$ at $E_{ads}/\Delta H_{vap} \approx 1.0$. With the exception of the weakest value of E_{ads}, the GNF promotes ice nucleation with a rate that remains relatively constant over the full range of E_{ads} (approximately 10 times faster than homogeneous nucleation). The snapshots show example nucleation events for the different systems: the NPs are shown in silver and ice-like molecules are shown in blue. We found that: (1) surfaces of different topography give rise to distinct ice nucleation mechanisms; and (2) the different nucleation mechanisms and rates have inequivalent sensitivity to the surface hydrophilicity. These results show that the 'requirements' for a material to be a good ice-nucleating agent depend strongly upon the mode of nucleation enhancement. Finally, we demonstrated how the microscopic understanding of heterogeneous ice nucleation obtained

from our simulations could be used to design a modified surface in silico with enhanced ice nucleating ability.

Quantum Voltages and Valence Electrons

Voltages inside matter are relevant to crystallization, materials science, biology, catalysis, and aqueous chemistry. The variation of voltages in matter can be measured by experiment. Using modern supercomputers and a sufficiently accurate level of theory allow the prediction of quantum voltages with spatial resolutions of bulk systems well beyond what can be currently measured. Of particular interest is the Mean Inner Potential (V_o) – the spatial average of these quantum voltages referenced to the vacuum. We establish a protocol to reliably evaluate V_o from quantum calculations. Voltages are very sensitive to the distribution of electrons and provide metrics to understand interactions in condensed phases (see Fig. 4). Interestingly, J.E. Hirsch recently pointed out that large increases in V_o should accompany the manifestation of the superconducting state in matter due to the electrons spilling out beyond the surface [*Annalen der Physik*, **526**, 63 (2014)]. In the present study, we find excellent agreement with measurements of V_o for vitrified water and salt crystals and demonstrate the impact of covalent and ionic bonding as well as intermolecular/atomic interactions (see Fig. 5). Certain aspects in this regard are highlighted making use of simple model systems/approximations. We predict V_o as well as the fluctuations of these voltages in aqueous NaCl electrolytes and characterize the changes in their behavior as the resolution increases below the size of atoms. The changes in V_o upon bond formation in a H_2O molecule reveal a far-field picture where an increase in electron density results in a decrease in voltage due to better screening of the nuclear cores. We found that, in contrast to the positive definite voltages of isolated atoms, once the electrons are allowed to transfer and redistribute to form bonds, lone pairs of electrons, and ions that ~40% of the total volume of the bulk electrolyte contains negative voltages. Furthermore, using the "strange relationship" between V_o and the diamagnetic susceptibility χ our calculations can be used to predict χ for aqueous NaCl electrolytes since no measurements exist.

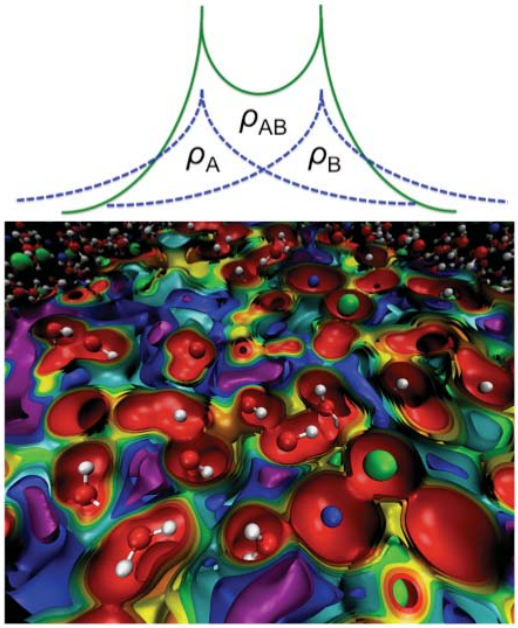

Figure 4. (upper) When isolated atoms (dashed blue) come together their interaction causes alterations/ deformations in the electron density (full green). There are large voltage changes that accompany these electron density changes and these voltage changes can be used to better understand and quantify phase transformations. (lower) Various voltage (V) isosurfaces are shown (red=1.4, orange=0.8, yellow=0.3, green=0, cyan=-0.3, blue=-0.8, purple=-1.4) for a configuration from a supersaturated aqueous NaCl solution (6.7M) demonstrating the complexity of the quantum voltage variations throughout space.

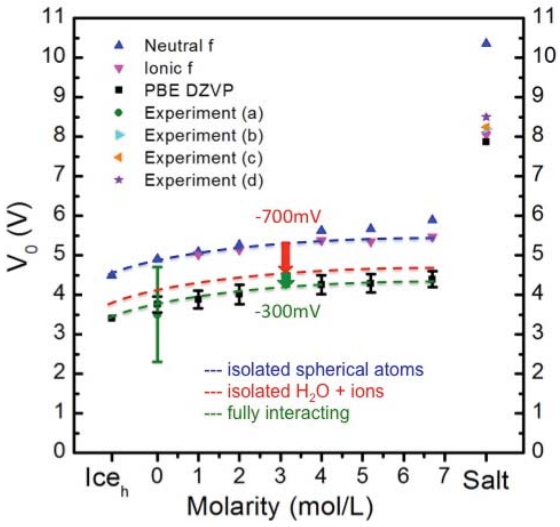

Figure 5. (at right) A comparison of calculated and experimental V_o of water aqueous NaCl electrolytes, and NaCl salt. Agreement between theory and experiment is excellent. Neutral scattering factors $f_{el}(0)$, as expected, overestimate *V*o , however, the ionic $f_{el}(0)$ predict the concentration trends. This shows that of the -1.1V difference between isolated atoms and condensed phase aqueous systems, -700mV (red) is intramolecular (e.g., covalent OH bonds) and -300mV (green) is intermolecular (e.g., ion-water and hydrogen bonding).

Some ongoing work includes: (1) performing *ab initio* MD in addition to using *ab initio* methods to resample the classical simulations to study charge transfer and radicalization, (2) using QM/MM hydrid DFT functionals to obtain distributions of excited (singlet and triplet) states to ground state singlet photon energies as well as spin-orbit interactions and oscillator strengths for the concentrated electrolytes, (3) use the quantum potential analysis to investigate the electrical properties of the crystal-aqueous phase interfaces, and (4) computing potentials of mean force for ions and cluster distribution functions in solutions from the *ab initio* MD to use in accelerated dynamics to model crystallization kinetics as well as deviations of the osmotic coefficient for electrolytes at high concentrations.

Direct PNNL collaborators on this project include M. Valiev, G.K. Schenter, C.J. Mundy, X. Wang, J. Fulton, L. Dang, and M. Baer and Postdoctoral Fellow Bernhard Sellner. Outside collaborations with the University College London include Stephen Cox and Angelos Michaelides on ice nucleation (Chemistry), Jake Stinson and Ian Ford on sulfuric acid-water nucleation (Physics), and Andrew Alexander (Chemistry) at the University of Edinburgh, Scotland.

Acknowledgement: This research was performed in part using the DOE NERSC facility. Battelle operates PNNL for DOE.

Publications of DOE Sponsored Research (2012-present)

G. Murdachaew, M. Valiev, S.M. Kathmann, and X. Wang, "Study of Ion Specific Interactions of Alkali Cations with Dicarboxylate Dianions", *Journal of Physical Chemistry A*, **116**, 2055 (2012).

Communication – S.J. Cox, S.M. Kathmann, J.A. Purton, M.J. Gillan, and A. Michaelides, "Non-hexagonal ice at hexagonal surfaces: the role of lattice mismatch", *Physical Chemistry Chemical Physics*, **14**, 7944 (2012).

Communication – H. Wen, G.L. Hou, S.M. Kathmann, M. Valiev, and X.B. Wang, "Solute anisotropy effects in hydrated anion and neutral clusters", *Journal of Chemical Physics*, **138**, 031101 (2013).

S.J. Cox, Z. Raza, S.M. Kathmann, B. Slater, and A. Michaelides, "The Microscopic Features of Heterogeneous Ice Nucleation May Affect the Macroscopic Morphology of Atmospheric Ice Crystals", *Faraday Discussions*, in press (2013).

S.M. Kathmann, B. Sellner, A.J. Alexander, and M. Valiev, "Beyond Classical Theories", *Proceedings of the 19th International Conference on Nucleation and Atmospheric Aerosols - AIP Conference Proceedings*, **1527**, 109, doi:10.1063/1.4803215 (2013).

J.L. Stinson, S.M. Kathmann, and I.J. Ford, "Empirical Valence bonds: A reactive classical potential for sulphuric acid and water", *Proceedings of the 19th International Conference on Nucleation and Atmospheric Aerosols - AIP Conference Proceedings*, **1527**, 266, doi:10.1063/1.4803255 (2013).

Cover Article – B. Sellner, M. Valiev, and S.M. Kathmann, "Charge and Electric Field Fluctuations in Aqueous NaCl Electrolytes", *Journ.al of Physical Chemistry B*, **117**, 10869 (2013). This work was highlighted in DOE's Pulse (Science and Technology Highlights from the DOE National Laboratories), "*Strong forces at work in simple table salt*", #397, Sept. 16, (2013) http://web.ornl.gov/info/news/pulse/no397/story3.shtml

J.L. Stinson, S.M. Kathmann, and I.J. Ford, "Dynamical consequences of a constraint on the Langevin thermostat in molecular cluster simulation", *Molecular Physics*, DOI:10.1080/00268976.2014.917732 (2014).

J.L. Stinson, S.M. Kathmann, and I.J. Ford, "Investigating the significance of zero-point motion in small molecular clusters of sulphuric acid and water", *Journal of Chemical Physics*, **140**, 024306 (2014).

S.J. Cox, S.M. Kathmann, B. Slater, and A. Michaelides, "Nanoscale Control of Ice Formation", *Nature Materials*, (2014).

B. Sellner and S.M. Kathmann, "A Matter of Quantum Voltages", **Invited - Special Issue** of *Journal of Chemical Physics*, accepted, (2014).

Chemical Kinetics and Dynamics at Interfaces

Structure and Reactivity of Ices, Oxides, and Amorphous Materials

Bruce D. Kay (PI), R. Scott Smith, and Zdenek Dohnálek
Chemical and Materials Sciences Division
Pacific Northwest National Laboratory
P.O. Box 999, Mail Stop K8-88
Richland, Washington 99352
bruce.kay@pnnl.gov

Collaborators include: GA Kimmel, J Matthiesen, RA May, and NG Petrik

Program Scope

The objective of this program is to examine physiochemical phenomena occurring at the surface and within the bulk of ices, oxides, and amorphous materials. The microscopic details of physisorption, chemisorption, and reactivity of these materials are important to unravel the kinetics and dynamic mechanisms involved in heterogeneous (i.e., gas/liquid) processes. This fundamental research is relevant to solvation and liquid solutions, glasses and deeply supercooled liquids, heterogeneous catalysis, environmental chemistry, and astrochemistry. Our research provides a quantitative understanding of elementary kinetic processes in these complex systems. For example, the reactivity and solvation of polar molecules on ice surfaces play an important role in complicated reaction processes that occur in the environment. These same molecular processes are germane to understanding dissolution, precipitation, and crystallization kinetics in multiphase, multicomponent, complex systems. Amorphous solid water (ASW) is of special importance for many reasons, including the open question over its applicability as a model for liquid water, and fundamental interest in the properties of glassy materials. In addition to the properties of ASW itself, understanding the intermolecular interactions between ASW and an adsorbate is important in such diverse areas as solvation in aqueous solutions, cryobiology, and desorption phenomena in cometary and interstellar ices. Metal oxides are often used as catalysts or as supports for catalysts, making the interaction of adsorbates with their surfaces of much interest. Additionally, oxide interfaces are important in the subsurface environment; specifically, molecular-level interactions at mineral surfaces are responsible for the transport and reactivity of subsurface contaminants. Thus, detailed molecular-level studies are germane to DOE programs in environmental restoration, waste processing, and contaminant fate and transport.

Our approach is to use molecular beams to synthesize “chemically tailored” nanoscale films as model systems to study ices, amorphous materials, supercooled liquids, and metal oxides. In addition to their utility as a synthetic tool, molecular beams are ideally suited for investigating the heterogeneous chemical properties of these novel films. Modulated molecular beam techniques enable us to determine the adsorption, diffusion, sequestration, reaction, and desorption kinetics in real-time. In support of the experimental studies, kinetic modeling and simulation techniques are used to analyze and interpret the experimental data.

Recent Progress and Future Directions

Mobility of supercooled liquid toluene, ethylbenzene, and benzene near their glass transition temperatures investigated using inert gas permeation Glasses and other non-crystalline solids are utilized in a variety of scientific and applied fields and are important in diverse disciplines ranging from art and architecture to catalysis and drug delivery. However, it

is experimentally difficult to measure the kinetic processes involved in creating these materials. Part of the difficulty is due to the inherent drive to crystallize as the temperature of the supercooled liquid approaches the glass transition. Recently, we have developed a technique in which the permeation rate of inert gases is used to determine the diffusivity of the supercooled liquid. In this technique, a layer of an inert gas (e.g., Ar, Kr, and Xe) is deposited beneath the amorphous solid overlayer. When the amorphous solid transforms into a supercooled liquid, the gas begins to permeate through the supercooled liquid. Desorption of the gas can be measured and is related to the diffusivity of the supercooled liquid itself.

We have applied this technique to investigate the mobility of supercooled liquid toluene, ethylbenzene, and benzene near their respective glass transition temperatures (T_g). For toluene and ethylbenzene the onset of inert gas permeation is observed at temperatures near T_g. Diffusivities of 10^{-14} to 10^{-9} cm^2/s were determined from 115 to 135 K, respectively. The diffusivities in toluene and ethylbenzene were the same over this temperature range, which is consistent with the behavior of their higher temperature liquids. The temperature dependence of the diffusivity approaching T_g was non-Arrhenius and was equally well-fit by either a VFT or the Corresponding States quadratic equation proposed by David Chandler and colleagues. At these temperatures, the relationship between the diffusivities and the viscosity did not obey the Stokes−Einstein equation but instead was well-fit by the fractional Stokes−Einstein equation with an exponent of ∼0.66. The diffusivity in neat supercooled benzene could not be determined using inert gas permeation due to the onset of crystallization at temperatures well below T_g. Mixtures of benzene and ethylbenzene were used to shift the benzene crystallization to higher temperature. A 50/50 mixture shifted the benzene crystallization to ∼120 K, but even at this temperature, the inert gas desorption spectra were far too complicated to extract meaningful diffusivities. This work is described in publication #8 below.

Future work will focus on expanding the inert gas permeation method to other systems and expanding the range of probe molecules used to further understand how their interactions with the material of interest alters the measured diffusivity.

Desorption Kinetics of Methanol, Ethanol, and Water from Graphene The desorption rates of astrophysically relevant molecules such as methanol, ethanol, and water are needed to understand and quantify the evaporation behavior of interplanetary ices and comets. Typically, the desorption kinetics are determined in the laboratory at temperatures where they can be measured in a reasonable amount of time (e.g. less than a day). These parameters are extrapolated to predict desorption rates at lower temperatures, which are usually more relevant to astrophysical processes. Dust grains, which are the core substrate for astrophysical ices, are believed to be composed of mostly carbonaceous and silicaceous materials. As such, many laboratory studies use carbon based surfaces such as amorphous carbon or highly oriented pyrolytic graphite (HOPG) as analogs for interstellar dust grains.

In a series of papers reported by others, the desorption of methanol, ethanol, water, and ammonia from an HOPG substrate was studied. In that work, the multilayers of these species were observed and reported to desorb with fractional-order desorption kinetics. For example, multilayer methanol, ethanol, water, and ammonia were reported to have desorption orders of 0.35, 0.08, 0.26, and 0.25 respectively. These results are in contrast to the zero-order desorption kinetics expected for multilayer desorption. The desorption order will affect the overall desorption rate kinetics and thus is an important factor for modeling the desorption behavior of astrophysical ices.

In some recent work we studied the desorption kinetics of methanol, ethanol, and water

deposited on a layer of graphene grown on Pt(111). Molecular beams were used to deposit well-calibrated doses onto the graphene substrate at 25 K and the desorption kinetics are determined using temperature programmed desorption (TPD). Our results show that both methanol and ethanol have well-resolved first, second, third, and multilayer layer desorption peaks. The alignment of the desorption leading edges is consistent with zero-order desorption kinetics from all layers. For water at low coverages (< 1 ML) we found that the initial desorption leading edges are aligned but then fall out of alignment at higher temperatures. In addition, the first and second layers are not resolved. For thicker water layers (10 to 100 ML), the desorption leading edges are in alignment throughout the desorption of the film. These observations are consistent with water dewetting from the graphene substrate at low water coverages and zero-order desorption at higher coverages. Kinetic simulations show that fractional-order desorption kinetics would be readily apparent in the experimental TPD spectra. The observed zero-order desorption observed in our work is in contrast to the fractional-order desorption kinetics reported for desorption on HOPG (graphite). The conflicting results may be due to differences in the substrate (HOPG versus graphene) or the film dosing technique (molecular beam versus background dosing). This work is described in publication #10 below.

Future work will focus on comparing the desorption behavior of a series of gases on graphene and amorphous solid water.

Adsorption, Desorption, and Displacement Kinetics of H_2O and CO_2 on TiO_2(110) Understanding the interaction dynamics of water and carbon dioxide with mineral surfaces is requisite for determining the feasibility of carbon capture and sequestration strategies whose goal is the formation of carbonates. Unfortunately mineral surfaces are complicated, making experimental determination of these interactions difficult. For example olivines, which are orthosilicates and comprise a large fraction of the earth's upper mantle, can have silicon, oxygen, and cation (Mg, Fe, Ca, etc.) surface adsorption sites. Impurities, such as cation substitutions that occur in "real-world" minerals, add a further level of complexity. In some recent work, we used TiO_2(110) as a model surface to begin learning about water and carbon dioxide surface interactions. While clearly not as complex as a true mineral surface, it has the advantage of having both metal and oxygen surface sites and as such should be a good reference point for interpreting results from more complicated substrates.

Temperature programmed desorption (TPD) and molecular beam techniques were used to determine the adsorption, desorption, and displacement kinetics of H_2O and CO_2 on a TiO_2(110) surface. As is known in the literature, H_2O and CO_2 have well-resolved peaks corresponding to desorption from bridge-bonded oxygen (O_b), five-fold coordinated Ti (Ti_{5c}), and oxygen vacancies (V_O) sites in order of increasing peak temperature. The results show that both species preferentially bind to the highest binding energy available, first occupying defects, followed by Ti_{5c} sites, and then O_b sites. Analysis of the saturated monolayer peak for both molecules reveals that the corresponding adsorption energies on all sites are greater for H_2O than for CO_2. Using sequential adsorption, we showed that, independent of the dose order (H_2O first then CO_2 and vice versa), H_2O displaces CO_2 from any occupied site before reaching the desorption temperature. Isothermal experiments reveal that the onset of H_2O displacement of CO_2 occurs between 75 and 80 K. These results mean that H_2O preferentially binds to the highest energy binding sites available and displaces CO_2 if need be. These results show that the relative strength of the adsorbate-substrate interactions is the dominant factor in the competitive adsorption/displacement kinetics. This work is described in publication #9 below.

Future work will focus on experiments with a more complex ortho-silicate mineral such as Forsterite. The CO_2 and H_2O adsorbate-substrate interaction kinetics on a well-characterized TiO_2(110) model system provide an excellent baseline for interpretation of experimental results on more complex, real-world substrates.

References to Publications of DOE sponsored Research (2012 - present)

1. R. S. Smith, N. G. Petrik, G. A. Kimmel, and B. D. Kay, *"Thermal and Nonthermal Physiochemical Processes in Nanoscale Films of Amorphous Solid Water"*, Accounts of Chemical Research **45**, 33 (2012).
2. R. A. May, R. S. Smith, and B. D. Kay, *"The Molecular Volcano Revisited: Determination of Crack Propagation and Distribution During the Crystallization of Nanoscale Amorphous Solid Water Films"*, Journal of Physical Chemistry Letters **3**, 327 (2012).
3. D. W. Flaherty, N. T. Hahn, R. A. May, S. P. Berglund, Y. M. Lin, K. J. Stevenson, Z. Dohnalek, B. D. Kay, and C. B. Mullins, *"Reactive Ballistic Deposition of Nanostructured Model Materials for Electrochemical Energy Conversion and Storage"*, Accounts of Chemical Research **45**, 434 (2012).
4. R. S. Smith and B. D. Kay, *"Breaking Through the Glass Ceiling: Recent Experimental Approaches to Probe the Properties of Supercooled Liquids near the Glass Transition"*, Journal of Physical Chemistry Letters **3**, 725 (2012).
5. J. Matthiesen, R. S. Smith, and B. D. Kay, *"Probing the mobility of supercooled liquid 3-methylpentane at temperatures near the glass transition using rare gas permeation"*, Journal of Chemical Physics **137**, 064509 (2012).
6. R. A. May, R. S. Smith, and B. D. Kay, *"The release of trapped gases from amorphous solid water films. I. "Top-down" crystallization-induced crack propagation probed using the molecular volcano"*, Journal of Chemical Physics **138**, 104501 (2013).
7. R. A. May, R. S. Smith, and B. D. Kay, *"The release of trapped gases from amorphous solid water films. II. "Bottom-up" induced desorption pathways"*, Journal of Chemical Physics **138**, 104502 (2013).
8. R. A. May, R. S. Smith, and B. D. Kay, *"Mobility of Supercooled Liquid Toluene, Ethylbenzene, and Benzene near Their Glass Transition Temperatures Investigated Using Inert Gas Permeation"*, Journal of Physical Chemistry A **117**, 11881 (2013). (Invited contribution for the Curt Wittig Festschrift.)
9. R. S. Smith, Z. J. Li, L. Chen, Z. Dohnalek, and B. D. Kay, *"Adsorption, Desorption, and Displacement Kinetics of H_2O and CO_2 on TiO_2(110)"*, Journal of Physical Chemistry B **118**, 8054 (2014). (Invited contribution for the James L. Skinner Festschrift.)
10. R. S. Smith, J. Matthiesen, and B. D. Kay, *"Desorption Kinetics of Methanol, Ethanol, and Water from Graphene"*, Journal of Physical Chemistry A, doi.org/10.1021/jp501038z (2014). (Invited contribution for the A. W. Castleman, Jr. Festschrift.)
11. R. S. Smith, Z. J. Li, Z. Dohnalek, and B. D. Kay, *"Adsorption, Desorption, and Displacement Kinetics of H_2O and CO_2 on Forsterite, Mg_2SiO_4(011)"*, Journal of Physical Chemistry C (2014). (Invited contribution for the John Hemminger Festschrift.)
12. G. A. Kimmel, T. Zubkov, R. S. Smith, N. G. Petrik, and B. D. Kay, *"Turning things downside up: Adsorbate induced water flipping on Pt(111)"*, The Journal of Chemical Physics (2014). (Invited contribution for JCP issue on interfacial and confined water.)

Probing Ultrafast Electron (De)localization Dynamics in Mixed Valence Complexes Using Femtosecond X-ray Spectroscopy

Lead PI: Munira Khalil, University of Washington, Seattle
PI: Niranjan Govind, EMSL, Pacific Northwest National Laboratory
PI: Shaul Mukamel, University of California, Irvine
PI: Robert Schoenlein, Lawrence Berkeley National Laboratory

The goal of this recently funded project (started on 9/1/2014) is to directly measure photoinduced electron delocalization/localization dynamics on a sub-50 fs timescale at the atomistic level in a series of solvated transition metal mixed valence complexes. The experiments will utilize the femtosecond X-ray pulses at LCLS (XPP/SXR instruments) to perform femtosecond X-ray absorption, emission and resonant inelastic X-ray scattering (RIXS) spectroscopies following photoexcitation of the sample. This study will aim to understand valence electron motion following metal-to-metal charge transfer (MMCT) excitation in the following mixed valence complexes dissolved in aqueous solution: $[(NH_3)_5Ru^{III}NCFe^{II}(CN)_5]^-$ (**1**, FeRu), *trans*-$[(NC)_5Fe^{II}CNPt^{IV}(NH_3)_4NCFe^{II}(CN)_5]^{4-}$ (**2**, FePtFe) and *trans*-$[(NC)_5Fe^{III}CNRu^{II}(L)_4NCFe^{III}(CN)_5]^{4-}$ (**3**, FeRuFe, L=pyridine). In the above complexes, the communication between the two metal atoms is varied by changing the identity and oxidation state of the metal atom and varying the ligand shell surrounding the metal atom. The chosen complexes provide a rich molecular playground to study the effects of electronic coupling, delocalization and electron-nuclear coupling between two transition metals connected with a cyanide bridge.

The ultrafast X-ray experiments will be performed by the Khalil and Schoenlein group members and will allow for an unprecedented view of the motion of the valence electrons between the metal centers and subsequent electronic and structural relaxation following MMCT. The success of the experiments will depend on the ability to interpret the core-level spectra of the photo-excited states of electron-rich transition metal molecular systems in solution. The experiments will be combined with theoretical X-ray spectroscopic and ultrafast electronic dynamics simulations performed by the Govind and Mukamel group members.

The results will provide a molecular-level understanding of “the extent of electron delocalization” *during* a photoinduced chemical reaction, which remains a fundamental question in the field of mixed valence chemistry and crucial to designing mixed valency in supramolecular complexes and in molecular electronics.

Chemical Kinetics and Dynamics at Interfaces

Non-Thermal Reactions at Surfaces and Interfaces

Greg A. Kimmel (PI) and Nikolay G. Petrik

Chemical and Materials Sciences Division
Pacific Northwest National Laboratory
P.O. Box 999, Mail Stop K8-88
Richland, WA 99352
gregory.kimmel@pnnl.gov

Program Scope

The objectives of this program are to investigate 1) thermal and non-thermal reactions at surfaces and interfaces, and 2) the structure of thin adsorbate films and how this influences the thermal and non-thermal chemistry. Energetic processes at surfaces and interfaces are important in fields such as photocatalysis, radiation chemistry, radiation biology, waste processing, and advanced materials synthesis. Low-energy excitations (e.g. excitons, electrons, and holes) frequently play a dominant role in these energetic processes. For example, in radiation-induced processes, the high energy primary particles produce numerous, chemically active, secondary electrons with energies that are typically less than ~100 eV. In photocatalysis, non-thermal reactions are often initiated by holes or (conduction band) electrons produced by the absorption of visible and/or UV photons in the substrate. In addition, the presence of surfaces or interfaces modifies the physics and chemistry compared to what occurs in the bulk.

We use quadrupole mass spectroscopy, infrared reflection-absorption spectroscopy (IRAS), and other ultra-high vacuum (UHV) surface science techniques to investigate thermal, electron-stimulated, and photon-stimulated reactions at surfaces and interfaces, in nanoscale materials, and in thin molecular solids. Since the structure of water near interface plays a crucial role in the thermal and non-thermal chemistry occurring there, a significant component of our work involves investigating the structure of aqueous interfaces. A key element of our approach is the use of well-characterized model systems to unravel the complex non-thermal chemistry occurring at surfaces and interfaces. This work addresses several important issues, including understanding how the various types of low-energy excitations initiate reactions at interfaces, the relationship between the water structure near an interface and the non-thermal reactions, energy transfer at surfaces and interfaces, and new reaction pathways at surfaces.

Recent Progress

Probing the photochemistry of chemisorbed oxygen on TiO_2(110) with Kr and other co-adsorbates

There are a limited number of methods that have sufficient sensitivity to probe the excited states of atoms and molecules on surfaces. Photon-stimulated desorption and electron-stimulated desorption are two of the most frequently used methods. Velocity and angular distributions, and electronic, vibrational, and rotational state distributions for the desorbing products can provide useful information about the reaction dynamics occurring on the surface. However, photo-induced processes do not always lead to desorption of the original molecule or a reaction product. For example, previous research by our group has shown that the majority of chemisorbed O_2 on TiO_2(110) does not desorb during UV irradiation. One possible solution to this problem is to co-adsorb weakly-interacting atoms or molecules that can act as "reporters" for the chemical reactions occurring on the surface. In that case, we could use the high sensitivity of the PSD method to investigate reactions that don't produce desorption events of their own.

In this study, we used weakly-bound atoms and molecules (Ar, Kr, Xe, CO, CH_4, CO_2, CH_3OH, N_2O, and N_2) to probe the photochemical interactions of chemisorbed oxygen on rutile TiO_2(110). Ultraviolet irradiation of chemisorbed oxygen co-adsorbed with the probe species led to photon-stimulated desorption (PSD) of some of the probe species (e.g. Kr and CH_4), but not others (e.g. CO_2 and

N_2O). Without chemisorbed oxygen, the PSD yields of all the probe species were very low or not observed. Surprisingly, both chemisorbed O_2 *and* oxygen adatoms, O_a, were photo-active for desorption of Kr and other weakly-bound species. To our knowledge, this is the first evidence for photo-activity of O_a on TiO_2(110). The Kr PSD yield increased with increasing coverage of Kr and of chemisorbed oxygen. For Kr, the angular distribution of the photodesorbed atoms was approximately cosine. The Kr distribution was quite different from the angular distribution for the O_2 PSD, which was sharply peaked along the surface normal. We proposed that various forms of chemisorbed oxygen were excited by reactions with electrons and/or holes created in the TiO_2 substrate by UV photon irradiation. The photo-excited oxygen collided with, and transferred energy to, neighboring co-adsorbed atoms or molecules. For co-adsorbates with a small enough binding energy to the substrate, the collision could induce desorption of the probe atom or molecule. The observed phenomenon provides a new tool for studying photochemical processes. This work is published in reference 5.

Electron-stimulated reactions in layered CO/H_2O films: Hydrogen atom diffusion and the sequential hydrogenation of CO to methanol

Non-thermal reactions in water ices, with or without other co-adsorbed molecules, are of interest in astrochemistry and planetary sciences. For example, dust grains in cold molecular clouds are coated with molecular ices for which water is typically the main component. Thermal and non-thermal processing of these icy dust grains produces some of the complex molecules that have been observed in interstellar space. Reactions in water ices are also important in comets and some of the moons of the gas-giant planets. In cold, dense molecular clouds, CO is an abundant component in icy grain mantles, and reactions in CO/H_2O ices contribute to the wide variety of organic molecules that have been observed in these environments. As a possible route to the production organic molecules, the non-thermal reactions in CO/H_2O ices have been investigated for photon, electron, and ion irradiation

We have previously investigated non-thermal reactions in ASW films and demonstrated that the non-thermal reactions and the electronic excitations that initiate those reactions do not necessarily occur at the same location in the ASW. For example, we showed that H_2 is preferentially produced at the ASW/substrate and ASW/vacuum interfaces. However, the energy that drives the reactions at the ASW/substrate interface is absorbed in the "bulk" of the ASW film. Molecular oxygen is also produced in electron-irradiated ices, but the reactions that produce O_2 occur primarily at or near the ASW/vacuum interface. This previous research on the spatial distribution of electron-stimulated reactions in neat ASW films motivated us to investigate the spatial distribution of the electron-stimulated reactions in CO/ASW films.

We investigated low-energy (100 eV) electron-stimulated reactions in layered H_2O/CO/H_2O ices. For CO layers buried in amorphous solid water (ASW) films at depths of 50 ML or less from the vacuum interface, both oxidation and reduction reactions were observed. However for CO buried more deeply in ASW films, only the reduction of CO to methanol was observed. Experiments with layered films of H_2O and D_2O showed that the hydrogen atoms participating in the reduction of the buried CO originate in the region that was 10 – 50 ML below the surface of the ASW films and subsequently diffused through the film. For deeply buried CO layers, the CO reduction reactions quickly increased with temperature above ~60 K. A simple chemical kinetic model that treats the diffusion of hydrogen atoms in the ASW and sequential hydrogenation of the CO to methanol accounted for the observations. This work is published in reference 6.

Multiple Non-Thermal Reaction Steps for the Photooxidation CO to CO_2 on Reduced TiO_2(110)

TiO_2 is a widely used photocatalyst. Its ability to oxidize organic contaminants makes it useful, for example, in air and water purification systems and as a thin-film coating for self-cleaning surfaces. As a result of titanium oxide's practical applications and its potential use in photocatalytic water spitting, it has been the subject of a tremendous amount of research. Because it is a prototypical photocatalytic reaction, the photooxidation of CO to CO_2 has received considerable attention, and some of the most detailed information has come from investigations of the reactions of CO and O_2 on single-crystal TiO_2(110).

Previous experiments have shown that the CO_2 photon-stimulated desorption (PSD) yield increased abruptly at the beginning of the UV irradiation and then monotonically decreased as the irradiation proceeds (see Fig. 1a). Similar kinetics are also observed for the CO_2 electron-stimulated desorption (ESD) yield when energetic electrons are used to create electron-hole pairs in the TiO_2 instead of UV photons. It has been proposed that the photooxidation of CO on TiO_2(110) proceeds in a single step via electron attachment, $CO + O_2^- + e^- \rightarrow CO_2 + O_b^{2-}$, and this mechanism is consistent with the observed kinetics. However, the typical time resolutions in the earlier experiments have been ~0.1 s, precluding investigation of the reaction kinetics at earlier times.

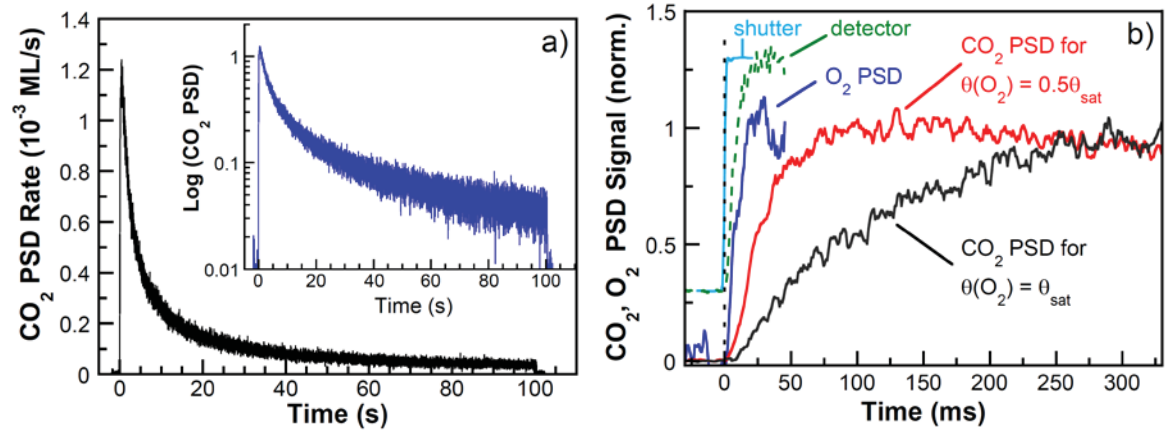

Figure 1. CO_2 and O_2 PSD signals versus time during UV irradiation of co-adsorbed O_2 and CO on TiO_2(110). a) On a longer timescale, the CO_2 PSD signal appears to increase abruptly when the UV light is switched on at t = 0 s, and then decays with complicated (non-exponential) kinetics. b) On a millisecond timescale, the CO_2 PSD signals (red and black lines) increase gradually from zero, reach a maximum and then decay at longer times. In contrast, the O_2 PSD signal (blue line) increases with the response time of the mass spectrometer detection system (green line).

We have investigated the photooxidation of CO adsorbed on reduced, rutile TiO_2(110) with an emphasis on the initial reaction kinetics on a millisecond timescale. For a saturation coverage of chemisorbed O_2 and half that coverage, we find that the CO_2 PSD signal is initially zero and gradually increases to a maximum value after several tens of milliseconds (Fig. 1b). The initial CO_2 PSD signal increases more quickly for the smaller O_2 coverage, but reaches approximately the same maximum value at intermediate times for both O_2 coverages. The results show that the photooxidation of CO on TiO_2(110) requires two or more non-thermal reaction steps and involves a metastable intermediate species. It is likely that both a hole and an electron are involved in the reactions, e.g. $CO + O_2^{2-} \xrightarrow{h^+} (CO \cdot O_2)^- \xrightarrow{e^-} O_b^{2-} + CO_2(gas)$. Alternatively, the order of the electron- and hole-mediated steps could be reversed. (Our results do not distinguish between the two possibilities.) The results also suggest that a non-thermal reaction involving this intermediate species is responsible for the non-cosine angular distribution of desorbing CO_2 that we have previously reported. This work is published in reference 4.

Future Directions:

Important questions remain concerning the factors that determine the structure of thin water films on various substrates. We plan to continue investigating the structure of thin water films on non-metal surfaces, such as oxides, and on metals where the first layer of water does not wet the substrate. For the

non-thermal reactions in water films, we will use IRAS to characterize the electron-stimulated reaction products and precursors. We will also continue our investigations into the photochemistry of small molecules on TiO_2(110).

References to publications of DOE-sponsored research (FY 2012 – present)

[1] R. Scott Smith, Nikolay G. Petrik, Greg A. Kimmel, and Bruce D. Kay, "Thermal and non-thermal physiochemical processes in nanoscale films of amorphous solid water," *Accounts of Chemical Research*, **45,** 33 (2012).

[2] G. A. Kimmel, M. Baer, N. G. Petrik, J. VandeVondele, R. Rousseau, and C. J. Mundy, "Polarization- and azimuth-resolved infrared spectroscopy of water on TiO_2(110): Anisotropy and the hydrogen-bonding network, " *J. Phys. Chem. Lett*, **3**, 778 (2012).

[3] Nikolay G. Petrik and Greg A. Kimmel, "Adsorption geometry of CO versus coverage on TiO_2(110) from s- and p-polarized infrared spectroscopy," *J. Phys. Chem. Lett*, **3**, 3425 (2012) (DOI: 10.1021/jz301413v)**.**

[4] Nikolay G. Petrik and Greg A. Kimmel, "Multiple Non-Thermal Reaction Steps for the Photooxidation CO to CO_2 on Reduced TiO_2(110)," *J. Phys. Chem. Lett*, **4**, 344 (2013) (DOI: 10.1021/jz302012j).

[5] Nikolay G. Petrik and Greg A. Kimmel, "Probing the photochemistry of chemisorbed oxygen on TiO_2(110) with Kr and other co-adsorbates," *Phys. Chem. Chem. Phys.* **16**, 2338 – 2346 (2014) (DOI: 10.1039/c3cp54195a).

[6] Nikolay G. Petrik, Rhiannon J. Monckton, Sven P. K. Koehler and Greg A. Kimmel, "Electron-stimulated reactions in layered CO/H2O films: Hydrogen atom diffusion and the sequential hydrogenation of CO to methanol," *J. Chem. Phys.* **140**, 204710 (2014) (DOI: 10.1063/1.4878658).

[7] Greg A. Kimmel, Tykhon Zubkov, R. Scott Smith, Nikolay G. Petrik and Bruce D. Kay, "Turning things downside up: Adsorbate induced water flipping on Pt(111)," *J. Chem. Phys.*, **submitted**.

Combinations of Aromatic and Aliphatic Radiolysis

Jay A. LaVerne
Notre Dame Radiation Laboratory, University of Notre Dame
Notre Dame, IN 46556
laverne.1@nd.edu

Program Scope

The radiation chemistry of simple organic molecules is derived mainly from the excited states following neutralization and this program thoroughly examines how those excited states lead to final product formation. Aliphatic compounds tend to readily decompose to a wide variety of radical species while aromatic compounds are thought to be radiation inert because of the low yields of final products. (Roder 1981) Recent studies from our laboratory have shown that aromatic compounds can in fact undergo extensive radiolytic decomposition under certain conditions. (Baidak, Badali et al. 2011; La Verne and Baidak 2012) This program seeks to understand the mechanism underlying how aromatic compounds decompose when exposed to ionizing radiation and to identify the final products formed. Of particular interest is identification of the relative contribution to radiolytic decomposition by molecules containing both aromatic and aliphatic components. Characterization of the conditions under which aromatic compounds are likely to be sensitive to radiation is an important part of this effort. Mixed organic compounds are found throughout the DOE complex. They are vital components of resins used in radioactive waste separations and the polymers used in construction components and waste storage containers. Aromatic entities are found in many of the solvents used in extraction processes including the newer “designer solvents” made from ionic liquids. Many building blocks of cells including DNA contain aromatic components so this research is also important for radiation protection purposes. The research focuses on the radiation chemistry of a variety of aromatic liquids containing different heteroatoms or aliphatic side chains. More complex aromatic compounds examined in this project include various polymers and resins. Molecular hydrogen production is the primary probe of radiation sensitivity, but a wide variety of spectroscopic and chromatographic techniques are also used. This effort differs substantially from the conventional radiation chemical approach in that heavy ion radiolysis makes up a substantial portion of the program.

Recent Progress

Aromatic compounds are found to be radiation inert when exposed to conventional γ-rays, but under certain heavy ion radiolysis conditions they exhibit substantial decomposition. This program tries to identify the characteristics under which aromatic compounds decompose and the mechanism involved. Since the decomposition of aromatic compounds is observed under heavy ion radiolysis this program relies extensively on exploiting the detailed characteristics of the track structure of radiation to probe the mechanisms involved. Ionizing radiation deposits energy along its path in localized regions leading to a nonhomogeneous distribution of reactive species that constitutes the radiation track. The general effects of track structure on the radiolysis of materials in the condensed phase are reasonably well understood, especially in liquid water. (LaVerne 2004) With increasing linear energy transfer (LET, equal to the stopping power, -dE/dx) the density of energy deposition becomes greater about the particle path. This increase in local energy density leads to higher concentrations of reactive species than are obtained using conventional fast electron or γ-radiolysis. Yields of products that

are formed due to second order reactions will be enhanced with increasing LET while those due to first order processes will be unaffected. Therefore, the yield dependence on LET can be used as a convenient probe of mechanisms in radiolysis. These so-called track effects elucidate the dominant process from the many possible pathways for product formation in the radiolysis of organic compounds. Studies on benzene and its analogs found a substantial increase in the production of H_2 on increasing the LET of the incident radiation. (LaVerne and Araos 2002; Enomoto, LaVerne et al. 2007) Organic radiolysis is primarily initiated by C-H bond breakage so the observation of H_2 implies that modification to the parent molecule decomposition must be occurring.

Most compounds consist of an aromatic and an aliphatic component so an attempt was made to determine the relative contributions to the overall radiolytic decomposition. Previous studies on the γ-ray irradiation of benzene and toluene (methyl-benzene) found an increase in H_2 production by about a factor of four by the addition of the aliphatic side chain. Examination of ethyl-, butyl-, and hexyl-benzene further confirms that the addition of the aliphatic component increases the overall net decomposition, but the additional H_2 is not linear. Clearly, some energy mixing is occurring. All of the compounds show the characteristic increase in H_2 yields with increasing LET showing how the aromatic entity dominates in certain conditions. The radiolysis of cyclohexane – benzene mixtures further elucidates the underlying mechanism. Energy deposition by ionizing radiation in each component of a mixture is proportional to the electron fraction. A mixture of 50% cyclohexane in benzene gives H_2 yields significantly lower than expected. Such a result suggests cation transfer reactions on the earliest timescales before neutralization. The LET results definitely show that the process leading to H_2 formation is second order and photolysis studies show that H_2 is formed from highly excited states of the medium molecules. (Baidak, Badali et al. 2011) Such a finding is contrary to contemporary thought that the lowest level excited states are responsible for radiolytic decomposition. The increase in local concentration of excited state species within the particle track is promoting a substantial amount of reaction between them before they normally decay to ground. The implication of this observation is that high energy states can undergo extensive chemistry, but that chemistry can be somewhat restricted because of the short lifetimes of these states.

An effort was made to determine how an aromatic entity within a compound could control the overall radiolytic effect. This work proceeded by examining the decomposition of Amberlite, a strongly basic ion exchange resin used in the treatment of nuclear reactor cooling water. The resin is a quaternary ammonium salt on a cross-linked polystyrene backbone. The gamma radiolysis of Amberlite gives a very low yield of 0.07 molecules of H_2 per 100 eV of energy absorbed, but that yield increases substantially to 0.27 molecules/100 eV for 5 MeV He ions, chosen to represent alpha particles. Gamma radiolysis yield of H_2 from polyethylene, polystyrene, and benzene are 3.3, 0.03 and 0.04 molecules/100 eV, respectively. Clearly, the results are not averaged over the various components making up the molecules since one would expect the radiolytic yield of H_2 with polystyrene to be somewhere between that for polyethylene and benzene. Apparently, the presence of an aromatic entity completely dominates the radiolytic formation of H_2. The yields of H_2 formation from all of these compounds show the characteristic increase with increasing LET suggesting similar formation mechanisms.

Future Plans

General trends for the production of H_2 have been observed, but the overall mechanism is still quite uncertain and there is little predictability. The cyclohexane – benzene mixture studies indicate that in addition to the very short excited state chemistry there seems to be some interchange of the cations before neutralization. Preliminary studies on selected deuterated ionic liquids with substituted imidazolium cations indicate

that the formation of H_2 is mainly from the aromatic ring. These studies will be extended to deuterated mixtures of benzene and cyclohexane as well as selectively deuterated toluene. The goal is to examine the isotopic distributions of hydrogen in order to determine the site of H_2 production in mixtures of aromatic and aliphatic compounds as well as in compounds containing both aromatic and aliphatic components. The outcome of the deuterated studies will be especially important at high LET were the aromatic entity seems to dominate the productions of H_2.

In addition to examination of H_2, a variety of spectroscopic techniques will be used to examine the carbon containing products. These products generally do not follow the trends of H_2 with respect to LET because of the radical precursors. However, the production of H_2 must be accompanied by a carbon containing product and LET dependences will definitely be instrumental in identification of these compounds.

References

Baidak, A., M. Badali, et al. (2011). "Role of the Low-energy Excited States in the Radiolysis of Aromatic Liquids." Journal of Physical Chemistry A **115**: 7418-7427.

Enomoto, K., J. A. LaVerne, et al. (2007). "Heavy Ion Radiolysis of Liquid Pyridine." Journal of Physical Chemistry A **111**(1): 9-15.

La Verne, J. A. and A. Baidak (2012). "Track Effects in the Radiolysis of Aromatic Liquids." Radiation Physics and Chemistry **81**: 1287-1290.

LaVerne, J. A. (2004). Radiation Chemical Effects of Heavy Ions. Charged Particle and Photon Interactions with Matter. A. Mozumder and Y. Hatano. New York, Marcel Dekker, Inc**:** 403-429.

LaVerne, J. A. and M. S. Araos (2002). "Heavy Ion Radiolysis of Liquid Benzene." Journal of Physical Chemistry A **106**(46): 11408-11413.

Roder, M. (1981). Aromatic Hydrocarbons. In Radiation Chemistry of Hydrocarbons. Amsterdam, Elsevier.

DOE Sponsored Publications in 2012-2014

El Omar, A. K.; Schmidhammer, U.; Rousseau, B.; La Verne, J. A.; Mostafavi, M. Competition Reactions of $H_2O^{\bullet+}$ Radical in Concentrated Cl^- Aqueous Solutions: Picosecond Pulse Radiolysis Study. *J. Phys. Chem. A* **2012**, *116*, 11509-11518.

Groenewold, G. S.; Elias, G.; Mincher, B. J.; Mezyk, S. P.; La Verne, J. A. Characterization of CMPO and its Radiolysis Products by Direct Infusion ESI-MS. *Talanta* **2012**, *99*, 909-917.

La Verne, J. A.; Baidak, A. Track Effects in the Radiolysis of Aromatic Liquids. *Radiat. Phys. Chem.* **2012**, *81*, 1287-1290.

Roth, O.; Dahlgren, B.; La Verne, J. A. Radiolysis of Water on ZrO_2 Nanoparticles. *J. Phys. Chem. C* **2012**, *116*, 17619-17624.

Dhiman, S.; La Verne, J. A. Radiolysis of Simple Quaternary Ammonium Salt Components of Amberlite Resin. *J. Nucl. Mater.* **2013**, *436*, 8-13.

El Omar, A. K.; Schmidhammer, U.; Balcerzyk, A.; La Verne, J. A.; Mostafavi, M. Spur Reactions Observed by Picosecond Pulse Radiolysis in Highly concentrated Bromide Aqueous Solutions. *J. Phys. Chem. A* **2013**, *117*, 2287-2293.

Lousada, C. M.; La Verne, J. A.; Jonsson, M. Enhanced Hydrogen Formation During the Catalytic Decomposition of H_2O_2 on Metal Oxide Surfaces in the Presence of HO Radical Scavengers *Phys. Chem. Chem. Phys.* **2013**, *15*, 12674-12679.

Mincher, B. J.; Mezyk, S. P.; Elias, G.; Groenewold, G. S.; La Verne, J. A.; Nilsson, A. R.; Pearson, J.; Schmitt, N. C.; Tillotson, R. D. and Olsen, L. G. **2014**, The Radiation Chemistry of CMPO: Part 2. Alpha Radiolysis, *Solv. Extr. Ion Exch. 32*, 167-178.

Interfacial Radiation Sciences

Jay A. LaVerne, David M. Bartels, Ian Carmichael, Sylwia Ptasinska
Notre Dame Radiation Laboratory, University of Notre Dame, Notre Dame, IN 46556
laverne.1@nd.edu, bartels.5@nd.edu, carmichael.1@nd.edu, sylwia.ptasinska.1@nd.edu

Program Scope

Radiation chemical effects at interfaces encompasses a wide range of fundamental disciplines brought together to investigate many different practical applications including those in the nuclear power industry. Fundamental radiation chemical effects in homogeneous media have been examined for many years at the NDRL and the expertise built up by these studies are now being used to address a wide variety of challenges involving interfaces in the generation of nuclear power. Three broad areas are being addressed: reactor chemistry, fuel and waste processing, and waste storage that are linked by the common factor of the influence of interfaces in association with radiation. Water and aqueous solutions are the focus of much of the research because they are found throughout the nuclear industry. Important questions to be answered include how the radiolysis of water either modifies or is modified by a nearby interface. In reactor water chemistry, specific topics to be addressed are rates of radical reactions at high temperature and the production and destruction of aqueous H_2O_2 at interfaces. The knowledge obtained aids in the management of existing reactors and in the development of next generation reactors. Specific topics investigated in separation systems include an examination of the stable products from various system components. Gas production in the radiolysis of resins and polymers, especially when associated with water, is being explored to aid in the management and development of waste separation streams. The third area of research focuses on the radiation chemistry associated with waste storage. This part examines the effects of water radiolysis on metal oxide interfaces and the radiolysis of polymers used in waste storage. Both topics address the production of hazardous gases, which are especially important in the storage and transportation of waste in sealed containers.

Recent Progress and Future Plans

Oxidation of solid surfaces by water radiolysis products in a reactor is the main factor leading to corrosion and ultimate failure of components. Water decomposition products are also the main concern in the storage of radioactive waste materials. Two main oxidizing species are produced in water radiolysis, the OH radical and H_2O_2. The OH radical is highly oxidizing, but has a very short lifetime leading to little effect on surfaces except when it is formed very close to an interface. On the other hand, H_2O_2 is responsible for much of the radiation-induced corrosion of nuclear reactor components because of its mobility. In most water cooled reactors, the addition of H_2 is typically used to minimize H_2O_2 production by scavenging the OH radicals before they can combine to give H_2O_2. In waste storage containers, the radiolytic buildup of H_2 will also lead to the same processes and many waste storage plans are engineered for these scenarios. Reduction of H_2O_2 yields in this system is actually caused by a chain process that also involves H atoms by the so called Allen cycle. (Allen et al. 1952) A variety of experiments combined with model calculations have characterized this system in gamma radiolysis. (Pastina and LaVerne 1999; Pastina and LaVerne 2001) However, nuclear reactors contain a variety of radiation types. Neutrons lead to proton and oxygen atom recoils from water. Alpha particles from actinide decay in waste products can be a significant fraction of the radiation field in

storage scenarios. Heavy ions such as protons, helium ions or oxygen ions have a significantly higher rate of linear energy transfer (LET = -dE/dx) than gamma rays. Water radiolysis products are well-known to be very dependent on the LET. (LaVerne 2004) An increase in LET leads to a decrease in the concentration of H atoms and OH radicals with a cessation of the chain process with a corresponding loss in H_2O_2 protection. Experiments have shown that the effect of H_2 on H_2O_2 production decreases with increasing LET. An LET of about 8 eV/nm corresponding to a 5 MeV proton is typically the breaking point where H_2 has an effect. At lower proton energies the LET is sufficiently large that the escaping H atoms and OH radicals cannot sustain the chain process and the production of H_2O_2 increases with dose. However, dose rate can also affect the escape yields of radicals. Dose rate effects vary from very high in nuclear reactors to low in waste storage systems. High dose rates enhance radical combination reactions and can lower OH radical and H atom concentrations sufficiently to stop the chain process with added H_2. A series of experiments were performed with various energy protons and helium ions to establish the effects of dose rate on H_2O_2 production with added H_2. Accelerator based studies with 5 MeV helium ions, corresponding to typical alpha particles, exhibited no dose rate effect over several orders of magnitude in the range of fluences available. The results suggest that for the most part the response of these systems is independent of dose rate for alpha particle radiolysis. A dose rate effect was observed for 5 MeV protons, where the cutoff between high and low LET effects occurs. Increasing the dose rate for these ions led to a lessening of the effect of added H_2. Model calculations are in agreement with the data for both gamma radiolysis and low LET heavy ion radiolysis. Further work is in progress to expand the model calculations and to examine other experimental parameters that might be affecting H_2O_2 yields in these systems. The addition of heterogeneous surfaces is found to have an additional effect on H_2O_2 production with added H_2. These experiments are extremely preliminary, but the added interface increases the rate of H_2O_2 decomposition with dose and a complete study is underway.

Radiation chemistry studies of simple volatile compounds condensed on alumina have been performed as part of the research examining the decomposition of molecules adsorbed on surfaces. These experiments made a tremendous step forward in understanding basic radiation decomposition processes of different compounds by the incorporation of a mass spectrometer for performing thermal desorption studies following radiolysis. Formic acid, acetonitrile, formamide and methyl formamide were examined in order to look at the effects due to systematic changes in the structure of the parent compound. Infrared examination showed some of the characteristic compounds, such as CO and CO_2, expected to be formed in the radiolysis of these compounds. Other products are typically lost in the busy spectrum of the parent compound and become more difficult to identify unambiguously. Thermal desorption shows water formation in all the oxygen containing compounds while the products in the nitrogen containing compounds are N_2, NH_3, and HCN. Further studies will examine thermal variations before irradiation; for instance, annealing the sample may lead to a different crystalline structure and possible variation in products. Another simple series of compounds, possibly alcohols, will be examined next.

Dissociative H_2O or O_2 adsorption onto a GaAs(100) surface was studied using X-ray Photoelectron Spectroscopy (XPS) carried out *in situ* under near ambient pressure conditions. These *in situ* XPS studies enable us to monitor the evolution of molecular dissociation on GaAs under elevated pressures and temperatures for the first time. In pressure-dependent XPS studies, the GaAs surface was exposed to H_2O or O_2 molecules at pressures ranging from ultra-high-vacuum (10^{-10} mbar) to 5 mbar at room temperature. In temperature-dependent XPS studies, the GaAs surface was annealed from room temperature up to 773 K at a gas pressure of 0.1 mbar. A

variety of surface species were detected forming oxide/hydroxide networks. Moreover, surface reactions on GaAs were monitored for two morphologies: a simple planar crystalline surface with (100) orientation and an ensemble of GaAs nanowires, both exposed to H_2O or O_2 environments. A significant enhancement in molecular dissociation in the case of nanowires was detected. This enhancement in oxidation and/or hydroxylation of GaAs nanowires is due to their higher surface area and the existence of more active sites for molecular dissociation. Characterization of the nature of these active sites will be pursued with the assistance of plane-wave super-cell Density Functional Theory calculations on the various Ga- and As- dominated surfaces and their reactivity towards OH and H radicals from water dissociation.

Resins are used for separations and filtering throughout the nuclear power industry and their radiolytic decay is important for proper maintenance. An extensive examination of the H_2 production from amberlite resin was undertaken recently in which the individual components of the resin were examined in the dry state in order to learn their contributions to overall gas production. The amine group was observed to have a large influence on H_2 production so different amines were examined with various amounts of water as will typically be encountered in realistic scenarios. Specifically, H_2 yields were measured from ammonium chloride, methyl ammonium chloride, dimethyl ammonium chloride, trimethyl ammonium chloride, and tetramethyl ammonium chloride with different amounts of water. There are three regions observed for all compounds with various amounts of water. Dry compounds or those with little water each had their own characteristic production of H_2 as previously reported. The range of about 20 – 80% water loading leads to H_2 yields of 1 – 1.5 molecules/100 eV for all these compounds. Finally there was a slight increase in H_2 production at about 90% water followed by a gradual decrease to the 0.45 molecules/100 eV found with only water. There appears to be a slight interaction between the amine and water at high water percentage for both the di- and tri-methyl ammonium chloride. Further work will try to elucidate the exact interactions between water and the amines.

References

Allen, A. O., C. J. Hochanadel, J. A. Ghormley, and T. W. Davis. 1952. Decomposition of Water and Aqueous Solutions under Mixed Fast Neutron and Gamma Radiation. *J. Phys. Chem.* 56: 575-586.

LaVerne, J. A. (2004). Radiation Chemical Effects of Heavy Ions. Charged Particle and Photon Interactions with Matter. A. Mozumder and Y. Hatano. New York, Marcel Dekker, Inc**:** 403-429.

Pastina, B., and J. A. LaVerne. 1999. Hydrogen Peroxide Production in the Radiolysis of Water with Heavy Ions. *J. Phys. Chem. A* 103: 1592-1597.

Pastina, B., and J. A. LaVerne. 2001. Effect of Molecular Hydrogen on Hydrogen Peroxide in Water Radiolysis. *J. Phys. Chem. A* 105: 9316-9322.

Publications with BES support since 2012

El Omar, A. K.; Schmidhammer, U.; Rousseau, B.; LaVerne, J. A.; Mostafavi, M. Competition Reactions of $H_2O^{\bullet+}$ Radical in Concentrated Cl^- Aqueous Solutions: Picosecond Pulse Radiolysis Study. *J. Phys. Chem. A* **2012**, *116*, 11509-11518.

Groenewold, G. S.; Elias, G.; Mincher, B. J.; Mezyk, S. P.; LaVerne, J. A. Characterization of CMPO and its Radiolysis Products by Direct Infusion ESI-MS. *Talanta* **2012**, *99*, 909-917.

La Verne, J. A.; Baidak, A. Track Effects in the Radiolysis of Aromatic Liquids. *Radiat. Phys. Chem.* **2012**, *81*, 1287-1290.

Roth, O.; Dahlgren, B.; LaVerne, J. A. Radiolysis of Water on ZrO_2 Nanoparticles. *J. Phys. Chem. C* **2012**, *116*, 17619-17624.

Jheeta, S.; Ptasinska, S.; Sivaraman, B.; Mason, N. **2012** The irradiation of 1:1 mixture of ammonia:carbon dioxide ice at 30 K using 1 keV electrons. *Chem. Phys. Lett.* 551, 144.

Jheeta, S.; Domaracka, A.; Ptasinska, S.; Sivaraman, B.; Mason, N. J. **2013** The irradiation of pure CH_3OH and 1:1 NH_3:CH_3OH ices at 30K using low energy electrons. *Chem. Phys. Lett*. 543 208.

Dhiman, S.; LaVerne, J. A. Radiolysis of Simple Quaternary Ammonium Salt Components of Amberlite Resin. *J. Nucl. Mater.* **2013**, *436*, 8-13.

El Omar, A. K.; Schmidhammer, U.; Balcerzyk, A.; LaVerne, J. A.; Mostafavi, M. Spur Reactions Observed by Picosecond Pulse Radiolysis in Highly concentrated Bromide Aqueous Solutions. *J. Phys. Chem. A* **2013**, *117*, 2287-2293.

Lousada, C. M.; LaVerne, J. A.; Jonsson, M. Enhanced Hydrogen Formation During the Catalytic Decomposition of H_2O_2 on Metal Oxide Surfaces in the Presence of HO Radical Scavengers *Phys. Chem. Chem. Phys.* **2013**, *15*, 12674-12679.

Mincher, B. J.; Mezyk, S. P.; Elias, G.; Groenewold, G. S.; LaVerne, J. A.; Nilsson, A. R.; Pearson, J.; Schmitt, N. C.; Tillotson, R. D. and Olsen, L. G. **2014**, The Radiation Chemistry of CMPO: Part 2. Alpha Radiolysis, *Solv. Extr. Ion Exch. 32*, 167-178.

Zhang, X. Q.; Lamere, E.; Liu, X. Y.; Furdyna, J. K. and Ptasinska, S. **2014**, Morphology dependence of interfacial oxidation states of gallium arsenide under near ambient conditions, *Appl. Phys. Lett. 104*,

Zhang, X. Q. ; Lamere, E.; Liu, X.; Furdyna, J. K. and Ptasinska, S. **2014**, Interface chemistry of H_2O on GaAs nanowires probed by near ambient pressure X-ray photoelectron spectroscopy, *Chem. Phys. Lett. 605*, 51-55.

Zhang, X. Q. and Ptasinska, S. **2014**, Dissociative Adsorption of Water on an H_2O/GaAs(100) Interface: *In Situ* Near-Ambient Pressure XPS Studies, *J. Phys. Chem. C 118*, 4259-4266.

Single-Molecule Interfacial Electron Transfer

H. Peter Lu
Bowling Green State University
Department of Chemistry and Center for Photochemical Sciences
Bowling Green, OH 43403
hplu@bgsu.edu

Program Scope

We focus our studies on molecular dynamics in condensed phase and at interfaces, especially, the complex reaction dynamics associated with electron and energy transfer rate processes, using single-molecule high spatial and temporal resolved spectroscopic approaches. The complexity and inhomogeneity of the interfacial ET dynamics often present a major challenge for a molecular level comprehension of the intrinsically complex systems, which calls for both higher spatial and temporal resolutions at ultimate single-molecule and single-particle sensitivities. Combined single-molecule spectroscopy and electrochemical atomic force microscopy (E-Chem AFM) approaches are unique for heterogeneous and complex interfacial electron transfer systems because the static and dynamic inhomogeneities can be identified and characterized by studying one molecule at a specific nanoscale surface site at a time. Single-molecule spectroscopy reveals statistical distributions correlated with microscopic parameters and their fluctuations, which are often hidden in ensemble-averaged measurements. Single molecules are observed in real time as they traverse a range of energy states, and the effect of this ever-changing "system configuration" on chemical reactions and other dynamical processes can be mapped. The goal of our project is to integrate and apply these spectroscopic imaging and topographic scanning techniques to measure the energy flow and electron flow between molecules and substrate surfaces as a function of surface site geometry and molecular structure. We have been primarily focusing on studying interfacial electron transfer under ambient condition and electrolyte solution involving both single crystal and colloidal TiO_2 and related substrates. Our understanding of the fundamental interfacial electron transfer processes will be important for developing efficient light harvesting systems and broadly applicable to problems in fundamental catalysis and interfacial chemistry.

Recent Progress

Single-Molecule Interfacial Electron Transfer Dynamics of Porphyrin on TiO_2 Nanoparticles: Dissecting the Complex Electronic Coupling Dependent Dynamics. We have studied the photosensitized interfacial electron transfer (ET) dynamics of the Zn(II)-5,10,15,20-tetra (3-carboxyphenyl) porphyrin (*m*/*p*-ZnTCPP)-TiO_2 nanoparticle (NP) system using single-molecule photon-stamping spectroscopy (Figure 1). The single-molecule fluorescence intensity trajectories of both *m*-ZnTCPP and *p*-ZnTCPP on TiO_2 NP surface show fluctuations and blinking between bright and dark states, which are attributed to the variations in the reactivity of interfacial ET, i.e., intermittent interfacial electron transfer dynamics (Figure 2). We also identified the effect of anchoring group binding geometry (*meta* or *para*), hence electronic coupling of sensitizer (*m*/*p*-ZnTCPP) and TiO_2 substrate, on interfacial ET dynamics. Compared to *p*-ZnTCPP on TiO_2 NP surface, with *m*-ZnTCPP, dark states are observed to dominate in single-molecule fluorescence intensity trajectories. This observation coupled with the large difference in lifetime derived from bright and dark states of *m*-ZnTCPP demonstrate higher charge injection efficiency of *m*-ZnTCPP than *p*-ZnTCPP. The nonexponential autocorrelation function decay and the power-law distribution of the dark-time probability density provide a detailed characterization of the inhomogeneous interfacial ET dynamics. The distribution of autocorrelation function decay times (τ) and power-law exponents (m_{dark}) for *m*-ZnTCPP are

found to be different from those for *p*-ZnTCPP, which indicates the sensitivity of τ and m_{dark} on the molecular structure, molecular environment, and molecule-substrate electronic coupling of the interfacial electron transfer dynamics. Overall, our results strongly suggest that the fluctuation and even intermittency of excited-state chemical reactivity are intrinsic and general properties of molecular systems that involve strong molecule-substrate interactions. Furthermore, the observed differences in the interfacial electron transfer reactivity of *m*-ZnTCPP and *p*-ZnTCPP can be associated with the difference in the redox reactivity intermittency with the fluctuation of molecule-TiO_2 electronic and Franck-Condon coupling.

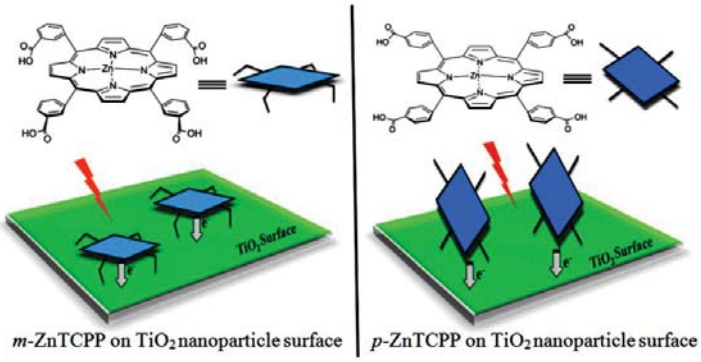

Figure 1. Schematic representation of *m*-ZnTCPP and *p*-ZnTCPP binding on TiO_2 surface. The different molecular binding geometry on TiO_2 surface contributes to different electronic coupling between the molecules and the substrate, and in turn, contributes to different interfacial electron transfer rate processes.

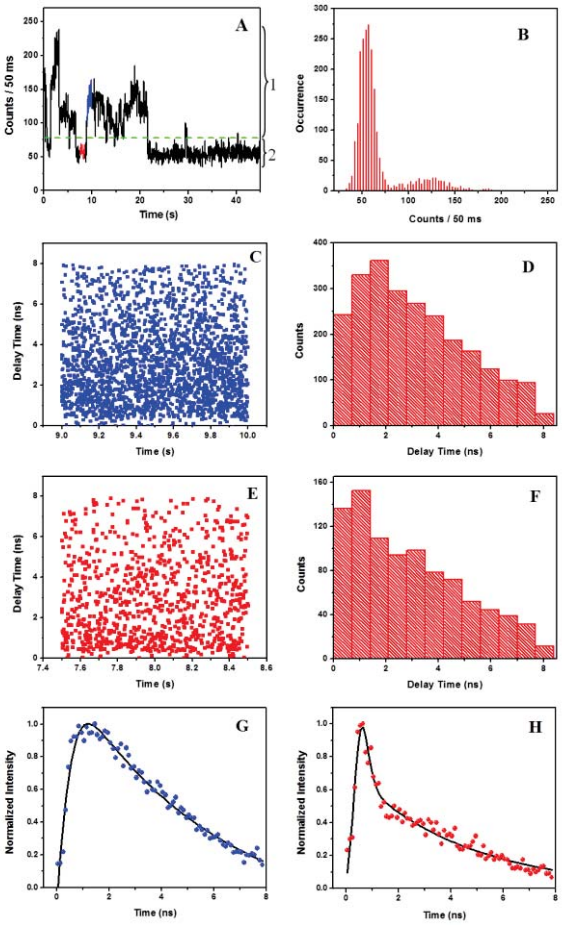

Figure 2. Single-molecule fluorescence decay profile of *m*-ZnTCPP on TiO_2 NP surface. The Fluorescence emission trajectory of *m*-ZnTCPP on TiO_2 NPs-coated cover glass and histogram of the emission intensity are displayed in (A) and (B). Using 77 photon-counts/50 ms as threshold, the fluorescence emission trajectory is separated into higher-level emission (marked as 1) and lower-level emission (marked as 2). (C, E) and (D, F) show the photon-stamping data and corresponding histogram for a typical bright state (in "blue", 9.0−10.0 s) and dark state (in "red", 7.5−8.5 s). The fluorescence decay profiles of higher-level emission and lower-level emission of the whole trajectory are displayed in (G) and (H). The fit to the decay profiles (solid line) shown in (G) and (H) are biexponential fit derived by deconvolution of instrument response function (IRF).

Probing Driving Force Dependent Single-Molecule Interfacial Electron Transfer Dynamics. There a number of key parameters that control an interfacial electron transfer dynamics in molecule/TiO_2 systems. The parameters which greatly influence ET dynamics include electronic coupling between the molecule and semiconductor, vibrational relaxation energy of adsorbed molecule, solvent reorganization energy, driving force of the free energy gap, the surface structures, and the defect

surface states. In this task, we have focused our studies on the electron transfer rate processes controlled by the electron transfer driving force (ΔG) as well as the interfacial electric field at a molecule-TiO_2 interface. Although, significant efforts made in this direction by ensemble average measurements (electrochemistry as well as spectroscopy) already indicate the importance of various factors in determining injection dynamics, further advancement of the understanding requires study at single molecule level and at specific nanoscale local environment. The complexity of the interfacial electron transfer dynamics often presents a major challenge for conventional ensemble-averaged measurements as the molecule-substrate interactions are inhomogeneous involving heterogeneous local environments. Single-molecule spectroscopy provides insightful details about interfacial ET dynamics which are beyond the realms of conventional solution-phase ensemble-averaged analyses; particularly with regard to complex mechanism and spatiotemporal heterogeneity. Combination of single-molecule fluorescence spectroscopy approach with various other techniques such as atomic force microscopy (AFM), electrochemistry, and Raman spectroscopy can further facilitate inspection of multiple-parameters with high chemical selectivity and wide temporal and spatial resolutions. Here we develop correlated single-molecule spectro-electrochemistry technique (Figure 3) to study photon-stamping measurements of individual Zn(II)-5,10,15,20-tetra (3-carboxyphenyl) porphyrin, *m*-ZnTCPP, molecule anchored to TiO_2 NP surface in aqueous solution while electrochemically controlling the energy states of TiO_2 NPs through applied electric bias. We thus concluded that the interfacial electron transfer dynamics, the excited-state lifetime of dye molecule anchored to TiO_2, and the single molecule blinking pattern can be controlled by tuning the relative energetics of the dye excited state relative to the unoccupied TiO_2 acceptor state.

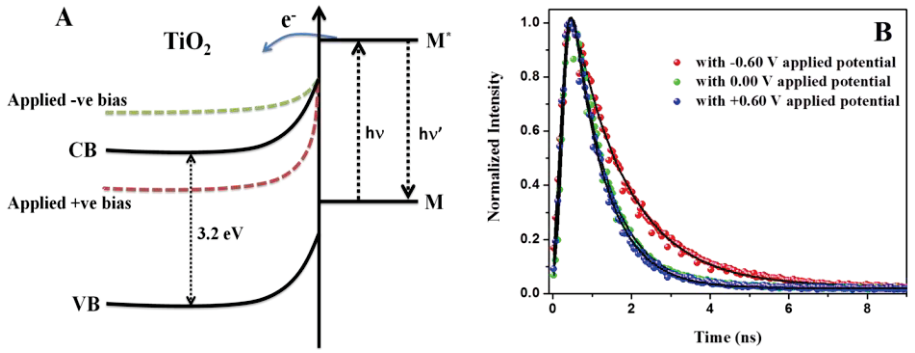

Figure 3: The fluorescence decay profiles of *m*-ZnTCPP on TiO_2 NP surface with different applied surface electric potentials. The initial study indicates that in absence of applied electric bias the single-molecule fluorescence intensity trajectories of *m*-ZnTCPP on TiO_2 NP surface show fluctuations and blinking between bright and dark states, which are attributed to the variations in the reactivity of interfacial ET, i.e., intermittent interfacial electron transfer dynamics. The blinking pattern changes significantly with –ve applied potential, whereas it remains almost same with applied +ve potential. The application of -0.6 V to the TiO_2 electrode also resulted in ~2-fold increase in excited state lifetime of *m*-ZnTCPP.

Characterizing Electric Field Effect on Covalent Interactions at a Molecule-TiO2 Interface. We have probed the change in the interface properties of alizarin-TiO_2 system as a result of the externally applied electric field by using surface-enhanced Raman spectroscopy (SERS) and supported our experimental results by *ab initio* calculations. The electric field effect on the interface properties has been probed by using single-molecule surface-enhanced Raman spectroscopy and supported by density functional theory calculations in alizarin-TiO_2 system. The perturbation, created by the external potential, has been observed to cause a shift and/or two-peak occurrence of the 648 cm^{-1} peak, typical indicator of the strong coupling between alizarin and TiO_2. This phenomenon evidence the field-dependent electronic coupling change that has a direct correlation with the electron transfer dynamics.

Future Research Plans

Interfacial ET dynamics strongly involves with and regulated by molecule-surface interactions. Following forward electron transfer (FET), the injected electrons go through different semiconductor processes such as charge trapping, detrapping, and electron Brownian and non-Brownian diffusion before (i) recombination with parent cation (back ET,BET) or (ii) diffusion away to generate photovoltaic potential energy. Unlike FET dynamics, which are predominately ultrafast in the femtosecond to several hundred picoseconds range, BET dynamics is often nonexponential or stretched exponential ranging from sub-nanoseconds to several milliseconds. Typically, it is the BET process that determines the solar energy conversion efficiency of a molecule-TiO_2 nanoparticle system. We plan to study the BET dynamics by manipulating the electric field distribution at the interface and the energetic trapping state distributions in the TiO_2 nanoparticles. Furthermore, the electronic coupling strength between excited states of dye molecule and the semiconductor can be modified through a number of ways including (i) the use of a bridge between the chromophore and the anchoring group of the dye molecule; (ii) the use of different anchoring groups, such as carboxylic acid and hydroxyl derivatives; and by (iii) the use of different numbers of anchoring groups. We will explore these possible chemical manipulations to systematically study further the electronic coupling regulated interfacial electron transfer dynamics. One of the most significant characteristics of our approach is that we will interrogate the complex interfacial electron transfer dynamics by actively pin-point energetic manipulation of the surface interaction and electronic couplings, beyond the conventional excitation and observation.

Publications of DOE sponsored research (FY2011-2014)

1. Papatya C. Sevinc, Yuanmin Wang, H. Peter Lu, “Probing Electric Field Effect on Covalent Interactions at a Molecule-Semiconductor Interface,” Submitted (2014).
2. Vishal Govind Rao, Bharat Dhital, Yufan He, H. Peter Lu, " Single-Molecule Interfacial Electron Transfer Dynamics of Porphyrin on TiO2 Nanoparticles: Dissecting the Complex Electronic Coupling Dependent Dynamics," Submitted (2014).
3. Vishal Govind Rao, Bharat Dhital, Yufan He, H. Peter Lu, " Single-Molecule Interfacial Electron Transfer Dynamics of Porphyrin on TiO2 Nanoparticles: Dissecting the Complex Electronic Coupling Dependent Dynamics," *J. Phys. Chem. C*., In press, Web released (2014).
4. H. Peter Lu, "Single-Molecule Interfacial Electron Transfer Dynamics," an invited book chapter in Handbook of Spectroscopy, Second Edition (G. Gauglitz and D. S. Moore. Eds), p. 877-910, Wiley-VCH Verlag GmbH & Co. (2014).
5. Desheng Zheng, Leonora Kaldaras, H. Peter Lu, “Total Internal Reflection Fluorescence Microscopy Imaging-Guided Confocal Single-Molecule Fluorescence Spectroscopy,” *Review of Scientific Instruments*, **83**, 013110 (2012).
6. Yuanmin Wang, Papatya C. Sevinc, Yufan He, H. Peter Lu, "Probing Ground-State Single-Electron Self-Exchange Across a Molecule-Metal Interface," *J. Am. Chem. Soc.,* **133**, 6989-6996 (2011).
7. Sevinc, Papatya; Wang, Xiao; Wang, Yuanmin; Zhang, Dai; Meixner, Alfred; Lu, H. Peter, "Simultaneous Spectroscopic and Topographic Near-Field Imaging of TiO2 Single Surface States and Interfacial Electronic Coupling," Nano Letters, 1490-1494 (2011).

Solution Reactivity and Mechanisms through Pulse Radiolysis

Sergei V. Lymar
Chemistry Department, Brookhaven National Laboratory, Upton, NY 11973-5000
e-mail: lymar@bnl.gov

Program Scope

This program applies pulse radiolysis for investigating reactive intermediates and inorganic reaction mechanisms. The specific systems are selected based on their fundamental significance or importance in energy and environmental problems.

The first project investigates physical chemistry of nitrogen oxides and their congeneric oxoacids and oxoanions. These species play an essential role in environmental chemistry, particularly in the terrestrial nitrogen cycle, pollution, bioremediation, and ozone depletion. Nitrogen-oxygen intermediates are also central to the radiation-induced reactions that occur in nuclear fuel processing and within attendant nuclear waste. Redox and radical chemistry of the nitrate/nitrite system mediates the most of radiation-induced transformations in these environments. Equally important are the biochemical roles of nitrogen oxides. We apply time-resolved techniques for elucidation of the prospective reactions in terms of their thermodynamics, rates and mechanisms, focusing on the positive nitrogen oxidation states, whose chemistry is of the greatest current interest. This abstract and meeting presentation will be focused mainly on new results from this project.

The goal of the second project is to gain mechanistic insight into redox catalysis through characterization of the catalyst transients involved in the catalytic cycle, with the focus on water oxidation catalysis. Development of catalysts to carry out the four-electron water oxidation remains the greatest challenge in the solar energy utilization. Growing recent interest in this field has triggered the discovery of a wide variety of catalytic systems, both molecular and heterogeneous, but the reaction mechanisms remain to be established. The major impediment has been the difficulties in identification and characterization of the reaction intermediates. In this project, we use radiolysis techniques to generate and characterize the redox states of the catalyst involved in water oxidation.

Collaborators on these projects include M. Valiev (PNNL),[1-2] Shafirovich (NYU),[3] J. Hurst (WSU, emeritus),[4-6] D. Polyansky (BNL),[4] D. Grills (BNL),[7] and H. Schwarz (BNL, emeritus).[8]

Progress

Nitrogen oxides.[1-2,4,9-10] Rapid one-electron reduction of NO is most readily accomplished through pulse radiolysis whereby the hydrated electron reacts with NO producing the nitroxyl anion ($^3NO^-$) in its triplet ground state as shown to the right. However, protonation of $^3NO^-$ primarily yields nitroxyl (^1HNO), whose ground state is singlet.[11] Undoubtedly, $^3NO^-$ and ^1HNO are the major species that mediate radiation-induced transformations in the nuclear fuel processing and nuclear wastes; the latter is evidenced by the NO and N_2O emissions from the Hanford waste storage tanks.

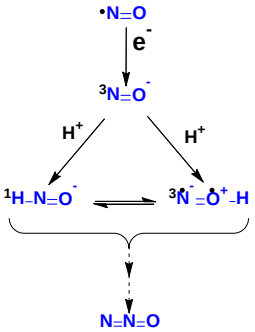

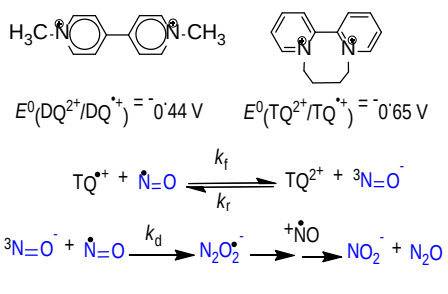

Although energetics of the nitroxyl species is germane for evaluating their reactivity, only the free energy of aqueous ^{1}HNO has been reliably established.[12] The most important poorly known quantity is $\Delta_{form}G^0(^3NO^-)$, that defines the reduction potentials for NO and pKa(^{1}HNO/^{3}NO$^-$). In the attempt to evaluate this potential, we have used pulse radiolysis to investigate the redox equilibria between ^{3}NO$^-$ and various viologens, diquat (DQ^{2+}) and tetraquat (TQ^{2+}). While no reaction was detected for the higher potential $DQ^{\bullet+}$ radical, the lower potential $TQ^{\bullet+}$ radical was found to be capable of the NO reduction (scheme above). The kinetic analysis allowed evaluating the equilibrium constant $K_{eq} = k_f/k_r$, which gave the first direct determination of $E^0(NO/^3NO^-) = -0.85$ V.

Our computations at the CCSD(T)/ COSMO theory level reveals the highly unusual manifold of nitroxyl species spin states that is diagramed to the right. The diagram shows the existence of the higher energy tautomer of protonated NO$^-$ with triplet ground state (^{3}NOH) and is drawn to scale using the relative computed energies for ^{1}HNO/^{3}HNO and ^{3}NOH/^{1}NOH, the above described $E^0(NO/^3NO^-)$, and the previously estimated $\Delta_{form}G^0(^1HNO)$.[12] The pattern of energy levels engenders an expectation of the unique acid-base chemistry, which we have indeed observed in the nitroxyl species production through the photochemical decomposition of trioxodinitrate($N_2O_3^{2-}$/$HN_2O_3^-$), as shown in the scheme below.

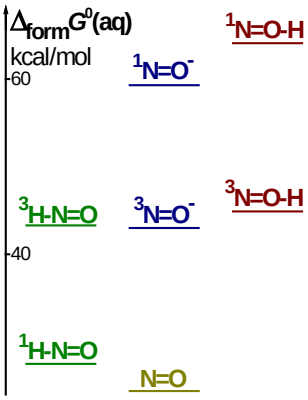

In variance with the long-held beliefs, our CCSD(T)/COSMO computations show that protonation of $N_2O_3^{2-}$ occurs on the lone terminal oxygen atom and not on the neighboring nitrogen atom. These finding has important implications for understanding our flash UV laser photolysis data. Counterintuitively, we find that only protonated ^{1}HNO nitroxyl species is produced from the fully deprotonated $N_2O_3^{2-}$ anion and observe a considerable amount of deprotonated ^{3}NO$^-$ product from fully protonated $HN_2O_3^-$; in this case decomposition bifurcates between ^{3}NO$^-$ and ^{1}HNO products. The most plausible interpretation of these findings is shown in the scheme above and involves a number of rapid, energetically favorable acid-base reactions along with the ^{1}HNO → ^{3}HNO intersystem crossing.

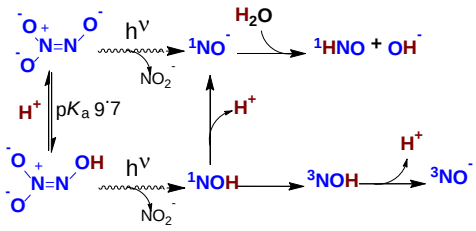

Intermediates in water oxidation catalysis.[3-4,6] Research from several laboratories, have established that water oxidation catalysis by the *cis,cis*-$[(bpy)_2(H_2O)Ru\text{-}O\text{-}Ru(OH_2)(bpy)_2]^{4+}$ (known as the *blue dimer* **{3,3}**, whose structure is shown to the left and the numbers in parenthesis indicate oxidation states of the Ru atoms) involves its progressive oxidation with the attendant loss of protons to the ruthenyl **{5,5}** dimer. Pulse radiolysis has figured prominently in the assignment of intermediary oxidation states formed upon sequential one-electron oxidations of the dimer.[4-5] Recently, we have investigated reaction of persulfate with the ruthenium blue dimer. This highly unusual reaction allows to quantitatively convert the {3,3} oxidation state into the {3,4} state and is a key ingredient of our research toward characterization of the redox transients formed

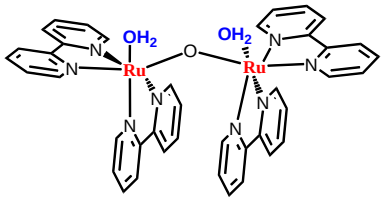

during water oxidation cycle. The combination of thermal kinetic, radical trapping, and pulse radiolysis experiments reveal the unusual apparent two-electron reaction mechanism with the intermediacy of radical species and allowed to obtain information about disproportionation reactions of the blue dimer, with important implication to understanding its catalytic mechanism.

Planned work will investigate:

- New pathways for generating nitroxyl species and their reactivity, including rate and mechanism of their self-decay.
- Spin-forbidden ground state bond breaking/making reactions involving $^1HNO/^3NO^-$.
- Thermodynamics of photochemical and spontaneous generation of $^1HNO/^3NO^-$ from trioxodinitrate ($HN_2O_3^-/N_2O_3^{2-}$) species.
- Redox and radical chemistry in the nitrite/nitrate system, including: formation pathways and thermodynamics of nitrate radical anion; rates and mechanisms of its acid-catalyzed and redox reactions.
- Nature of catalyst states involved in water oxidation by the ruthenium "blue dimer", including reduction potential and decay mechanism for the Ru^{IV}-Ru^{IV} and higher oxidation states.
- Mechanistic studies of radiation-induced radical and redox reactions on solid/liquid interfaces.

References (DOE sponsored publications in 2011-present are marked with asterisk)

(1*)Valiev, M.; Lymar, S. V. "Structural and Mechanistic Analysis through Electronic Spectra: Aqueous Hyponitrite Radical ($N_2O_2^-$) and Nitrosyl Hyponitrite Anion ($N_3O_3^-$)" *J. Phys. Chem. A* **2011**, *115*, 12004-12010.
(2*)Shaikh, N.; Valiev, M.; Lymar, S. V. "Decomposition of Amino Diazeniumdiolates (NONOates): Molecular Mechanisms" *J. Inorg. Biochem.*, (published online 23 August 2014).
(3*)Zidki, T.; Zhang, L.; Shafirovich, V.; Lymar, S. V. "Water Oxidation Catalyzed by Cobalt(II) Adsorbed on Silica Nanoparticles" *J. Am. Chem. Soc.* **2012**, *134*, 14275-14278.
(4*)Polyanskiy, D. E.; Hurst, J. K.; Lymar, S. V. "Application of Pulse Radiolysis to Mechanistic Investigations of Water Oxidation Catalysis" *Eur. J. Inorg. Chem.* **2014**, 619-634.
(5*)Cape, J. L.; Lymar, S. V.; Lightbody, T.; Hurst, J. K. *Inorg. Chem.* **2009**, *48*, 4400-4410.
(6*)Stull, J. A.; Britt, R. D.; McHale, J. L.; Knorr, F. J.; Lymar, S. V.; Hurst, J. K. "Anomalous Reactivity of Ceric Nitrate in Ruthenium "Blue Dimer"-Catalyzed Water Oxidation," *J. Am. Chem. Soc.* **2012**, *134*, 19973-19976.
(7*)Grills, D. C.; Farrington, J. A.; Layne, B. H.; Lymar, S. V.; Mello, B. A.; Preses, J. M.; Wishart, J. F. "Mechanism of the Formation of a Mn-Based CO_2 Reduction Catalyst Revealed by Pulse Radiolysis with Time-Resolved Infrared Detection" *J. Am. Chem. Soc.* **2014**, *136*, 5563-5566.
(8*)Lymar, S. V.; Schwarz, H. A. *J.* "Hydrogen Atom Reactivity toward Aqueous *tert*-Butyl Alcohol" *Phys. Chem. A* **2012**, *116*, 1383-11389.
(9)Armstrong, D. A.; Huie, R. E.; Lymar, S.; Koppenol, W. H.; Merényi, G.; Neta, P.; Stanbury, D. M.; Steenken, S.; Wardman, P. *Bioinorg. React. Mech.* **2013**, *9*, 59-61.
(10)Armstrong, D. A.; Huie, R. E.; Lymar, S.; Koppenol, W. H.; Merényi, G.; Neta, P.; Ruscic, B.; Stanbury, D. M.; Steenken, S.; Wardman, P. *Pure Appl. Chem.*, (accepted).
(11)Lymar, S. V.; Shafirovich, V.; Poskrebyshev, G. A. *Inorg. Chem.* **2005**, *44*, 5212-5221.
(12)Shafirovich, V.; Lymar, S. V. *Proc. Natl. Acad. Sci. USA* **2002**, *99*, 7340-7345.

Geminate Recombination in Tetrahydrofuran

Principal Investigators: John R. Miller and Andrew R. Cook

Department of Chemistry, Brookhaven National Laboratory, Upton, NY, 11973 USA

jrmiller@bnl.gov, acook@bnl.gov

Program Scope:

This program applies both photoexcitation and ionization by short pulses of fast electrons to investigate fundamental chemical problems relevant to the production and efficient use of energy and thus obtain unique insights not attainable with other techniques. These studies may play an important role in the development of safer, more effective, and environmentally beneficial processes for the chemical conversion of solar energy. Picosecond pulse radiolysis is employed to generate and study reactive chemical intermediates or other non-equilibrium states of matter in ways that are complementary to photolysis and electrochemistry and often uniquely accessible by radiolysis. This program also develops new tools for such investigations, applies them to chemical questions, and makes them available to the research community. Advanced experimental capabilities, such as Optical Fiber Single-Shot detection system, allow us to work on fascinating systems with 5-10 ps time-resolution that were previously prohibitive for technical reasons.

Recent Progress:

Charge recombination in THF: different fates for conjugated molecules. Ionization of THF, one of the best solvents for conjugated polymers, produces free ions, which move independently of each other, and a somewhat larger amount of geminate (or spur) ions consisting of electrons and holes that are separated by 1-7 nm, but are bound by their mutual Coulomb attraction. When THF was used in past work to investigate electron transfer and the Marcus theory, the geminate ion-pairs presented only a minor problem because they annihilate upon recombination. Electrons in long conjugated molecules behave differently. Geminate recombination of positive and negative charge carriers was observed in THF. Pulse radiolysis gives rapid creation of solvated protons (RH_2^+) and anions ($M^{\bullet -}$) in THF. These were expected to recombine by diffusion within their mutual Coulomb potential. Such annihilations of the carriers are due to proton transfer(PT) from the donor, RH_2^+, to the acceptor, $M^{\bullet -}$.

In 1938, Onsager applied the Debye-Smoluchowski (DS) equation to the case in which positive ions and negative ions annihilate upon contact (infinite annihilation rate: ion annihilation is diffusion-controlled). He discussed ion recombination under influence of Coulomb potential, predicted the free ion yield (F_h) as a function of initial separation distance, and defined a critical radius (r_c), now often called the Onsager radius, at which the attractive Coulomb potential energy, $V(r_c)$, equals thermal energy, $V(r_c)=k_BT$. An ion thermalized at r_c from its geminate counter ion has a 50% probability to escape to become free ion and a 50% probability to escape. For the primary ion pairs, the probabilities of escape and recombination change with the initial distance. We will refer to the free ion yield arising from escape by diffusion from their initial separation distances as the Type I free ion yield (F_h^I). Rice, Flannery, Hong, and Noolandi, extended Onsager's work to solve the DS equation for the case in which the rate of annihilation was not infinite, and suggested that an additional contribution to F_h could arise from ion-pairs

that escape after coming together. We will refer this additional contribution as the Type II free ion yield (F_h^{II}).

The data indicate the two step nature of the recombination: Coulomb driven formation of ion pairs followed by proton transfer. With large driving force (ΔG^0=-0.3 to -1.6 eV) for PT reaction, some of ion pairs react rapidly ($k_{MPT} > 10^9\ s^{-1}$) but others react more slowly. For 17 molecules studied the amplitude of the long-lived homogenous (free) ion yield is constant at 0.356±0.03 of the total regardless of k_{MPT}, indicating no geminate ions escape to become free ions. For anions of oligo(9,9-dihexyl)fluorenes, $F_n^{\bullet-}$ (n=2-4), some of $F_n^{\bullet-}$ (n=2-4) do escape to become free ions. This escape suggests the ion's charge distribution is crucial for an ion to survive geminate recombination.

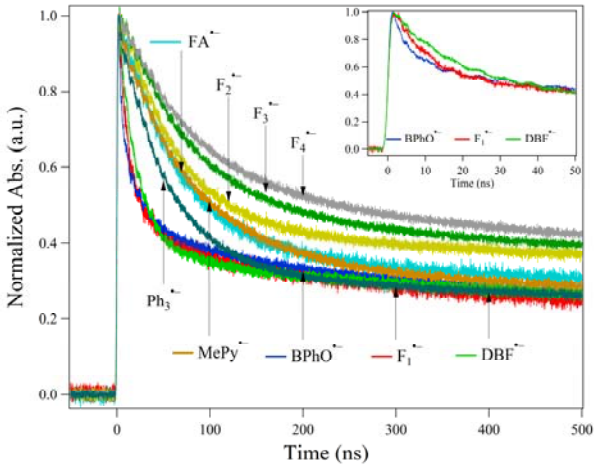

The rate constants for proton transfer within the ($M^{\bullet-}$,RH_2^+) ion pairs show some correlation with free energy change, ΔG°, for the proton transfer (PT) reactions. The correlation is only roughly known, because values of ΔG° are only roughly estimated, but the results yield conclusions that 1) PT reactions to oxygen or nitrogen are much faster than PT to carbon and 2) The slow PT rates to carbon are due to large reorganization energies.

Electron Transfer by Excited Benzoquinone Anions: Slow Rates for Two-Electron Transitions. Electron transfer (ET) rate constants from the lowest excited state of the radical anion of benzoquinone, $BQ^{-\bullet *}$, were measured in THF solution. Rate constants for bimolecular electron transfer reactions typically reach the diffusion-controlled limit when the free-energy change, ΔG°, reaches −0.3 eV. The rate constants for ET from $BQ^{-\bullet *}$ are one-to-two decades smaller at this energy and do not reach the diffusion-controlled limit until −ΔG° is 1.5−2.0 eV. The rates are so slow probably because a second electron must also undergo a transition to make use of the energy of the excited state. Similarly, ET, from solvated electrons to neutral BQ to form the lowest excited state, is slow, while fast ET is observed at a higher excited state, which can be populated in a transition involving only one electron. A simple picture based on perturbation theory can roughly account for the control of electron transfer by the need for transition of a second electron. The picture also explains how extra driving force (−ΔG°) can restore fast rates of electron transfer.

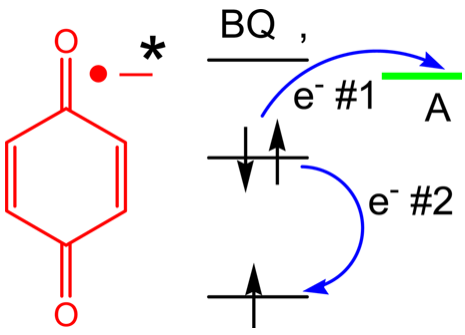

Pressure Tuning of Electron Attachment to Benzoquinones in Nonpolar Fluids: Continuous Adjustment of Free Energy Changes. Experiments above found unusually slow rates for transfer of an electron from the lowest excited state of $BQ^{-\bullet}$ to acceptors with varying ΔG°. Experiments below provide further evidence of the inability of the lower excited state to participate rapidly in electron transfer. Changing pressure from 1-2500 bar continuously tunes

free energy changes for electron attachment to molecules in nonpolar liquids by nearly 0.3 eV. Rate constants for electron attachment to substituted benzoquinones were determined over an extended free energy range of nearly 1 eV by a combination of solute, pressure, temperature and use of solvents with differing V_0: tetramethylsilane (TMS) and 2,2,4-trimethylpentane (TMP). The rates of attachment to both benzoquinone (BQ) and 2,5-dichlorobenzoquinone in TMS increase as the pressure increases to 2500 bar, while in TMP the rates are higher but change little with pressure; the rate of attachment to fluoranil in TMS is similarly high at 1 bar but decreases with increasing pressure. Together the observed rate constants can be qualitatively interpreted to yield a rate vs. free energy relation having both normal and Marcus inverted region behavior, seen in the figure to the right. The solid line is a fit of Marcus electron transfer theory with 1 vibrational mode to the rates for BQ and F_4Q in TMS. Parameter values: V(r) = 348 ± 4 cm^{-1}, λ_s = 0.105 ± 0.006, λ_v = 0.24± 0.007, T = 296, ω = 1296 cm^{-1}. The fit was performed using the known mobility μ = 100 cm^2/Vs, in TMS.

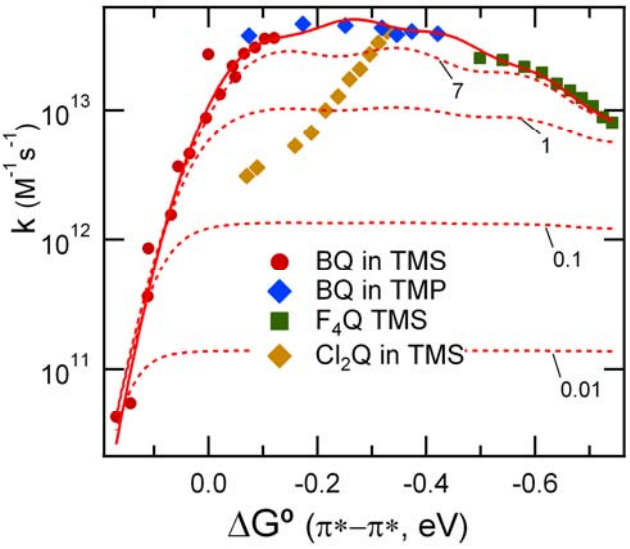

An important issue is which electronic state is formed by electron attachment. Analysis concludes that observable attachment rates to BQ and F_4Q occur only into the *second* π^* orbital. ΔG_o was therefore calculated for electron attachment to form the corresponding π^*-π^* excited states, $BQ^{-\bullet **}$ and $F_4Q^{-\bullet **}$. While excited state energies are uncertain, reasonable estimates are obtained from absorption, excitation and fluorescence spectra of the product radical anions measured here. Consistent with previous results, the n-π^* excited states, $BQ^{-\bullet *}$ and $F_4Q^{-\bullet *}$ appear to play no role in the kinetics. For $BQ^{-\bullet}$ the n-π^* excited state lies 0.5 eV below the π^*-π^* state, so electron attachment to form the n-π^* state would be more exoergic by 0.5 eV. At p=1 bar, where electron attachment to form the π^*-π^* excited state is endoergic by 0.17 eV, the observed rate constant is almost three decades below the maximum. Attachment to form the n-π^* state would have been exoergic by 0.33 eV. With reorganization energies similar to those determined, the rates to form the n-π^* state are predicted to be near the maximum at 1 bar, but the observed rates are much slower, and can be fully accounted for by formation of only the higher, π^*-π^* excited state.

This analysis thus finds that electron attachment to BQ overwhelmingly forms the upper π^*-π^* excited state, consistent with previous results in THF. We attribute the absence of ground state formation to suppression of rate by a Marcus inverted effect by a factor of at least 10^3, due to a nuclear overlap (Franck-Condon) effect. In the case of the n-π^* state, Franck-Condon factors for formation should be nearly optimal, so the absence of a contribution indicates slowing of rates by a factor >10^3 due to a small electronic coupling, H_{ab}. As described by Zamadar, this small H_{ab} may be understood in terms of the two-electron rearrangement in formation n-π^* excited state. Zamadar found several reactions that were slowed by factors >10 due to the need for a coupled transition of a second electron. The present experiments find a factor of 10^3 or larger.

Future Plans:

We have previously reported fast step capture of holes that seems contrary to intuition. Like those for electron capture the mechanism is not clearly identified. The generality of this phenomenon is the subject of future studies. Experiments will utilize both polymers and small molecules in a variety of solvents with different IP's as well as mixtures to shed some light on the mechanism. A consequence of large amounts of hole capture appears to be large amounts of excited states produced from recombination also on very short times scales. This will be further explored.

Efforts will be made to observe electrons and holes attached to aggregates and crystallites, that may simulate the behavior of charges in films. We will also be seeking to investigate production of charges in actual films comprised of or containing conjugated polymers.

Publications of DOE sponsored research that have appeared in the last 2 years:

1. Musat, R. M.; Cook, A. R.; Renault, J. P.; Crowell, R. A. "Nanosecond Pulse Radiolysis of Nanoconfined Water" *J. Phys. Chem. C* **2012**, *116*, 13104-13110. doi:10.1021/jp301000c.
2. Takeda, N.; Miller, J. R. "Poly(3-Decylthiophene) Radical Anions and Cations in Solution: Single and Multiple Polarons and Their Delocalization Lengths in Conjugated Polymers" *J. Phys. Chem. B* **2012**, *116*, 14715-14723. doi:10.1021/jp3096242.
3. Wishart, J. F.; Funston, A. M.; Szreder, T.; Cook, A. R.; Gohdo, M. "Electron Solvation Dynamics and Reactivity in Ionic Liquids Observed by Picosecond Radiolysis Techniques" *Faraday Discuss.* **2012**, *154*, 353-363. doi:10.1039/c1fd00065a.
4. Zaikowski, L.; Kaur, P.; Gelfond, C.; Selvaggio, E.; Asaoka, S.; Wu, Q.; Chen, H. C.; Takeda, N.; Cook, A. R.; Yang, A.; et al. "Polarons, Bipolarons, and Side-by-Side Polarons in Reduction of Oligofluorenes" *J. Am. Chem. Soc.* **2012**, *134*, 10852-10863. doi:10.1021/ja301494n.
5. Cook, A. R.; Bird, M. J.; Asaoka, S.; Miller, J. R. "Rapid "Step Capture" of Holes in Chloroform During Pulse Radiolysis" *J. Phys. Chem. A* **2013**, *117*, 7712-7720. doi:10.1021/jp405349u.
6. Shkrob, I. A.; Marin, T. W.; Hatcher, J. L.; Cook, A. R.; Szreder, T.; Wishart, J. F. "Radiation Stability of Cations in Ionic Liquids. 2. Improved Radiation Resistance through Charge De Localization in 1-Benzylpyridinium" *J. Phys. Chem. B* **2013**, *117*, 14385-14399. doi:10.1021/jp408242b.
7. Zamadar, M.; Asaoka, S.; Grills, D. C.; Miller, J. R. "Giant Infrared Absorption Bands of Electrons and Holes in Conjugated Molecules" *Nat. Commun.* **2013**, *4*, 7. doi:10.1038/ncomms3818.
8. Zamadar, M.; Cook, A. R.; Lewandowska-Andralojc, A.; Holroyd, R.; Jiang, Y.; Bikalis, J.; Miller, J. R. "Electron Transfer by Excited Benzoquinone Anions: Slow Rates for Two-Electron Transitions" *J. Phys. Chem. A* **2013**, *117*, 8360-8367. doi:10.1021/jp403113u.
9. Bakalis, J.; Cook, A. R.; Asaoka, S.; Forster, M.; Scherf, U.; Miller, J. R. "Polarons, Compressed Polarons, and Bipolarons in Conjugated Polymers" *J. Phys. Chem. C* **2014**, *118*, 114-125. doi:10.1021/jp408910a.
10. Bird, M. J.; Reid, O. G.; Cook, A. R.; Asaoka, S.; Shibano, Y.; Imahori, H.; Rumbles, G.; Miller, J. R. "Mobility of Holes in Oligo- and Polyfluorenes of Defined Lengths" *J. Phys. Chem. C* **2014**, *118*, 6100-6109. doi:10.1021/jp5010874.
11. Holroyd, R.; Miller, J. R.; Cook, A. R.; Nishikawa, M. "Pressure Tuning of Electron Attachment to Benzoquinones in Nonpolar Fluids: Continuous Adjustment of Free Energy Changes" *J. Phys. Chem. B* **2014**, *118*, 2164-2171. doi:10.1021/jp412090k.

Ab initio approach to interfacial processes in hydrogen bonded fluids

Christopher J. Mundy
Physical Sciences Division
Pacific Northwest National Laboratory
902 Battelle Blvd, Mail Stop K1-83
Richland, WA 99352
chris.mundy@pnnl.gov

Program Scope

The long-term objective of this research is to develop a fundamental understanding of processes, such as transport mechanisms and chemical transformations, at interfaces of hydrogen-bonded liquids. Liquid surfaces and interfaces play a central role in many chemical, physical, and biological processes. Many important processes occur at the interface between water and a hydrophobic liquid. Separation techniques are possible because of the hydrophobic/hydrophilic properties of liquid/liquid interfaces. Reactions that proceed at interfaces are also highly dependent on the interactions between the interfacial solvent and solute molecules. The interfacial structure and properties of molecules at interfaces are generally very different from those in the bulk liquid. Therefore, an understanding of the chemical and physical properties of these systems is dependent on an understanding of the interfacial molecular structure. The adsorption and distribution of ions at aqueous liquid interfaces are fundamental processes encountered in a wide range of physical systems. In particular, the manner in which solvent molecules solvate ions at the interface is relevant to problems in a variety of areas. Another major focus lies in the development of models of molecular interaction of water and ions that can be parameterized from high-level first principles electronic structure calculations and benchmarked by experimental measurements. These models will be used with appropriate simulation techniques for sampling statistical mechanical ensembles to obtain the desired properties.

This work was done in collaboration with G. K. Schenter and John L. Fulton.

Progress Report

The role of short-range structure in hydrophobic solvation [2]

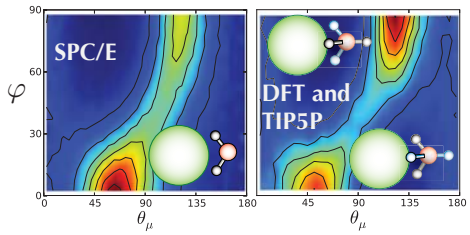

Figure 1: Schematic of the solvation patterns of different water models around a hard sphere [2]. The left panel is SPC/E water and shows only one distinct population for the orientation of water around the hard sphere favoring the configurations consistent with donation of hydrogen bonds. The left panel shows the results of TIP5P and DFT water models where the there is clear population in both donating and accepting configurations.

Here we study the structural and electrostatic consequences of the various broken symmetries that arise from inserting the simplest model of an uncharged ion core, a hard sphere solute of varying radius into water as described by two classical water models, SPC/E and TIP5P, and by state-of the art quantum density functional calculations. We show, the solvent response to a hard sphere (HS) solvation generate special configurations that are particularly sensitive to small differences between donor and acceptor hydrogen bonds and to

local variations in the induced charge density as shown in **Figure 1** [2]. This system provides a stringent test of classical water models in a physically important application where accurate quantum calculations can be carried out to assess their predictions. These results have implications for nonzero ionic charge and needed improvements to the Born model. In our study we derive explicit expressions for the calculation of the potential at the center of the HS cavity due to the structure of water. Thus, the relationship between local hydration structure and the cavity potential provides an important insight into the sensitivity of on hydration free energies to forms of molecular interaction (*e.g.* quantum versus classical). These results in conjunction with our previous studies provide further evidence that the differences in the solvent response to broken symmetries have measurable consequences that can influence the underlying thermodynamics of ions in solution.

Acids in the vicinity of the air-water interface [1,3]

The role of the first solvation shell as an important ingredient for ion adsorption has lead to a unique program at PNNL to determine the accurate local hydration structure of ions using X-ray adsorption fine structure (EXAFS) in conjunction with molecular dynamics (MD) using *ab initio* based interaction potentials. Although there is a theoretical and experimental consensus that ions can be present at the air-water interface, there is no such consensus regarding the self-ions of water (H_3O^+ and OH^-) that comprise acids and bases. Recently we have established the use of *ab initio* based interaction potentials to study hydrochloric acid (HCl) over a variety of concentrations [5]. Our recent joint simulation/experimental study has verified the emergence and experimental assignment of a contracted contact ion pair between chorine and H_3O^+ moiety. This observation and prediction suggests a picture of acids where the chloride anion is not a mere spectator but an active participant in the determination of the activity of the excess proton. In our previous study it was found that the solvation structure of HNO_3 in bulk at high concentrations resembled the interfacial solvation of HNO_3 at low concentrations (*e.g.* isolated molecule). The differences in the local solvation structure between HNO_3 under interfacial and bulk solvation was correlated to the measured degree of dissociation in both environments.

Extensions of the aforementioned work on nitric acid were initiated to explain the observed proton exchange from HCl to DCl in molecular beam experiments on the liquid-air interface of salty glycerol solutions [1]. To this end we performed *ab initio* MD simulations and computed the potentials of mean force (PMF) for acid dissociation of HCl in bulk and in the vicinity of the air-water interface. Our finding, consistent with our previous studies on nitric acid, is that the preponderance of the contracted contact ion-pair between chorine and H_3O^+ in high concentration HCl is observed at low concentrations of HCl in the vicinity of the air-water interface. The abundance of this contracted ion pair at the air-water interface preconditions the likelihood for fast proton exchange as shown schematically in **Figure 2.** Moreover, when the acid is changed to HBr no fast proton exchange is observed. This was also corroborated in our simulations where we found that HBr has little to no propensity to form contact ion pairs and favors reactive channels to complete dissociation.

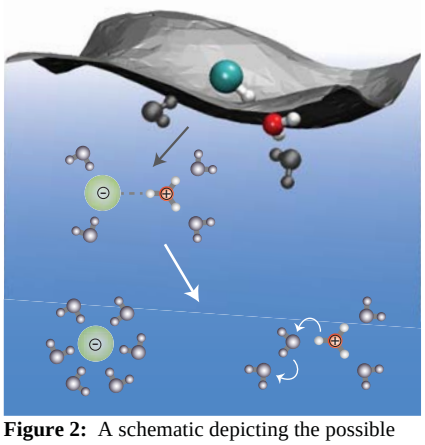

Figure 2: A schematic depicting the possible channels for acid dissociation in the vicinity of the air-water interface [1]

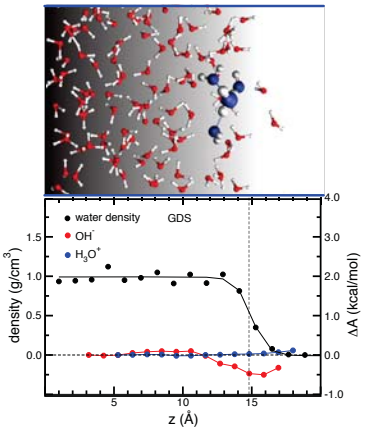

Figure 3: Intrinsic free energies of adsorption for H_3O^+ (blue) and OH^- (red) at the air water interface (black) [3].

Connections of the aforementioned work to our recent study of the intrinsic PMFs of H_3O^+ to the air-water interface[3] can provide clues to understanding the controversial topic of the surface propensity of protons to the air-water interface. Indeed, our intrinsic PMFs indicate that there is no strong driving or repelling force for the isolated H_3O^+ to air-water interface as shown in **Figure 3.** Rather our research suggests a picture where the correlated interactions of the proton and the counter ion must be considered to form a complete picture of acids in the vicinity of the air-water interface. This is distinct from our understanding of the inorganic electrolytes where the independent ion picture seems to hold for concentrations below 1 M.

Future directions

Future research will be extended to elucidation of the solvation and surface properties of more complex anions such as the oxyanions (with G.K. Schenter and J.L. Fulton) such as ClO_3^- and BrO_3^- where both exhibit very interesting behavior in the context of the Hofmeister series. We are currently extending our previous work with John D. Weeks to investigate the charging of hard spheres using *ab initio* interaction potentials. We are using multiple representations of the molecular interaction for water (*e.g.* TIP5P, SPC/E, flavors of DFT) to understand the role of the non-linear structural response to charged hard spheres to separate short- and long-ranged electrostatic response to the free energy of solvation.

Acknowledgements. This work was performed with Yan Levin (Brazil) John D. Weeks (U. Maryland), D.J. Tobias (UC-I), Ilja Siepmann (U. Minn.), and I.-F.W. Kuo (LLNL), Greg Schenter (PNNL), Marcel D. Baer (PNNL), Shawn M. Kathmann, Abe Stern (UC-I), Joost VandeVondele (U. Zurich), Greg Kimmel (PNNL), John Fulton (PNNL), and Roger Rousseau (PNNL). We also acknowledge computer resources from NERSC and a 2008-2012 INCITE award. Battelle operates Pacific Northwest National Laboratory for the US Department of Energy.

Publications with BES support (2012-present):

1. Baer, MD; Tobias, DJ; **Mundy CJ**, "Investigation of Interfacial and Bulk Dissociation of HBr, HCl, and HNO_3 Using Density Functional Theory-Based Molecular Dynamics Simulations," *Journal of Physical Chemistry B*, **DOI**: 10.1021/jp5062896
2. Remsing, RC; Baer, MD; Schenter, GK; **Mundy, CJ**; Weeks, JD, "The Role of Broken Symmetry in Solvation of a Spherical Cavity in Classical and Quantum Water Models," *Journal of Physical Chemistry Letters* **5**, 2767 (2014)
3. Bear, MD; Kuo, I-FW; Tobias, DJ; **Mundy, CJ**, "Toward a unified picture of the water self-ions at the air-water interface," *Journal of Physical Chemistry B* **118**, 8364 (2014)

4. Pluharova, E; Baer, MD; **Mundy, CJ**; Schmidt, B; Jungwirth, P, "Aqueous Cation-Amide Binding: Free Energies and IR Spectral Signatures by Ab Initio Molecular Dynamics," *Journal of Physical Chemistry Letters* **5**, 2235 (2014)

5. Baer, MD; Fulton, JL; Balasubramanian, M; Schenter, GK; **Mundy, CJ**, "Persistent ion-pairing in aqueous hydrochloric acid," (Frontiers Article) *Journal of Physical Chemistry B* **118**, 7211 (2014).

6. Devanathan, R; Idupulapati, N; Baer, MD; **Mundy, CJ**; Dupuis, M, "*Ab initio* molecular dynamics simulation of proton hopping in a model polymer membrane," *Journal of Physical Chemistry B* **117**, 16522 (2013)

7. Tobias, DJ; Stern, AC; Baer, MD; Levin, Y; **Mundy, CJ**, "Simulation and theory of atmospherically relevant aqueous liquid-air interfaces," *Annual Reviews of Physical Chemistry* **64**, 339 (2013)

8. McGrath, MJ; Kuo, I-FW; Ngouana, BF; Ghogomu, JN; **Mundy, CJ**; Marenich, AV; Cramer, CJ; Truhlar, DG; Siepmann, JI, "Calculation of the Gibbs free energy of solvation and dissociation of HCl in water via Monte Carlo simulations and continuum solvation models," *Physical Chemistry Chemical Physics* **15**, 13578 (2013)

9. Stern, AC; Baer, MD; **Mundy, CJ**; Tobias, DJ, "Thermodynamics of iodide adsorption at the instantaneous air-water interface," *Journal of Chemical Physics* **138**, 114709 (2013)

10. Tobias, DJ; Stern, AC; Baer, MD; Levin, Y; **Mundy CJ,** "Simulation and theory of ions at atmospherically relevant liquid-air interfaces," *Annual Reviews of Physical Chemistry* **64**, 339 (2013)

11. Baer, MD and **Mundy, CJ**, "An *ab initio* approach to understanding the specific ion effect," *Faraday Discussions* **160**, 89-101 (2013)

12. Baer, MD; Stern, AC; Levin, Y; Tobias, DJ; **Mundy, CJ**, "Electrochemical Surface Potential Due to Classical Point Charge Models Drives Anion Adsorption to the Air-Water Interface," *Journal of Physical Chemistry Letters* **3**, 1948-7185 (2012)

13. Kimmel, GA; Baer, M; Petrik, NG; VandeVondele, J; Rousseau, R; **Mundy, CJ**, "Polarization and Azimuth-Resolved Infrared Spectroscopy of Water on TiO_2(110): Anisotropy and the Hydrogen-Bonding Network," *Journal of Physical Chemistry Letters* **3,** 1948-7185 (2012)

DYNAMIC STUDIES OF PHOTO- AND ELECTRON-INDUCED REACTIONS ON NANOSTRUCTURED SURFACES - *DE-FG02-90ER14104*

Richard Osgood,
Center for Integrated Science and Engineering, Columbia University, New York, NY 10027, Osgood@columbia.edu

Progress Report

Program Scope or Definition:

Our current research program examines the photon- and electron-initiated reaction mechanisms, half-collision dynamics, and other nonequilibrium-excited dynamics effects, occurring with excitation of adsorbates on well-characterized metal-oxide and nanocrystal surfaces. In order to explore these dynamics, our program has developed new synthesis methods for uncapped nanocrystals *with specific reconstructions and orientation in situ* in a UHV STM instrument. To identify these nanocrystals and their structure, our program utilizes a new technique developed in our lab, which enables STM nanocrystallography. The technique uses tunneling from the tip of our STM or an *in situ* flood UV lamp to excite adsorbate molecules at specific sites in these nanocrystals. The resulting chemistry and surface dynamics are investigated via imaging of the reaction fragments in the vicinity of the reaction sites.

Our recent experiments have been directed toward electronic-tunneling reactions involving a series of linear aromatics on rutile TiO_2(110) surfaces (although we have recently examined other iron-oxide surfaces), as well as exploration of the unexpected "inverse" catalytic activity of uncapped TiO_2 nanocrystals, with known atomic structure, on single-crystal Au. Our adsorbate molecules have been chosen to enable thermal and tip-induced studies of physisorbed molecules at room temperature [1,2]. In addition, our experiments have included preliminary studies of the tip-induced dynamics from a single TMMA molecule. This acid molecule was chosen since it is known to exhibit light-induced chemistry on TiO_2; note that its light induced chemistry has been examined extensively in experiments at PNNL. During this last year, our program has included a study of the reactivity and structure of TMMA molecules on nanocrystal TiO_2 on Au(111), stress-induced chemistry of H and H_20 on nanopatterned TiO_2, and initial studies of deuterated CH_3OH on TiO_2.

Recent Progress:

STM studies of photoreactions on supported single-crystal & single-nanocrystal TiO_2.

In order to establish the dynamics of light-induced reactions on TiO_2 surfaces that could serve as a platform for more complex studies of single-molecule electron-induced reactions, a series of experiments have been carried out, in which surfaces with adsorbed target molecules were controllably exposed to photon-energy-tuned UV light. Trimethyl acetic acid (TMAA) was chosen as a model photoreaction active molecule due to its ease of handling and the existence of numerous prior studies of its photoreactivity, including studies at other DOE Labs. UV doses were administered from a Xe-Hg arc lamp, light from, which was spectrally narrowed with a UV monochromator and focused onto the

sample inside our STM stage. An optical power density of ~5 mW/cm^2 could be achieved on the surface of the sample. This experimental arrangement allowed us to image the same area of the sample before and after a dose of UV radiation. The photoreactivity of TMAA on the surfaces of either a single-crystal rutile(110) or a TiO_2 nanocrystal sample, grown on a Au(111) substrate was explored.

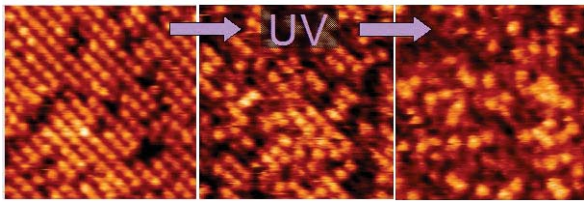

Fig 1: 10 × 10 nm STM images of a TiO_2 rutile(110) surface with near-saturation coverage of TMAA molecules (left) and after consecutive doses of 300 nm UV light

Figure 1 shows a series of STM images of the same bulk single-crystal TiO_2(110) surface with a saturation coverage of TMAA (~0.5 ML) before and after consecutive 5 and 10min doses of UV light, having a 15nm bandwidth centered at λ = 300 nm. Individual TMAA molecules are clearly visible in the images, thus allowing measuring their areal density simply via direct "counting" of the molecules in a known area. Thus the molecular desorption rates could be measured from these images. Using this approach, a 4 × 10^{-5} quantum efficiency of this light-induced process was measured at this wavelength. However, the identical experiment with 360 nm wavelength UV light did not show noticeable desorption even after a 4.5-hour dose. While photolysis of TMAA on the TiO_2(110) surface is a well-studied reaction, our experiments are the first spectrally resolved measurements that directly demonstrate hole-mediated dynamics of this photoreaction. Indeed, the energy of λ = 360 nm photons is well above the TiO_2 bandgap and such light is readily adsorbed in TiO_2 bulk. However, the characteristic adsorption depth for 360 nm light is about 250 nm, which is much greater than diffusion range of holes in TiO_2 (10 nm) thus explaining negligible reaction rates. In comparison, adsorption depth for 300 nm light is about 12 nm, thus allowing a measurable photoreaction rate to be determined.

In addition, single-site resolved TMAA photolysis experiments have been performed with TiO_2 nanocrystals prepared on the Au(111) substrate through the procedure, developed earlier in our group. This procedure leads to formation of 10 – 30 nm wide and 1 – 3 nm tall crystallites with predominantly the rutile (100) crystallographic orientation on the top face. Since this was the first study of TMAA interaction with TiO_2 nanocrystals, the initial experiments explored the adsorption state of TMAA on the nanocrystals. Using both STM imaging and temperature programmed desorption (TPD) spectroscopy, our experiments established that TMAA readily adsorbs on the surfaces of TiO_2 nanocrystals at room temperature with the local surface density of the adsorbed molecules being comparable to that on the single-crystal rutile(110) surface. The adsorbed molecules follow a nearly identical thermal decomposition pattern on nano-TiO_2 and rutile(110) with the important exception being that nanocrystals of TiO_2 generate more hydrogen-depleted products compared to bulk single crystal rutile(110).

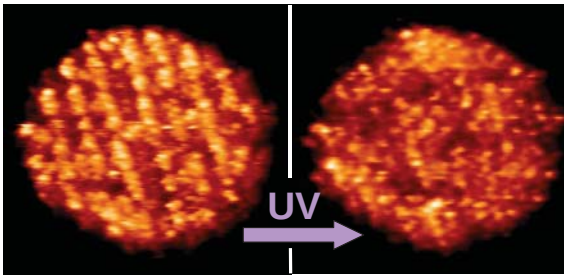

Fig. 2: 25 × 25 nm STM images on TMAA-covered TiO_2 nanocrystal on Au(111) substrate before (left) and after (right) a dose of 300nm UV light.

One example of a photoreaction experiment for TMAA on a nano-TiO_2/Au(111) surface is shown in **Fig. 2**. The left STM image shows a TMAA-saturated 20nm-wide TiO_2 nanocrystal and the left image shows the same nanocrystal after a 15min exposure to 300nm UV light. The light-induced desorption is evident from the molecular surface density in the images and counting of individual molecules suggests that ~50% of the initially adsorbed TMAA molecules have been removed by irradiation. This result was further supported by independent TPD experiments when the TPD spectra from as-prepared and UV-irradiated TMAA/nano-TiO_2/Au(111) surfaces were collected. The comparison of the corresponding TPD peak areas confirmed ~50 % depletion of TMAA molecules resulting from UV irradiation. Interestingly, this percentage appears to be the limiting extent of the photoreaction and higher doses of UV light did not result in further TMAA desorption. To the best of our knowledge, this is the first atomically-resolved study of any photo-induced reaction on the surfaces of TiO_2 nanocrystals.

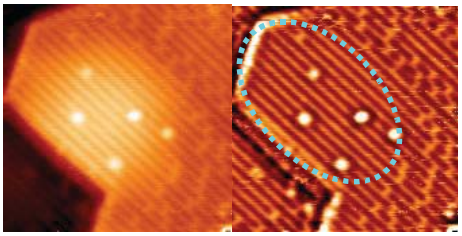

Fig. 3: Two STM images showing absence of oxygen vacancies, V_o, in strained region above a subsurface Ar cluster; features due to V_o appear as lighter streaks against the brown background in the right image. Bright spots are surface impurities

Catalytic studies on iron-oxide surfaces.

In order to expand our oxide substrate capability, our group begun to examine processes on Fe_3O_4(111) surfaces – a collaboration with the Flynn Group and the Flytzani-Stephanopoulos Group at Tufts[3]. In particular, our group chose to study the surface reactivity of deuterated methanol, which is of interest for fuel-cell applications. The unique combination of STM and TPD capabilities of our experimental chamber allowed us to relate specific reactivity patterns to different surface phases of Fe_3O_4(111) that included Fe_2O_3(0001) and FeO(111). These phases were formed by varying the sample preparation conditions; the phases could be easily distinguished in the STM images. Methanol species were observed to be dissociatively adsorbed only on the Fe-terminated Fe_3O_4(111) surface and physisorbed on the O-terminated FeO(111) and bi-phase surfaces. Methanol is first dissociated into methoxy (CD_3O) attached to surface terminating Fe sites and D-atom atop the under-coordinated oxygen sites of Fe_3O_4(111). A fraction of these surface species then recombined to desorb as molecular methanol (CD_3OD) from the surface at 365 K. Methoxy (CD_3O) is further dissociated into formaldehyde (CD_2O) and D-atoms at higher temperatures. The gas-phase formaldehyde (CD_2O) and methanol molecules recombinatively desorb from the surface at 635 K. In general, the reaction of methanol on the iron-oxide surface has shown high sensitivity to atomic-level surface reconstructions.

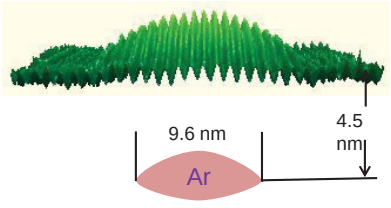

Fig. 4: 3D cross-sectional figure combining STM images taken before explosive removal of the TiO_2 lid above buried Ar cluster and schematic sketch of cluster.

Stress-Induced Reactivity on Oxide Surfaces.

Our Group has recently demonstrated the use of nanoscale local strain to control surface reactions on oxide surfaces [5,6]. This research uses STM imaging in a UHV environment to show that this strain locally alters reactivity of the surface. Our experiments used a nanoscale template of extremely small, buried-atom Ar clusters to provide

nm-scale strain in near-surface layers of metal oxides.

The experiments showed that local (i.e. atomic scale) stress in TiO_2 layers results in a change in the reactivity of that surface and that this change may be used in conjunction with reactions of adsorbate molecules to change the surface composition and thus promote local etching, functionalization, or growth. This effect is shown in the image in **Fig 3**. In particular, a clean, bare surface of reduced TiO_2(110) has atomic rows of five-fold coordinated Ti and bridging O, appearing light and dark in the STM image. Some surface O atoms are missing, creating oxygen vacancies V_O that appear as bright point features between neighboring bright rows. It is then possible to use a low-energy (i.e. 1-2 kV) ion beam in combination with high-temperature annealing to implant nm-scale clusters of Ar atoms beneath the sample's surface. In the vicinity of the buried Ar blister, the atomic layers are deformed upward and a local strain field is established. Within this strain field oxygen vacancies are eliminated, apparently due to the higher binding energy of oxygen in the strained region; this effect is shown clearly by comparing the regions within and outside of the blue circle surrounding the implanted cluster in **Fig. 3**. It is also possible to control or vary the strain field above such blisters via several experimental parameters including temperature and ion flux.

In order to explore the nature of the buried Ar clusters, extensive research was made, including STM-probe-tip- controlled nanoetching, combined with numerical simulation of mechanical deformation of TiO_2 around buried clusters, to determine the magnitude and directionality of the surface strain. Thus an important component to our work has been to develop the experimental techniques to use STM to probe the dimensions of our strained nanoregions shown in **Fig. 4**. For this we used short +8V voltage pulses from the STM tip to cause "rupture" of clusters that left up to 11 nm deep craters on the surface. The conclusion of the study has been that argon forms near-surface horizontal cracks in the volume of TiO_2 filled with highly pressurized solid argon. The values of surface strain induced by these pockets of Ar have been calculated to reach 3% - the values well outside of the limits of the macroscopic sample-deformation experiments and allow direct observation of the effects of strain on surface reactivity. *Due to its potential as a method for achieving nanoscale pattering we have now initiated a new program, funded by NSF DMR to support the patterning aspect of this work.*

Recent Grant-Sponsored Publications

1. D. V. Potapenko, N. Choi, and R.M. Osgood, Jr., "Adsorption Geometry of Anthracene and 4-Bromobiphenyl on TiO_2(110) Surfaces." J. Phys. Chem. 114, 19419 (2010)
2. D. V. Potapenko, Z. Li, R. Osgood, "Dissociation of single 2-chloroanthracene molecules by STM-tip electron injection." J. Chem. Phys. 116, 4679 (2012)
3. Z. Li, D. V. Potapenko, K. T. Rim, M. Flytzani-Stephanopoulos, G. W. Flynn, R. M. Osgood, X-D. Wen, E. R. Batista, "Catalytic studies on iron-oxide surfaces: Reactions of fully deuterated methanol (CD_3OD) on Fe_3O_4(111)" (Submitted J. Phys. Chem.)
4. D.V. Potapenko, Z.Li, Y. Lou, R. M. Osgood Jr.," 2-Propanol Reactivity on I*n Situ* Prepared Au(111)-Supported TiO_2 Nanocrystals." J. Catal. 297, 281-288 (2012)
5. D. V. Potapenko, Z. Li, J. W. Kysar, R. M. Osgood, "Nanoscale strain engineering on the surface of a bulk TiO_2 crystal." (In review, Nano Letters)
6. Z. Li, D. V. Potapenko, R. M. Osgood, "Controlling surface reactions with elastic strain in nanometer regions." (Submitted, ACS Nano)

Studies of surface adsorbate electronic structure and femtochemistry at the fundamental length and time scales

Hrvoje Petek
Department of Physics and Astronomy and Chemistry
University of Pittsburgh
Pittsburgh, PA 15260

Our research focuses on the electronic structure and dynamics of solids, their surfaces, and molecule covered surfaces. We are interested in dynamical surface processes initiated by optical excitation or chemical stimulation. The correct description of surface electronic structure, surface optical processes leading to photoexcitation, interfacial charge transfer, energy and momentum relaxation of carriers, and femtochemistry is essential for description of surface phenomena such as photovoltaic and photocatalytic energy conversion. Here we report the experimental results on femtosecond time-resolved multi-photon photoemission (TR-MPP) and low-temperature STM studies of electronic surfaces and interfaces.[1-8]

Multidimensional photoelectron spectroscopy. Multidimensional electronic and vibrational spectroscopies are emerging as powerful means to study coherent phenomena in condensed matter. In the past year we have developed 3D photoelectron spectroscopy as a means for studying coherent dynamics at the solid/vacuum interface. Imaging photoelectron energy (E) and momentum (k) distributions as the delay between two identical <15 fs pump and probe pulses is advanced in 100 as steps provides information on the coherent polarization dynamics that drive a multiphoton process. Fourier transforms (FT) of 3D (E, k, t) movies reveal the dominant coherent polarization components that define the outcome of an MPP process. We have applied the technique to the coherent dynamics in silver and copper.

Transient excitons at Ag(111) surface. In three photon photoemission (3PP) process from the Shockley surface state (SS) of Ag(111) via the n=1 image potential (IP) state, we observe evidence for formation of an excitonic state.[9] The dispersive SS and IP states observed in nonresonant process are overwhelmed by a nondispersive feature that appears near the SS-IP two-photon resonance. The non-dispersive spectrum is a signature of a localized state formed by

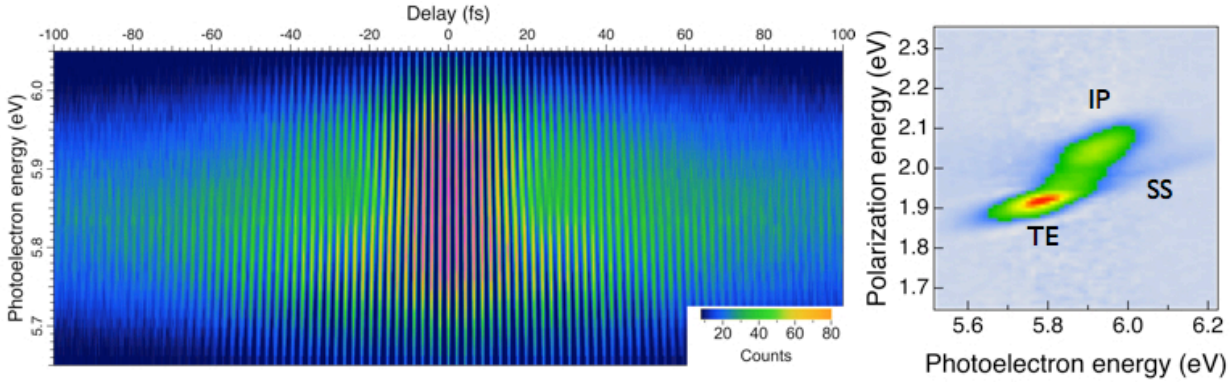

Figure 1. *a) The interferogram for normal emission form Ag(111) extracted from a 3D movie of 3PP, which measures the coherent polarization dynamics excited with 2.05 eV light. b) the 2D photoelectron spectrum (induced polarization vs photoelectron energy. The IP state is emitted by the external field, whereas the TE oscillates at ½ the SS to IP state resonant frequency.*

exciting an electron from the SS. The transition moment enhancement and participation of the entire SS band is consistent with the assignment to an exciton composed of a surface electron interacting with the SS hole; however, by definition a metal cannot support a bound state of the Coulomb potential. We explain the excitonic state as a transient in the excitation process where the primary excitation creates and electron-hole pair interacting through the bare Coulomb potential, whereupon charge density fluctuations evolve this transient to the asymptotic, fully screened surface electron, in other words, the image potential state. This transient exciton (TE) evolution is captured on Ag(111) surface due to its relatively slow screening.

As an example of multidimensional MPP in Fig. 1a we show the interferogram for normal emission ($k_{||}$=0) obtained by scanning the delay between the pump and probe pulses in 100 as intervals and its FT. The fringes in the interferogram indicate that upon 2.04 eV photon excitation the coherent polarization in Ag(111) surface persists for tens of fs for certain *E* and *k*, even though we expect that the coherent response of metals, e.g. reflection of light, to be essentially instantaneous. FT of the interferogram indicates that the dominant component of the coherent polarization oscillates at the frequency of the SS-IP two-photon resonance rather than that of the laser driving field. The photoemission of the IP state, however, is driven at the laser frequency, because the IP state is the delayed consequence of saturation of screening. Based on the 2D spectra in Fig. 1b we conclude that the external driving field of the laser excites local fields (coherent polarization) associated with the SS-IP two-photon resonance. The local fields, which fluctuate on the atomic scale, couple to the MPP process more efficiently than the external field, and therefore dominate the 2D spectra. The analysis of the photoemission yield with *E, k,* and *t* resolution thus a differential picture of the coherent response of a Ag. Because screening is universal, the transient exciton dynamics observed for Ag should also play a role in the transient regime of other materials (molecules, semiconductors), which support bound excitons.

Polaritonic multiphoton photoemission in copper. The excitonic photoemission in Ag begs the question whether this is a common feature of metals. The answer is yes and no. Analogous TR-MPP measurements on Cu(111) surface show no evidence for an excitonic intermediate state. This is expected on account of the more efficient screening in Cu, which limits the transient exciton regime to the sub-femtosecond time scale. Nevertheless, MPP from Cu(111) surface

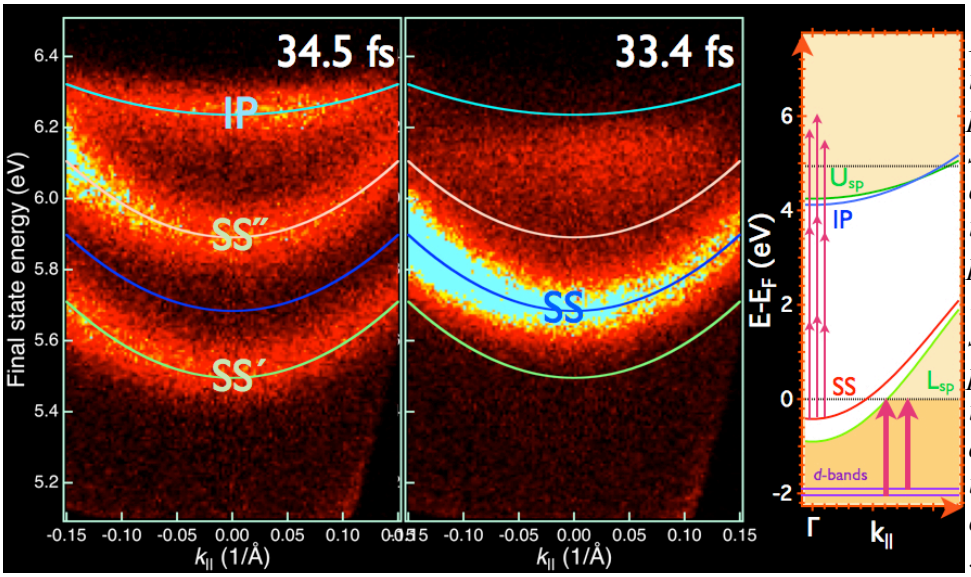

Figure 2. *Two images from a 3D photoemission movie showing the main and satellite SS images for different pump-probe delays. The band structure shows the dominant polarization excited in the sample due to d-band to E_F transitions, which contributes to the 3PP process.*

indicates that polarization associated with the *nonresonant* excitation from the SS of Cu(111) persists on >15 fs time scale, whereas energy-time uncertainty would demand that the polarization decay time of a nonresonant transition should decrease inversely with the energy detuning from a real resonance (<1 fs in the performed experiments). Considering the local fields excited in Cu upon visible light absorption solves this conundrum.

Interband transitions dominate the optical response in Cu above the threshold for d- to sp-band excitation at 2 eV. In MPP experiments with >2 eV photons monitoring the signal from SS on Cu(111) surface the dominant polarization excited in the sample is that of the interband transitions. At the threshold for excitation from the top of the d-bands to the crossing of the sp-band with the Fermi level (~2 eV), the dephasing of the coherent polarization due to carrier-carrier scattering is expected to be slow because of phase space constraints. Therefore, the slow dephasing allows strong local polaritonic fields associated with the interband polarization to build up in the course of ultrafast excitation. Together with the external field, these local fields 3PP from the SS of Cu(111). This is evident in experiments where we record 3PP spectra and TR-MPP movies at the d- to sp-band threshold. The spectra show a tripling of the SS band seen in two frames from a TR-2PP movie (Fig. 2a). The main SS band is accompanied by two satellites representing 3PP by the external field and the induced polaritonic local fields associated with the *d*-band for E_F excitation (Fig. 2). The polaritonic contribution to 3PP in Cu is general and should affect optical absorption in solid state systems whenever interband transitions can be excited resonantly. Although the concept of local fields is implicit in the theories of dielectric response, its implications in energy transductions processes is essentially unexplored.[10]

CO_2 capture by metal-organic chains. By means of low-temperature STM, we have studied the CO_2 capture on Au surfaces.[10] On bare Au surfaces CO_2 molecules are physisorbed and cannot be imaged even at 5K. Continuing our studies of 1D surfaces, we have explored the interactions of CO_2 molecules with self-assembled chains of Au adatoms and 4-phenylene diisocyanide (PDI) molecules, $[\text{-Au-PDI-}]_n$. The Au-PDI chains form upon adsorbing PDI molecules onto Au(111) and Au(100) surfaces at 300 K. The chains form ordered parallel arrays with a minimum ~1.4 nm spacing most likely due to interchain repulsion (Fig. 3a). Upon CO_2 adsorption, even for sparse chain arrays with several nm spacing, the chains collapse into tight bundles with a ~1 nm spacing (Fig. 3b). High-resolution imaging shows that CO_2 molecules become sandwiched between two Au-PDI chains in ordered, single molecule wide ranks (Fig. 3c).

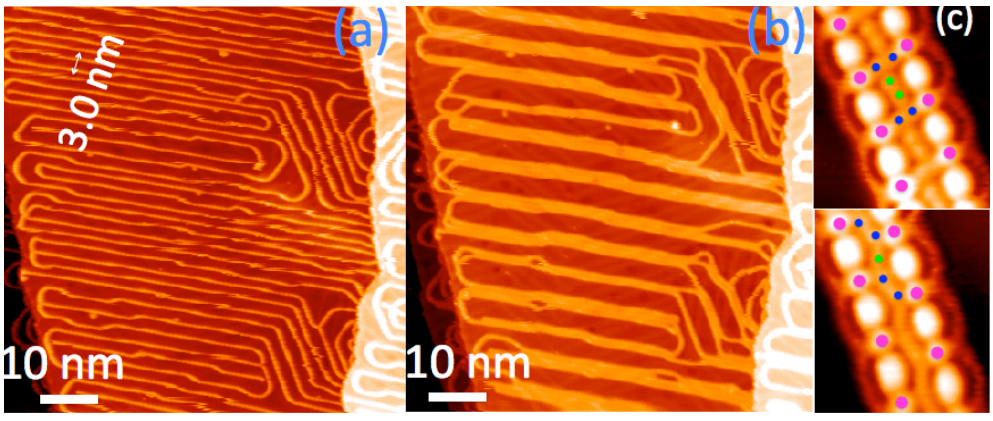

Figure 3. *a) Au-PDI chains on Au(111) surface at low coverage and 77K. b) The same surface after exposure to CO_2 gas. The Au-PDI chains coalesce into bundles. c) High resolution images of two Au-PDI chains sandwiching CO_2 molecules. Pink dots indicate Au atoms, blue the chemisorbed CO_2, and green physisorbed CO_2. The halos are loosely bound peripheral CO_2.*

STM imaging at 5K reveals that the CO_2 capture is seeded by CO_2 chemisorption at Au adatom seeding sites. The chemisorption of CO_2 molecules at low coverages is confirmed by vibrational spectroscopy and XPS measurements, which confirm the presence of reduced CO_2 molecules and low coverages. As the CO_2 coverage is increased, other CO_2 molecules cluster around these seeding sites until a full monolayer of CO_2 molecules in between Au-PDI chains is formed. We plan to use the Au-PDI chains as a platform for studying CO_2 capture and reduction.

Molecular electronic level alignment on metals. Electronic level alignment for molecules on metals controls many interfacial phenomena. How the intrinsic properties of the interacting systems define the electronic structure of their interface remains one of the most important problems in molecular electronics and nanotechnology. We address this fundamental problem through experimental and computational studies of molecular electronic level alignment of thin films of C_6F_6 on noble metal surfaces. The unoccupied electronic structure of C_6F_6 is characterized with single molecule resolution using low-temperature scanning tunneling microscopy and spectroscopy. The experiments are performed on Cu and Au surfaces with different work functions and distinct surface-normal projected band structures. In parallel, the electronic structure of the quantum wells (QWs) formed by LUMO state of C_6F_6 monolayer and multilayer films and their alignment with respect to the vacuum level of the metallic substrates are calculated by solving the Schrödinger equation for a semiempirical one dimensional (1D) potential of the combined system using input from density functional theory. Our analysis shows that the level alignment for C_6F_6 molecules bound through weak van der Waals interaction to noble metal surfaces is primarily defined by the image potential of metal, the electron affinity of molecule, and the molecule surface distance. We expect the same factors to determine to the interfacial electronic structure for a broad range of molecule/metal interfaces.

DOE Basic Energy Sciences Sponsored Publications 2012-2014

1 Feng, M., Lin, C., Zhao, J., & Petek, H. Orthogonal Intermolecular Interactions of CO Molecules on a One-Dimensional Substrate. *Annu. Rev. Phys. Chem.* **63**, 201-224 (2012).

2 Dougherty, D.B. *et al.* Band Formation in a Molecular Quantum Well via 2D Superatom Orbital Interactions. *Phys. Rev. Lett.* **109**, 266802 (2012).

3 Lin, C. *et al.* Theory of orthogonal interactions of CO molecules on a one-dimensional substrate. *Phys. Rev. B* **85**, 125426 (2012).

4 Petek, H. Photoexcitation of adsorbates on metal surfaces: One-step or three-step. *J. Chem. Phys.* **137**, 091704-091711 (2012).

5 Feng, M. *et al.* Energy stabilization of the s-symmetry superatom molecular orbital by endohedral doping of C_{82} fullerene with a lanthanum atom. *Phys. Rev. B* **88**, 075417 (2013).

6 Winkelmann, A. *et al.*, Ultrafast multiphoton photoemission microscopy of solid surfaces in real and reciprocal space in *Dynamics of interfacial electron and excitation transfer in solar energy conversion: theory and experiment*, P. Piotrowiak, ed. (Royal Society of Chemistry, Cambridge, 2013).

7 Petek, H. Single-Molecule Femtochemistry: Molecular Imaging at the Space-Time Limit. *ACS Nano* **8**, 5-13 (2014).

8 Zhao, J. *et al.* Molecular Electronic Level Alignment at Weakly Coupled Organic Film/Metal Interfaces. *ACS Nano* **ASAP** (2014).

9 Cui, X. *et al.* Transient excitons at metal surfaces. *Nat Phys* **10**, 505-509 (2014).

10 Feng, M., Sun, H., Zhao, J., & Petek, H. Self-Catalyzed Carbon Dioxide Adsorption by Metal–Organic Chains on Gold Surfaces. *ACS Nano* **8**, 8644-8652 (2014).

Ultrafast electron transport across nanogaps in nanowire circuits

Eric O. Potma

Department of Chemistry
University of California, Irvine
Irvine, CA 92697
e-mail: epotma@uci.edu

Program Scope

In this Program we aim for a closer look at electron transfer through single molecules. To achieve this, we use ultrafast laser pulses to time stamp an electron tunneling event in a molecule that is connected between two metallic electrodes, while reading out the electron current. A key aspect of this project is the use of metallic substrates with plasmonic activity to efficiently manipulate the tunneling probability. In the first phase of this program we developed highly sensitive tools for the ultrafast optical manipulation of tethered molecules through the evanescent surface field of plasmonic substrates. In the second phase of the program we use these tools for exercising control over the electron tunneling probability.

Recent progress

During Year I and II of this project, we have unambiguously shown that surface plasmon polarition (SPP) excitations can be used to carry out precise nonlinear optical manipulations of molecular systems at designated target sites.[1, 2, 3, 4] The ability to control the density and duration of the electric field at the target site is crucial for performing light-induced tunneling events through molecules. In Year III we have rebuilt our ultrafast microscope, including the construction of a custom designed optical parametric oscillator and the assembly of ultra-sensitive electronics for light-induced current measurements. In Year IV we have perfected the design and fabrication of reproducible nano junctions consisting of gold electrodes on silica substrates through a combination of lithography and focus ion beam milling. During Year V, we have completed our SPP-induced electron tunneling experiments in nanometer-scale junctions.

This report summarizes the advances made during Year V. We have made the following advances:

- Experimental demonstration of light-controlled electron current across nanometer-sized junctions. We have shown that light-induced electron tunneling can be accomplished in nm-sized junctions in a controllable fashion. The electron currents are stable and reproducible at ambient temperatures and pressures.
- Mechanism of electron current across nm junctions. Electron tunneling typically occurs in sub-nm junctions. For much larger junctions, the mechanism of field emission is prevalent. In nm-sized junctions, however, an intermediate regime exists where a transition from tunneling to field emission can be observed. We have characterized the mechanism of electron transport in this regime.

Below we highlight some of the details and implications of these achievements:

Experimental demonstration of light-controlled electron current across nanometer-sized junctions
Previously, in Year IV, we had developed a method for fabricating nanometer-sized junctions between two gold electrodes using a combination of lithography, focused ion beam milling and electromigration. We have fabricated nano junctions in the 4 nm to 15 nm range. Light-induced tunneling is accomplished by launching a SSP wave at a distance ~ 10 μm from the nano-junction. The SPP wave is propagating across the junction, while modulating the electric field. The electric field modulation gives rise an alternate current across the junction at the optical frequency of the SPP wave. This optical ac modulation forms the driving force for a dc current. The basic layout of the experiment is shown in Figure 1.

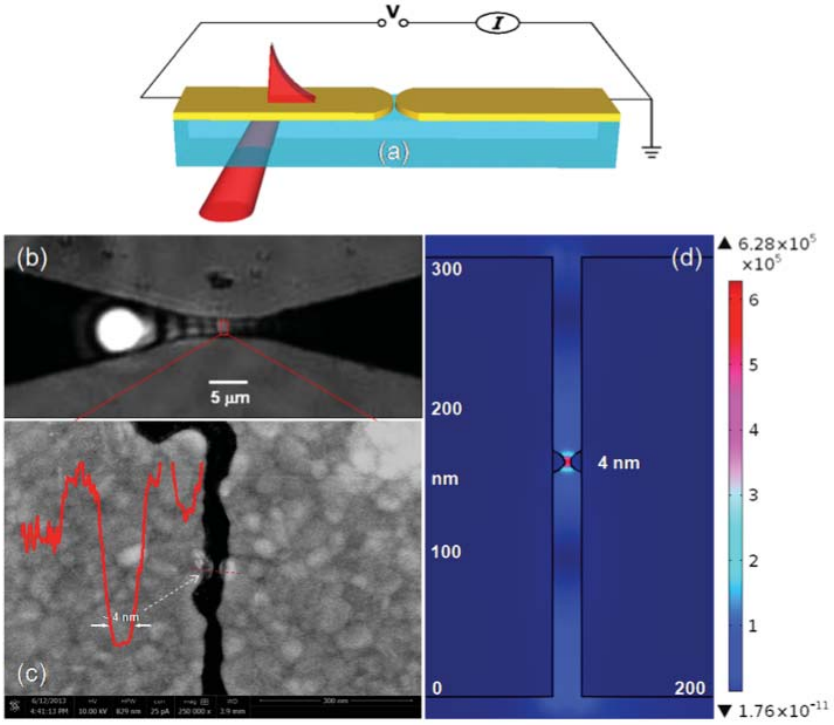

Figure 1: (a) Basic scheme for measuring the SPP induced current. (b) Nanojunction prepared by partial FIB milling and electromigration. (c) The smallest gap size at the closest point in the junction is 4 nm. (d) Simulation of the electric field amplitude in the junction. Highest fields are found at the protrusions of closest proximity.

Figure 2 shows the electron current across the gap as a function of laser power. The current increases with higher illumination power. For a 12 nm gap, the profile is indicative of field emission of electrons. This process occurs when the field amplitude in the junction is high enough to significantly bend the potential, allowing electrons to tunnel to the altered barrier. The field emission process is independent of the size of the junction. For smaller gaps, like the 4 nm gap shown in red, a different profile is observed. The different dependence of the current with laser power reflects the transitional regime from field emission to electron tunneling.

Mechanism of electron current across nm junctions
We have developed a model for electron transport across nm-scale junctions. The model retrieves

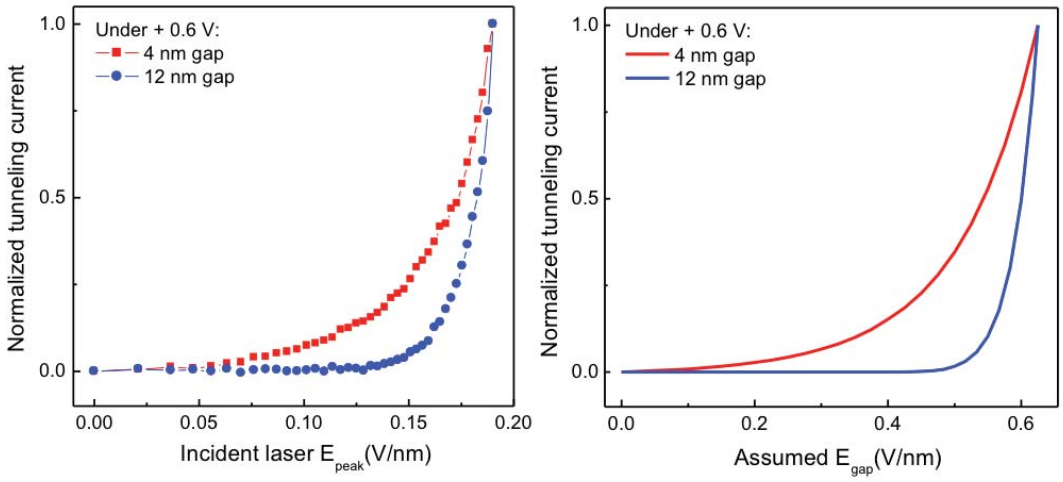

Figure 2: Dependence of electron current measured across a nano-junction as a function of laser field amplitude. Left panel: experiments for a 4 nm and a 12 nm gap. Right panel: simulations based on image potentials under the influence of ac modulation at optical frequencies. The difference between the 4 nm and the 12 nm is qualitatively reproduced.

Fowler-Nordheim type field emission in the large junction limit while predicting Tien-Gordon type rectification in the small junction limit. Importantly, this model is capable to explain electron currents in the intermediate regime between electron tunneling (<1 nm) and field emission, a regime not studied before. We observe that in gaps smaller than 5 nm, light can induce rectifying currents, where the magnitude of the current scales roughly linearly with the power of the incident light. Rectifying tunneling currents have been observed in sub-nm gaps, but have not been seen before in gaps larger than a nm. Our model establishes that for gaps smaller than 5 nm, the image potential is sufficiently bent in the presence of weak ac fields to allow linear rectification to occur. This new mechanism explains why efficient electron currents in sub 5 nm gaps can be observed. Electron currents in this regime are important, as junctions in this limit can be reliably fabricated with modern ion milling techniques. This regime is also relevant to chemistry, where junctions with bridging molecules are typically in the nm regime.

Future Plans

During Year IV and V, we have accomplished our goal of controlling electron tunneling currents across engineered nano-gaps with femtosecond light pulses. We are now in a position to use our scheme for controlling the flow of electrons through a molecule that bridges the gap. In this last phase of the program, we have focused our efforts on incorporating DNA molecules into the nano-circuit. We have chosen an approach that makes use of pre-engineered DNA between two 30 nm gold nano-beads. The nano-bead system can be placed across a junction formed by two gold electrodes. When there is contact between the gold bead and the electrode, currents can flow through the DNA. We are currently optimizing this assay.

Publications with acknowledged DOE support:

[1] Y. Wang, X. Liu, D. Whitmore, W. Xing, and E. O. Potma, "Remote multi-color excitation using femtosecond propagating surface plasmon polaritons in gold films," *Opt. Express* **19**, 13454–13463 (2011).

[2] X. Liu, Y. Wang, and E. O. Potma, "Surface-mediated four-wave mixing of nanostructures with counterpropagating surface plasmon polaritons," *Opt. Lett.* **36**, 2348–2350 (2011).

[3] Y. Wang, X. Liu, A. R. Halpern, K. Cho, R. M. Corn, and E. O. Potma, "Wide field, surface-sensitive four-wave mixing microscopy of nanostructures," *Appl. Opt.*, **51** 3305–3312 (2012).

[4] X. Liu, Y. Wang, and E. O. Potma, "A dual-color plasmonic focus for surface-selective four-wave mixing," *Appl. Phys. Lett.* **101**, 081116 (2012).

[5] J. Brocious and E. O. Potma, "Lighting up micro-structured materials with four-wave mixing microscopy," *Materials Today* **16**, 344-350 (2013).

Interfacial Chemistry between Gas-Phase Molecules and GaAs Surfaces Probed by Near-Ambient Pressure X-ray Photoelectron Spectroscopy

Sylwia Ptasinska

Radiation Laboratory and Department of Physics, University of Notre Dame

The elucidation of interactions between air components and surfaces at the atomic scale is crucial for a comprehensive picture of many physical, chemical and technological processes. Due to the importance of Ga-based semiconductors in photoelectrochemical solar cells, we have focused recently on a developing a fundamental understanding of the surface interaction between GaAs and common gaseous molecules. In the present studies, Near-Ambient Pressure X-ray Photoelectron Spectroscopy was used to track the evolution of surface chemistry at elevated pressures and elevated temperatures. The obtained spectra revealed the nature of the molecular interactions and allowed the detection of changes in the electronic structure of surface Ga, As and O atoms under the reaction conditions.

Water adsorption onto a GaAs(100) surface exhibited a strong dissociation with simultaneous oxygenation and hydroxylation of surface Ga atoms with an increase in H_2O pressure at room temperature. While oxygen interaction with the GaAs surface induced dynamic oxidation processes, which involved the formation of gallium oxides (i.e., Ga_2O and Ga_2O_3) with an increase of O_2 pressure and/or temperature, as well as arsenic oxides, the latter mainly following an increase of temperature. Two other oxidants, N_2O and NO were also investigated under near-ambient conditions. Based on changes in the photoelectron spectra, the extent of surface oxidation due to the dissociative adsorption of oxidants was in the order of $NO>O_2>N_2O$, at higher pressures and at room temperature. While at higher temperatures and elevated pressures, this extent was in the order of $O_2>NO>N_2O$.

Richard J. Saykally; Department of Chemistry, University of California *and*
Chemical Sciences Division, Lawrence Berkeley National Laboratory
Berkeley, CA 94720-1460
saykally@berkeley.edu *http://www.cchem.berkeley.edu/rjsgrp/index.html*

Spectroscopy of Liquids and Interfaces

Program Scope or Definition

The goal of this project is to explore, develop, and apply novel methodologies for atom-specific characterization of liquids, solutions, and and their interfaces, employing combinations of liquid microjet technology with synchrotron X-ray and Raman spectroscopies, and to apply nonlinear optical spectroscopy and close connection with state-of-the-art theory for characterization of electrolyte interfaces, seeking to establish the general principles that govern interfacial behavior and of liquid-vapor and solid-liquid interfaces and fundamental processes such as evaporation and surface adsorption.

Recent Progress

Towards a Complete Molecular Mechanism for Ion Adsorption to Aqueous Interfaces [1-4]

As a route to clarifying the mechanism that selectively drives ions to and away from the air/water interface, we have measured the temperature dependence of the adsorption free energy of the thiocyanate ion by UV resonant SHG spectroscopy. Adsorption of aqueous thiocyanate ions from bulk solution to the liquid/vapor interface was measured as a function of temperature . The resulting adsorption enthalpy and entropy changes of this prototypical chaotrope were both determined to be negative. This surprising result is supported by molecular simulations, which clarify the microscopic origins of observed thermodynamic changes. Calculations reveal energetic influences of adsorbed ions on their surroundings to be remarkably local. Negative adsorption enthalpies thus reflect a simple repartitioning of solvent density among surface, bulk, and coordination regions. A different, and much less spatially local, mechanism underlies the concomitant loss of entropy. Simulations indicate that ions at the interface can significantly bias surface height fluctuations even several molecular diameters away, imposing restrictions consistent with the scale of measured and computed adsorption entropies. Based on these results, we expect an ion's position in the Hofmeister lyotropic series to be determined by a combination of driving forces associated with the pinning of capillary waves and with a competition between ion hydration energy and the neat liquid's surface tension.

Characterization of Ion Pairing Between Like-charged Ions in Aqueous Solution[5]

We have recently reported the observation and characterization of "contact pairing" between positively charged ions in aqueous solution, using the combination of synchrotron X-ray spectroscopy of liquid microjets and first principles' theory. The ion(guanidinium-$CN_3H_6^+$) is very important in biology, used routinely as a protein denaturant, and comprising the side chain of one of the 20 natural amino acids(arginine). The cation-cation pairing is driven by the solvent(water) binding energy. The planar guanidinium ions form strong N-H donor hydrogen bonds in the plane of the molecule, but weak acceptor hydrogen bonds with the pi electrons orthogonal to the plane. When fluctuations bring the solvated ions near each other, the strong van der Waals attraction between the pi electron clouds squeezes out the wekly held water molecules, which move into the bulk solution and form much stronger hydrogen bonds with other waters. This mechanism is similar to that recently identified as responsible for weakly hydrated molecules residing at the surface of aqueous solutions .

Contact pairing between guanidinium ions in water had been predicted theoretically by a number of methodologies, but never definitively observed before. The observation by X-ray spectroscopy et al may set a general precedent for such unexpected behavior. For example, mobility studies have evidenced an affinity of guanidinium ions for polymers of arginine, and it is known that arginine interacts strongly with nucleotides. So perhaps "Like charges attract!" may become an accepted paradigm for aqueous solutions.

Towards a Predictive Theory of Water Evaporation [6]

Liquid microjet technology affords the opportunity to study the details of water evaporation, free from the obfuscating effects of condensation that have plagued previous studies. Studying small (diameter < 5 μm) jets with Raman thermometry, we find compelling evidence for the existence of a small but significant energetic barrier to evaporation, in contrast to most current models. Studies of heavy water indicate a similar evaporation coefficient, and thus an energetic barrier similar to that of normal water[. A transition state model developed for this process provides a plausible mechanism for evaporation in which variations in libration and translational frequencies account for the small observed isotope effects. The most important practical result of this work is the quantification of the water evaporation coefficient (0.6), which has been highly controversial, and is a critical parameter in models of climate and cloud dynamics. A molecular-level description of the mechanism for water evaporation has been developed by the Chandler group using their TPS methodology for simulating such rare events, and a paper has recently been published by them.

We have measured the effects of ionic solutes on water evaporation rates. Ammonium sulfate, the most common ionic solute in atmospheric aerosols, was shown to have no statistically significant effect on the rate, whereas sodium perchlorate effected a 25% reduction. The presence of acetic acid-a surface active component of natural aerosols- was likewise shown not to effect significant changes in the evpaoration rate[6]. Most recently, we have determined that addition of up to 0.5M concentrations of HCl has similarly negligible effects on the rate.

Towards a Complete Understanding of CO_2 – Carbonate Equilibria

The dissolution of carbon dioxide in water and the ensuing hydrolysis reactions are of profound importance for understanding the behavior and control of carbon in the terrestrial environment, but essential aspects of these reactions remain poorly understood, particularly those involving aqueous carbonic acid. Using newly developed liquid microjet mixing technology, the first X-ray absorption spectra of aqueous carbonates, *including the short-lived carbonic acid species itself,* have been measured as a function of pH to characterize the evolution of electronic structure of carbonate, bicarbonate, carbonic acid and dissolved CO_2. The corresponding carbon K-edge core-level spectra were calculated using a first-principles electronic structure approach which samples molecular dynamics trajectories. Measured and calculated spectra are in excellent agreement. Each species exhibits similar, but distinct, spectral features which are interpreted in terms of the relative C–O bond strengths, molecular configuration, and hydration strength. This work provides benchmarks for future studies of this system.

Electrokinetic detection for X-ray spectra of weakly interacting liquids: n-decane and n-nonane[7]

Our introduction of liquid microjets into soft X-ray absorption spectroscopy enabled the windowless study of liquids by this powerful atom-selective high vacuum methodology. However, weakly interacting liquids produce large vapor backgrounds that strongly perturb the liquid signal. Consequently, solvents (e.g., hydrocarbons, ethers, ketones, etc.) and solutions of central importance in chemistry and biology have been inaccessible by this technology. Here we

describe a new detection method, upstream detection, which greatly reduces the vapor phase contribution to the X-ray absorption signal while retaining important advantages of liquid microjet sample introduction (e.g., minimal radiation damage). The effectiveness of the upstream detection method is demonstrated in this first study of room temperature liquid hydrocarbons: n-nonane and n-decane. Good agreement with first principles' calculations indicates that the eXcited electron and Core Hole(XCH) theory adequately describes the subtle interactions in these liquids that perturb the electronic structure of the unoccupied states probed in core-level experiments.

Structure and Properties of Lithium Battery Elecrolytes from X-ray Spectroscopy(9)

Since their introduction into the commercial marketplace in 1991, lithium ion batteries have become increasingly ubiquitous in portable technology. Nevertheless, improvements to existing battery technology are necessary to expand their utility for larger-scale applications, such as electric vehicles. Advances may be realized from improvements to the liquid electrolyte; however, current understanding of the liquid structure and properties remain incomplete. X-ray absorption spectroscopy of solutions of $LiBF_4$ in propylene carbonate (PC), interpreted using first-principles electronic structure calculations within the eXcited electron and Core Hole (XCH) approximation, yields new insight into the solvation structure of the Li^+ ion in this model electrolyte. By generating linear combinations of the computed spectra of Li^+-associating and free PC molecules and comparing to the experimental spectrum, we find a Li^+-solvent interaction number of 4.5. This result suggests that computational models of lithium ion battery electrolytes should move beyond tetrahedral coordination structures.

Future Plans

1. Perfect our microfluidics-based mixing system for generating short lived species, e.g. carbonic acid, in liquid microjets for study by X-ray spectroscopy. Apply this technology to the study of hydration and hydrolysis of carbon dioxide, nitrogen oxides, and sulfur oxides.
2. Explore the generality of like-charge ion pairing in aqueous solution by examining other candidate systems, such as arginine-guanadinium and arginine-arginine.
5. Temperature dependences for surface adsorption of some other prototype salts will be measured, as we work with the Geissler group to develop a general understanding and predictive theory of the forces that drive some ions to the surface and repel others.
6. Extension of these measurements to solid/liquid interfaces will be explored, seeking to develop ways to study electrode interfaces.

References (DOE supported papers: 2012-present) – 9 total

[available at http://www.cchem.berkeley.edu/rjsgrp/opening/pubs.htm]

1. D.E. Otten, R. Onorato, R. Michaels, J. Goodknight, R. J. Saykally "Strong Surface Adsorption of Aqueous Sodium Nitrite as an Ion Pair," *Chem. Phys. Lett.* **519-520**, 45-48 (2012).
2. *D.E. Otten, P. Shaffer, P. Geissler, R.J. Saykally "Elucidating the Mechanism of Selective Ion Adsorption to the Liguid Water Surface," PNAS **109** (3), 701-705 (2012).
*featured in Editor's Choice *Science* **335,** 505(2012), "Sacrifices at the Surface".
3. Otten, D. E., Saykally, R. J., "*Spectroscopy and Modeling of Aqueous Interfaces"*, Proceedings of the Varenna School - Course CLXXXVII "Water: Fundamentals as the basis of understanding the environment and promoting technology (8-13 July 2014)-In Press.

4. Saykally, R. J., "*Aqua incognita: liquor aquae superficies"*, in AQUA INCOGNITA: Why Ice Floats on Water and Galileo 400 years on, Pierandrea Lo Nostro & Barry W Ninham (Editors), (ISBN: 9781925138214; Connor Court, Australia; 2014).
5. Shih, O., England, A.H., Dallinger, G.C., Smith, J.W., Duffey, K.C., Cohen, R.C., Prendergast, D., and Saykally, R. J. "*Cation-Cation Contact Pairing in Water: Guanidinium" J. Chem. Phys* ***139,*** Article Number: 035104 DOI: 10.1063/1.4813281 (2013).
6. *Duffey, K.C., Shih, O., Wong, N.L., Drisdell, W.S., Saykally, R.J., and Cohen, R.C. "Evaporation kinetics of aqueous acetic acid droplets: effects of soluble organic aerosol components on the mechanism of water evaporation"*Phys. Chem. Chem. Phys.* ***2013*****,** 15 (28), 11634 - 11639. ***Cover Article.**
7. Lam, R. K., Shih, O., Smith, J. W., Sheardy, A. T., Rizzuto, A. M., Prendergast, D., Saykally, R. J., "*Electrokinetic detection of X-ray spectra of weakly interacting liquids: n-decane and n-nonane"*, *J. Chem. Phys.*, **2014**, 140, 234202.
8. Saykally, R.J. "Air/Water Interface: Two Sides of the Acid Base Story" *Nature Chem.* **5,**82-84*,* 2013.
9. Smith, J. W., Lam, R. K., Sheardy, A. T., Shih, O., Rizzuto, A. M., Borodin, O., Harris, S. J., Prendergast, D., and Saykally, R. J., "X-Ray Absorption Spectroscopy of $LiBF_4$ in Propylene Carbonate: A Model Lithium Ion Battery Electrolyte" *Phys. Chem. Chem. Phys*.(2014)

COVER ARTICLE: DOI: 10.1039/c4cp03240c

10. Lam, R. K., England, A. H., Sheardy, A. T., Shih, O., Smith, J. W., Rizzuto, A. M., Prendergast, D. P., Saykally, R. J., *The Hydration Structure of Aqueous Carbonic Acid from X-ray Absorption Spectroscopy, Chem. Phys. Lett.*, **614,** 282-286 (2014). **COVER ARTICLE**

Molecular Theory & Modeling

Development of Statistical Mechanical Techniques for Complex Condensed-Phase Systems

Gregory K. Schenter
Physical Sciences Division
Pacific Northwest National Laboratory
902 Battelle Blvd.
Mail Stop K1-83
Richland, WA 99352
greg.schenter@pnnl.gov

This work was done in collaboration with Chris Mundy and John Fulton.

The long-term objective of this project is to advance the development of molecular simulation techniques to better understand fundamental properties and processes of molecular and nanoscale systems in complex environments, such as condensed phases and interfaces. We seek to develop a systematic connection between models of molecular interactions and collective behavior of molecular systems. This will lead to an improved knowledge of complex collective behavior on a macroscopic scale. It involves the investigation of representations of molecular interaction as well as statistical mechanical sampling techniques and finding the balance between efficiency and accuracy in the description of molecular interaction. We search for the appropriate amount of explicit treatment of electronic structure that allows for efficient sampling of a statistical mechanical ensemble of a system of interest.

Recent investigations have focused on complexity associated with broken symmetries corresponding to vacuum/liquid, liquid/solid, and liquid/liquid interfaces or highly concentrated electrolytes. The characterization of these systems requires a description of molecular interaction that is more robust than what is required to describe bulk, homogeneous systems. Understanding the balance between descriptions of molecular interaction and complexity will continue to be the focus of future research efforts.

We have established that a Density Functional Theory (DFT) description of molecular interaction provides a quantitative representation of the short-range interaction and structure when compared to Extended X-ray Absorption Fine Structure (EXAFS) measurements. To do this it is essential to develop a simulation protocol that places you in the correct region of the bulk phase diagram. We established that a BLYP DFT simulation of 100's of H2O's at 300K, with Grimme's D2 dispersion correction, and a MOLOPT DZ basis set effectively does this. [a] This allowed us to successfully characterize the solvation structure of the two ions, I^- [b] and IO_3^- [c] and have confidence in our MD-EXAFS approach. In these studies we generated a statistical ensemble of configurations using the CP2K electronic structure/statistical mechanics package [d]. From this ensemble, a series of electron multiple scattering calculations are performed using the FEFF9 code [e] to generate a configuration average EXAFS spectra to compare to experimental measurement. A similar protocol yielded unprecedented agreement between measured structural signal and the ensemble generated using a DFT description of molecular interaction for cations. [Refs. 2 and 3]

MD-EXAFS of HCl

The established techniques have allowed us to characterize in detail the equilibrium associated with the dissociation of a protic acid, HCl, in water. [Ref. 5]

$$\underset{a}{Cl{-}H{\cdots}OH_2} \underset{k_{ba}}{\overset{k_{ab}}{\rightleftharpoons}} \underset{b}{Cl^{-}{\cdots}H{-}OH_2^{+}} \underset{k_{cb}}{\overset{k_{bc}}{\rightleftharpoons}} \underset{c}{Cl^{-}_{aq} + H_3O^{+}_{aq}}$$

Here we distinguish from the the proton transfer from the acid (Cl-H) to a hydrogen-bonded water molecule (a → b) and the formation of the fully dissociated anion and cation (b → c). In this work we verify the distinct intermediate contact ion species consisting of the anion and the hydronium cation (b) at moderate concentrations using the MD-EXAFS approach. We are able to quantitatively reproduce the trends in the EXAFS signal with increasing acid concentration from our generated statistical mechanical ensemble. (See Figure 1) Additional discussion of this work is contained in Chris Mundy and John Fulton's CPIMS Abstract.

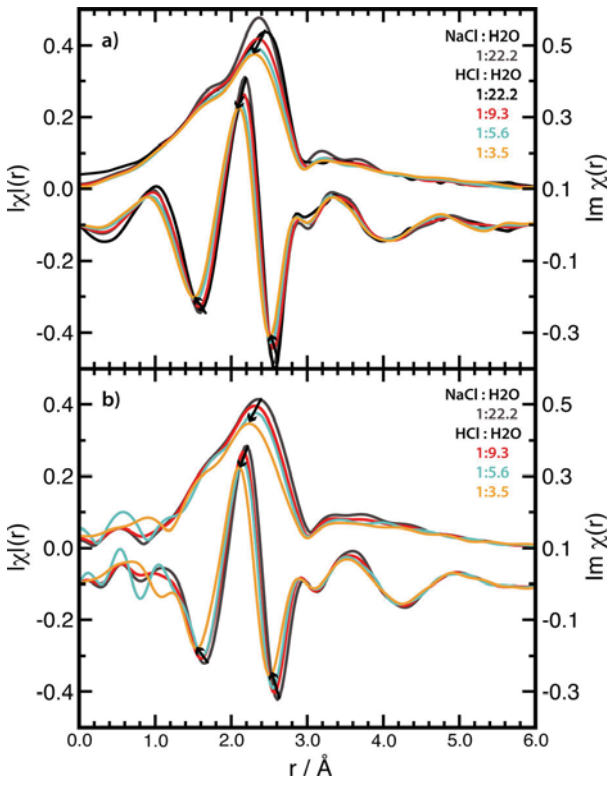

Figure 1. Experimental and theoretical EXAFS Cl K-edge as a function of the concentration of the electrolyte solution. Experimental and theoretical data, respectively (top and bottom). The top curves in each panel correspond to k^2-weighted |χ(R)| (left axis), and the bottom curves in each panel correspond to Im[χ (R)] (right axis). The loss of coordinated oxygens in the first solvation shell are manifest in the change of intensity in the peaks in |χ (R)| (top curves). The Im[χ (R)] (bottom curves) is sensitive to the contraction of the Cl-O distance in the formed contact ion pair between hydronium and chloride that is not present in the salt solution. Ratios of HCl to water of the experiment and simulation are in the legend in each panel. Black arrows are shown as guides to elucidate the evolution of the EXAFS signal to shorter Cl-O distances as a function of increasing acid concentration.

In the future we will extend these studies to concentrated electrolytes and more complex ions such as the oxyanion series: IO_3^-, BrO_3^-, ClO_3^-, and ClO^-. We will continue to explore the relation of EXAFS analysis to neutron and X-ray diffraction measurements.

The Role of Broken Symmetry in Solvation of a Spherical Cavity

The insertion of a hard sphere cavity in liquid water breaks the translational symmetry and generates an electrostatic potential difference between the bulk and the center of the cavity. Recently we explored the structure of water about small, medium and large cavities (2Å, 4Å, and 6Å radii) comparing empirical potential models (SPC/E and TIP5P) and DFT response to the induced broken symmetry. We explored both the structural response of the fluid as well as resulting electic field response as characterized by the scalar electrostatic potential. [Ref. 4]

The perturbation of the number density is displayed in Figure 2

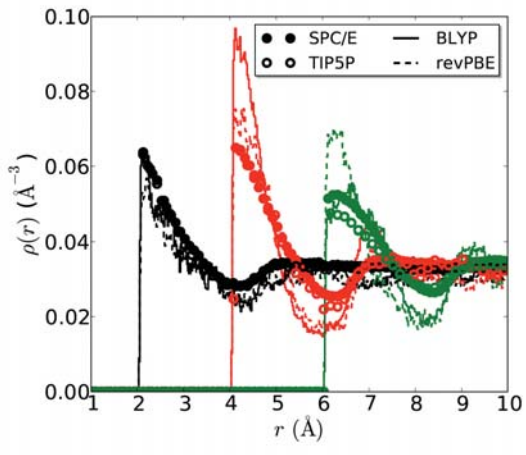

Figure 2. Comparing oxygen number density, for models of molecular interaction.

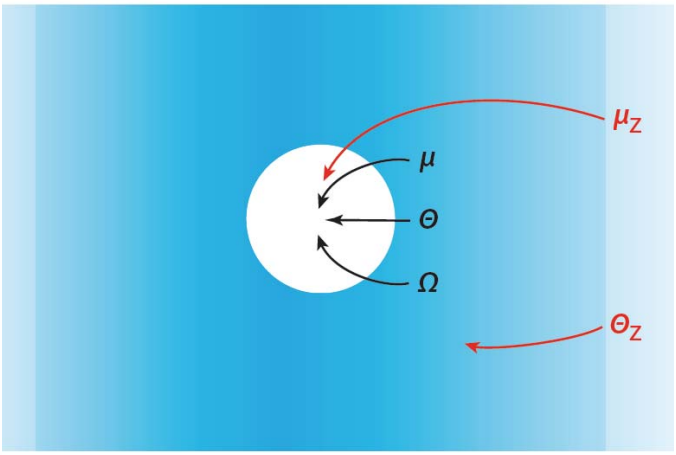

Figure 3. Multipole contributions to the electric field inside a cavity in response to the broken symmetry.

In this work we were able to decompose the contributions to the electric field in terms of a multipole analysis. [See Figure 3. μ represents dipole density, Θ represents quadrupole density and Ω represents octupole density.] For the empirical potential we are able to unambiguously decompose multipole contributions to the cavity potential [See Table 1.] Such an analysis in terms of traceless multipole moments for the continuous distribution corresponding to the DFT charge density is a challenge and represents the focus of future work. Such an analysis lays at the foundation of model reduction techniques. Additional details of this work are contained in Chris Mundy's CPIMS abstract.

Model	R_C	μ	Θ	Ω	μ_z	$\Phi^{HW'}$
SPC/E	2	-47	-134	-204	260	-140
	4	-237	-195	-90	260	-262
	6	-297	-167	-35	260	-239
TIP5P	2	-35	-20	-59	103	-16
	4	-72	-40	-24	103	-33
	6	-104	-32	-8	103	-41

Table 1. Multipole decomposition of the scalar potential, $\Phi^{HW'}$ (mV) vs. cavity radius R_C (Å).

Acknowledgements: Direct collaborators on this project include C. J. Mundy, M. Baer and J. Fulton. Interactions with S. S. Xantheas, L. X. Dang and S. M. Kathmann have significantly influenced the course of this work.

This research was performed in part using the computational resources in the National Energy Research Supercomputing Center (NERSC) at Lawrence Livermore National Laboratory. Battelle operates Pacific Northwest National Laboratory for the US Department of Energy.

References

a. M. D. Baer, C. J. Mundy, M. J. McGrath, I. F. W. Kuo, J. I. Siepmann, and D. J. Tobias. "Re-Examining the Properties of the Aqueous Vapor-Liquid Interface Using Dispersion Corrected Density Functional Theory." J. Chem. Phys. **135** (12), 124712 (2011).
b. J. L. Fulton, G. K. Schenter, M. D. Baer, C. J. Mundy, L. X. Dang, and M. Balasubramanian, "Probing the Hydration Structure of Polarizable Halides: A Multiedge XAFS and Molecular Dynamics Study of the Iodide Anion," J. Phys. Chem. B **114** (40), 12926-12937 (2010).
c. M. D. Baer, V. T. Pham, J. L. Fulton, G. K. Schenter, M. Balasubramanian, and C. J. Mundy, "Is Iodate a Strongly Hydrated Cation?," J. Phys. Chem. Lett. **2** (20), 2650-2654 (2011).
d. The CP2K developers group, http://cp2k.berlios.de/ (2008) J. VandeVondele, M. Krack, F. Mohamed, M. Parrinello, T. Chassaing and J. Hutter, Comp. Phys. Comm. **167**, 103 (2005).
e. J. J. Rehr, R. C. Albers, S. I. Zabinsky, Phys. Rev. Lett. **69**, 3397 (1992); M. Newville, B. Ravel, D. Haskel, J. J. Rehr, E. A. Stern, and Y. Yacoby, Physica B, **208-209**, 154 (1995); A. L. Ankudinov, C. Bouldin, J. J. Rehr, H. Sims, and H. Hung, Phys Rev. B **65**, 104107 (2002).

References to publications of DOE sponsored research (2012-present)

1. R. Atta-Fynn, D. F. Johnson, E. J. Bylaska, E. S. Ilton, G. K. Schenter, and W. A. de Jong, "Structure and Hydrolysis of the U(IV), U(V), and U(VI) Aqua Ions from Ab Initio Molecular Simulations," Inorg. Chem. **51** (5), 3016-3024 (2012).
2. J. L. Fulton, E. J. Bylaska, S. Bogatko, M. Balasubramanian, E. Cauet, G. K. Schenter, and J. H. Weare, "Near-Quantitative Agreement of Model-Free DFT-MD Predictions with XAFS Observations of the Hydration Structure of Highly Charged Transition-Metal Ions," J. Phys. Chem. Lett. **3** (18), 2588-2593 (2012).
3. S. Bogatko, E. Cauet, E. Bylaska, G. K. Schenter, J. Fulton, and J. Weare, "The Aqueous Ca^{2+} System, in Comparison with Zn^{2+}, Fe^{3+}, and Al^{3+}: An Ab Initio Molecular Dynamics Study," Chem.-Eur. J. **19** (9), 3047-3060 (2013).
4. R. C. Remsing, M. D. Baer, G. K. Schenter, C. J. Mundy, and J. D. Weeks, "The Role of Broken Symmetry in Solvation of a Spherical Cavity in Classical and Quantum Water Models," J. Phys. Chem. Lett., **5** (16), 2767–2774 (2014).
5. M. D. Baer, J. L. Fulton, M. Balasubramanian, G. K. Schenter, and C. J. Mundy, "Persistent Ion Pairing in Aqueous Hydrochloric Acid," J. Phys. Chem. B, **118** (26), 7211–7220 (2014).

An Atomic-scale Approach for Understanding and Controlling Chemical Reactivity and Selectivity on Metal Alloys

E. Charles H. Sykes (charles.sykes@tufts.edu)
Department of Chemistry, Tufts University, 62 Talbot Ave, Medford, MA 02155

Program Scope:

Catalytic hydrogenations are critical steps in many industries including agricultural, chemicals, foods and pharmaceuticals. In the petroleum refining industry, for instance, catalytic hydrogenations are performed to produce light, hydrogen rich products like gasoline. Hydrogen activation, uptake, and reaction are also important phenomena in fuel cells, hydrogen storage devices, materials processing, and sensing. Typical heterogeneous hydrogenation catalysts involve nanoparticles composed of expensive noble metals or alloys based on metals like Pt, Pd, and Rh. Our goal is to alloy very small amounts of these types of reactive metals with more inert and often much cheaper hosts and to understand how the local atomic geometry affects reactivity. We have focused on understanding the adsorption, diffusion, spillover and reactivity of hydrogen in a number of these types of systems. We designed well-defined Pd, Co, Au and Cu alloy surfaces that are amenable to high resolution scanning probe studies, X-ray photoelectron spectroscopy, and chemical analysis of adsorbate binding, spillover and reaction [1-12].

We demonstrated for the first time how single Pd atoms can convert the otherwise catalytically inert surface of an inexpensive metal, in this case Cu, into an ultraselective catalyst [12]. We used high resolution imaging to characterize the active sites in what we call "*single atom alloys*" in which Pd is atomically dispersed in a Cu single crystal surface, and we probed the chemistry of these surfaces with temperature programmed reaction spectroscopy. The mechanism of activation involves facile dissociation of molecular hydrogen at the individual palladium atoms followed by spillover onto the Cu surface, where highly selective catalysis occurs by virtue of weak binding. The observed reaction selectivity is much higher than that measured on Pd alone, illustrating the unique synergy of the system.

Using the Pd/Cu single atom alloy, we discovered a new phenomenon that we term the "*molecular cork effect*" in which the hydrogen spillover pathway from atomic Pd dissociation sites to Cu reaction sites is controlled via molecular adsorption of a spectator molecule on the minority sites [4]. This effect enables the creation of a non-equilibrium form of hydrogen that is weakly bound to Cu but prevented from desorbing from the surface. We showed that the molecular cork effect is present during the surface catalyzed hydrogenation of styrene and illustrated how it can be used as a method for controlling uptake and release of hydrogen in a model storage system.

The Pd single atom alloy system also allowed us to probe the diffusion of large amounts of weakly adsorbed hydrogen on Cu(111). Using high resolution, time-resolved scanning tunneling microscopy imaging, we were able to investigate the quantum tunneling enabled diffusion and assembly of hydrogen atoms and compare their behavior to deuterium atoms. In contrast to other catalytic metals, this work revealed the complex interaction and structures formed by hydrogen on Cu(111).

Continuing our work on bimetallics, by studying Co nanoparticles grown on Cu we discovered a previously unreported, but catalytically relevant, high coverage phase of hydrogen that could only be formed by virtue of Co/Cu interface sites [1, 5, 6, 11]. We also discovered that adsorbed CO and H, the two reactants in Fischer-Tropsch Synthesis, are segregated on Co nanoparticle surfaces [5]. CO adsorbs on the Co nanoparticles via spillover from the Cu, and we found that by depositing CO onto preadsorbed

H layers, the CO is able to induce a two-dimensional phase compression of H, providing the first direct visualization of this long proposed phenomenon in a catalytically relevant system.

These types of alloy systems allow us to address previously unobtainable structures, densities and phases of hydrogen due to the limitations of single crystal work in ultra-high vacuum. By understanding the energy landscape for hydrogen activation, adsorption and spillover we have been able to generate catalytically relevant high coverage hydrogen phases, design efficient and selective hydrogenation sites, and trap hydrogen on surfaces beyond its normal desorption point yielding novel catalytic intermediates.

Recent Progress:

Towards a Molecular Level Understanding of Fischer-Tropsch Reactants on Cobalt Nanoparticles

Building upon our work with hydrogen on single atom alloy surfaces, we have undertaken the study of Co/Cu alloys. Cobalt is an active metal for a variety of commercially and environmentally significant heterogeneously catalysed processes, not least Fischer-Tropsch Synthesis (FTS) that involves the formation of hydrocarbons via the catalytic conversion of syngas (CO and H_2), which can be derived from biomass, a renewable energy resource. Currently, FTS accounts for the production of 200,000 barrels per day of synthetic fuel. Yet despite its importance as an industrial catalyst, Co's surface chemistry is less studied compared to other key catalyst metals, stemming in part from the difficulties associated with Co single crystal preparation and stability. Given that Co-based catalysis is affected by the adsorption state of reactants, as well as nanoparticle shape and size, we have begun to study this surface chemistry using a novel model system. We have utilized a method for preparing model Co catalysts by depositing Co onto Cu single crystals (an inert metal for FTS), yielding well-defined Co nanoparticles that offer an excellent platform to investigate the adsorption, diffusion, dissociation, and reaction of catalytically relevant molecules [1, 5, 6, 11]. Using LT-STM we have studied these model nanoparticles and the interaction of syngas with their surfaces on the molecular scale.

We studied the dissociative adsorption of H_2, a process central to a number of catalytic reactions, on the Co surfaces. Despite the importance of H_2 adsorption on Co, there are relatively few studies examining this system. We have utilized the Co/Cu(111) bimetallic, instead of the traditional planar Co single crystals, to study this process with a more catalytically-relevant form of Co nanoparticles with well-defined terraces and step edges. Using STM we discovered three different phases of H on the close-packed Co nanoparticle surfaces with a range of densities [5, 6]. Our data reveal a so-far unreported high coverage phase of H with a (1x1) structure and provides the first visualization of the 6H-(3x3) structure, which has previously only been predicted based on coverage measurements. These high-density phases, which are undoubtedly important in catalytic systems at elevated pressure, are only amenable to surface science techniques via a nanoparticle model system with a high step to terrace ratio, as spillover from step edges to the terrace sites plays a critical role in populating reaction sites on the Co close-packed nanoparticle surfaces. In contrast to the low density phases, the H-(1x1) structure can only be formed at an intermediate temperature, indicating that compression to this higher-density phase is activated [5,6]. Thus, we demonstrated that the coverage of H on Co nanoparticles may, in fact, be much higher than previously expected from single crystal work, especially considering the elevated pressures that are employed during catalysis.

Furthering our work examining hydrogen on Co nanoparticles, we have coadsorbed H_2 and CO on the Co/Cu system. We have shown for the first time that H and CO segregate on the Co surfaces, and we propose that atomic H blocks CO adsorption, preventing complete overlayer formation and causing the

build-up of CO at the cobalt nanoparticle step edges. Our STM images reveal that CO and H atoms form phase separated domains on cobalt multilayer islands. This indicates that the available interface for reaction between the two adsorbed reactants will strongly depend on cobalt particle size. In other words the FTS reactivity must be subject to unforeseen kinetic restraints as a function of particle size due to the limitation of the boundary between reactants. This phenomenon is still under investigation in our labs.

Since competitive adsorption and lateral pressure between surface-bound intermediates are important effects that dictate chemical reactivity, we wanted to further explore the mixed CO/H system on Co to study these effects [5]. We found that by depositing CO, which adsorbs on the Co nanoparticles *via* spillover from the Cu(111) support, onto preadsorbed adlayers of H, the CO exerts two-dimensional pressure on H, compressing it into a higher-density, energetically less-preferred structure [5]. *This result provides the first direct visualization of this long proposed phenomenon in a catalytically relevant system.* By depositing an excess of CO, we found that H on the Co surface is forced to spill over onto the Cu(111) support. Thus, spillover of H from Co onto Cu, where it would not normally reside due to the high activation barrier, is preferred over desorption. These results may have ramifications for Fischer–Tropsch synthesis kinetics on Co, as the displacement of H by CO, in addition to the segregation of the adsorbates, limits the interface between the two molecules.

Future Plans:

Our approach offers the opportunity to study the atomic-scale composition and structure of active sites and relate this information to their ability to activate, spillover and react industrially relevant small molecules. We will use these guiding principles to examine catalytic metal alloys from a new perspective and discover new processes. Future work is aimed at:

1) Extending our single atom alloy (SAA) approach to understanding hydrogenations on PdAg and PdAu
2) Using the “molecular cork” effect to control the activity and selectivity of surface catalyzed hydrogenation reactions
3) Understanding and controlling C-C bond formation on Cu adatoms and Co nanoparticles
4) Elucidating the optimal atomic geometry of AgCu for oxygen activation

These model systems will allow us a fundamental understanding of many important elementary steps in surface catalyzed chemistry. The atomic-scale structure of the active sites in metal alloy catalysts is hard, if not impossible, to characterize by conventional methods. Our surface science approach that includes scanning probes offers methods to characterize the structure, stoichiometry, and reactivity, and provides an atomic-scale view of local structure and adsorbate binding/diffusion. However, when working on well-defined model systems it is imperative to work with the same elements, structures and ensembles that are present in the real catalysts under working conditions. Implementation of the SAA approach to the design of real catalysts requires consideration of the effect of higher reaction temperature and pressure, which may cause the minority active element to segregate into the bulk of the more inert host and hence cause a loss in activity. Understanding and controlling surface segregation under reaction conditions will also be crucial for the efficient use of costly elements of the alloy by keeping them in active sites on or near the surface. Promisingly, there are now many experimental and theoretical examples of metal alloys under realistic conditions in which the more active element is stabilized at the surface by adsorbates. This adsorbate-induced reverse segregation effect is understood in terms of the adsorbate binding more strongly to the element which would normally segregate to the

bulk and results in a reversal of the normal surface segregation behavior. For example, in the case of the Cu/Pd system the stabilization due to segregation of Cu to the surface is small (0.02 eV) compared to the ~0.4 eV increase in binding of H to Pd vs. Cu. The fact that Pd segregation to the Cu surface has been observed experimentally in Pd/Cu catalysts under realistic hydrogenation operating conditions bodes well for the utility of these types of atomic geometries in real catalysts.

All our proposed systems have been chosen with these considerations in mind. Active elements will be added/alloyed into more inert Cu, Ag, and Au surfaces. The (111) facet is chosen, as it is often the most commonly exposed facet on metal nanoparticles. While minority structures like step edges or defects often dominate the reactivity of metal surfaces, the chemistry of our alloyed systems is expected to be driven at the added metal atom sites and this will be checked with control experiments of the reactivity before and after alloying.

DOE-Sponsored Research Publications in the Last Two Years:

1) "Segregation of Fischer-Tropsch Reactants on Colbalt Nanoparticle Surfaces" E. A. Lewis, D. Le, A. D. Jewell, C. J. Murphy, T. S. Rahman, and E. C. H. Sykes - ***Chemical Communications*** 2014, *50*, 6537-6539
2) "Significant Quantum Effects in Hydrogen Activation" G. Kyriakou, E. R. M. Davidson, G. Peng, L. T. Roling, S. Singh, M. B. Boucher, M. D. Marcinkowski, M. Mavrikakis, A. Michaelides, and E. C. H. Sykes - ***ACS Nano*** 2014, *8*, 4827-4835
3) "Atomic-Scale Insight into the Formation, Mobility and Reaction of Ullmann Coupling Intermediates" E. A. Lewis, C. J. Murphy, M. L. Liriano, and E. C. H. Sykes - ***Chemical Communications*** 2014, *50*, 1006-1008
4) "Controlling the Spillover Pathway with the Molecular Cork Effect" M. D. Marcinkowski, A. D. Jewell, M. Stamatakis, M. B. Boucher, E. A. Lewis, C. J. Murphy, G. Kyriakou and E. C. H. Sykes - ***Nature Materials***, 2013, *12*, 523-528
5) "Visualization of Compression and Spillover in a Coadsorbed System: Syngas on Cobalt Nanoparticles" E. A. Lewis, D. Le, A. D. Jewell, C. J. Murphy, T. S. Rahman and E. C. H. Sykes - ***ACS Nano***, 2013, *7*, 4384-4392
6) "Dissociative Hydrogen Adsorption on Close-Packed Cobalt Nanoparticle Surfaces" E. A. Lewis, D. Le, C. J. Murphy, A. D. Jewell, M. F. G. Mattera, M. L. Liriano, T. S. Rahman and E. C. H. Sykes - ***Journal of Physical Chemistry C***, 2012, *116*, 25868-25873 [Cover Story]
7) "Quantum Tunneling Enabled Self-Assembly of Hydrogen Atoms on Cu(111)" A. D. Jewell, G. Peng, M. F. G. Mattera, E. A. Lewis, C. J. Murphy, G. Kyriakou, M. Mavrikakis and E. C. H. Sykes - ***ACS Nano***, 2012, *6*, 10115-10121
8) "Viewing and Inducing Symmetry Breaking at the Single-Molecule Limit" H. L. Tierney, A. D. Jewell, A. E. Baber, E. V. Iski and E. C. H. Sykes - ***Chirality***, 2012, *24*, 1051-1054
9) "Hydrogen Bonding and Chirality in Functionalized Thioether Self-Assembly" - A. F. McGuire, A. D. Jewell, T. J. Lawton, C. J. Murphy, E. A. Lewis and E. C. H. Sykes - ***Journal of Physical Chemistry C***, 2012, *116*, 14992-14997
10) "Molecular-Scale Surface Chemistry of a Common Metal Nanoparticle Capping Agent: Triphenylphosphine on Au(111)" - A. D. Jewell, E. C.H. Sykes and G. Kyriakou - ***ACS Nano***, 2012, *6*, 3545-3552
11) "Rediscovering Cobalt's Surface Chemistry" E. A. Lewis, A. D. Jewell, G. Kyriakou, E. C. H. Sykes - ***Physical Chemistry Chemical Physics***, 2012, *14*, 7215-7224 [Cover Story]
12) "Isolated Metal Atom Geometries as a Strategy for Selective Heterogeneous Hydrogenations" - G. Kyriakou, M. B. Boucher, A. D. Jewell, E. A. Lewis, T. J. Lawton, A. E. Baber, H. L. Tierney, M. Flytzani-Stephanopoulos and E. C. H. Sykes - ***Science***, 2012, *335*, 1209-1212

Solvation Dynamics in Nanoconfined and Interfacial Liquids

Ward H. Thompson
Department of Chemistry, University of Kansas, Lawrence, KS 66045
wthompson@ku.edu

Program Scope

There is currently significant interest in nanostructured materials that can confine liquids in nanoscale pores, due to both the appearance of new fundamental phenomena in these systems and their wide range of potential applications, including catalysis, sensing, separations, electrochemistry, and optical materials. However, the design principles are still lacking for the development of such mesoporous (2 nm $\leq$ *diameter* $\leq$ 50 nm) materials for practical applications that take advantage of their large surface area-to-volume ratio and their high degree of tunability through pore size, shape, roughness, and chemical functionality. At the same time, this gap points to the need to improve our fundamental understanding of how complex liquid dynamics can arise from nanoscale confinement and vary strongly with the confining environment properties.

We are addressing some of the outstanding questions regarding these nanoconfined liquid dynamics and the implications for chemical reactions – *i.e.*, *How does a chemical reaction occur differently in a nanoconfined solvent than in a bulk solvent?* – by using solvation dynamics as a basis. Solvation dynamics is closely related to the reaction coordinate for charge transfer reactions such as electron or proton transfer reactions and is often dramatically affected by nanoconfinement.

Recent Progress & Future Plans

Dynamics of Nanoconfined Water.

Reorientational motion of the solvent molecules is a key component in a wide variety of chemical processes, including solvation dynamics and proton transfer reactions. Thus, it is important to understand how liquid molecules rotate when confined within nanoscale frameworks. We have examined this question by examining the reorientational dynamics of water in ~ 2.4 nm diameter hydrophilic (OH-terminated) silica pores. The results are generally expressed in terms of a reorientational correlation function, $C_2(t) = \langle P_2[\mathbf{e}(0)\cdot\mathbf{e}(t)]\rangle$ with $\mathbf{e}$ the OH unit vector, which provides a measure of the rotational times of the OH bonds in the liquid. We have previously found[1] that the long-time decay of $C_2(t)$ for water confined in hydrophilic pores, appears to follow a power law, *i.e.*, $C_2(t) \sim (t/\tau)^{\alpha}$ with exponent $\alpha = -1.1$. (Similar, but even slower, non-exponential decays are observed for nanoconfined methanol and ethanol.)

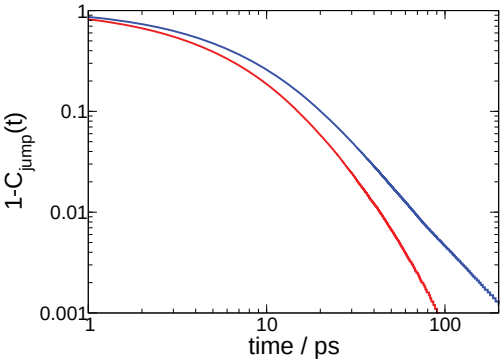

Figure 1: The hydrogen-bond exchange correlation function, $1 - C_{jump}(t)$, for nanoconfined water including all jumps (red) and only jumps to new water acceptors (blue)

We have recently made inroads into understanding the origin of this power-law decay by noting that it arises from an analogous power-law behavior in the hydrogen-bond exchange, or jump, times. It is important to note that this is true only for jumps to a new water acceptor – jumps to a new acceptor on the pore surface do not result in complete reorientation and do not yield a power-law decay (Fig. 1). However, the hydrogen-bond exchange for a water near a specified site at the surface can be characterized by a single timescale, the "jump" time, but that those timescales are themselves widely distributed.[1,2] It is interesting, then, to ask What determines the jump time for a particular location on the pore surface? Detailed analysis shows that there are two dominant factors, both of which are entropic. The first is associated with the volume excluded by the pore that inhibits the approach of a new hydrogen-bonding partner. The second is related to the structure of the hydrogen-bonding network imposed by the pore surface that suppresses elongation of the initial hydrogen bond in the exchange process. Enthalpic effects arising from the chemical heterogeneity of the pore surface represent only a minor contribution. We have also demonstrated that the heterogeneity observed in the water dynamics is mainly static, arising from the spatial heterogeneity of the pore surface, and that dynamical heterogeneity in the water dynamics plays at most a minor role.

These results implicate the surface roughness as a key factor in the non-exponential dynamics. We are constructing silica pores of varying roughness to explore this relationship. We are also examining the effect of steric bulk through simulations of confined methanol and ethanol; these systems also provide insight into how the effect of surface chemistry on dynamics can vary with the liquid. Further, we are examining the mechanism of water diffusion in these pores, which has been suggested to be relatively isotropic.[3]

Influence of Steric Bulk on the Reorientational Dynamics of Alcohols.

Preliminary simulations of the reorientation of nanoconfined alcohols induced us to examine the reorientation of bulk alcohols. Generally, NMR measurements on linear alcohols have found that reorientation is slower the longer the alkyl chain, a result reproduced in molecular dynamics simulations. We previously found that the extended jump mechanism developed for water, which predicts that the OH reorientation is governed by the switching of hydrogen-bonding partners and the reorientation of intact hydrogen bonds, also describes OH reorientation in the lower alcohols (methanol and ethanol).[4] The results show that the steric bulk of the alcohol significantly lengthens the time to switch hydrogen-bond partners.

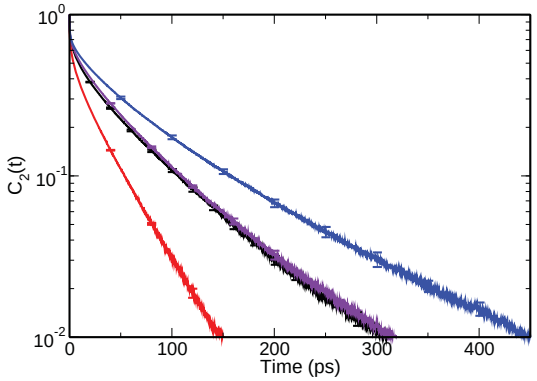

Figure 2: Reorientation correlation functions for *n*-butanol (black), *iso*-butanol (red), *sec*-butanol (violet), and *tert*-butanol (blue).

We have then addressed how the arrangement of the steric bulk affects the dynamics by comparing the four isomeric butanols. The reorientation time of the OH group, measured by the decay of the $C_2(t)$ function defined above and shown in Fig. 2, is fastest for *iso*-butanol and, not surprisingly, slowest for *tert*-butanol. Interestingly, *sec*-

butanol and *n*-butanol have nearly identical reorientation times; this is due to a cancellation of two effects: *n*-butanol displays faster exchanges between hydrogen-bonding partners but *sec*-butanol exhibits more rapid reorientation of intact hydrogen bonds. Moreover, the dynamics of all the butanols can be understood within the context of the extended jump model. Excluded volume effects slow down hydrogen-bond jumps differently for the four alcohols due to their individual arrangements of steric bulk. An additional effect is due to changes in the hydrogen-bonded networks in the four liquids; cluster analysis of these networks is in progress to determine the influence of these networks on the dynamics.

Solvation in Nanoscale Silica Pores.

Solvation dynamics in nanoconfined solvents are generally marked by dramatic changes relative to the corresponding bulk solvent. In particular, long time scales not seen in the bulk solvent – often as long as hundreds of picoseconds or several nanoseconds – are observed in the time-dependent fluorescence signal. A number of models have been proposed to explain the origin of this multi-exponential, long-time decay. However, clear comparisons of theoretical predictions with experimental measurements is lacking as is, by extension, a rigorous test of the models.[5] To address this, we have developed a number of models for both the dye molecule and the confining framework[7,8] to allow for more general exploration of the phenomena and driving forces involved in TDF experiments, and chemistry in general, in nanoconfined solvents.

We have used replica exchange molecular dynamics to investigate the position and orientational distribution of a commonly used dye molecule, Coumarin 153 (C153), dissolved in ethanol confined within $\sim$ 2.4 nm diameter hydrophilic silica pores.[8] The molecule was modeled in its ground electronic state. The simulations found that the C153 carbonyl oxygen is almost always found at the pore surface, as shown in Fig. 3, where the free energy is plotted as a function of the oxygen atom distance from the pore wall. However, the molecule was found to lie primarily in two orientations: one in which the carbonyl oxygen points at the pore wall with C153 being nearly perpendicular and another where the carbonyl oxygen moves away from the pore wall and the whole molecule sits relatively flat against the surface. The free energy barriers between these orientations are found to be comparatively small ($\sim 1-2$ kcal/mol), a result that is particularly surprising in light of the slow dynamics of confined C153 and suggests retardation of the solvent motions is primarily responsible.

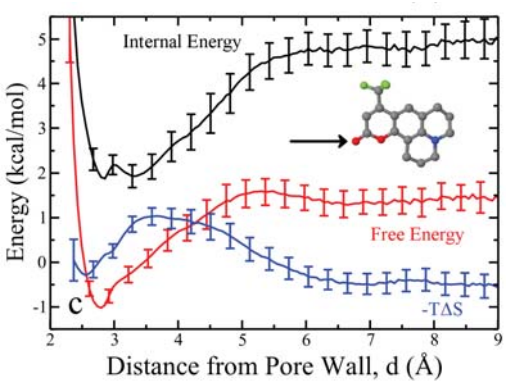

Figure 3: Free energy, $\Delta A(d)$, internal energy, $\Delta U(d)$, and entropic contribution, $-T\Delta S(d)$, are shown as a function of solute distance from the pore wall for the carbonyl oxygen of C153.

Ongoing work includes exploration of other system properties. For example, the analogous properties of C153 in its electronic excited state are being examined. In addition, the effect of surface chemistry is being investigated through simulations of hydrophobic pores and pores with hydrogen-bonding artificially "turned off." The relationship of dye location and orientation to time-dependent fluorescence measurements will also be probed using nonequilibrium molecular dynamics

simulations. Finally, the results will be compared to simulations of dye molecules at planar silica surfaces to understand the effects of surface curvature and solvent confinement.

References

[1] †D. Laage and W.H. Thompson *J. Chem. Phys.* **136**, 044513 (2012). "Reorientation Dynamics of Nanoconfined Water: Power-law Decay, Hydrogen-bond Jumps, and Test of a Two-State Model"

[2] †A.C. Fogarty, E. Duboué-Dijon, D. Laage, and W.H. Thompson, *J. Chem. Phys.* (submitted). "Origins of the Non-exponential Reorientation Dynamics of Nanoconfined Water"

[3] A.A. Milischuk and B.M. Ladanyi, *J. Chem. Phys.* **135**, 174709 (2011). "Structure and Dynamics of Water Confined in Silica Nanopores"

[4] A.A. Vartia, K.R. Mitchell-Koch, G. Stirnemann, D. Laage, and W.H. Thompson, *J. Phys. Chem. B* **115**, 12173-12178 (2011). "On the Reorientation and Hydrogen-Bond Dynamics of Alcohols"

[5] W.H. Thompson, *Annu. Rev. Phys. Chem.* **62**, 599-619 (2011). "Solvation Dynamics and Proton Transfer in Nanoconfined Liquids"

[6] †B.J. Ka and W.H. Thompson, *J. Phys. Chem. A* **116**, 832-838 (2012). "Sampling the Transition State of a Proton Transfer Reaction in Mixed Quantum-Classical Molecular Dynamics Simulations"

[7] †A.A. Vartia and W.H. Thompson, *J. Phys. Chem. B* **116**, 5414-5424 (2012). "Solvation and Spectra of a Charge Transfer Solute in Nanoconfined Ethanol"

[8] †J.A. Harvey and W.H. Thompson, *J. Phys. Chem. B* (submitted). "Thermodynamic Driving Forces for Dye Molecule Position and Orientation in Nanoconfined Solvents"

†DOE-sponsored publication past 2 years

Imaging Interfacial Electric Fields on Ultrafast Timescales

William A. Tisdale
Department of Chemical Engineering
Massachusetts Institute of Technology, Cambridge, MA 02139
tisdale@mit.edu

Program Scope

The objective of this project is to explore a novel methodology for visualization of ultrafast electronic processes at interfaces. The method, which is based on optical stimulation, builds upon previous success using spontaneous second-order nonlinear optical probes to track the temporal evolution of interfacial electric fields resulting from charge separation across an interface. A goal is to speed signal acquisition by orders of magnitude so that laser scanning ultrafast microscopy becomes feasible. The ultimate aim is to generate movies of interfacial electronic phenomena occurring on femtosecond timescales and submicron length scales, thereby informing our understanding of disorder, heterogeneity, and morphology, and how these factors affect ensemble behavior in photovoltaic, electrochemical, and optoelectronic systems.

Recent Progress I: *Stimulated SHG*

Second harmonic generation (SHG) is a second order nonlinear optical process in which two photons at a fundamental frequency ω combine to form a single photon at frequency 2ω. Like any even-ordered nonlinear optical process, SHG is dipole-forbidden in the bulk of centrosymmetric media such as many crystal structures, amorphous solids, liquids, and gases; observed SHG signals in these media originate from materials' interfaces. SHG experiments selectively probe interfaces and are sensitive to the interfacial environment. SHG is an inefficient process, and high incident fundamental fluences are necessary to produce measurable signals. The incident fundamental fluence is often limited by the sample's optical damage threshold, and signals are usually very weak. Even with an optimal detection system, the signal to noise ratio (SNR) in SHG experiments is limited by the presence of shot noise. It is desirable to amplify the weak spontaneous SHG signal allowing high quality measurements to be taken in a shorter period of time. Such an advance would enable SHG measurements with time and spatial resolution, which are currently infeasible due to intractably long acquisition times resulting from spontaneous SHG's notoriously low SNR. As a major project milestone, we have successfully demonstrated the amplification of weak spontaneous SHG signals by optical stimulation (manuscript in preparation).

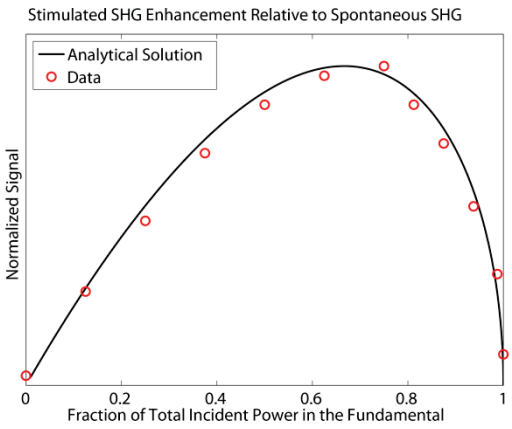

Figure 1. Open circles represent stimulated SHG experiments performed with constant incident power. The horizontal axis describes the fraction of the power in the fundamental field. The black line is the result predicted by the wave mixing formalism.

To assess the feasibility of stimulated SHG, experiments were initially conducted in a model system, β-barium borate (BBO). Experiments with BBO revealed that stimulated SHG is well-modelled by a wave-mixing formalism first described by Armstrong *et al.* in 1962. This model describes plane waves at the fundamental and second harmonic frequencies propagating through a nonlinear medium. The fundamental field generates a nonlinear polarization that radiates the second harmonic, acting as a nonlinear source term in the wave equation for the second harmonic field. As the fields add coherently, energy is transferred between them. This process is described by the coupled set of differential equations,

(1) $\frac{dA_1}{dz} = -\frac{2\omega^2 d_{eff}}{k_1 c^2} A_1 A_2 \sin\theta$

(2) $\frac{dA_2}{dz} = \frac{4\omega^2 d_{eff}}{k_2 c^2} A_1^2 \sin\theta$

(3) $\frac{d\theta}{dz} = \Delta k - 4\omega^2 \frac{d_{eff}}{c^2}\left[\frac{A_2}{k_1} - \frac{A_1^2}{A_2 k_2}\right]\cos\theta$

1 = fundamental, 2 = second harmonic

A_i = field amplitude, k_i = wave vector magnitude

Δk = momentum mismatch, θ = relative phase

d_{eff} = effective nonlinear optical coefficient

In experiments where the interaction length is short, or the sample is weakly nonlinear, the generated signal is described by the derivative, $dA_1^2/dz = 2A_1 dA_1/dz$. From the first equation, this is proportional to $A_1^2 A_2$. The linear dependence of the signal on the second harmonic field amplitude represents the stimulating effect. In the absence of an applied stimulating field, spontaneous SHG still occurs at a low rate in the presence of nonzero vacuum occupation of the stimulating field mode. Maximum enhancement due to stimulation is obtained when two photons at the fundamental frequency are available for every photon at the second harmonic frequency, as shown in Fig. 1. The data (open circles) are plotted on the same graph with the analytical prediction based on the wave mixing formalism (solid line).

Beyond predicting the correct power dependence of stimulated SHG, further insight can be found by examining the system of differential equations. In the first two equations, there is a $\sin(\theta)$ term where θ indicates the relative phase between the fundamental and second harmonic field. This dependence indicates that by altering the relative phase, it is possible to change the direction of power flow between the two fields from second harmonic generation (SHG) to degenerate difference frequency generation (DFG). This is experimentally observed by purposefully cycling the relative phase of the stimulating and fundamental field in increments smaller than the wavelength of an optical cycle. These data are plotted in Fig. 2. As the relative phase is cycled by π, the detected SHG signal fluctuates from in-phase to out-of-phase with the modulated fundamental beam indicating the shift from SHG to DFG. The signal magnitude follows the expected $|\sin\theta|$ dependence described by the system of differential equations. The detected signal magnitude and the lock-in amplifier phase are plotted against the numerically obtained results predicted by the set of coupled differential equations, demonstrating a strong fundamental understanding of stimulated SHG and DFG phenomena.

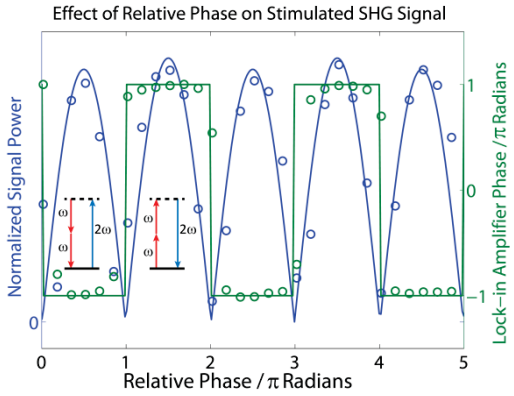

Figure 2. Dependence of the stimulated SHG signal on the relative phase of the two fields. Open circles are experimental data. Lines are predictions of the wave mixing formalism. Blue (left axis) represents the magnitude of the stimulated SHG signal and oscillates with period π. The phase of the signal relative to the chopper is plotted in green and captures transitions between SFG and DFG.

Recent Progress II: *PbS QD Synthesis and Self-Assembly*

Lead sulfide (PbS) nanocrystals, also called quantum dots (QDs) have a size-dependent, tunable near-infrared band gap which makes them particularly attractive for use in photovoltaics, photodetectors, IR-emitting LEDs and lasers, and optoelectronic components at telecom wavelengths. Additionally, PbS QDs have been implicated in a variety of novel photophysics, including multiple exciton generation and hot-electron transfer. Since their band gap is linked to their physical size, it is critical that monodisperse ensembles of QDs can be readily synthesized. Monodispersity provides narrow and well-controlled absorption and emission features – essential for spectroscopic investigations – and maximizes exciton and charge carrier transport efficiency. Despite their technological importance, existing methods for synthesizing PbS QDs cannot produce monodisperse nanocrystals over a wide range of sizes. By carefully controlling the stoichiometric ratio of Pb and S precursors, we have been able to synthesize record-monodispersity PbS QDs over a size range twice as large as was previously attainable (see publication #1).

Due to their monodispersity, the QDs self-assemble into well-ordered two and three dimensional superlattices. Transmission and scanning electron micrographs such superlattices are shown in Fig. 3a-c. Grazing transmission

small-angle X-ray scattering data obtained at Brookhaven National Lab (GT-SAXS; Fig. 3d) confirm the formation of a well-ordered superlattice hundreds of microns large. Furthermore, the wide-angle X-ray scattering data (WAXS; Fig. 3e) show that atomic planes on neighboring nanocrystals are aligned as well. These data reveal a body-centered cubic PbS QD supracrystal with a high degree of structural, orientational, and energetic ordering. Such materials should be highly interesting for the exploration of coherent excitonic phenomena in self-assembled solids.

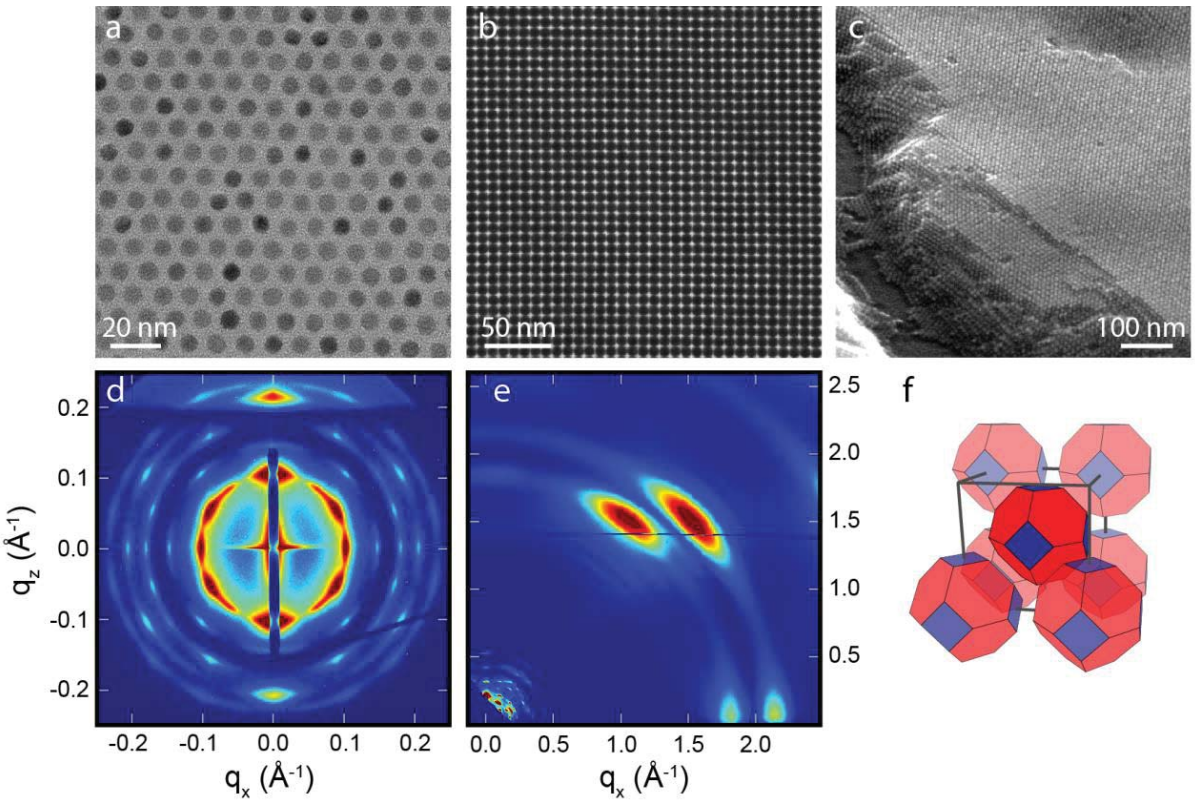

Figure 3. Characterization of a PbS QD superlattice. (a-c) Transmission and scanning electron micrographs showing an ordered arrangement of QDs.(d, e) Small- and wide-angle X-ray scattering, showing body-centered cubic packing and oriented alignment of neighboring atomic lattices. (f) Space-filling model of the aligned BCC superlattice.

Future Plans

Stimulated SHG. Immediate plans are to demonstrate the sensitivity benefits of stimulated SHG in a scientifically interesting system and further quantify the enhancements that are possible *via* this new technique. Additionally, we will soon receive a new ultrafast laser system, which will enable integration into a laser scanning optical microscope.

QD materials. Ongoing work includes tuning interparticle coupling within the self-assembled array *via* ligand exchange, and searching for evidence of coherent exciton delocalization.

CPIMS-Supported Publications (2013-2014)

1. M.C. Weidman, M.E. Beck, R.S. Hoffman, F. Prins, W.A. Tisdale; "Monodisperse, Air-Stable PbS Nanocrystals *via* Precursor Stoichiometry Control," *ACS Nano* **8**, 6363-6371 (2014).

Structural Dynamics in Complex Liquids Studied with Multidimensional Vibrational Spectroscopy

Andrei Tokmakoff

Department of Chemistry, James Franck Institute, and Institute for Biophysical Dynamics
The University of Chicago, Chicago, IL 60637
E-mail: tokmakoff@uchicago.edu

The physical properties of water and aqueous solutions are inextricably linked with efforts to develop new sustainable energy sources. Energy conversion, storage, and transduction processes, particularly those that occur in biology and soft matter, make use of water for the purpose of storing and moving charge. Water's unique physical and chemical properties depend on the ability of water molecules to participate in up to four hydrogen bonds, and the rapid fluctuations and ultrafast energy dissipation of its hydrogen-bonded networks. The goal of our research is a fundamental description of the properties of water at a molecular level, and how it participates in proton transport in aqueous media. Our work over the course of the past year can be divided into four areas: (1) the generation of short pulses of broadband infrared light (BBIR) and use in two-dimensional spectroscopy (2D IR); (2) the investigation of intra- and intermolecular coupling in the vibrational relaxation process in H_2O; and (3) the study of aqueous hydroxide and strong acids to describe the interaction of the ion and water and explore the dynamics of proton transfer in water, and (4) the coupled motion of water and its hydrogen-bonding solutes.

All of the experimental studies of water and aqueous solutions that we have published during the past year have been enabled by our development of a new ultrafast infrared light source that allows unprecedented access to the study of dynamical intermolecular interactions. Our newest spectrometer, built since moving to the University of Chicago last year, uses a laser plasma source to generate coherent pulses of broadband infrared light that are shorter than 70 fs and have a spectrum spanning the entire mid-IR vibrational spectrum, from 3800 cm^{-1} to <1000 cm^{-1}. This source is integrated as a probe pulse in ultrafast pump–probe and 2D IR experiments. In our 2DIR spectrometer, a pulse pair of two 45 fs pulses from a homebuilt OPA source, centered at 3400 cm^{-1}, vibrationally excites the system and the subsequent response is studied using the BBIR as a probe. This capability allows us to correlate the vibrational OH stretching motions in water to other molecular vibrations across the mid-IR. It provides the opportunity to directly observe correlated motion of solute and solvent, and the redistribution and cascade of energy throughout the various states of the system. Our development of this spectrometer continues and future plans involve amplification of this source to use for excitation and detection in 2D IR experiments.

The large bandwidth of our BBIR probe pulse has afforded us the opportunity to study the broad absorption features in neat H_2O. In the broadband 2D IR and transient absorption spectra of H_2O, we observed several unique features that differ qualitatively from the observations of other researchers. The most striking feature is the broad excited state absorption between the $\nu = 1$ and $\nu = 2$ states of the OH stretch, which is over 1000 cm^{-1} broad and relaxes with a 275 fs time constant. Additionally, the long-time transient absorption spectrum characteristic of a temperature rise grows in on a 722 fs timescale resulting in an appreciable amount of low-frequency mode excitation on timescales faster than the period of oscillation. The extreme broadening and ultrafast energy dissipation indicate that the OH stretching vibrations are not localized to a single bond, but rather, the vibrational wave functions are delocalized over many molecules. Further, our 2D IR spectra show that the OH stretch and bend are strongly coupled. Pump-probe anisotropy measurements on the cross-peak showed that there was no correlation between the transition dipole orientation of the OH stretch and the HOH bend—consistent with our conclusions regarding the localized nature of the OH stretch. The rapid growth of the long-time spectrum suggests that it is inappropriate to treat relaxation in the weak coupling limit. We instead attribute the extreme relaxation rate to vibrational non-adiabatic effects arising from strong couplings between the OH

stretching and bending modes and low frequency intermolecular motions. Ongoing work is aimed at theoretically modeling the collective vibrational dynamics of H_2O.

Proton transport in aqueous alkali hydroxide solutions has been described in terms of proton transfer from water to hydroxide resulting in shifting of the OH^- unit in space combined with the interconversion between different solvated structures of the ion. Because of large variation in the strength of hydrogen bonds in this system, the linear IR spectra of aqueous hydroxides show a broad continuum absorption feature across the mid-IR region with a handful of distinguishable features. We have performed BB 2D IR experiments to probe the entire continuum absorption upon exciting OH stretching motion. Our first effort was to draw conclusions as to the origin of the continuum absorption and assign the vibrational features. Our 2D IR spectra showed a distinct band at 2850 cm^{-1} and a cross-peak to a second band at 3250 cm^{-1} that is obscured in the FTIR spectrum beneath the bulk water. In order to help assign the vibrations responsible for the spectral features, we performed a normal mode analysis of solvated hydroxide clusters taken from an empirical valence bond molecular dynamics simulation. From the density of vibrational states (DOS) calculated from ~1000 clusters, we concluded that the 2850 cm^{-1} band involved the asymmetric (*E*) vibration of the OH bonds of the water molecules solvating the ion, whereas the 3250 cm^{-1} band involves the symmetric (A_1) vibration. Furthermore, we find that these stretch vibrations are delocalized over 5–8 water molecules.

Focusing on our long-term objective to characterize the structure and transport of excess protons in water, we have performed BB 2D IR spectroscopy of aqueous strong acids. Similar to hydroxide solutions, excess protons in water give rise to a continuum absorption in the mid-infrared that is largely featureless and spans over 2000 cm^{-1}. This continuum is thought to be related to varying hydrogen bond configurations of the proton, ranging from a hydronium or Eigen complex to a Zundel complex. Rapid interchange between proton configurations is also thought to lead to the observed line broadening. 2D IR spectroscopy reveals that the entire continuum responds immediately upon exciting OH stretching vibrations and the relaxation of this continuum occurs on sub-100 fs timescales. Additionally, we found strong evidence for the presence of Zundel species in the form of a cross-peak between the Zundel bending vibration at 1750 cm^{-1} and the OH stretching vibration of the Zundel flanking waters at 3200 cm^{-1}. Our current data points toward a 250 fs timescale for the exchange time between Zundel species and bulk water. Our ongoing work is aimed at studying spectral regions associated with Eigen complexes, improving vibrational assignments to features within the continuum, and using excitation and probing throughout the IR to follow the ultrafast exchange of proton structures.

Finally, in an effort to understand the 2D IR spectroscopic signatures of a model hydrogen-bonding interaction, we performed BB 2D IR experiments to watch the correlated vibrational motion of the hydrogen bond donor and acceptor. Here we used dimers of N-methylacetamide, in which the N–H group donates a hydrogen bond to the C=O group of another molecule. We identified a series of cross-peaks, which arise solely from the intermolecular interaction, and demonstrated that the N–H C=O and C–N bonds on both partners move synchronously as a result of the hydrogen bond. These results are being extended to water–solute systems, where the water forms a hydrogen bond with the solute.

DOE Supported Publications (2011-2014)

1. "A Fast-Scanning Fourier Transform 2D IR Interferometer," Sean T. Roberts, Joseph J. Loparo, Krupa Ramasesha, and Andrei Tokmakoff, *Optics Communications*, **284** (2011) 1062–1066.
2. "Proton Transfer in Concentrated Aqueous Hydroxide Visualized using Ultrafast Infrared Spectroscopy," Sean T. Roberts, Krupa Ramasesha, Poul B. Petersen, Aritra Mandal, and Andrei Tokmakoff, *Journal of Physical Chemistry A*, **115** (2011) 3957–3972.
3. "Collective Hydrogen Bond Reorganization in Water Studied with Temperature-Dependent Ultrafast Infrared Spectroscopy," Rebecca A. Nicodemus, S. A. Corcelli, J. L. Skinner, and Andrei Tokmakoff, *Journal of Physical Chemistry B*, **115** (2011) 5604–5616.
4. "Ultrafast 2D IR Anisotropy of Water Reveals Reorientation during Hydrogen-Bond Switching," Krupa Ramasesha, Sean T. Roberts, Rebecca A. Nicodemus, Aritra Mandal and Andrei Tokmakoff, *Journal of Chemical Physics*, **135** (2011) 054509.
5. "A Phenomenological Approach to Modeling Chemical Dynamics in Nonlinear and Two-Dimensional Spectroscopy," Krupa Ramasesha, Luigi De Marco, Andrew D. Horning, Aritra Mandal, and Andrei Tokmakoff, *Journal of Chemical Physics*, **135** (2012) 134507.
6. "Experimental Evidence of Fermi Resonances in Isotopically Dilute Water from Ultrafast Broadband IR Spectroscopy," Luigi De Marco, Krupa Ramasesha, and Andrei Tokmakoff, *Journal of Physical Chemistry B*, **117** (2013) 15319–15327.
7. "Water Vibrations have Strongly Mixed Intra- and Inter-Molecular Character," Krupa Ramasesha, Luigi De Marco, Aritra Mandal, and Andrei Tokmakoff, *Nature Chemistry*, (2013) **5** (2013) 935–940.
8. "Local and Collective Reaction Coordinates in the Transport of the Aqueous Hydroxide Ion," Sean T. Roberts, Aritra Mandal, and Andrei Tokmakoff, *Journal of Physical Chemistry B*, **118** (2014) 8062–8069.
9. "Collective Vibrations of Water-Solvated Hydroxide Ions Investigated with Broadband 2D IR Spectroscopy," Aritra Mandal, Krupa Ramasesha, Luigi De Marco, and Andrei Tokmakoff, *Journal of Chemical Physics*, **140** (2014) 204508.
10. "Direct Observation of Intermolecular Interactions Mediated by Hydrogen Bonding," Luigi De Marco, Martin Thämer, Mike Reppert, and Andrei Tokmakoff, *Journal of Chemical Physics*, **141** (2014) 034502.

The Role of Electronic Excitations on Chemical Reaction Dynamics at Metal, Semiconductor and Nanoparticle Surfaces

John C. Tully
Department of Chemistry, YaleUniversity, 225 Prospect Street, P. O. Box 208107, New Haven, CT, 06520-8107 USA
john.tully@yale.edu

Program Scope

Achieving enhanced control of the rates and molecular pathways of chemical reactions at the surfaces of metals, semiconductors and nanoparticles will have impact in many fields of science and engineering, including heterogeneous catalysis, photocatalysis, materials processing, corrosion, solar energy conversion and nanoscience. However, our current atomic-level understanding of chemical reactions at surfaces is incomplete and flawed. Conventional theories of chemical dynamics are based on the Born-Oppenheimer separation of electronic and nuclear motion. Even when describing dynamics at metal surfaces where it has long been recognized that the Born-Oppenheimer approximation is not valid, the conventional approach is still used, perhaps patched up by introducing friction to account for electron-hole pair excitations or curve crossings to account for electron transfer. There is growing experimental evidence that this is not adequate. We are examining the influence of electronic transitions on chemical reaction dynamics at metal and semiconductor surfaces. Our program includes the development of new theoretical and computational methods for nonadiabatic dynamics at surfaces, as well as the application of these methods to specific chemical systems of experimental attention. Our objective is not only to advance our ability to simulate experiments quantitatively, but also to construct the theoretical framework for understanding the underlying factors that govern molecular motion at surfaces and to aid in the conception of new experiments that most directly probe the critical issues.

Recent Progress

Independent Electron Surface Hopping (IESH)

We have now completed a thorough testing of IESH on NO scattering from Au(111) in which the N—O stretching coordinate is treated by quantum mechanics. This is the first attempt of which we are aware to combine quantum mechanical electronic and vibrational transitions on an equal footing by surface hopping. Our studies demonstrate: (1) Such calculations are computationally feasible, albeit more laborious than our prior IESH simulations with the N—O vibration treated classically. Including N quantum vibrational modes for each electronic state increases the number of quantum levels by a factor of N, resulting in roughly a factor of N to N^2 increase in computational cost. (2) The classical vibration and quantum vibration results for state-to-state vibrational excitation of scattering of NO (v=0) are in surprisingly good accord.This is not necessarily expected, since vibrational spacings of NO are large compared to kT and because classical simulations must impose a somewhat arbitrary procedure to bin the final vibrational energies in order to compare to quantum mechanical state populations. (3) The quantum vibration simulations are in quite good accord with state-selected measurements of vibrational excitation of NO (v=0) scattered from the Au(111) surface measured by the Göttingen group headed by Alec Wodtke. The comparison of experiment and IESH, with

classical treatment of NO vibration, was published in 2012. A manuscript reporting the quantized vibration results is in preparation. The success of this procedure for employing surface hopping to describe quantum mechanical transitions involving both electronic and nuclear degrees of freedom simultaneously promises to open up the possibility of simulating new classes of nonadiabatic dynamics, notably proton coupled electron transfer.

Exact Potential Energy Surfaces for Nonadiabatic Dynamics

An underlying goal of our research program is to develop a theoretical framework for simulating molecular dynamics subject to motion on multiple potential energy surfaces, i.e., nonadiabatic molecular dynamics. E. K. U. Gross and coworkers (*J. Chem. Phys*. **137**, 22A530, 2012) have recently derived an "exact" factorization of the total molecular wavefunction into electronic and nuclear factors. The solution looks like the adiabatic (Born-Oppenheimer) approximation, but with full inclusion of nonadiabatic interactions. This is a very appealing idea. Whereas accurate solution of these equations must ultimately be equivalent to quantum mechanical evolution on multiple states, there may be computational advantages and, in any case, the simplified form of the wavefunction may suggest new approximations and new insights. We have made a preliminary examination of this approach, applying it to several model problems that exhibit two coupled electronic states and for which numerically exact quantum solutions can be obtained by conventional methods. First, our results verify that the exact factorization method does indeed reproduce the exact results. However, the potential energy surfaces that emerge can display severe spatial and time dependences. Moreover, the potential energy surfaces are not unique. The non-uniqueness results from the fact that multiplying the nuclear wavefunction by any arbitrary phase factor $\exp[-S(R,t)]$, with $S(R,t)$ real-valued, and multiplying the electronic wavefunction by the conjugate factor $\exp[+S(R,t)]$ does not change the overall wavefunction, but it does alter the potential energy surface governing nuclear motion. A number of interesting results have emerged from our calculations. For example, for the simple parabolic double well with constant coupling, the exact potential energy surface exhibits a higher barrier than the adiabatic potential energy surface, as is necessary to reproduce the reduction in tunneling rate due to nonadiabatic interactions with the upper electronic state.

The Influence of Phase Transitions on Chemical Reaction Rates

The experimental group of Elsa C. Y. Yan (Yale University) has recently measured the thermal rate of isomerization of the 11-cis retinyl chromophore in the visual pigment rhodopsin, <u>in the absence of light</u>. The motivation for this study was to put limits on the dark noise, i.e., the background signal in the dark that limits vision in dim light. In the course of this study they made a remarkable discovery: at temperatures between 52.0 and 64.6°C, the measured rate constants fit well to an Arrhenius straight line with, however, an unexpectedly large activation energy of 114 ± 8 kcal/mol, much larger than the 60 kcal/mol photoactivation energy at 500 nm. Moreover, they obtained an unprecedentedly large prefactor of $10^{72 \pm 5}$ s^{-1}, about 45 orders of magnitude larger than any previously reported prefactor for a unimolecular reaction and 60 orders of magnitude larger than typical frequencies of molecular motions! At lower temperatures the measured Arrhenius parameters were found to be more normal: E_a = 22 ± 2 kcal/mol and $A_{pref} = 10^{9 \pm 1}$ s^{-1} in the range 37.0 – 44.5°C. We have developed a model, based on transition state theory (TST), that convincingly explains this very unusual and surprising behavior. A key factor is that the temperatures for which the huge values of E_a and A_{pref} were found were fairly close to the 71°C melting temperature of the rhodopsin protein. A second key,

supported by QM/MM calculations by the group of Victor Batista (Yale University), is that the reaction barrier is somewhat lower when the protein is melted than when the chromophore is more constrained in the folded state. This barrier lowering produces a driving force to lower the melting temperature when the system is constrained to be at the transition state. If the initial state is ordered and the transition state is partially or completely melted, there will be huge increases in both the enthalpy and entropy of activation, as observed. At lower temperatures where both the initial and transition states are ordered, and at higher temperatures where both states are disordered, activation energies and entropies will be more normal, producing distinct "elbows" in the Arrhenius plot. This behavior may well prove to be quite general, not only in biological reactions, but also in condensed phase and surface reactions carried out at temperatures and pressures close to 2D or 3D phase transitions. The theoretical model underlying these observations was derived by the PI under this DOE grant. The qualitative picture emerging from the model was published recently in *PNAS*. A paper presenting the theoretical details is in preparation.

Future Plans

Constrained Density Functional Theory

We plan to further develop constrained density functional theory (CDFT) for computing "diabatic" potential energy surfaces and their off-diagonal couplings for molecules interacting with surfaces. The IESH method appears capable of accurately simulating nonadiabatic dynamics at metal and semiconductor surfaces, provided the required input is available and reliable. The necessary input is a diabatic Hamiltonian matrix that accurately represents the charge and excited states of the molecule embedded in the continuum of conduction band levels, and does so for all relevant molecule and surface atom positions. For NO interacting with the gold surface, we were able to construct a satisfactory diabatic Hamiltonian using density functional theory with the application of fictitious electric fields to modulate the energies of ionic states. This procedure is not applicable to most systems of experimental interest, however. The most critical challenge to further progress is to develop more generally applicable *ab initio* procedures for computing the necessary diabatic Hamiltonians. We propose to further develop and apply CDFT for this purpose. CDFT is conceptually simple; a DFT calculation is carried out with an imposed constraint, such as constraining the net local charge on a molecule to be negative one. This will produce the lowest energy potential energy surface consistent with this charge constraint. This can be repeated with different constraints to produce diagonal elements of the desired diabatic Hamiltonian. However, there are unsolved issues with computing the off-diagonal elements, including the absence of a proper wave function in DFT and non-orthogonality of Kohn-Sham determinants corresponding to different constraints. We will address these issues. In particular, we are exploring the possibility of enforcing orthogonality via an additional constraint. As we overcome these obstacles, we will apply this approach to two important adsorbate-surface interactions. The first will be hydrogen atom scattering from metals, particularly gold and silver, currently under experimental study by the Wodtke group. Second, we will apply CDFT with spin constraints to oxygen atoms and oxygen molecules interacting with metals surfaces. For both of these adsorbates, transitions between the ground state triplet and low-lying singlet states can occur without spin-orbit interactions via a two-electron exchange with the conduction band, possibly with major implications to chemical reactivity.

Exact Potential Energy Surfaces for Nonadiabatic Dynamics

As discussed above, a number of compelling research directions are suggested by the prospect of factoring the total electronic-nuclear wavefunction exactly for nonadiabatic dynamics. We plan to pursue this project with emphasis on three aspects. First, we will explore optimal ways to choose the arbitrary phase factor so as to either simplify computational effort or reveal insights, or both. The choice of phase is related to the choice of representation, i.e., diabatic or adiabatic, but their precise relationship is not direct, nor is it understood. Second, we will attempt to develop practical methods in which nuclear motion is propagated classically but governed by the exact potential energy surface, in contrast to current Ehrenfest and surface hopping methods. If successful, this strategy could be particularly advantageous for nonadiabatic dynamics at metal and semiconductor surfaces by avoiding the somewhat cumbersome discretization of the electronic continuum required by our IESH method. Third, while exact, it is not obvious how nuclear motion evolving on a single potential energy surface can properly describe situations where discrete transitions occur between different electronic states. We will examine this question in the context of the surface hopping theory which, although very different in flavor, often provides an accurate description of nuclear motion subject to multiple potential energy surfaces.

The Influence of Phase Transitions on Chemical Reaction Rates

The PI is developing a mean-field-based quantitative model to place this phenomenon on a more solid footing. Ongoing experiments in the Yan group on various mutant proteins will provide the data against which to validate the model. In addition, molecular dynamics simulations, with appropriately designed non-Boltzmann sampling methods, will be used to compute the huge changes in activation enthalpy and entropy that occur near the melting temperature, and to monitor the nature and degree of disorder in the isomerizing protein.

References to Publications of DOE-Sponsored Research in last two years:

Nonadiabatic dynamics at metal surfaces: Independent electron surface hopping with phonon and electron thermostats, N. Shenvi, J. C. Tully, *Faraday Disc***157**, 325-335 (2012).

Unusual Kinetics of Thermal Decay of Dim-Light Photoreceptors in Vertebrate Vision, Y. Guo, S. Sekharan, J. Liu, V. S. Batista, J. C. Tully*, E. C. Y. Yan*, *PNAS***111**, 10438-10443, (2014).

Reactive Processes in Aqueous Environment

Marat Valiev
[1]Environmental Molecular Sciences Laboratory and
Pacific Northwest National Laboratory
902 Battelle Blvd.
Mail Stop K9-90
Richland, WA 99352
marat.valiev@pnl.gov

The major objective of our research is to gain fundamental understanding of reactive processes in aqueous systems ranging from clusters to bulk solvation environments. We are interested in the impact of solvation environment on the specific observable properties of the solute molecules, as well as the effect of the solute specific properties on the solvent structure. Our investigation is focused mainly on polyatomic solutes, which can adopt different structural forms, electronic states, and tautomeric configurations.

One of the important directions in our research is to provide molecular-level understanding of selectivity and specificity effects of ion solvation in aqueous environments. It is now accepted that the spherically symmetric representation of the solute species gives inadequate description even in the case of monoatomic ions. In the latter case the first non-vanishing symmetry-breaking contribution comes from the induced dipole moment proving to be critical for understanding the surface propensity of these species on the basis of their size and polarizability (soft vs. hard). The effects of solute anisotropy are expected to be even more important for the solvation of complex polyatomic species. Unlike monatomic ions, the presence of internal molecular structure leads to permanent inhomogeneities in the charge density distribution, which can have a bigger impact on the solute-solvent interactions than induced (polarization) effects. Similar to polarization, these charge density distribution effects are specific (they depend on the particular molecule) and have an inherent capacity to differentiate or select between bulk (isotropic) and surface (anisotropic) solvent environments. Our research is aimed to provide first-principles

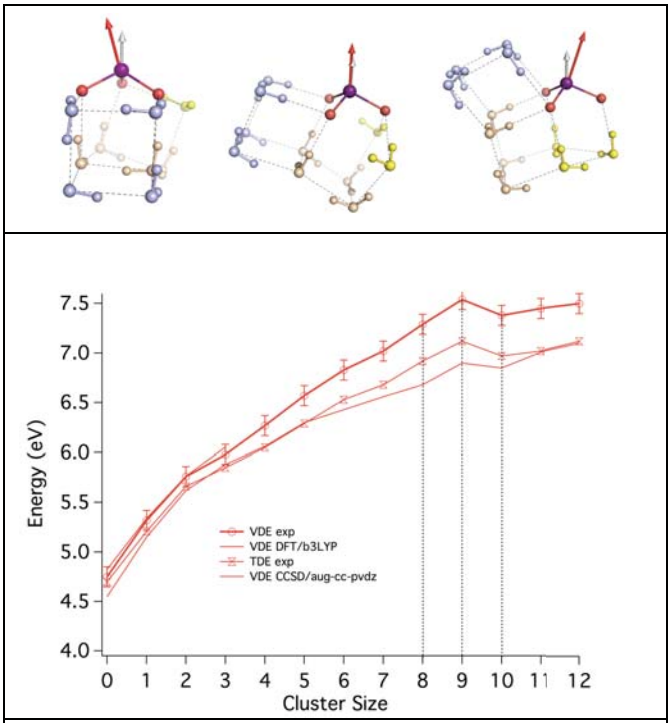

Figure 1: (top) global minimum structures of n= 9, 10, 11 iodate water cluster; (bottom) comparison between experimental and calculated EBE binding energy as a function of water cluster size.

description of these effects based on combined molecular modeling in conjunction with experimental photoelectron spectroscopy (PES) measurements performed by Dr. Xuebin Wang (PNNL). The relevant quantity of interest is the electron binding energy (EBE) – the vertical energy difference between the anion and neutral complex at the stable structure of the anion. Sensitive to the solvent environment, the EBE provides a precise measure of the incremental solvation process. The absence of "bulk" solvent in the cluster environment exposes the fine details of the solute-solvent interactions and provides an ideal setting to assess the potential impact of charge anisotropy effects. The latter can have a significant impact on the PES spectrum, as was the case with iodate $(IO_3^-)(H_2O)_n$ water clusters that showed an unusual drop in EBE value at n=10 (see Fig.1). Our investigation showed that this anomalous behavior is a result of strong anisotropic effects resulting from highly ordered solvent structure. These results indicate the observed PES anomaly that may be a general feature in the cluster solvation of polyatomic solutes. Currently we are investigating SCN-, which also exhibits an unusual signature PES spectrum.

In addition to bulk aqueous environment, we are also investigating chemical properties of radical anion species in cluster environments. In particular, we have studied the effects of amine group functionalization of dicarboxylates ($^-CO_2–(CH_2)_n–CO_2^-$, n=2, 3), which results in well known aspartate and glutamate amino acids. Combining ab-initio calculations with experimental PES measurements performed by Dr. Xuebin Wang, we have determined that for singlet dianion states, the addition of amine group results leads to the increase of vertical electron binding energies. For the anion radical states, the main effect is the appearance of resonance structure, which weakens the binding of adjacent carboxylate group. The reduced binding of the carboxylate group observed computationally suggests the increase in the rate of post photo-detachment auto-decarboxylation reaction of radical species, which is confirmed experimentally by the enhanced production of zero kinetic energy electrons.

Another direction of our research is focused on fundamental chemistry of radical and anion molecular species in aqueous solution. This work is done in close collaboration with Sergei Lymar at BNL and aimed at understanding thermodynamics, electronic structure, and reactivity of nitrogen-oxide base compounds. The two systems that are of particular interest to us are NONOate (XN(O)NO-) and nitrate/nitrite systems. NONOates compounds can be viewed as adducts of NO dimer with general electron donating group X^-. The latter provides the necessary "electron" glue that holds together otherwise weakly bound NO dimers. Depending on nature of the electron-donating group the strength of this bond can be varied, which can be employed in the engineered delivery of

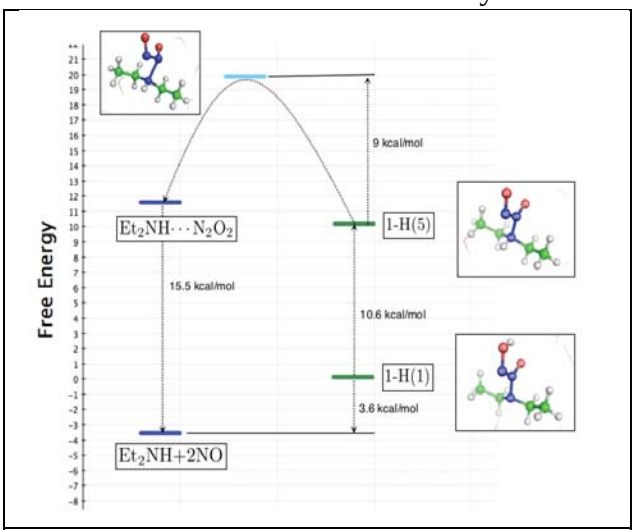

Figure 2: Thermodynamic cycle of pH-driven NO release in amino NONOate.

NO species. In our earlier work, we have investigated the case of X = e- resulting in hyponitrite radical N(O)NO- species. Presently we are looking at other members of NONOate family – amino NONOates ($X=Et_2N^-$) and Angeli salt ($X=O_2^-$). In addition to equilibrium properties, our investigation is also focused on the kinetics of the pH-induced NO release(see Fig. 2). The challenging feature of these systems is that high levels of ab-initio theory (e.g. CCSD(T)) are require for proper description of electron correlation effects.

Both of the application areas discussed above require high levels of ab-initio treatment to properly capture the changes in the electronic structure as well as the sufficient amount of statistical sampling to account for the aqueous environment. While QM/MM approach remains our main method for these types of simulations, we are investigating other methodologies including combination of quantum mechanical and classical density functional approach (QM/cDFT).

1. G. N. Chuev, M. Valiev, and Mq. V. Fedotova, (2012). “Integral Equation Theory of Molecular Solvation Coupled with Quantum Mechanical/Molecular Mechanics Method in NWChem Package”, Journal of Chemical Theory and Computation, 8, 1246-54.
2. G. Murdachaew, M. Valiev, S. M. Kathmann, and X. B. Wang, (2012). “Study of Ion Specific Interactions of Alkali Cations with Dicarboxylate Dianions”, Journal of Physical Chemistry A, 116, 2055-61.
3. T. T. Wang, H. Y. Yin, D. Y. Wang, and M. Valiev, (2012). “Hybrid Quantum Mechanical and Molecular Mechanics Study of the S(N)2 Reaction of Ccl4 + Oh- in Aqueous Solution: The Potential of Mean Force, Reaction Energetics, and Rate Constants”, 116 , 2371-76.
4. Benjamin E. Van Kuiken, Marat Valiev, Stephanie L. Daifuku, Caitlin Bannan, Matthew L. Strader, Hana Cho, Nils Huse, Robert W. Schoenlein, Niranjan Govind, and Munira Khalil: Simulating Ru L3-Edge X-ray Absorption Spectroscopy with Time-Dependent Density Functional Theory: Model Complexes and Electron Localization in Mixed-Valence Metal Dimers, *The Journal of Physical Chemistry A* 2013 *117* (21), 4444-4454
5. Wen, H.; Hou, G.-L.; Kathmann, S. M.; Valiev, M.; Wang, X.-B.: Communication: Solute anisotropy effects in hydrated anion and neutral clusters. *The Journal of Chemical Physics* 2013, *138*, 031101.
6. Sellner, B.; Valiev, M.; Kathmann, S. M.: Charge and Electric Field Fluctuations in Aqueous NaCl Electrolytes. *The Journal of Physical Chemistry B* 2013.
7. Shihu H. M. Deng, Gao-Lei Hou, Xiang-Yu Kong, Marat Valiev, and Xue-Bin Wang: Examining the Amine Functionalization in Dicarboxylates: Photoelectron Spectroscopy and Theoretical Studies of Aspartate and Glutamate. *The Journal of Physical Chemistry A* **2014** *118* (28), 5256-5262
8. Shaikh N, Marat Valiev, V. Shafirovich, and S.V. Lymar: Decomposition of Amino Diazeniumdiolates (NONOates): Molecular Mechanisms, Inorganic Chemistry, 2014 (accepted)

Probing the Actinide-Ligand Binding and the Electronic Structure of Gaseous Actinide Molecules and Clusters Using Anion Photoelectron Spectroscopy

PI: Lai-Sheng Wang

Department of Chemistry
Brown University
324 Brook Street
Providence, RI 02912
Email: lai-sheng_wang@brown.edu

Program Scope

The broad scope of this program is to better understand actinide chemistry using new spectroscopic techniques and to provide accurate spectroscopic data for the validation of new theoretical methods aimed at actinide chemistry. This program contains three thrust areas:

- probing ligand-uranyl (UO_2^{2+}) interactions in gaseous anionic complexes in the form of $[UO_2L_x]^{n-}$ produced by electrospray ionization
- probing the electronic structure and bonding of inorganic and organometallic compounds of actinides in the gas phase
- probing the metal-metal bonding and size-dependent electronic structures in U_x^-, $U_xO_y^-$, and $U_xF_y^-$ clusters as a function of size and composition.

Understanding the chemistry of the actinide elements is of critical importance to the mission of DOE. My group has developed a number of experimental apparatuses, including a magnetic-bottle photoelectron spectroscopy instrument equipped with a laser vaporization supersonic cluster source, a combined photoelectron imaging and magnetic-bottle instrument equipped with an electrospray ionization source, and a newly-built high-resolution photoelectron imaging system equipped with a laser vaporization cluster source. This suite of state-of-the-art instruments are uniquely suitable to investigate the three classes of actinide compounds. Photodetachment involves removal of electrons from occupied molecular orbitals and probes directly the chemical bonding properties of the underlying molecular species. Photoelectron spectroscopy of anions yields electron affinities and low-lying electronic state information for the corresponding neutral species. The application of *anion* photoelectron spectroscopy to actinide molecules opens up new research opportunities and yields accurate and systematic electronic structure and spectroscopic information that can be used to verify computational methods and advance our understanding of the reactivity, structure, and bonding of actinide molecules.

Recent Progress (August 2013 to August 2014)

In this funding period, we have made significant progresses in the investigation of monouranium fluoride and oxide complexes (UF_x^- and UO_x^-), as well as UCl_6^- and UCl_6^{2-}. In particular, we have been able to obtain vibrationally-resolved photoelectron spectra for UO^- and UO_2^- for the first time, using our newly-built photoelectron imaging system. A publication is under preparation for the new results. We have also constructed a second-generation temperature-controlled ion trap, which allows us to produce cold anions and significantly enhanced our ability to obtain well-resolved photoelectron spectra. Preliminary data have been obtained on UCl_6^- and UO_6^{2-}. The photoelectron data on these hexachloride complexes are in contrast with the hexafluoride counterparts. We were able to observe strong mass signals for

UF_6^- previously, but were not able to measure its photoelectron spectra, due to the extremely low detachment cross sections of the 5f electrons.[2] Our new data on UCl_6^- and UCl_6^{2-} are being analyzed and prepared for publication.

Strong Electron Correlation in UO_2^-: A Photoelectron Spectroscopy and Relativistic Quantum Chemistry Study. The electronic structures of actinide systems are extremely complicated and pose considerable challenges both experimentally and theoretically because of significant electron correlation and relativistic effects. We have investigated the electronic structure and chemical bonding of uranium dioxides, UO_2^- and UO_2, using photoelectron spectroscopy and relativistic quantum chemistry. Photoelectron spectra of UO_2^- were measured at four different photon energies (**Fig. 1**). The electron affinity of UO_2 is measured to be 1.159(20) eV. Intense detachment bands are observed from the UO_2^- low-lying $(7s\sigma_g)^2(5f\phi_u)^1$ orbitals (labeled as X, A, B) and the more deeply-bound O2p-based molecular orbitals (labeled as D and E), which are separated by a large energy gap from the U-based orbitals (**Fig. 1d**). Remarkably, numerous weak photodetachment transitions are observed in the gap region due to extensive two-electron transitions (features labeled as b to s), suggesting strong electron correlations among the $(7s\sigma_g)^2(5f\phi_u)^1$ electrons in UO_2^- and the $(7s\sigma_g)^1(5f\phi_u)^1$ electrons in UO_2. These observations are interpreted using multi-reference *ab initio* calculations with inclusion of spin-orbit coupling. The strong electron correlations and spin-orbit couplings generate orders-of-magnitude more detachment transitions from UO_2^- than expected on the basis of the Koopmans' theorem. The current experimental data on UO_2^- provide a long-sought opportunity to arbitrating various relativistic quantum chemistry methods aimed at handling systems with strong electron correlations.

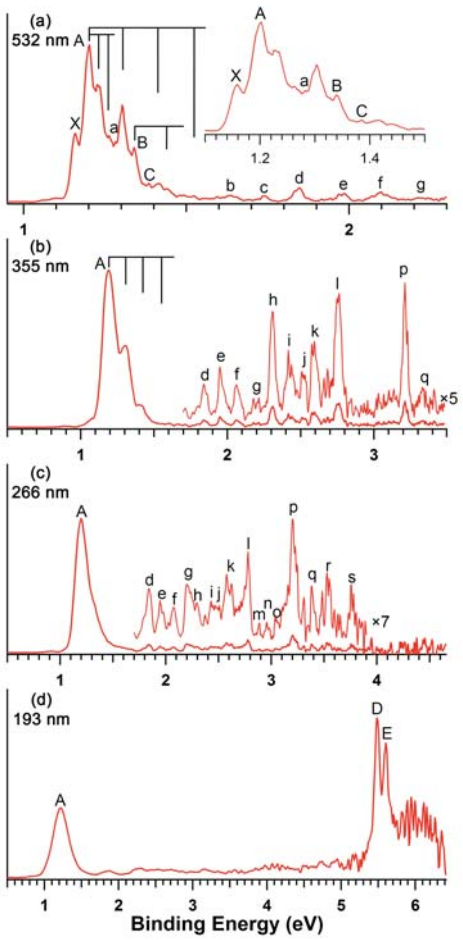

Fig. 1. Photoelectron spectra of UO_2^- at (a) 532 nm, (b) 355 nm, (c) 266 nm and (d) 193 nm.

Probing the Electronic Structures of Low Oxidation-State Uranium Fluoride Molecules UF_x^- (x = 2−4). We have produced gaseous UF_x^- (x = 2−4) anions and investigated their electronic structure and U−F bonding using photoelectron spectroscopy and relativistic quantum chemistry. Vibrationally-resolved photoelectron spectra are obtained for all three monouranium fluoride species and the electron affinities of UF_x (x = 2−4) are measured to be 1.16(3), 1.09(3), and 1.58(3) eV, respectively. Significant multi-electron transitions are observed in the photoelectron spectra of $U(5f^37s^2)F_2^-$, as a result of strong electron correlation effects of the two 7s electrons. The U−F symmetric stretching vibrational modes are resolved for the ground states of all UF_x (x = 2−4) neutrals. Theoretical calculations are performed to qualitatively understand the photoelectron spectra. The entire UF_x^- and UF_x (x = 1−6) series are considered theoretically to examine the trends of U−F bonding and the electron affinities as a function of fluorine coordination. The increased U−F bond lengths and decreased bond orders

from UF_2^- to UF_4^- indicate that the U−F bonding becomes weaker as the oxidation state of U increases from I to III.

A High-Resolution Velocity-Map Photoelectron Imaging Study on UO^- and UO_2^-. Using our newly-built high-resolution velocity-map imaging system, we have obtained preliminary highly-resolved photoelectron spectra for UO^- and UO_2^- (**Fig. 2**). The new spectra for UO_2^- are consistent with those shown in **Fig. 1a**, but are much highly resolved. The electron affinities of UO and UO_2 are measured accurately as 1.1407 ± 0.0007 eV and 1.1688 ± 0.0006 eV, respectively. In addition, the new data allow as to obtain vibrational frequencies for the symmetric U–O stretching modes for the neutral ground state, anionic ground state, and two neutral excited states for UO_2, along with the bending mode for the neutral ground state. Vibrational frequencies for the U–O stretching are also measured for the ground and first excited state of UO. These preliminary results for UO and UO_2 are in good agreement with previous experimental and theoretical studies. Such highly accurate experimental data on the ground and low-lying excited states of the simplest uranium oxide molecules provide much better benchmarks for theoretical methods. These data also suggest that high-resolution photoelectron spectral data on these actinide systems are complementary and comparable to optical experiments, such as resonant-two photon ionization spectroscopy.

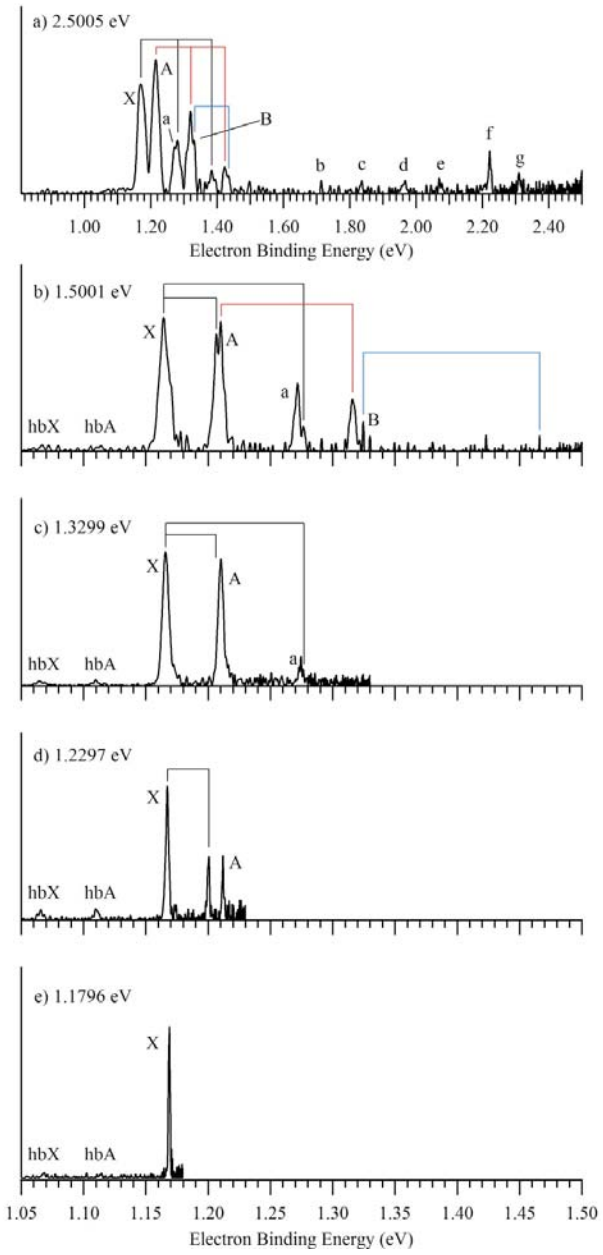

Fig. 2. High-resolution photoelectron spectra of UO_2^- at photon energies between 1.1796 and 2.5005 eV, using velocity-map imaging. The labeled features are the same as in Fig. 1. Vibrational progressions are indicated.

Future Plans

In the next funding period, we will continue to investigate the uranium oxide and fluoride systems using both our magnetic-bottle photoelectron apparatus and the high-resolution velocity-map imaging system. We will extend the monouranium systems to include higher oxides, UO_x^- (x = 3–6). Studies on multi-nuclear uranium oxides ($U_xO_y^-$) will be initiated to study the U–U bonding. Mixed uranium oxide and fluoride systems have also been observed in our cluster source and will be investigated. In addition, we will complete the study on UCl_6^- and UCl_6^{2-}.

Publications from DOE Supported Research (FY12-FY14)

1. "Observation and Investigation of the Uranyl Tetrafluoride Dianion ($UO_2F_4^{2-}$) and Its Solvation Complexes with Water and Acetonitrile" (P. D. Dau, J. Su, H. T. Liu, J. B. Liu, D. L. Huang, J. Li, and L. S. Wang), *Chem. Sci*. **3**, 1137-1146 (2012). (DOI: 10.1039/c2sc01052f)

2. "Photoelectron Spectroscopy and Theoretical Studies of UF_5^- and UF_6^-" (P. D. Dau, J. Su, H. T. Liu, D. L. Huang, F. Wei, J. Li, and L. S. Wang), *J. Chem. Phys.* **136**, 194304 (2012). (DOI: 10.1063/1.4716182)

3. "Photoelectron Spectroscopy and the Electronic Structure of the Uranyl Tetrachloride Dianion: $UO_2Cl_4^{2-}$" (P. D. Dau, J. Su, H. T. Liu, D. L. Huang, J. Li, and L. S. Wang), *J. Chem. Phys.* **137**, 064315 (8) (2012). (DOI: 10.1063/1.4742062)

4. "Photoelectron Spectroscopy of Cold UF_5^-" (P. D. Dau, H. T. Liu, D. L. Huang, and L. S. Wang) *J. Chem. Phys*. **137**, 116101 (2) (2012). (DOI: 10.1063/1.4753421)

5. "Probing the Electronic Structure and Chemical Bonding in Tricoordinate Uranyl Complexes $UO_2X_3^-$ (X = F, Cl, Br, I): Competition between Coulomb Repulsion and U–X Bonding" (J. Su, P. D. Dau, Y. H. Qiu, H. T. Liu, C. F. Xu, D. L. Huang, L. S. Wang, and J. Li), *Inorg. Chem*. **52**, 6617-6626 (2013). (DOI: 10.1021/ic4006482)

6. "A Joint Photoelectron Spectroscopy and Theoretical Study on the Electronic Structure of UCl_5^- and UCl_5" (J. Su, P. D. Dau, C. F. Xu, D. L. Huang, H. T. Liu, F. Wei, L. S. Wang, and J. Li, *Chem. Asian J.*, Jul 12, 2013. (DOI: 10.1002/asia.201300627)

7. "Probing the Electronic Structures of Low Oxidation-State Uranium Fluoride Molecules UF_x^- (x = 2−4)" (W. L. Li, H. S. Hu, T. Jian, G. V. Lopez, J. Su, J. Li, and L. S. Wang), *J. Chem. Phys.* 139, 244303 (2013). (DOI: 10.1063/1.48514750)

8. "Strong Electron Correlation in UO_2^-: A Photoelectron Spectroscopy and Relativistic Quantum Chemistry Study" (W. L. Li, J. Su, T. Jian, G. V. Lopez, H. S. Hu, G. J. Cao, J. Li, and L. S. Wang), *J. Chem. Phys*. **140**, 084306 (9 pages) (2014). (DOI: 10.1063/1.4867278).

Chemical Kinetics and Dynamics at Interfaces

Cluster Model Investigation of Condensed Phase Phenomena

Xue-Bin Wang
Physical Sciences Division, Pacific Northwest National Laboratory, P.O. Box 999, MS K8-88, Richland, WA 99352. E-mail: xuebin.wang@pnnl.gov

Program Scope

We aim at obtaining a microscopic understanding of solution chemistry and condensed phase phenomena using gas phase clusters as model systems. Clusters occupy an intermediate region between gas phase molecules and the condensed states of matter and play an important role in heterogeneous catalysis, aerosol chemistry, and biological processes. We use electrospray ionization (ESI) to generate a wide variety of molecular and ionic clusters to simulate key species involved in the condensed phase reactions and transformations, and characterize them using low temperature, and temperature-controlled negative ion photoelectron spectroscopy (NIPES). Inter- and intra-molecular interactions and their variation as function of size and composition, important to understand complex chemical reactions and nucleation processes in condensed and interfacial phases can be directly obtained. Experiments and *ab initio* calculations are synergistically combined to (1) probe solute anisotropic effects in hydrated anion and neutral clusters; (2) obtain a molecular-level understanding of the solvation and stabilization of complex singly- and multiply-charged anions important in condensed phases; (3) quantify thermodynamic driving forces resulted from hydrogen-bonded networks formed in aerosol nucleation processes and enzymatic catalytic reactions; (4) study temperature-dependent conformation changes and isomer populations of complex solvated clusters; (5) investigate intrinsic electronic structures of environmentally and catalytically important species and reactive diradicals; and (6) understand the molecular processes and initial steps of dissolution of salt molecules in polar solvents. The central theme of this research program lies at obtaining a fundamental understanding of environmental materials and solution chemistry important to many primary DOE missions (waste storage, subsurface and atmospheric contaminant transport, catalysis, etc.), and enhances scientific synergies between experimental and theoretical studies towards achieving such goals.

Recent Progress

Study of ion specific effects in solvation and cation-anion interactions: Specific ion effects are ubiquitous in solvation and play important roles in biological processes and functions. Collaborating with PNNL theoreticians, Drs. Valiev and Kathmann, we provided compelling experimental and theoretical evidence that the anisotropic nature of complex polyoxyanion solutes can have a critical influence on the solvation process. Combined photoelectron spectroscopy and theoretical modeling results show that the electron binding energy of $IO_3^-(H_2O)_n$ (n = 0 – 12) clusters is characterized by an anomalous drop at n = 10. Such behavior is unprecedented for rigid solute molecules, and is related to the anisotropy of the neutral iodate radical that displays a strong selectivity to solvent configurations generated by the charged anion complex (Wen, Hou, Kathmann, Valiev, and Wang, **2013**. *J. Chem. Phys. 138*, 031101). We also carried out a direct spectroscopic probe of interactions between alkali metal cations with a series of differently sized dicarboxylate dianions in simulating cation-anion specific interactions, which demonstrates the delicate interplay among several factors (electrostatic interaction, size matching, and strain energy) that play critical roles in determining the structures and energetics of gaseous clusters as well as ion specificity and selectivity in solutions and biological systems (Murdachaew, Valiev, Kathmann, and Wang **2012**. *J. Phys. Chem. A*, *116*, 2055).

***Probing electronic structures of diradicals*:** Diradicals are exotic and reactive species. Their electronic structures and electron affinities are important fundamental information to understand their chemistry. In collaboration with Wes Borden's group at University of North Texas we have carried out a series of joint

experimental and theoretical studies on a variety of diradicals, which not only confirmed previous theoretical predictions, but also provided electronic structure information to benchmark theoretical methods (Fu, Yang, and Wang **2011**. *J. Phys. Chem. A 115*, 3201; Chen, Hrovat, Deng, Zhang, Wang, and Borden **2014**, *J. Am. Chem. Soc., 136*, 3589; Guo, Hou, Li, and Wang **2012**. *J. Phys. Chem. Lett. 3*, 304; Bao, Hrovat, Borden, and Wang **2013**, *J. Am. Chem. Soc. 135*, 4291).

Studying hydrogen bond network (HBN) and implications in enzymatic reactions and anion recognition: Many enzymes catalyze a wide variety of chemical processes by using two or even three hydrogen bonds. The energies of these hydrogen bonding interactions are important in catalysis but are not well understood. In collaboration with Steven Kass at University of Minnesota, We used NIPES to directly probe the energetic consequences of hydrogen bond arrays in small covalently bound model compounds, and their binding ability to various anions in charactering the cooperative effects of HBN and its effects on selective anion recognition (Shokri, Schmidt, Wang, and Kass **2012**, *J. Am. Chem. Soc.*. *134*, 2094; Beletskiy, Schmidt, Wang, and Kass **2012**. *J. Am. Chem. Soc. 134*, 18534; Shokri, Wang, and Kass **2013**, *J. Am. Chem. Soc. 135*, 9525).

Negative ion photoelectron spectroscopy study of atmospherically related clusters and species: Recent lab and field measurements have indicated critical roles of organic acids in enhancing new atmospheric aerosol formation. Such findings have stimulated theoretical and experimental studies with the aim of understanding interaction of organic acids with common aerosol nucleation precursors like bisulfate (HSO_4^-). We carried out a combined negative ion photoelectron spectroscopic and theoretical investigation of molecular clusters formed by HSO_4^- with succinic acid (SUA) along with $HSO_4^-(H_2O)_n$ and $HSO_4^-(H_2SO_4)_n$. It is found that one SUA molecule can stabilize HSO_4^- by ca. 39 kcal/mol, triple the corresponding value that one water molecule is capable of (ca. 13 kcal/mol). This work provides direct experimental evidence showing significant thermodynamic advantage by involving organic acid molecules to promote formation and growth in bisulfate clusters and aerosols (Hou, Lin, Deng, Zhang, Zheng, Paesani, and Wang **2013**. *J. Phys. Chem. Lett. 4*, 779).

Photoelectron spectroscopic studies of organometallic complexes and green fluorescence protein chromophore: In collaboration with Xantheas of PNNL we carried out NIPES study of Zeise's anion $[PtCl_3(C_2H_4)]^-$**,** the quintessential organometallic compound first synthesized by William Zeise in the 1820s**,** and its Br- and I- analogs in the gas phase. Well-resolved and rich spectral features are obtained for each species, yielding detailed electronic structure information, which is assigned with the aid of high-level electronic structure calculations at the coupled cluster level of theory (Hou, Wen, Lopata, Zheng, Kowalski, Govind, Wang, and Xantheas **2012**. *Angew. Chem. Int. Ed. 51*, 6356). The detailed insights of the chemical bonding and underlying electronic structure can be used to benchmark interactions between olefins and transition metal complexes, which are crucial to a wide range of catalytic processes.

Very recently, we reported a negative ion photoelectron spectroscopy study on the model green fluorescence protein chromophore anion. Despite the considerable size and low symmetry of the molecule, well resolved vibrational structures were obtained with the 0–0 transition being the most intense peak. The adiabatic (ADE) and vertical detachment energy (VDE) therefore are determined, revealing the photon excited S_1 state being both adiabatically and vertically bound against the electron detached continuum D_0. The accurate ADE and VDE values and the well-resolved photoelectron spectra provide much needed, robust benchmarks for future theoretical investigations for this important molecule (Deng, Kong, Zhang, Yang, Zheng, Sun, Zhang, and Wang, **2014**. *J. Phys. Chem. Lett. 5*, 2155).

Photoelectron spectroscopy study of energy-related clusters: superhalogens, hyperhalogens, and functionalized fullerenes, polycyclic aromatic hydrocarbons. We (in collaboration with Boltalina and Strauss of Colorado State University) have conducted systematic and intensive research on functionalized carbon clusters, polyaromatic hydrocarbons (PAHs) and their derivatives, aimed for better electron acceptors and organic photovoltaic active layers. The intrinsic electronic structure properties of those composited clusters and molecules (e.g., electron affinity, HOMO-LUMO gap) and the extent of tunable

range induced by peripheral electron donating or withdrawing groups have been probed by NIPES, and correlated with solution measured reduction potentials. Such correlation bridges molecules to materials, shedding light on rational synthesis of carbon-based nanomaterials for constructing more efficient photovoltaic devices (Kuvychko, Castro, Deng, Wang, Strauss, and Boltalina, **2013**. *Angew. Chem. Int. Ed 52*, 4871; Clikeman, Deng, Avdoshenko, Wang, Popov, Strauss, and Boltalina, **2013**. *Chem. Eur. J. 19*, 15404).

Future Directions

The main thrust of our BES program will continue to be on cluster model studies of condensed phase phenomena in the gas phase. The experimental capabilities that we have developed give us the opportunity to attack a broad range of fundamental chemical physics problems pertinent to ionic solvation, solution chemistry, homogeneous / heterogeneous catalysis, aerosol chemistry, biological processes, and material synthesis. The ability to cool and control ion temperature enables us to study different isomer populations and conformation changes of environmentally important hydrated clusters. Another major direction is to use gaseous clusters to model ion-specific interactions in solutions, ion transport and ion-receptor interactions in biological systems, and initial nucleation processes relevant to atmospheric aerosol formation.

References to Publications of DOE CPIMS Sponsored Research (2012 - present)

1. A Shokri, JC Schmidt, XB Wang, and SR Kass, "Hydrogen Bonded Arrays: The Power of Multiple Hydrogen Bonds", *J. Am. Chem. Soc.*134, 2094-2099 (2012).
2. JC Guo, G Hou, SD Li, and XB Wang, "Probing the Low-lying Electronic States of Cyclobutanetetraone (C_4O_4) and its Radical Anion: A Low-Temperature Anion Photoelectron Spectroscopic Approach", *J. Phys. Chem. Lett.* 3, 304-308 (2012).
3. G Murdachaew, M Valiev, SM Kathmann, and XB Wang, "Study of Ion Specific Interactions of Alkali Cations with Dicarboxylate Dianions", *J. Phys. Chem. A* 116, 2055-2061 (2012).
4. IV Kuvychko, JB Whitaker, BW Larson, TC Folsom, NB Shustova, SM Avdoshenko, YS Chen, H Wen, XB Wang, L Dunsch, AA Popov, SH Strauss, and OV Boltalina, "Substituent Effects in a Series of 1,7-$C_{60}(R_F)_2$ Compounds (R_F = CF_3, C_2F_5, *n*-C_3F_7, *i*-C_3F_7, *n*-C_4F_9, *s*-C_4F_9, *n*-C_8F_{17}): Electron Affinities, Reduction Potentials and *E*(LUMO) Values Are Not Always Correlated", *Chemical Science* 3, 1399-1407 (2012).
5. GH Hou, H Wen, KA Lopata, W Zheng, K Kowalski, N Govind, XB Wang, and SS Xantheas, "A Combined Gas-Phase Photoelectron Spectroscopic and Theoretical Study of Zeise's Anion and Its Br- and I-Analogs", *Angew. Chem. Int. Ed.* 51, 6356-6360 (2012).
6. A Shokri, JC Schmidt, XB Wang, and SR Kass, "Characterization of a Saturated and Flexible Aliphatic Polyol Anion Receptor", *J. Am. Chem. Soc.* 134, 16944-16947 (2012).
7. EV Beletskiy, JC Schmidt, XB Wang, and SR Kass, "Three Hydrogen Bond Donor Catalysts: Oxyanion Hole Mimics and Transition State Analogues", *J. Am. Chem. Soc.*134, 18534-18537 (2012).
8. H Wen, GL Hou, SM Kathmann, M Valiev, and XB Wang, "Solute Anisotropy Effects in Hydrated Anion and Neutral Clusters", *J. Chem. Phys.* 138, 031101-1-4 (2013).
9. X Bao, DA Hrovat, WT Borden, and XB Wang, "Negative Ion Photoelectron Spectroscopy Confirms the Prediction that $(CO)_5$ and $(CO)_6$ Each Has a Singlet Ground State", *J. Am. Chem. Soc.* 135, 4291-4298 (2013).
10. GL Hou, W Lin, SH Deng, J Zhang, W Zheng, F Paesani, and XB Wang, "Negative Ion Photoelectron Spectroscopy Reveals Thermodynamic Advantage of Organic Acids in Facilitating Formation of Bisulfate Ion Clusters: Atmospheric Implications", *J. Phys. Chem. Lett.* 4, 779-785 (2013).
11. IV Kuvychko, KP Castro, SH Deng, XB Wang, SH Strauss, and OV Boltalina, "Taming Hot CF_3 Radicals: Incrementally Tuned Families of Polyarene Electron Acceptors for Air-Stable Molecular Optoelectronics", *Angew. Chem. Int. Ed.* 52, 4871-4874 (2013).

12. EF van der Eide, GL Hou, SH Deng, H Wen, P Yang, RM Bullock, and XB Wang, "Metal-Centered 17-Electron Radicals $CpM(CO)_3^{\bullet}$ (M = Cr, Mo, W): A Combined Negative Ion Photoelectron Spectroscopic and Theoretical Study", *Organometallics* 32, 2084-2091 (2013).
13. IV Kuvychko, C Dubceac, SH Deng, XB Wang, AA Granovsky, AA Popov, MA Petrukhina, SH Strauss, and OV Boltalina, "$C_{20}H_4(C_4F_8)_3$: A Fluorine-Containing Annulated Corannulene that Is a Better Electron Acceptor Than C_{60}", *Angew. Chem. Int. Ed.* 52, 7505-7508 (2013).
14. A Shokri, XB Wang, and SR Kass, "Electron-Withdrawing Trifluoromethyl Groups in Combination with Hydrogen Bonds in Polyols: Brønsted Acids, Hydrogen-Bond Catalysts, and Anion Receptors", *J. Am. Chem. Soc.* 135, 9525-9530 (2013).
15. BW Larson, JB Whitaker, XB Wang, AA Popov, G Rumbles, N Kopidakis, SH Strauss, and OV Boltalina, "Electron Affinity of Phenyl−C_{61}−Butyric Acid Methyl Ester (PCBM)", *J. Phys. Chem. C* 117, 14958-14964 (2013).
16. GL Hou, MM Wu, H Wen, Q Sun, XB Wang, WJ Zheng, "Photoelectron spectroscopy and theoretical study of $M(IO_3)_2^-$ (M=H, Li, Na, K): Structural evolution, optical isomers, and hyperhalogen behavior", *J. Chem. Phys.*139, 044312-1-7 (2013).
17. J Zhang, DA Hrovat, ZR Sun, X Bao, WT Borden, and XB Wang, "The Ground State of $(CS)_4$ Is Different from that of $(CO)_4$: An Experimental Test of a Computational Prediction by Negative Ion Photoelectron Spectroscopy", *J. Phys. Chem. A* 117, 7841-7846 (2013).
18. TT Clikeman, SHM Deng, S Avdoshenko, XB Wang, AA Popov, SH Strauss, and OV Boltalina, "Fullerene "Superhalogen" Radicals: the Substituent Effect on Electronic Properties of 1,7,11,24,27-$C_{60}X_5$", *Chemistry – A European Journal* 19, 15404-15409 (2013).
19. A Shokri, Y Wang, GA O'Doherty, XB Wang, and SR Kass, "Hydrogen-Bond Networks: Strengths of Different Types of Hydrogen Bonds and An Alternative to the Low Barrier Hydrogen-Bond Proposal", *J. Am. Chem. Soc.* 135, 17919-17924 (2013).
20. J Zhang, P Yang, ZR Sun, and XB Wang, "Covalently Bound Tetracoordinated Organoborons as Superhalogens: A Combined Negative Ion Photoelectron Spectroscopy and Theoretical Study", *J. Phys. Chem. A* (ASAP) (dx.doi.org/10.1021/jp410009a) (2014).
21. A Shokri, SHM Deng, XB Wang, and SR Kass, "Molecular Recognition: Preparation and Characterization of Two Tripodal Anion Receptors", *Organic Chemistry Frontiers* 1, 54-61 (2014).
22. B Chen, DA Hrovat, SHM Deng, J Zhang, XB Wang, and WT Borden, "The negative ion photoelectron spectrum of meta-benzoquinone radical anion (MBQ•-): A joint experimental and computational study", *J. Am. Chem. Soc.* 136, 3589-3596 (2014).
23. TT Clikeman, EV Bukovsky, IV Kuvychko, LK San, SH M Deng, XB Wang, YS Chen, SH Strauss, and OV Boltalina, "Poly(trifluoromethyl)azulenes: structures and acceptor Properties" *Chem. Comm.* 50, 6263-6266 (2014).
24. SHM Deng, XY Kong, GX Zhang, Y Yang, WJ Zheng, ZR Sun, DQ Zhang, and XB Wang, "Vibrationally Resolved Photoelectron Spectroscopy of the Model GFP Chromophore Anion Revealing the Photoexcited S_1 State Being Both Vertically and Adiabatically Bound against the Photodetached D_0 Continuum" *J. Phys. Chem. Lett.* 5, 2155-2159 (2014).
25. SHM Deng, GL Hou, XY Kong, M Valiev, and XB Wang, "Examining the Amine Functionalization in Dicarboxylates: Photoelectron Spectroscopy and Theoretical Studies of Aspartate and Glutamate" *J. Phys. Chem. A* 118, 5256-5262 (2014).
26. M Samet, XB Wang, and SR Kass, "A Preorganized Hydrogen Bond Network and Its Effect on Anion Stability" *J. Phys. Chem. A* (ASAP) (dx.doi.org/10.1021/jp505308v) (2014).
27. B Chen, DA Hrovat, R West, SHM Deng, XB Wang, and WT Borden, "The Negative Ion Photoelectron Spectrum of Cyclopropane-1,2,3-Trione Radical Anion, $(CO)_3^{\bullet-}$ – A Joint Experimental and Computational Study" *J. Am. Chem. Soc.* (ASAP) (dx.doi.org/10.1021/ja505582k) (2014).

Free Radical Reactions of Hydrocarbons at Aqueous Interfaces

Principal Investigator: Kevin R. Wilson
Lawrence Berkeley National Laboratory, 1 Cyclotron Road, MS 6R2100, Berkeley, CA 94720
Email: krwilson@lbl.gov

Program Scope and Long Term Objectives: This project will probe the surface chemistry of hydrocarbon molecules residing on nanometer and micron-sized aqueous droplets exposed to gas phase hydroxyl radicals using atmospheric pressure surface sensitive mass spectrometry and ambient pressure photoelectron spectroscopy. This program aims to:

(1) Quantify the link between molecular structure and surface reactivity at an aqueous interface using model hydrocarbon architectures (e.g. isomers)

(2) Determine how the presence and distribution of interfacial ions control the surface reactivity of a hydrocarbon at an aqueous interface.

This work broadly supports the Department of Energy's Basic Energy Sciences program to better assess, mitigate and control the efficiency, utilization, and environmental impacts of energy use. This work seeks a rigorous molecular understanding of how heterogeneous reaction pathways lead to either bulk solvation of a surface active organic molecule or its removal from the interface through decomposition into gas phase products. Understanding these fundamental processes are critical for predicting the chemical fate of hydrocarbon byproducts of energy use and consumption.

Recent Progress: During the last year, we have sought to understand how thermodynamic phase (solid versus aqueous) controls the heterogeneous hydroxyl radical (OH) reaction pathways of organic molecules. Nanometer-sized succinic acid ($C_4H_6O_4$) particles were selected as a model system since it is straightforward to control the phase of these particles by simply changing relative humidity. The heterogeneous reaction was investigated using an aerosol flow tube reactor. The molecular and elemental transformation of the particles is quantified using Direct Analysis in Real Time (DART), a soft atmospheric pressure ionization source, coupled to a high resolution mass spectrometer.

Particle phase, controlled by liquid water content in the particle, is observed to have a pronounced effect on the reaction kinetics, the distribution of the oxidation products and the average aerosol carbon oxidation state. In highly concentrated aqueous droplets (~9 Molar), succinic acid within the particle reacts 41 times faster with OH than in solid aerosol producing a larger quantity of both functionalization and fragmentation reaction products. These observations are consistent with the more rapid diffusion of succinic acid to the surface of aqueous droplets than solid particles. For aqueous droplets at an OH exposure of 2.5×10^{12} molecule cm^{-3} s, the average aerosol carbon oxidation state is +2, with higher molecular weight functionalization products accounting for ~5% and lower carbon number (C<4) fragmentation products comprising 70% of the mass. The remaining 25% of the aqueous droplet is unreacted succinic acid. This is in contrast with solid

particles, at an equivalent oxidation level, where unreacted succinic acid is the largest particle phase constituent with functionalization products accounting for <1% and fragmentation products ~8% of the aerosol mass yielding an average aerosol carbon oxidation of only +0.62. Based on exact mass measurements of the oxidation products and a proposed reaction mechanism, succinic acid in both phases is preferentially reacts with OH to form smaller carbon number monoacids and diacids (e.g. oxalic acid). These results illustrate the importance of water in controlling the rate at which the average particle carbon oxidation state evolves through the formation and evolution of C-C bond scission products with high carbon oxidation states and small carbon numbers. These results also point more generally to potential complexity of heterogeneous reactions, whose pathways may ultimately depend upon the "exposure history" of particles to relative humidity.

These initial studies on succinic acid have been extended to more branched analogs (methyl-succinic acid and 2,3-dimethylsuccinic acid) in order to elucidate how molecular structure of the carbon backbone impacts the chemistry of peroxy and alkoxy radical intermediates. For these compounds, the formation of more oxygenated products can be explained by well-known condensed-phase reaction mechanisms. The abundance of fragmentation products is found to increase with the number of methyl groups, which can be attributed to the increased number of tertiary carbon atoms and the enhanced probability for alkoxy radical decomposition at these sites. A quantitative model of how methyl groups on succinic acid affect reaction kinetics and C-C bond scission reaction pathways is currently being developed.

Finally, we have spent considerable effort understanding water uptake and droplet formation on nanometer-sized particles. This work seeks to understand how organic molecules are arranged at the interface of a micron sized aqueous droplet—a key feature in determining a molecule's availability for a heterogeneous reaction with gas phase radicals. Sensitive measurements of the droplet size were conducted, at a relative humidity (~99.9%) just below saturation, on submicron particles containing an ammonium sulfate core and an organic layer of a model compound of varying thickness. The 12 model organic compounds are a series of di-carboxylic acids (C_3 to C_{10}), *cis*-pinonic, oleic, lauric, and myristic acids, which represent a broad range in solubility from miscible (malonic acid) to insoluble. The growth in droplet size with increasing organic fraction cannot be explained by assuming the organic material is dissolved in the bulk droplet. Instead, the wet droplet diameters exhibit a complex and non-linear dependence on organic volume fraction, leading to droplet growth that is in some cases smaller and in others larger than that predicted by bulk solubility alone. For palmitic and stearic acid, small droplets at or below the detection limit of the instrument are observed, indicating significant kinetic limitations for water uptake, which are consistent with maximum mass accommodation coefficients on the order of 10^{-3}.

A model based on the two-dimensional van der Waals equation of state is used to explain the complex droplet growth with organic aerosol fraction and dry diameter. The model suggests that mono- and di-carboxylic acids with limited water solubility partition to the droplet interface and reduce surface tension only after a two dimensional (2D) condensed monolayer is formed. Two relatively soluble compounds, malonic and glutaric acid, also appear to form surface phases, which

increase water uptake. There is a clear alternation in the threshold for droplet growth observed for odd and even carbon number diacids, which is explained in the model by differences in the excluded molecular areas of even (~40 $Å^2$/molecule) and odd (~20 $Å^2$/molecule) diacids. These differences are consistent with the odd diacids being are arranged at the droplet interface in "end-to-end" configurations with only one acid group in contact with the aqueous phase; in contrast to even carbon numbered diacids forming "folded" films with both acids groups in contact with the bulk phase. These results reveal a new and complex relationship between the composition of an organic particle and its water uptake, suggesting that organic surface films might strongly influence the multiphase chemistry of organic particles as well as cloud droplet formation. These results are a guide for designing new heterogeneous reactions to probe how reaction pathways might depend upon interfacial orientation (odd vs. even diacids) and structure of organic molecules at the liquid vapor interface.

Future Plans: In the next year, our focus will be on understanding how C-C bond scission reactions produced by surface reactions of OH radicals depend upon molecular structure (i.e. carbon chain length), interfacial orientation, and particle viscosity. As described above, there is emerging evidence that the degree of branching on the hydrocarbon skeleton plays a controlling influence on the formation of smaller molecular weight reaction products. By measuring the heterogeneous reaction of OH with a series of compounds that differ only in the number of methyl substituents should quantify the relationship between the number of tertiary carbon reaction sites and C-C bond scission propensity.

Initial results (described above) suggest that the OH reactivity of odd and even numbered di-carboxylic acids should be rather different due to differences in molecular orientation at the droplet vapor interface. This will be explored through careful measurements of how the reaction rate and product distributions depend upon diacid carbon number. For example, one might expect that reaction of OH with interfacial odd diacids to occur primarily at the terminus of the molecule and thus form different reactions products compared to even diacids that are arranged in a "folded" motif at the droplet vapor interface.

In collaborative work with Dr. Frances Houle (LBNL-Chemical Sciences) we are applying spatially resolved stochastic reaction-diffusion simulations of droplet chemistry to better explain our experimental results; with a key objective of understanding how particle phase viscosity influences heterogeneous reaction mechanisms. This work will elucidate how the onset of glassy dynamics in nanometer-sized particles controls heterogeneous reaction pathways. These simulations of our experimental data will elucidate new details about the location of various free radical reaction pathways within the particle (bulk vs. subsurface vs. surface) which are significant insights that are difficult to observe via experiments alone. These simulations are also being used to understand in molecular detail how the formation and subsequent decomposition of alkoxy radicals (a key intermediate formed via an OH surface reaction) controls the evolution of particle mass, with the general objective of elucidating the coupling of free radical chemistry with changes in particle size, density and ultimately viscosity.

Finally, we will use a new laser tweezers setup to probe the surface chemistry of individual micron sized droplets over long reaction times (hours to days). Here we will use Raman scattering for chemical composition determination and the droplet's whispering gallery modes for high precision droplet sizing (~1 nm) to elucidate changes in single droplet chemistry as a function of reaction time to OH. We will also design a novel interface to our mass spectrometer to obtain single droplet mass spectra as a function of reaction time. Future efforts will be devoted to interfacing the single droplet laser trap to the Molecular Environmental Science Beamline (with Dr. Hendrik Bluhm, LBNL) to measure single droplet X-ray photoelectron spectra during a chemical reaction. The science objective of these technical efforts is to obtain a new depth-resolved chemical description of the droplet/vapor interface during a chemical reaction.

Publications Acknowledging the Office of Science Early Career Award:

1. F.A. Houle, W.D. Hinsberg and K.R. Wilson, *"Oxidation of a model alkane aerosol by OH radical: the emergent nature of reactive uptake",* Submitted to Environmental Science and Technology, (2014).

2. C. Ruehl and K.R. Wilson, *"Surface organic monolayers control the hygroscopic growth of submicron particles at high relative humidity,"* J. Phys. Chem. A, DOI: 10.1021/jp502844g (2014)

3. M.N. Chan, H. Zhang, A. H. Goldstein, and K. R. Wilson, *"The Role of Water and Phase in the Heterogeneous Oxidation of Solid and Aqueous Succinic Acid Aerosol by Hydroxyl Radicals,"* J. Phys. Chem. C, DOI: 10.1021/jp5012022 (2014).

4. H. Zhang, C. Ruehl, A. Chan, T. Nah, D. Worton, G. Isaacman, A. Goldstein, and K. R. Wilson, *"OH Initiated Heterogeneous Oxidation of Cholestane: A Model System for Understanding the Photochemical Aging of Cyclic Alkane Aerosols,"* J. Phys. Chem. A. 117, 12449 (2013).

5. T. Nah, M.N. Chan, S. R. Leone, and K. R. Wilson, *"Real Time in Situ Chemical Characterization of Sub-micrometer Organic Particles Using Direct Analysis in Real Time-Mass Spectrometry,"* Anal. Chem., **85**, 2087 (2013).

6. M.N. Chan, T. Nah, and K. R. Wilson, *"In-Situ Chemical Detection of Sub-micron Organic Aerosols using Direct Analysis in Real Time Mass Spectrometry (DART-MS): The Effect of Aerosol Size and Volatility,"* Analyst, 138, 3749-37577 (2013).

7. C. R. Ruehl, T. Nah, G. Isaacman, D. R. Worton, A. W. H. Chan, K. R. Kolesar, C. D. Cappa, A. H. Goldstein, and K. R. Wilson, *"The influence of molecular structure and aerosol phase on the heterogeneous oxidation of normal and branched alkanes by OH,"* J. Phys. Chem. A., **117**, 3990 (2013)

8. C. W. Harmon, C. R. Ruehl, C. D. Cappa, and K. R. Wilson, *"A Statistical Description of the Evolution of Cloud Condensation Nuclei Activity during the Heterogeneous Oxidation of Squalane and Bis (2-ethylhexyl) Sebacate Aerosol by Hydroxyl Radicals,"* Phys. Chem. Chem. Phys., **15**, 9679 (2013).

Transition Metal Reactions and Highly Accurate Electronic Structure Methods

Theresa L. Windus
Ames Laboratory, 125 Spedding Hall,
Iowa State University, Ames, IA 50011
twindus@iastate.edu

PROGRAM SCOPE:

This component of the Chemical Physics Program at Ames Laboratory focuses on modeling of transition metal catalytic and photo-activated reactions, the development of highly accurate electronic structure methods and their use in non-adiabatic chemical reactions. The modeling of transition metal reactions are in collaboration with the experimental groups of Aaron Sadow and Andreja Bakac in the Catalysis program at Ames Laboratory. The highly accurate electronic structure methods have been developed in collaboration with Klaus Ruedenberg and are focused on extending the correlation energy extrapolation by intrinsic scaling (CEEIS) method to larger molecular systems. In addition, the development of R12 technology with a local multi-reference configuration interaction (MRCI) is in progress. The development of non-adiabatic chemical methods is in collaboration with Mark Gordon's group.

RECENT PROGRESS:

TRANSITION METAL REACTIONS:

(i) Reactions of metal-carbon bonds and O_2 are important potential components of new approaches to green oxidative catalysis. Often these reactions can be complicated by unselective product formation from overoxidation rather than formation of metallo-alkylperoxides that might be used as mediators of selective oxidation. Zn metal centers, in particular, tend to initiate overoxidation. In a collaboration with the Sadow group in the Catalysis program at Ames Laboratory, a new mixed oxazoline-carbene borate Zn compound, $\{PhB(Ox^{Me2})_2Im^{Mes}\}ZnCH_3$, was examined and found to provide isolable monomeric Zn alkylperoxide [5]. An interesting feature of this catalyst is there is a significant distortion of the Zn methyl group from the pseudo tetrahedral position. Starting with the X-ray structure, gas phase calculations were performed to determine the nature of this distortion. The optimized structures showed the same distortion and examination of the wavefunction and the densities suggests that there are subtle electronic rather steric effects in play.

(ii) The reaction mechanism for stereospecific cycloamination reactions with cyclopentadienyl-bis(oxazolinyl)borato zirconium complexes is being examined in collaboration with the Sadow group. While experimental and computational models agree on the structures and IR spectrum of the complexes [2], the reaction mechanism is proving to be elusive. Multiple possible mechanisms agree with the experimental kinetics and there is debate in the experimental community on the mechanisms of cylcoamination in general (especially with d^0 metals). The major proposed mechanisms involve insertion, $2\pi+2\pi$ cycloaddition, or concerted CN/CH bond formation. In collaboration with Mark Gordon, each of these mechanisms (and several others) are being examined using density functional methods (B3LYP, PBE0 and M06-2L) for structures and energetics with additional MP2 single point energies to improve the energetics. The structures change minimally between the different functionals, which implies (unsurprisingly) that the structures can be represented without too much difficulty. Interestingly, though, the newer M06-

2L functionals give energetics similar to the MP2, while the others give reaction barriers that are much higher in energy. While work is still ongoing, ligand effects on the reaction barriers for the different mechanisms have proven to be very important. In particular, additional amines in the solvation sphere of the Zr catalyst have an effect on which mechanisms dominate the kinetics. These concentration effects are also seen in the experimental results.

(iii) In collaboration with the Bakac group in the Catalysis Program at Ames Laboratory, transition metal complexes $(NH_3)_5CoX^{2+}$ (X = CH_3, Cl) and $L(H_2O)MX^{2+}$, where L = [14]aneN_4 or *meso*-Me_6-[14]aneN_4, M = Rh or Co, and X is a variety of axial ligands, are examined by both experiment and computation to better understand their electronic spectra and associated photochemistry [6]. Specifically, irradiation into weak visible bands of $(NH_3)_5CoCH_3^{2+}$ and $L(H_2O)MX^{2+}$ (X = CH_3 or NO) leads to photohomolysis of Co-CH_3 and M-X bonds, respectively. On the other hand, when X = halide or NO_2, visible light photolysis leads to dissociation of X^- and/or cis/trans isomerization. Computations show that visible bands for alkyl and nitrosyl complexes involve M-X bonding-to-antibonding transitions. In contrast, complexes with X = Cl or NO_2 exhibit only d-d bands in the visible, so that homolytic cleavage of the M-X bond requires UV photolysis. UV-Vis spectra are not significantly dependent on the structure of the equatorial ligands, as shown by similar spectral features for $(NH_3)_5CoCH_3^{2+}$ and $L^1(H_2O)CoCH_3^{2+}$.

(iv) Flowing afterglow experiments have shown that Nb mono- and di-cations activate the C-O bond in CO_2 to form the metal oxide and carbon monoxide. However, the mono-cation is much more efficient at catalyzing the reaction. A complicating factor is that each of the reactions involves a change in spin state near the transitions states of the potential energy surfaces. By using multi-reference methods, it was found that the barrier for the mono-cation reaction is approximately 6 kcal/mol, while that for the di-cation is approximately 18 kcal/mol explaining the difference in the reactivity of the Nb cations.[7]

HIGHLY ACCURATE ELECTRONIC STRUCTURE CALCULATIONS:

(i) Windus and Ruedenberg have extended the CEEIS method to take advantage of many-body effects in a new correlation energy extrapolation by many body expansion method (CEEMBE). The CEEMBE method combines several ideas to obtain a reliable estimate for the configuration interaction (CI) energy of the chemical system. First, the valence orbitals in the reference MCSCF calculation are separated into groups (or "bodies"), each with a preset number of valence electrons using occupationally restricted multiple active space (ORMAS). Next, a series of computations are performed for each of the smaller ORMAS references where a certain level of excitations (doubles, triples, quadruples, etc.) are made into a limited number of virtual orbitals, n, where n increases toward the full virtual space. Many body expansion techniques are then used to approximate the value of the total CI energy from the energies of the smaller CI calculations. Additional accuracy can then be obtained by linearly extrapolating the changes that occur in the approximate energy against the changes that occur in the exact energy as the number of virtual orbitals is varied. Applications to F_2 and ozone show that this is a promising technique for decreasing the overall size of the computations needed to obtain accurate results.

(ii) Windus and Ruedenberg have also initiated a careful examination of important portions of the ozone potential energy surface using SA-MCSCF and CEEIS. The stationary points include the "traditional" open ring structure, the equilateral ring structure (yet, to be found experimentally), and the transition state between the two. In addition, the minimum on the excited state surface and the conical intersection between the ground and lowest excited state have been located. Interestingly, the ground state transition state, excited state minimum and the conical intersection

all lie quite close to one another. Using a small 2 orbital, 2 electron active space, the CEEIS method was applied including up to quadruple excitations. By double excitations, most of the full valence active space is recovered and by quadruple excitations the difference between the small active space and the full valence active space is less than about 5 millihartree. Relative energy differences are much less. Of course, the CEEIS calculations with the smaller active space are much less expensive than those for the full valence active space.

NON-ADIABATIC DYNAMICS:

The dynamics package NEWTON-X and GAMESS were interfaced for nonadiabatic and adiabatic "on-the-fly" dynamics simulations [4]. In particular, this interface allows for the first study of nonadiabatic dynamics with the occupation restricted multiple active space (ORMAS) approximation, which is unique to GAMESS. Several dynamics simulations using methaniminium as an example were performed with various computationally feasible active space choices (or schemes) in order to test the qualitative accuracy and relative expense of different active space choices. Overall, for ORMAS orbital subspace divisions, schemes with no excitations between orbital subspaces give qualitatively incorrect state populations while schemes with single excitations between orbital subspaces recover the qualitatively correct state populations relative to the CASSCF level of theory at a lower computational expense. All active spaces show a large number of trajectories with an orbital integrity issue that is not caught by the energy conservation checks. So, trajectories must be monitored carefully and more overall trajectories are likely to be needed to obtain quantitative statistical information.

FUTURE PLANS:

HOMOGENEOUS CATALYSTS:

Collaborations with the catalysis groups at Ames continue by examining catalytic and photocatalytic mechanisms. The study of the Zr catalyzed hydromination reaction mechanism will be completed. Interestingly, the Y substituted catalysis provides the opposite stereochemical products than the Zr catalyst does and will be examined. Rhodium catalyzed decarbonylation reactions for alcohols will also be examined since they react both thermally and photochemically and provide a rich chemistry to explore. Understanding the different reaction pathways and the modifications of these paths when interacting with a nanocrystal and mesoporous silica nanoparticles is a long term goal of the research.

HIGHLY ACCURATE ELECTRONIC STRUCTURE CALCULATIONS:

(i) Development of the CEEMBE method will continue and be expanded to allow for much larger molecular systems than previously explored using the CEEIS method. In particular, different virtual space specifications to allow for a more localized virtual space will be used to decrease the number of determinants in the calculations. Early explorations into this approach appear promising, but many more computations will be required to verify the approach. In addition, the CEEMBE method will be applied to the new CEPA method implemented in GAMESS. This promises to be produce a very economical method for high accuracy.

(ii) In a collaboration with Professors Emily Carter and Mark Gordon, a local MRCI and MRACPF program has been implemented into GAMESS, which allows much larger systems and their excited states to be examined. In an effort to improve the convergence of the excited and ground state calculations with respect to basis set, the explicitly correlated R12 method as

formulated by Valeev is being integrated with the localized code. The R12 approach has shown that quadruple zeta quality results can be obtained using a double zeta basis set for small ground state molecules – decreasing the overall cost by using a smaller basis set. To date, the second-order density matrix (SODM) - required by the R12 perturbative approach - has been implemented within the local MRCI code symmetric group approach (SGA) and has been parallelized. Technical issues associated with the different data representations and integration will be addressed to allow for larger computations.

NON-ADIABATIC DYNAMICS:

With the integration of GAMESS and NEWTON-X, multiple directions for using ORMAS are being explored. As discussed above, the use of MCSCF methods can often results in active space corruption during the dynamics. While use of TDDFT or spin flip TDDFT is appealing, there are significant issues when near conical intersections and when multiple surfaces are involved. Therefore, additional methods are being explored for maintaining the MCSCF active spaces during the reactions. These include using the recent density distance criteria of Head-Gordon and state tracking methods of Tretiak that have been used on single reference methods, but not for multi-reference methods. Simple models such as methaniminium will be examined first since there is good benchmark information available. Then more complicated systems such as urocanic acid and photochemical catalytic systems will be studied.

PUBLICATIONS:

[1] "Intermolecular β-hydrogen abstraction in ytterbium, calcium and potassium tris(dimethylsilyl)methyl compounds.", K. Yan, G. Schoendorff, B.M. Upton, A. Ellern, T.L. Windus, and A.D. Sadow, *Organomettallics*, **2013**, *32*, 1300–1316.

[2] "Highly Enantioselective Zirconium-Catalyzed Cyclization of Aminoalkenes", K. Manna, W.C. Everrett, G. Schoendorff, A. Ellern, T.L. Windus, and A.D. Sadow, *J. Am. Chem. Soc.*, **2013**, *13*, 7235–7250.

[3] "Accurate ab initio potential energy curves and electronic and vibrational spectra for C_2", J. Boschen, L. Bytautas, K. Ruedenberg, T.L. Windus, *Theor. Chem. Acc.*, **2014**, *133*, 1425,invited.

[4] "Nonadiabatic dynamics study of methaniminium with ORMAS: Challenges of incomplete active spaces in dynamics simulations.", A.C. West, M. Barbatti, H. Lischka, and T.L. Windus, *Comp. Theor. Chem.*, **2014**, *1040-1041*, 158-166, invited submission.

[5] "Oxygen Insertion Reactions of Mixed *N*-Heterocyclic Carbene-Oxazolinylborato Zinc Alkyl Complexes", S. Xu, W.C. Everett, A. Ellern, T.L. Windus, and A.D. Sadow, *Dalton Transactions*, accepted

[6] "UV-Visible Spectroscopy of Macrocyclic Nitrosyl Complexes of Cobalt and Rhodium. Experiment and Calculation", E.A. Hull, A.C. West, O. Pestovsky, K.E. Kristian, A. Ellern, J.F. Dunne, J.M. Carraher, A. Bakac, T.L. Windus, *Inorg. Chem.*, submitted.

[7] "Reactions of Niobium mono and dications with CO and CO_2" E.A. Hull, G. Davico, T.L. Windus, *J. Phys. Chem. A*, submitted.

Ionic Liquids: Radiation Chemistry, Solvation Dynamics and Reactivity Patterns

James F. Wishart
Chemistry Department, Brookhaven National Laboratory, Upton, NY 11973-5000
wishart@bnl.gov

Program Definition

Ionic liquids (ILs) are a rapidly expanding family of condensed-phase media with important applications in energy production, storage and consumption, including advanced devices and processes and nuclear fuel and waste processing. ILs generally have low volatilities and are combustion-resistant, highly conductive, recyclable and capable of dissolving a wide variety of materials. They are finding new uses in dye-sensitized solar cells, chemical synthesis, catalysis, separations chemistry, batteries, supercapacitors and other areas. Ionic liquids have dramatically different properties compared to conventional molecular solvents, and they provide a new and unusual environment to test our theoretical understanding of primary radiation chemistry, charge transfer and other reactions. We are interested in how IL properties influence physical and dynamical processes that determine the stability and lifetimes of reactive intermediates and thereby affect the courses of reactions and product distributions. We study these issues by characterization of primary radiolysis products and measurements of their yields and reactivity, quantification of electron solvation dynamics and scavenging of electrons in different states of solvation. From this knowledge we wish to learn how to predict radiolytic mechanisms and control them or mitigate their effects on the properties of materials used in nuclear fuel processing, for example, and to apply IL radiation chemistry to answer questions about general chemical reactivity in ionic liquids that will aid in the development of applications listed above.

Soon after our radiolysis studies began it became evident that the slow solvation dynamics of the excess electron in ILs (which vary over a wide viscosity range) increase the importance of pre-solvated electron reactivity and consequently alter product distributions and subsequent chemistry. This difference from conventional solvents has profound effects on predicting and controlling radiolytic yields, which need to be quantified for the successful use under radiolytic conditions. Electron solvation dynamics in ILs are measured directly when possible and estimated using proxies (e.g. coumarin-153 dynamic emission Stokes shifts or benzophenone anion solvation) in other cases. Electron reactivity is measured using ultrafast kinetics techniques for comparison with the solvation process.

A second important aspect of our interest in ionic liquids is how their unusual sets of properties affect charge transfer and charge transport processes. This is important because of the many applications of ionic liquids in devices that operate on the basis of charge transport. While interest in understanding these processes in ionic liquids is growing, the field is still in an early stage of development. We are using donor-bridge-acceptor systems to study electron transfer reactions across variable distances in a series of ionic liquids with a range of structural motifs and whose dynamical time scales vary from moderately fast to extremely slow, and to compare them with conventional solvents.

Methods. Picosecond pulse radiolysis studies at BNL's Laser-Electron Accelerator Facility (LEAF) are used to identify reactive species in ionic liquids and measure their solvation and reaction rates. This work is aided greatly by the development of Optical Fiber Single-Shot (OFSS) detection at LEAF by A. Cook (DOI: 10.1063/1.3156048) and its present extension into the NIR regime. LEAF's new capability in mid-infrared transient absorption detection allows precise identification of radiolytic intermediates and their reaction kinetics. IL solvation and rotational dynamics, and electron transfer reactions, are measured by TCSPC in the laboratory of E. W. Castner, Jr. at Rutgers Univ. Picosecond transient absorption measurements of excited state dynamics and electron transfer reactions are done in our lab at BNL. Diffusion rates of anions, cations and solutes are obtained by PGSE NMR in the S. Suarez and S.

Greenbaum labs at CUNY and by Castner's group at Rutgers. We have extensive collaborations with other major groups in ionic liquid synthesis, physical chemistry, simulations and radiation chemistry.

Ionic liquid synthesis and characterization. Our work often involves novel ILs that we design to the requirements of our radiolysis and solvation dynamics studies and are not commercially available. We have developed in-house capabilities and a network of collaborations (particularly with S. Lall-Ramnarine of Queensborough CC and R. Engel of Queens College) to design, prepare and characterize ILs in support of our research objectives. Cation synthesis is done by several methods, including a CEM microwave reactor, resulting in higher yields of purer products in much shorter time than traditional methods. We have a diverse instrumentation cluster including DSC, TGA, viscometry, AC conductivity, Karl Fischer moisture determination, ion chromatography and ESI-mass spec (for purity analysis and radiolytic product identification). The cluster serves as a resource for our collaborators in the New York Regional Alliance for Ionic Liquid Studies and other institutions (Penn State, ANL, ORNL). Our efforts are substantially augmented by student internships from the BNL Office of Educational Programs, particularly the VFP (formerly FaST) program, which brings collaborative faculty members and their students into the lab for ten weeks each summer. Since 2003, a total of 41 undergrads, three graduate students, one pre-service teacher, two high school students and four junior faculty have worked on IL projects in our lab, many of them for more than one summer.

Recent Progress

Effects of ionic liquids on intramolecular ET processes. Over the years, we have used oligoproline-bridged electron donor-bridge-acceptor (D-B-A) systems to probe various aspects of the energetics and distance dependence of ET processes in conventional solvents. We are now using these D-B-A systems to study how ionic liquids affect ET processes. Our first study (in collaboration with Castner) looked at the DMPD-pro_1-C343 D-B-A system in four solvents, including two ILs with short butyl chains, and showed how slow IL dynamics leads to distributed ET kinetics as predicted by theory. We have now extended our studies to include *N*-methyl-*N*-decylpyrrolidinium bistriflylamide (C_{10}mPyrr NTf_2), which has been shown via X-ray scattering and MD simulations to have distinct non-polar and polar domains, as distinguished from the short-chain ILs we have been using (C_4mPyrr NTf_2 and N_{1444} NTf_2) that do not show heterogeneity on that scale. The question of local environment effects (dynamical and energetic) is very important in ILs because of their molecular-scale polar/non-polar heterogeneity. We extended our measurements of photoinduced ET to the longer-bridged DMPD-pro_2-C343 system, with analysis by the distributed kinetics methods applied in the previous study. The increased conformational freedom afforded by the second bridging proline results in multiple conformations that are energetically accessible. The multiple conformations have significant variations in donor-acceptor electronic coupling, leading to the observation of dynamics that include both adiabatic and nonadiabatic contributions. We are now measuring photo-induced ET in these systems by femtosecond transient absorption to capture processes too fast for TCSPC and to observe the kinetics of back electron transfer.

Mid-infrared observation and kinetics of radicals in ionic liquids. LEAF recently added a third beam line dedicated to mid-infrared (1050-2330 cm^{-1}) transient absorption pulse radiolysis on the nanosecond time scale, based on quantum cascade laser IR sources. After considerable development work to master the still-evolving QCL technology, the mid-IR detection system is in routine use on diverse projects such as charge transport in molecular wires, mechanisms of transition metal catalysis[1] and identification of radiolytically-produced intermediates in ionic liquid radiolysis. In collaborative work with the Kuwabata Group at Osaka University on polymerizable ionic liquids used to fabricate nanopolymer patterns and structures, we demonstrated that we could easily use the LEAF mid-IR TA system to follow the radiation-induced polymerization of a vinylimidazolium IL on timescales up to seven minutes (a software limitation since removed) by following the bleaching of the vinyl monomer

C=C stretch. This result indicates that mid-IR detection coupled with pulse radiolysis will be extremely useful for studying polymer synthesis and grafting in many different systems.

Future Plans

Effects of ionic liquids on intramolecular ET processes. To probe deeper intramolecular ET in D-B-A systems in ILs, we have prepared D-B-A systems of different charge types, which we expect to occupy different regions within the IL. The neutral DMPD-pro$_n$-C343 system (n = 0-2) undergoes photoinduced charge separation to form a zwitterion, followed by charge recombination during the back electron transfer. For comparison, we will study the charged $[(bpy)_2Ru^{II}MCbpy\text{-}(pro)_n\text{-}ampyRu^{III}(NH_3)_5]^{5+}$ (n = 1, 2, and longer) system that we have investigated extensively in water, which should preferably be located in the polar region of the IL. The $(bpy)_2Ru^{II}MCbpy$ center is an excited-state electron donor, so the forward and back ET reactions are charge-shift (2+,3+/3+,2+) instead of separation and recombination. Given that the redoxcenters in this system are cations, the choice of IL anion is expected to influence the ET dynamics. In addition to the TCSPC method we have been using, the ET kinetics in the bimetallic system will be measured at by picosecond pulse radiolysis and laser-pumped femtosecond transient absorption (with E. W. Castner (Rutgers, TCSPC) and R. Rached (Fordham, synthesis)).

Cage escape and recombination in ILs. The early steps of photoinduced reactions often involve a competition between recombination and escape of the photoproducts, whether they are radicals or charge-separated states, which largely determines the quantum efficiency of energy capture and in some cases, photodegradation yields in catalytic systems. Recent quantum MD simulations by our collaborators imply that cage escape/recombination of radiation-induced radical species is important to explain yields of early radiolysis products as well. Compared to molecular solvents, ionic liquids may show unusual dynamical effects in cage relaxation, in addition to slower cage escape due to higher viscosity. In previous work, we observed such effects in the photolysis of *ortho*-chloro-hexaarylbisimidazole (*o*-Cl-HABI, L-L in the adjacent scheme) where quantum yields of the lophyl radical (L•) were much lower in three ILs than in DMSO. Work by others showed that even the recombination of lophyl radical pairs that are covalently constrained in a near-optimal configuration is quite slow ($t_{1/2}$ = 33 ms, $\Delta G^{\neq}$ = 65.5 kJ/mol) due to the large structural rearrangement required. We would like to know if ILs promote recombination through slower cage structural relaxation, holding the radical pair close to the transition state configuration for a longer time, and whether the viscosity-lengthened cage escape time promotes recombination of the relaxed pair through interactions with the IL environment. The BNL LEAF Optical Fiber Single Shot (OFSS) system is extremely useful for this effort because the diffusive recombination of lophyl radicals takes many seconds in ILs and in ordinary solvents, making typical repetitive pump-probe experiments completely impractical. In contrast, OFSS provides picosecond-resolution, 5-nanosecond-range transient absorption data using relatively small numbers of shots that can be collected at arbitrarily long delays in-between. Recently we undertook some studies of HABI/lophyl dynamics using the OFSS system. We demonstrated that the desired measurements are possible, but the default pump wavelengths of the LEAF laser system (400 and 266 nm) fall at points where HABI absorption is too low (400) or too high (266) to maximize the signal of the lophyl radical intermediate. Given the key importance of cage escape to photoinduced processes, we will reconfigure the experiment (pump wavelengths and HABI dyes) to enable the desired measurements. We will examine the kinetics of cage escape and recombination in ILs of different viscosities, and the effects of slow IL relaxation dynamics on the planarization of the lophyl radical, which provides the very large reorganization barrier for radical dimerization. (Collaboration with Prof. V. Strehmel (U. of Applied Sci., Krefeld, Germany) and A. Cook (BNL))

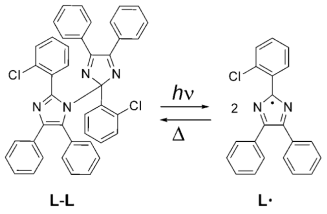

Scavenging and solvation processes of pre-solvated electrons in ionic liquids. Our early work in the reactivity of excess electrons in ionic liquids demonstrated the importance of pre-solvated electron scavenging in trying to understand and predict the distributions of early radiolysis products and radiolytic damage accumulation. It was also clear that the slower relaxation dynamics of ILs made them excellent media for the general study of fundamental radiolysis processes without the need to use cryogenic techniques, in combination with the advanced instrumentation of the LEAF Facility. We recently connected our observed electron solvation dynamics to the kinetics of electron scavenging. In other preliminary work we have observed that selected scavengers (e.g., nitrate, benzophenone) in ILs show different reaction profiles towards the various precursor states to the solvated electron. Different scavenger reactivities towards pre-solvated and solvated electrons have been known empirically for many years and cryogenic kinetic work by Jonah and Lewis showed specific mechanistic differences between scavengers similar to what we have seen in ILs. However, the combination of extended IL dynamical time scales and the time resolution of the LEAF OFSS detection system, coupled with the fact that it uses only small amounts of samples that do not have to be flowed, as well as the ability of ILs to dissolve polar and nonpolar scavengers, provides a unique opportunity to characterize the fundamental reactivity of pre-solvated electron species and understand how the properties of scavengers control their reaction profiles. The extension of the LEAF OFSS detection capability to the NIR (900-1700 nm) will greatly facilitate the study of dynamical and electron solvation processes in our ILs. This knowledge will permit the design of better systems to control radiation-induced reactivity, for example in the processing of radioactive materials (whether in ionic liquids or not), in systems for radiation processing and sterilization, and during long-term exposure to space, for example. (with A. Cook, BNL)

Publications

1. *Mechanism of the Formation of a Mn-Based CO_2 Reduction Catalyst Revealed by Pulse Radiolysis with Time-Resolved Infrared Detection* D. C. Grills, J. A. Farrington, B. H. Layne, S. V. Lymar, B. A. Mello, J. M. Preses, J. F. Wishart, *J. Am. Chem. Soc.*, **136**, 5563-5566 (2014).
2. *Binary Ionic Liquid Mixtures for Supercapacitor Applications* S. I. Lall-Ramnarine, S. N. Suarez, N. V. Zmich, D. Ewko, S. Ramati, D. Cuffari, M. Sahin, Y. Adam, E. Rosario, D. Paterno and J. F. Wishart, *ECS Transactions* **64**, 57-69 (2014).

Intermolecular interactions in the gas and condensed phases

Sotiris S. Xantheas
Physical Sciences Division, Pacific Northwest National Laboratory
902 Battelle Blvd., Mail Stop K1-83, Richland, WA 99352
sotiris.xantheas@pnnl.gov

The objective of this research effort aims at developing a comprehensive, molecular-level understanding of the collective phenomena associated with intermolecular interactions occurring in the gas phase, in guest/host molecular systems and in aqueous environments. The motivation of the present work stems from the desire to establish the key elements that describe the structural and associated spectral features of solutes in a variety of hydrogen bonded environments such as bulk water, aqueous interfaces and aqueous hydrates. Simple model systems including small molecules of complex electronic structure as well as aqueous clusters offer a starting point in this process by providing the test bed for validating new approaches for analyzing the electronic structure as well as the nature of interactions and the magnitude of collective phenomena at the molecular level. For instance, high level first-principles electronic structure calculations of the structures, energetics, and vibrational spectra of aqueous neutral and ionic clusters provide useful information needed to assess the accuracy of reduced representations of intermolecular interactions, such as classical potentials used to model the macroscopic structural and thermodynamic properties of those systems. The database of accurate cluster structures, binding energies, and vibrational spectra can, furthermore, aid in the development of new density functionals, which are appropriate for studying the underlying interactions. Representative applications include the development of novel descriptions of the electronic structure of simple molecules, the modeling of liquid water and ice, the quantitative description of aqueous ion solvation, the structure of clathrate hydrates and the interaction of host molecules with those guest networks. The detailed molecular-scale account of aqueous systems provided by these studies is relevant to Department of Energy programs in contaminant fate and transport and waste processing as well as hydrogen storage.

The modeling of intermolecular interactions over a wide spectrum ranging from the very weak (i.e. rare gas dimers) to the very strong (i.e. charge-dipole) interactions with universal, *simple* potential energy functions (PEFs) is hampered by their fixed $1/r$ dependence. To this end, existing popular PEFs such as the Mie, Lennard-Jones (*LJ*), Morse and Buckingham exponential-6 (*Be-6*) have been used to describe weak intermolecular interactions. An alternative way to make those PEFs more flexible, so they can describe a wide range of interactions, is to add an additional term with a variable $(1/r)^k$ dependence to describe the long-range part of the potential. The PEFs are cast in terms of the dimensionless reduced variables $r^*=r/r_m$ and $\varepsilon^*=\varepsilon/\varepsilon_m$, where the subscript m denotes the value at the minimum and they are required to obey the scalability constraints, viz. $\varepsilon^*(r^*)\big|_{r^*=1} = -1$, $\lim_{r^*\to\infty} \varepsilon^*(r^*) = 0$ and $\left.\frac{\partial \varepsilon^*}{\partial r^*}\right|_{r^*=1} = 0$.

The *generalized* (reverting back to the original form for some value of the additional parameter) and *extended* (not reverting back to the original form for any value of the additional parameter) new forms of these PEFs are:

$$(gLJ)^*: \quad \varepsilon^*_{gLJ}(r^*;\beta) = \frac{\beta}{6}\left[\left(\frac{1}{r^*}\right)^{12} - \left(\frac{1}{r^*}\right)^{6}\right] - \left(\frac{1}{r^*}\right)^{\beta}$$

$$(gMie)^*: \quad \varepsilon^*_{gMie}(r^*;n,m,\beta_\mu) = \frac{\beta_\mu}{n-m}\left[\left(\frac{1}{r^*}\right)^{n} - \left(\frac{1}{r^*}\right)^{m}\right] - \left(\frac{1}{r^*}\right)^{\beta_\mu}, \quad n > m$$

$$(gM)^*: \quad \varepsilon^*_{gM}(r^*;a^*_M,\gamma^*_1) = \frac{\gamma^*_1}{a^*_M}\left[e^{2a^*_M(1-r^*)} - e^{a^*_M(1-r^*)}\right] - e^{\gamma^*_1(1-r^*)}$$

$$(eM)^*: \quad \varepsilon^*_{eM}(r^*;a^*_M,\gamma_2) = \frac{\gamma_2}{a^*_M}\left[e^{2a^*_M(1-r^*)} - e^{a^*_M(1-r^*)}\right] - \left(\frac{1}{r^*}\right)^{\gamma_2}$$

$$(gBe\text{-}6)^*: \quad \varepsilon^*_{gBe-6}(r^*;\alpha_B,\delta) = \frac{\alpha_B\delta}{6(1-\alpha_B)}\left[e^{\frac{6(1-r^*)}{\alpha_B}} - \left(\frac{1}{r^*}\right)^{6}\right] - \left(\frac{1}{r^*}\right)^{\delta}$$

As a stringent test of their flexibility, they have been used to describe the strong ion-water interactions present in halide- and alkali metal-water interactions obtained from high level [CCSD(T)/triple ζ quality basis set] *ab-initio* calculations. The results with the extended Morse (*eM*) PEF, shown in Figure 1 for the 1-dimensional minimum energy cuts corresponding to the approach of the ion to water in the halide-water series, demonstrate that the additional parameter (describing the long-range) also affects the accuracy of the short-range part. Results of similar accuracy are obtained for the alkali metal-water interactions. Overall the new forms of the PEFs produce fits to the *ab-initio* data for these two classes of interactions that are between one and two orders of magnitude better in the χ^2 than the original forms (shown in dashed lines in Fig. 1).

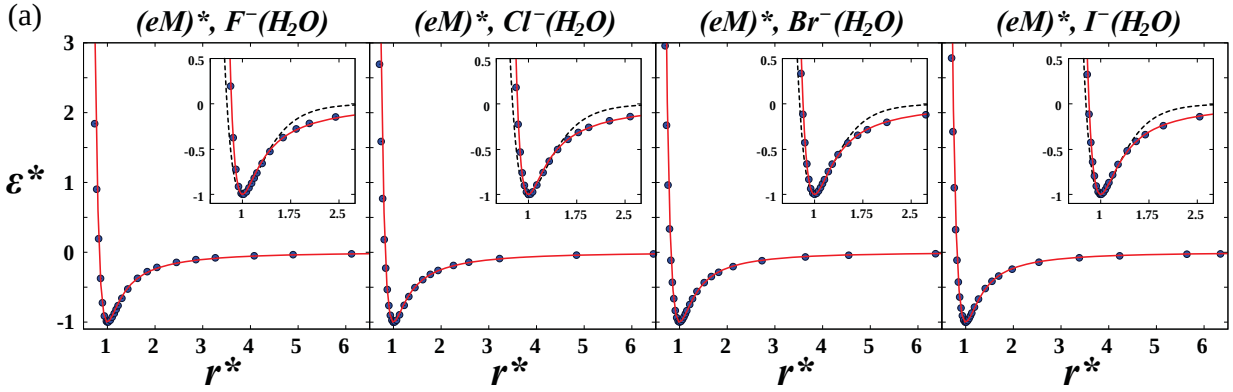

Figure 1. Fits of the (*eM*) PEF to the halide-water *ab-initio* data. The dotted lines trace the original Morse PEF.

For the halide- and alkali metal-water interactions the 1-dimensional Potential Energy Surfaces (PESs) in terms of the dimensionless variables r^* and ε^* differ just in the repulsive walls. For the $(eM)^*$ PEF these between the various ions in the repulsive wall are mainly controlled by the different values of the α^*_M parameter, whose fitted values vary monotonically with the ion size. Figure 2 shows that the fitted values of α^*_M correlate remarkably well with various sets of the ionic radii (Pauling, Shannon, Gourary, Latimer) for the halide-water (left panel) and the alkali metal-water (right panel) systems.

Future studies will investigate the performance of those newly introduced PEFs in describing a wide spectrum of intermolecular interactions ranging from the very weak (i.e. rare gas dimers) to the very strong (i.e. alkali metal halide dimers). It is anticipated that this will lead to a unified description of dissimilar interactions using a single, universal PEF with the values of its parameters providing additional physical insight into the nature of the underlying interactions.

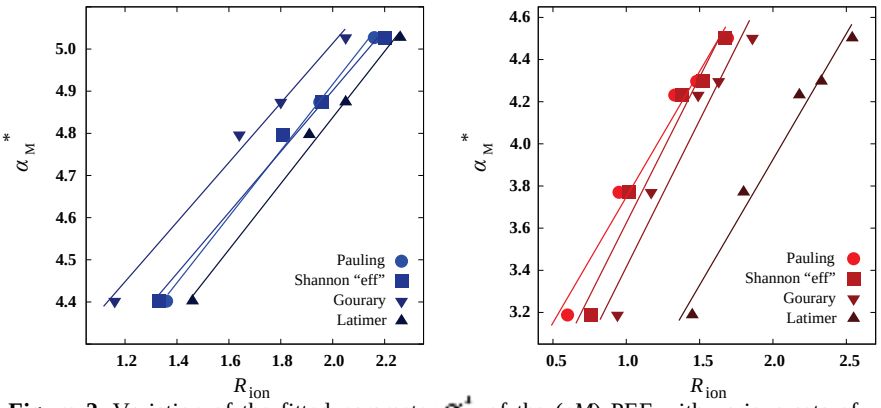

Figure 2. Variation of the fitted parameter α'_{gj} of the (*eM*) PEF with various sets of ionic sizes for the halide-water (left) and alkali metal-water (right) systems.

This research was performed in part using the computational resources in the National Energy Research Supercomputing Center (NERSC) at Lawrence Livermore National Laboratory. Battelle operates Pacific Northwest National Laboratory for the US Department of Energy.

References to publications of DOE sponsored research (2012 - present)

1. S. Yoo and S. S. Xantheas, "Structures, Energetics and Spectroscopic Fingerprints of Water Clusters *n*=2-24" in *Handbook of Computational Chemistry*, J. Leszczynski (ed.), Springer Science+Business Media B. V., ISBN 978-94-007-0710-8, Chapter 21, pp. 761-792 (2012)

2. S. Yoo and S. S. Xantheas, "Enhancement of Hydrogen Storage Capacity in Hydrate Lattices", *Chemical Physics Letters*, **525-526**, 13-18 (2012). Editor's Choice article. Featured in DOE's *In Focus* online publication: http://science.energy.gov/news/in-focus/2012/02-06-12/, Science Daily, EV Driven, Deixis magazine (Computational Science at the National Laboratories) http://www.deixismagazine.org/2012/07/twice-stuffed-permafrost/?utm_source=rss&utm_medium=rss&utm_campaign=twice-stuffed-permafrost

3. R. L. Sams, S. S. Xantheas, and T. A. Blake, "Vapor Phase Infrared Spectroscopy and *ab initio* Fundamental Anharmonic Frequencies of Ammonia Borane", *Journal of Physical Chemistry A* **116**, 3124 (2012)

4. G.-L. Hou, H. Wen, K. Lopata, W.-J. Zheng, K. Kowalski, N. Govind, X.-B. Wang, and S. S. Xantheas, "Zeise's Anion and Its Br- and I-Analogs: A Combined Gas-Phase Photoelectron Spectroscopic and Theoretical Study", Communication to the Editor, *Angewandte Chemie International Edition* **51**, 6356 (2012). Journal Cover

5. S. S. Xantheas, "Low-lying energy isomers and global minima of aqueous nanoclusters: Structures and corresponding spectroscopic features of the pentagonal dodecahedron $(H_2O)_{20}$ and $(H_3O)^+(H2O)_{20}$", Special issue on "Nano-Thailand: Nanotechnology for A Sustainable World" (invited), *Canadian Journal of Chemical Engineering* **90**, 843 (2012)

6. D. S. Lambrecht, L. McCaslin, S. S. Xantheas, E. Epifanovsky, and M. Head-Gordon, "Refined energetic ordering for sulfate-water (n=3-6) clusters using high-level electronic structure calculations", Peter Taylor Special Issue (invited), *Molecular Physics* **110**, 2513 (2012)

7. X. He, O. Sode, S. S. Xantheas, and S. Hirata, "Second-order many-body perturbation study of Ice Ih", *Journal of Chemical Physics* **137**, 204505 (2012)

8. S. Imoto, S. S. Xantheas, S. Saito, "Molecular origin of the difference in the HOH bend of the IR spectra between liquid water and ice", *Journal of Chemical Physics* **138**, 054506 (2013)

9. N. Mardirossian, D. S. Lambrecht, L. McCaslin, S. S. Xantheas, and M. Head-Gordon, "The Performance of Density Functionals for Sulfate-Water Clusters", *Journal of Chemical Theory and Computation* **9**, 1368 (2013)

10. K. Doi, E. Togano, S. S. Xantheas, R. Nakanishi, T. Nagata, T. Ebata and Y. Inokuchi, "Microhydration Effects on the Intermediates of the (I^- + CH_3I) S_N2 Reaction", Communication to the Editor, *Angewandte Chemie International Edition* **52**, 4380 (2013). Highlighted in the "Science Concentrates" section, Chemical & Engineering News, vol. **91** (8), p. 34-35 (2013)

11. E. Miliordos, K. Ruedenberg and S. S. Xantheas, "Unusual inorganic biradicals: A Theoretical Analysis", Communication to the Editor, *Angewandte Chemie International Edition* **52**, 5736 (2013)

12. S. Imoto, S. S. Xantheas, S. Saito, "Ultrafast Dynamics of Liquid Water: Frequency Fluctuations of the OH stretch and the HOH Bend", *Journal of Chemical Physics* **139**, 044503 (2013)

13. S. Iwata, P. Bandyopadhyay, and S. S. Xantheas, "Cooperative roles of charge-transfer and dispersion terms in hydrogen-bonded networks of $(H_2O)_n$, n = 6, 11 and 16", *Journal of Physical Chemistry A* **117**, 6641 (2013)

14. E. Miliordos and S. S. Xantheas, "Efficient procedure for the numerical calculation of harmonic vibrational frequencies based on internal coordinates" Joel M. Bowman Special Issue (invited), *Journal of Physical Chemistry A* **117**, 7019 (2013)

15. E. Miliordos, E. Aprà and S. S. Xantheas, "Optimal geometries and harmonic vibrational frequencies of the global minima of water clusters $(H_2O)_n$, n=2-6, and several hexamer local minima at the CCSD(T) level of theory" *Journal of Chemical Physics* **139**, 114302 (2013)

16. E. Miliordos and S. S. Xantheas, "Unimolecular and hydrolysis channels for the detachment of water from microsolvated alkaline earth dication (Mg^{2+}, Ca^{2+}, Sr^{2+}, Ba^{2+}) clusters", Thom H. Dunning Jr. Special Issue (invited), *Theoretical Chemistry Accounts* **133**, 1450 (2014)

17. E. Miliordos and S. S. Xantheas, "On the bonding nature of ozone (O_3) and its sulfur-substituted analogues, SO_2, OS_2, and S_3: Correlation between their biradical character and molecular properties" *Journal of the American Chemical Society* **136**, 2808 (2014)

18. E. Miliordos and S. S. Xantheas, "Elucidating the mechanism behind the stabilization of multi-charged metal cations in water: A case study of the electronic states of microhydrated Mg^{2+}, Ca^{2+} and Al^{3+}". Hot article for the week Oct 22, 2013 (http://blogs.rsc.org/cp/2013/10/22/this-weeks-hot-articles-11/). Highlighted in NERSC's web page, June 2014, http://www.nersc.gov/news-publications/news/science-news/2014/thirsty-metals-key-to-longer-battery-lifetimes/. Highlighted in DOE's Pulse (Science and Technology Highlights from the DOE National Laboratories, #417, 7 July 2014 http://web.ornl.gov/info/news/pulse/no417/story1.shtml, Communication to the Editor, *Physical Chemistry Chemical Physics* **16**, 6886 (2014). Journal cover

19. A. E. Vasdekis, M. J. Wilkins, J. W. Grate, R. T. Kelly, A. Konopka, S. S. Xantheas, T.-M. Chang "Solvent Immersion Imprint Lithography" *Lab on a Chip* **14**, 2072 (2014)

20. T. Yoshida, W. A. Farone and S. S. Xantheas, "Isomers and conformational barriers of gas phase nicotine, nornicotine and their protonated forms", James L. Skinner special issue (invited), *Journal of Physical Chemistry B* **118**, 8273 (2014)

21. S. S. Xantheas and J. C. Werhahn, "Universal Scaling of Potential Energy Functions describing Intermolecular Interactions: I. Foundations and scalable forms for new generalized Lennard-Jones, Mie, Morse and Buckingham exponential-6 potentials", *Journal of Chemical Physics* **141**, 064117 (2014)

22. J. C. Werhahn, D. Akase and S. S. Xantheas, "Universal Scaling of Potential Energy Functions describing Intermolecular Interactions: II. The halide- and alkali metal-water interactions", *Journal of Chemical Physics* **141**, 064118 (2014)

23. E. Miliordos, E. Aprà and S. S. Xantheas, "A benchmark theoretical study of the π-π interaction energy in the benzene dimer", Kenneth D. Jordan special issue (invited), *Journal of Physical Chemistry* DOI: 10.1021/jp5024235 (2014)

24. C. C. Pradzynski, C. W. Dierking, F. Zurheide, R. M. Forck, T. Zeuch, U. Buck and S. S. Xantheas, "Infrared detection of a fully coordinated water molecule in a $(H_2O)_{20}$ cluster: The smallest drop of water" Communication to the Editor, *Physical Chemistry Chemical Physics* (accepted 1-Sept-2014)

Room Temperature Single-Molecule Detection and Imaging by Stimulated Raman Scattering Microscopy

Principle Investigator: X. Sunney Xie

Department of Chemistry and Chemical Biology
Harvard University, Cambridge, MA 02138
xie@chemistry.harvard.edu

Program Scope:

The scope of this program is to push the detection sensitivity limit of stimulated Raman scattering (SRS) imaging to single molecule. Raman provides specific vibrational signatures of chemical bonds, which enables new modes of chemical imaging without labels. Unlike fluorescence, which has a large cross-section, single molecule Raman detection without surface enhancement has long been a major technical challenge. We attempt to tackle this challenge with our newly developed SRS imaging technique and study long chain conjugated molecules using near-resonance enhancement.

Recent Progress:

Towards the goal of single molecule SRS detection, we attempted both further technological development of lasers sources and imaging approaches as well as synthesis of new molecules with large Raman cross-section and high photostability for SRS imaging. However, due to the limitation of the photobleaching of the molecule (β-carotene or its analogs), we were unable to achieve single molecule detection limit. The photostabilizing effect of cyclooctatetraene conjugated to β-carotene was not large enough to decrease its photobleaching in SRS detection. Therefore, we conclude that it is difficult to achieve single molecule limit with the proposed SRS detection scheme.

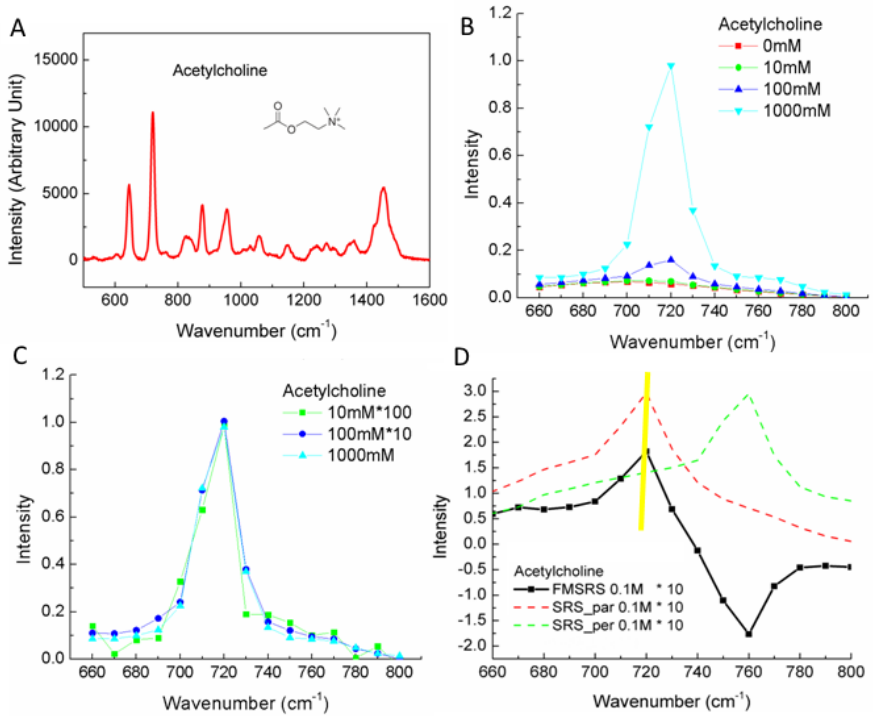

Figure 1: A. Spontaneous Raman spectrum of acetylcholine. B. SRS spectra of acetylcholine solutions. C. SRS spectra of acetylcholine solutions after background removal. D. SRS spectra of 0.1M acetylcholine solution with 30 cm^{-1} frequency offset for the two arms of FMSRS (dotted curves) and FMSRS spectrum (black solid curve).

However, we were able to adapt the constructed SRS system for high sensitivity detection of other small molecules. One such molecular target is acetylcholine. Acetylcholine is a small molecule that plays important roles in neurotransmission. It is a good model molecule for developing SRS imaging technology that could be broadly applicable to other small molecules. Figure 1A shows the Raman spectrum of acetylcholine and its molecular structure. We concentrated on the 720 cm^{-1} peak, which is attributed to the symmetric stretch vibration of choline group $N^{+}(CH_3)_3$. Using hyperspectral SRS imaging, we obtained the SRS spectra of acetylcholine solutions at different concentrations from 660 cm^{-1} to 800 cm^{-1} (Figure 1B). At 10 mM concentration, the SRS spectrum is dominated by a broad background that originates from cross-phase modulation. We can remove the background by subtracting the spectra with that from pure water. After this procedure, we observed linear concentration dependence of SRS spectra over two orders of magnitude as expected (Figure 1C). However, this post-processing procedure is not applicable to real samples because such background spectrum is unavailable. We used the frequency-modulation SRS (FMSRS) method developed for single molecule SRS to overcome this problem. Because SRS signal from acetylcholine has a sharp peak, while the background spectrum is broad, we can obtain SRS signal from acetylcholine by subtracting its SRS signal at 720 cm^{-1} from its SRS signal at 690 cm^{-1}. By doing so, the background contribution is largely removed while the acetylcholine signal is mostly intact. Experimentally this is achieved by FMSRS, which performs real-time subtraction of two SRS signals with spectral difference of 30 cm^{-1} (Figure 1D). Using this detection scheme, the detection limits reaches 20 mM at a pixel integration time of 4μs.

Lastly, we are developing a new super-resolution SRS imaging technique. SRS imaging resolution is limited by diffraction of both the pump and the Stokes beam. In a typical SRS setup that uses a 1064nm beam as the Stokes and 810 nm beam as the pump, the lateral resolution is ~ 350 nm and axial resolution is ~1.4 μm. Axial resolution is almost four times worse than lateral resolution. To improve axial resolution, we propose to combine temporal focusing with spectral focusing technique. Spectral focusing allows the use of broadband lasers to selectively excite a narrow Raman band of interests, while temporal focusing ensures that only at the focus different colors overlap and reach high peak intensity to excite the molecular vibration. We expect this novel technique will enhance the axial resolution by two-fold. Currently we are running computer simulation and designing experimental setup to implement this SRS detection scheme.

DOE Publications/Manuscripts 2013-present

1. Fu, Dan; Holtom, Gary; Freudiger, Christian; Zhang, Xu; Xie, X. Sunney. "Hyperspectral Imaging with Stimulated Raman Scattering by Chirped Femtosecond Lasers," J Phys. Chem. B 117, 4634-4640 (2013).
2. Fu, Dan; Xie, X. Sunney, Reliable Cell Segmentation Based on Spectral Phasor Analysis of Hyperspectral Stimulated Raman Scattering Imaging Data. Anal. Chem. 86 (9), 4115-4119 (2014).

List of Participants

LIST OF PARTICIPANTS

Dr. Musahid Ahmed
Lawrence Berkeley National Laboratory
https://commons.lbl.gov/display/csd/Musahid+Ahmed

Professor Scott Anderson
University of Utah
http://www.chem.utah.edu/directory/anderson/

Dr. David Bartels
Notre Dame Radiation Laboratory
http://www.rad.nd.edu/faculty/bartels.htm

Dr. Ali Belkacem
Lawrence Berkeley National Laboratory
http://amo-csd.lbl.gov/about.php

Dr. Hendrik Bluhm
Lawrence Berkeley National Laboratory
http://actinide.lbl.gov/hbluhm/

Dr. Nicholas Camillone
Brookhaven National Laboratory
http://www.bnl.gov/chemistry/bio/Camillone%20IIINicholas.asp

Benjamin Caplins
Lawrence Berkeley National Laboratory
http://chem.berkeley.edu/faculty/harris_c/index.php

Professor Ian Carmichael
Notre Dame Radiaton Laboratory
http://www.rad.nd.edu/faculty/carmichael.htm

Dr. Andrew Cook
Brookhaven National Laboratory
http://www.bnl.gov/chemistry/bio/CookAndrew.asp

Professor Tanja Cuk
Lawrence Berkeley National Laboratory
http://www.cchem.berkeley.edu/tkgrp/

Dr. Liem Dang
Pacific Northwest National Laboratory
http://www.pnl.gov/science/staff/staff_info.asp?staff_num=5604

Professor Michael Duncan
University of Georgia
http://www.chem.uga.edu/research/people/1976

Professor Michael Fayer
Stanford University
http://www.stanford.edu/group/fayer/

Dr. Christopher Fecko
DOE/Basic Energy Sciences
http://science.energy.gov/bes/csgb/about/staff/dr-christopher-fecko/

Dr. Gregory Fiechtner
DOE/Basic Energy Sciences
http://science.energy.gov/bes/csgb/about/staff/dr-gregory-j-fiechtner/

Mr. John L. Fulton
Pacific Northwest National Laboratory
http://www.pnnl.gov/science/staff/staff_info.asp?staff_num=5587

Professor Etienne Garand
University of Wisconsin
http://garand.chem.wisc.edu/

Dr. Bruce Garrett
Pacific Northwest National Laboratory
http://www.pnl.gov/science/staff/staff_info.asp?staff_num=5496

Professor Phillip Geissler
Lawrence Berkeley National Laboratory
http://www.cchem.berkeley.edu/plggrp/index.html

Dr. Mary K. Gilles
Lawrence Berkeley National Laboratory
https://commons.lbl.gov/display/csd/Mary+K.+Gilles

Professor Mark Gordon
Ames Laboratory
http://www.msg.ameslab.gov/

Dr. Jeffrey Guest
Argonne National Laboratory
http://www.anl.gov/cnm/person/jeffrey-guest

Dr. Alexander Harris
Brookhaven National Laboratory
http://www.bnl.gov/chemistry/bio/HarrisAlex.asp

Professor Mark Hersam
Northwestern University
http://www.hersam-group.northwestern.edu/

Dr. Wayne Hess
Pacific Northwest National Laboratory
http://www.pnl.gov/science/staff/staff_info.asp?staff_num=5505

Professor Wilson Ho
University of California, Irvine
http://www.physics.uci.edu/~wilsonho/whoghp.htm

Professor Bret Jackson
University of Massachusetts Amherst
http://www.chem.umass.edu/faculty/jackson.html

Dr. Ireneusz Janik
Notre Dame Radiation Laboratory
http://www.rad.nd.edu/faculty/Janik.htm

Professor Caroline Chick Jarrold
Indiana University
http://mypage.iu.edu/~cjarrold/index.htm

Dr. Cynthia J. Jenks
Ames Laboratory
https://www.ameslab.gov/users/cjenks

Professor Mark Johnson
Yale University
http://jlab.chem.yale.edu/

Professor Kenneth Jordan
University of Pittsburgh
http://www.pitt.edu/~jordan/

Dr. Shawn Kathmann
Pacific Northwest National Laboratory
http://www.pnl.gov/science/staff/staff_info.asp?staff_num=5601

Dr. Bruce Kay
Pacific Northwest National Laboratory
http://www.pnl.gov/science/staff/staff_info.asp?staff_num=5530

Professor Munira Khalil
University of Washington
http://depts.washington.edu/chem/people/faculty/mkhalil.html

Dr. Greg Kimmel
Pacific Northwest National Laboratory
http://www.pnl.gov/science/staff/staff_info.asp?staff_num=5527

Dr. Jeff Krause
DOE/Basic Energy Sciences
http://science.energy.gov/bes/csgb/about/staff/dr-jeffrey-l-krause/

Dr. Jay LaVerne
Notre Dame Radiation Laboratory
http://www.rad.nd.edu/faculty/laverne.htm

Dr. Da-Jiang Liu
Ames Laboratory
https://www.ameslab.gov/cbs/dajiang

Professor H. Peter Lu
Bowling Green State University
http://www.bgsu.edu/departments/chem/faculty/hplu/peterlu.htm

Dr. Sergei Lymar
Brookhaven National Laboratory
http://www.bnl.gov/chemistry/bio/LymarSergei.asp

Diane Marceau
DOE/Basic Energy Sciences
http://science.energy.gov/bes/csgb/about/staff/

Dr. John Miller
Brookhaven National Laboratory
http://www.bnl.gov/chemistry/bio/MillerJohn.asp

Dr. Christopher Mundy
Pacific Northwest National Laboratory
http://www.pnl.gov/science/staff/staff_info.asp?staff_num=5981

Professor Richard Osgood
Columbia University
http://cumsl.msl.columbia.edu/

Dr. Mark Pederson
DOE/Basic Energy Sciences
http://science.energy.gov/bes/csgb/about/staff/dr-mark-r-pederson/

Professor Hrvoje Petek
University of Pittsburgh
http://www.ultrafast.phyast.pitt.edu/Home.html

Dr. Tanja Pietraß
DOE/Basic Energy Sciences
http://science.energy.gov/bes/csgb/about/staff/dr-tanja-pietrass/

Professor Eric Potma
University of California, Irvine
http://www.chem.uci.edu/~potma/webpage_test.htm

Professor Sylwia Ptasinska
University of Notre Dame
http://www3.nd.edu/~sptasins/

Professor Krishnan Raghavachari
Indiana University
http://php.indiana.edu/~krgroup/

Professor Richard Saykally
Lawrence Berkeley National Laboratory
http://www.cchem.berkeley.edu/rjsgrp/

Dr. Gregory Schenter
Pacific Northwest National Laboratory
http://www.pnl.gov/science/staff/staff_info.asp?staff_num=5615

Dr. David K. Shuh
Lawrence Berkeley National Laboratory
http://actinide.lbl.gov/gtsc/Staff/dkshuh/

Dr. Wade Sisk
US DOE/Basic Energy Sciences
http://science.energy.gov/bes/csgb/about/staff/dr-wade-sisk/

Professor Charles Sykes
Tufts University
http://ase.tufts.edu/chemistry/sykes/Sykes%20Lab%20Research%20Group.html

Professor Ward Thompson
University of Kansas
http://thompsongroup.ku.edu/

Professor William A. Tisdale
Massachusetts Institute of Technology
http://web.mit.edu/tisdalelab

Professor Andrei Tokmakoff
University of Chicago
http://tokmakofflab.uchicago.edu/

Professor John Tully
Yale University
http://www.chem.yale.edu/~tully/

Dr. Marat Valiev
Pacific Northwest National Laboratory
http://www.emsl.pnl.gov/emslweb/people/marat-valiev

Professor Lai-Sheng Wang
Brown University
https://vivo.brown.edu/display/lw28

Dr. Xue-Bin Wang
Pacific Northwest National Laboratory
http://www.emsl.pnl.gov/emslweb/people/xuebin-wang

Professor Michael White
Brookhaven National Laboratory
http://www.bnl.gov/chemistry/bio/WhiteMichael.asp

Dr. Kevin R. Wilson
Lawrence Berkeley National Laboratory
http://wilsonresearchgroup.lbl.gov/home

Professor Theresa L. Windus
Ames Laboratory
https://www.ameslab.gov/users/theresa

Dr. James Wishart
Brookhaven National Laboratory
http://www.chemistry.bnl.gov/SciandTech/PRC/wishart/wishart.html

Dr. Sotiris Xantheas
Pacific Northwest National Laboratory
http://www.pnl.gov/science/staff/staff_info.asp?staff_num=5610

Professor X. Sunney Xie
Harvard University
http://bernstein.harvard.edu/